



FAMU-FSU
Engineering

Civil and Environmental Engineering

**FLORIDA A&M UNIVERSITY-
FLORIDA STATE UNIVERSITY
(FAMU-FSU) COLLEGE OF
ENGINEERING**

Improving Safety at Highway-Rail Grade Crossings in Florida while Maintaining Continuity of Passenger and Freight Flows: A Multi-Objective Approach

Project Number: BDV30-977-33

A Technical Report Prepared for the Florida Department of Transportation, Freight & Multimodal
Operations Office

FINAL REPORT

FDOT Project Manager: **Rickey Fitzgerald**, Freight & Multimodal Operations Office Manager

Principal Investigator:

Maxim A. Dulebenets, Ph.D., P.E.

Assistant Professor

Department of Civil & Environmental Engineering

Florida A&M University-Florida State University

Phone: +1(850) 410-6621

E-mail: mdulebenets@eng.famu.fsu.edu

Co-Principal Investigator:

John Sobanjo, Ph.D., P.E.

Professor

Department of Civil & Environmental Engineering

Florida A&M University-Florida State University

Phone: +1(850) 410-6153

E-mail: sobanjo@eng.famu.fsu.edu

Co-Principal Investigator:

Junayed Pasha, Ph.D.

Postdoctoral Research Associate

Department of Civil & Environmental Engineering

Florida A&M University-Florida State University

Phone: +1(850) 339-3666

E-mail: junayed729@gmail.com

Co-Principal Investigator:

Eren E. Ozguven, Ph.D.

Associate Professor

Department of Civil & Environmental Engineering

Florida A&M University-Florida State University

Phone: +1(850) 410-6146

E-mail: eozen@eng.famu.fsu.edu

Co-Principal Investigator:

Ren Moses, Ph.D., P.E.

Professor

Department of Civil & Environmental Engineering

Florida A&M University-Florida State University

Phone: +1(850) 410-6191

E-mail: moses@eng.famu.fsu.edu

Research Assistant:

Prashant Singh, P.E., C.Eng.

Graduate Research Assistant

Department of Civil & Environmental Engineering

Florida A&M University-Florida State University

Phone: +1(813) 970-5900

E-mail: prashant1.singh@famu.edu

December 2021

DISCLAIMER

The opinions, findings, and conclusions expressed in this report are those of the authors and not necessarily those of the State of Florida Department of Transportation.

METRIC CONVERSION CHART

When You Know	Multiply by	To Find
Length		
inches (in)	25.4	millimeters (mm)
feet (ft)	0.305	meters (m)
yards (yd)	0.914	meters (m)
miles (mi)	1.61	kilometers (km)
Volume		
fluid ounces (fl oz)	29.57	milliliters (mL)
gallons (gal)	3.785	liters (L)
cubic feet (ft ³)	0.028	meters cubed (m ³)
cubic yards (yd ³)	0.765	meters cubed (m ³)
Area		
square inches (in ²)	645.1	millimeters squared (mm ²)
square feet (ft ²)	0.093	meters squared (m ²)
square yards (yd ²)	0.836	meters squared (m ²)
acres	0.405	hectares (ha)
square miles (mi ²)	2.59	kilometers squared (km ²)

TECHNICAL REPORT DOCUMENTATION PAGE

1. Report No.	2. Government Accession No.	3. Recipient's Catalog No.	
4. Title and Subtitle Improving Safety at Highway-Rail Grade Crossings in Florida while Maintaining Continuity of Passenger and Freight Flows: A Multi-Objective Approach		5. Report Date 12/31/2021	
		6. Performing Organization Code 59-1961248	
7. Author(s) Maxim A. Dulebenets, Ph.D., P.E.; Junayed Pasha, Ph.D.; Ren Moses, Ph.D., P.E.; John Sobanjo, Ph.D., P.E.; Eren E. Ozguven, Ph.D.; Prashant Singh, P.E., C.Eng.		8. Performing Organization Report No. 045780	
9. Performing Organization Name and Address Florida A&M University-Florida State University 2525 Pottsdamer Street, Building A, Suite A124 Tallahassee, FL 32310-6046, USA		10. Work Unit No. (TRAVIS)	
		11. Contract or Grant No. BDV30-977-33	
12. Sponsoring Agency Name and Address Florida Department of Transportation 605 Suwannee Street, MS 30 Tallahassee, FL 32399		13. Type of Report and Period Covered Final Report Period Covered: 06/15/2020-12/31/2021	
		14. Sponsoring Agency Code	
15. Supplementary Notes			
16. Abstract The State of Florida is one of the most populous states in the United States. Because of this increasing population, a substantial amount of freight is transported in Florida. Rail is an important mode of freight transportation in Florida. Increasing railroad transportation-based activities have led to greater economic impacts as well as more highway-rail crossing accidents. Installation of various countermeasures at crossings will improve safety but can cause traffic delays. This project proposed a multi-objective mathematical model, which aimed to minimize the overall hazard severity and to minimize the overall traffic delay at the considered highway-rail grade crossings. A total of three solution algorithms was developed for the model, and the most effective one was identified based on the solution quality and computational time criteria. Furthermore, a standalone application "HRX Safety Improvement" was developed as a part of this project to assist the Florida Department of Transportation (FDOT) personnel with resource allocation for the considered highway-rail grade crossings. A set of computational experiments was performed to illustrate applicability of the proposed methodology for conducting multi-objective resource allocation. The experiments explicitly demonstrated that the developed methodology could serve as an effective decision support system for the FDOT personnel and assist with reducing the overall hazard severity and the overall traffic delay at the highway-rail grade crossings in Florida under different budget availability, countermeasure availability, hazard severity weight, and crossing type scenarios. Moreover, the introduction of alternative countermeasures, such as LED signs, could facilitate multi-objective resource allocation among highway-rail grade crossings and make it more efficient.			
17. Key Words Highway-rail grade crossings; crossing accidents; traffic delays; multi-objective optimization; decision support systems		18. Distribution Statement No restrictions	
19. Security Classif. (of this report) Unclassified	20. Security Classif. (of this page) Unclassified	21. No. of Pages 242	22. Price

ACKNOWLEDGEMENTS

This project was sponsored by the State of Florida Department of Transportation (FDOT). The Principal Investigators would like to thank the FDOT Project Manager, Mr. Rickey Fitzgerald, and FDOT Freight & Multimodal Operations Office for their valuable feedback throughout the project activities.

EXECUTIVE SUMMARY

The State of Florida is one of the most populous states in the United States. Because of this increasing population, a substantial amount of freight is transported in Florida. A large volume of freight is handled in the state by various modes (e.g., road, rail, sea). Rail is an important mode of freight transportation in Florida, as 15.8% of freight tonnage is exported by rail in Florida. Railroad transportation-based activities have increased in Florida, leading to greater economic impacts as well as more highway-rail crossing accidents. Since the number of highway-rail grade crossing accidents in Florida has been increasing, safety issues at the state highway-rail grade crossings should be mitigated. The latter objective can be achieved with various countermeasures, such as installation of various warning devices, traffic signal preemption, grade separation, and others. However, installation of countermeasures along with halting of the associated highway traffic, because of passing trains, may add delays at a highway-rail grade crossing.

In order to address the aforementioned issues, this project has developed a mathematical model, named the Multi-Objective Resource Allocation Problem (**MORAP**), which aims to minimize the overall hazard severity and to minimize the overall traffic delay at the considered highway-rail grade crossings. A total of three solution algorithms was developed for the **MORAP** mathematical model, and the most effective one was identified based on the solution quality and computational time criteria. Furthermore, a standalone application “HRX Safety Improvement” was developed as a part of this project to assist the Florida Department of Transportation (FDOT) personnel with the following functions: (1) estimation of the overall hazard severity for the considered highway-rail grade crossings; (2) estimation of the overall traffic delay for the considered highway-rail grade crossings before and after application of the candidate countermeasures; and (3) resource allocation for the considered highway-rail grade crossings.

A set of computational experiments was performed to illustrate applicability of the proposed methodology for conducting multi-objective resource allocation in order to minimize the overall hazard severity and to minimize the overall traffic delay at the existing highway-rail grade crossings in Florida. A comprehensive description of the computational experiments was presented in this report. Specifically, the following analyses were performed as a part of the experiments: (1) sensitivity analysis for the total available budget; (2) sensitivity analysis for the number of available countermeasures; (3) sensitivity analysis for the hazard severity weight values; (4) resource allocation among various crossing types; and (5) evaluation of an alternative countermeasure (i.e., light-emitting diode [LED] signs).

The computational experiments explicitly demonstrated that the developed methodology, including the **MORAP** mathematical model, the proposed solution algorithm (named Multi-Objective Profitable Severity and Delay Reduction [MPSDR] heuristic), and the “HRX Safety Improvement” standalone application, can serve as an effective decision support system for the FDOT personnel and assist with reducing the overall hazard severity and the overall traffic delay at the highway-rail grade crossings in Florida under different budget availability, countermeasure availability, hazard severity weight, and crossing type scenarios. Moreover, the introduction of alternative countermeasures, such as LED signs, could facilitate multi-objective resource allocation among highway-rail grade crossings and make it more efficient.

TABLE OF CONTENTS

DISCLAIMER	ii
METRIC CONVERSION CHART	iii
TECHNICAL REPORT DOCUMENTATION PAGE	iv
ACKNOWLEDGEMENTS	v
EXECUTIVE SUMMARY	vi
TABLE OF CONTENTS.....	vii
LIST OF FIGURES	ix
LIST OF TABLES.....	xvi
1. INTRODUCTION	1
1.1. Freight Mobility in Florida	1
1.2. Role of Rail Transportation in Florida.....	1
1.3. Highway-Rail Grade Crossings	3
1.4. Continuity of Passenger and Freight Flows at Highway-Rail Grade Crossings.....	21
1.5. Objectives of This Project.....	23
1.6. Report Structure	24
2. REVIEW OF THE RELEVANT STUDIES AND TECHNOLOGIES	25
2.1. Approaches for Quantifying Continuity of Passenger and Freight Flows at Highway-Rail Grade Crossings	25
2.2. Warning Devices and Advanced Technology at Highway-Rail Grade Crossings	31
2.3. Connected and Autonomous Vehicle Applications at Highway-Rail Grade Crossings	70
3. MATHEMATICAL MODEL DEVELOPMENT	79
3.1. Problem Definition.....	79
3.2. Proposed Mathematical Formulation.....	80
3.3. Estimation of the Overall Hazard Severity	81
3.4. Estimation of the Overall Traffic Delay	88
3.5. Model Complexity	93
4. DEVELOPMENT OF CANDIDATE SOLUTION ALGORITHMS	98
4.1. Epsilon-Constraint (ECON) Method	99
4.2. Multi-Objective Profitable Severity and Delay Reduction (MPSDR) Heuristic.....	101
4.3. Multi-Objective Effective Severity and Delay Reduction (MESDR) Heuristic.....	105
5. EVALUATION OF SOLUTION ALGORITHMS	109
5.1. Required Input Data.....	109
5.2. CPU Settings.....	113

5.3. Comparison of Pareto Fronts	113
5.4. Computational Time	121
5.5. Solution Algorithm Recommendation	125
5.6. Pareto Front Size Effects	125
6. DEVELOPMENT OF THE STANDALONE APPLICATION	128
6.1. Purpose of the Application.....	128
6.2. Installation Guidelines	129
6.3. User Guidelines.....	134
7. METHODOLOGY APPLICATION	171
7.1. Sensitivity Analysis for the Total Available Budget	171
7.2. Sensitivity Analysis for the Number of Available Countermeasures	180
7.3. Sensitivity Analysis for the Hazard Severity Weight Values	184
7.4. Resource Allocation among Various Crossing Types	195
7.5. Evaluation of an Alternative Countermeasure	203
8. CONCLUSIONS AND FUTURE RESEARCH	214
REFERENCES	217

LIST OF FIGURES

Figure 1 Rail mileage in Florida.	2
Figure 2 Locations of the private and public crossings in Florida.....	4
Figure 3 Distribution of Florida’s crossings by crossing position.....	4
Figure 4 Locations of different types of crossings in Florida.....	5
Figure 5 Distribution of Florida’s highway-rail grade crossings by ownership type.	6
Figure 6 Distribution of Florida’s highway-rail grade crossings by AADT.....	7
Figure 7 Distribution of Florida’s highway-rail grade crossings by total number of trains per day.	8
Figure 8 Distribution of Florida’s highway-rail grade crossings by maximum timetable speed....	8
Figure 9 Distribution of Florida’s highway-rail grade crossings by total number of tracks.....	9
Figure 10 Distribution of Florida’s highway-rail grade crossings by roadway type.	10
Figure 11 Distribution of Florida’s highway-rail grade crossings by illumination type.	10
Figure 12 Distribution of Florida’s highway-rail grade crossings by number of traffic lanes crossing railroad.....	12
Figure 13 Distribution of Florida’s highway-rail grade crossings by functional classification of road at crossing.	12
Figure 14 Highway-rail grade crossing accident statistics in Florida (2009 to 2019).	13
Figure 15 Distribution of Florida’s highway-rail grade crossings that experienced accidents between 2015 and 2019 by ownership type.....	14
Figure 16 Distribution of Florida’s highway-rail grade crossings that experienced accidents between 2015 and 2019 by AADT.	15
Figure 17 Distribution of Florida’s highway-rail grade crossings that experienced accidents between 2015 and 2019 by total number of trains per day.....	16
Figure 18 Distribution of Florida’s highway-rail grade crossings that experienced accidents between 2015 and 2019 by maximum timetable speed.	17
Figure 19 Distribution of Florida’s highway-rail grade crossings that experienced accidents between 2015 and 2019 by total number of tracks.	18
Figure 20 Distribution of Florida’s highway-rail grade crossings that experienced accidents between 2015 and 2019 by roadway type.....	18
Figure 21 Distribution of Florida’s highway-rail grade crossings that experienced accidents between 2015 and 2019 by illumination type.	19
Figure 22 Distribution of Florida’s highway-rail grade crossings that experienced accidents between 2015 and 2019 by number of traffic lanes crossing railroad.	20
Figure 23 Distribution of Florida’s highway-rail grade crossings that experienced accidents between 2015 and 2019 by functional classification of road at crossing.	21
Figure 24 Total rail fleet count in the U.S. for 2004-2014.	22
Figure 25 Heavy rail fleet count in the U.S. for 2004-2014.	23
Figure 26 Traffic queues starting from a highway intersection approach a highway-rail grade crossing.	25

Figure 27 Traffic queues starting from a highway-rail grade crossing approach a highway intersection.....	26
Figure 28 Regular pavement markings.....	32
Figure 29 Symbol and word pavement marking.....	33
Figure 30 Diagonal exclusion zone pavement markings at pre-signal locations.....	34
Figure 31 Alternative pavement markings at highway-rail grade crossings.....	35
Figure 32 Regulatory signs and plaques for highway-rail grade crossings.....	37
Figure 33 Warning signs and plaques for highway-rail grade crossings.....	38
Figure 34 An example of a stop sign.....	39
Figure 35 An example of a crossbuck sign.....	39
Figure 36 An example of wigwags.....	40
Figure 37 An example of a crossing bell.....	40
Figure 38 An example of flashing light signals.....	41
Figure 39 An example of basic gates.....	41
Figure 40 Examples of a LED preemptive train warning sign.....	42
Figure 41 Examples of a LED blinker sign.....	43
Figure 42 An example of a flip disk or flip dot display.....	44
Figure 43 An example of a LED display board.....	44
Figure 44 An example of two-quad gates with a raised median.....	47
Figure 45 An example of four-quad gates.....	47
Figure 46 An example of a microwave radar.....	51
Figure 47 An audible warning device (upper right corner) near a blank-out sign.....	55
Figure 48 An architecture of the DSRC.....	57
Figure 49 An example of an ASD.....	58
Figure 50 Example cues provided by an RSD.....	59
Figure 51 A truck equipped with the RSD device and DSRC antennas (pointed by an arrow).....	59
Figure 52 A typical VAD.....	60
Figure 53 The RCVW application concept.....	61
Figure 54 An example of the HRI-2000 system installation.....	62
Figure 55 An example of the PTC technology.....	63
Figure 56 An example of a mountable raised curb system.....	66
Figure 57 An example of bollards.....	66
Figure 58 An example of dynamic envelope zone pavement markings.....	67
Figure 59 An example of a dynamic envelope zone modified signage.....	68
Figure 60 The CAV technology and highway-rail grade crossing communication.....	70
Figure 61 Alternate routing with the Internet of Things.....	71
Figure 62 An example of an autonomous vehicle.....	72
Figure 63 Levels of automation for autonomous vehicles.....	73
Figure 64 An example of an autonomous vehicle with sensor-based technologies.....	75
Figure 65 Advanced train technologies.....	76

Figure 66 LEADER controls by New York Air Brake.....	77
Figure 67 Overview of an autoBAHN.....	78
Figure 68 Queue dissipation time estimations.....	91
Figure 69 Euler diagram for computational complexity classes.....	94
Figure 70 The knapsack problem prevailing in the railway industry.....	95
Figure 71 An illustrative example of a Pareto Front for the MORAP mathematical model.....	98
Figure 72 An illustrative example of the ECON method application.....	99
Figure 73 Pareto Fronts produced by ECON, MPSDR, and MESDR for the selected scenarios of problem instance with TAB = \$4.5M.....	119
Figure 74 Detailed evaluation of Pareto Fronts produced by ECON, MPSDR, and MESDR for the problem instance with $ X = 6109$, $ C = 11$, and TAB = \$4.5M.....	120
Figure 75 Relationship between the Pareto Front size and computational time required.....	126
Figure 76 Examples of Pareto Fronts with different Pareto Front sizes.....	127
Figure 77 The folder containing the installation file.....	129
Figure 78 The installer of the standalone application “HRX Safety Improvement”.....	130
Figure 79 The installation window of the standalone application “HRX Safety Improvement”.....	130
Figure 80 The installation directory of the standalone application “HRX Safety Improvement”.....	131
Figure 81 The installation directory of MATLAB Runtime.....	131
Figure 82 Accepting the terms of the license agreement.....	132
Figure 83 The confirmation window showing the installation directories.....	132
Figure 84 The installation progress.....	133
Figure 85 The installation completion.....	133
Figure 86 The user interface of the standalone application “HRX Safety Improvement”.....	137
Figure 87 Loading the database with highway-rail grade crossings and countermeasures.....	139
Figure 88 Specifying the location to export the results.....	140
Figure 89 Loading the crossing inventory data.....	141
Figure 90 Specifying the prediction year and loading the accident data.....	142
Figure 91 Selection of the crossing type.....	143
Figure 92 The progress bar of “FPI and Delay Estimation”.....	144
Figure 93 The “Output_FPI” sheet of the “Tool_Output.xlsx” file.....	145
Figure 94 The “Legend_FPI” sheet of the “Tool_Output.xlsx” file.....	145
Figure 95 The “Output_Delay” sheet of the “Tool_Output.xlsx” file.....	147
Figure 96 The “Legend_Delay” sheet of the “Tool_Output.xlsx” file.....	147
Figure 97 The “EBT(x,c)” sheet of the “Tool_Output.xlsx” file.....	148
Figure 98 The “VQ(x,c)” sheet of the “Tool_Output.xlsx” file.....	149
Figure 99 The “QDT(x,c)” sheet of the “Tool_Output.xlsx” file.....	149
Figure 100 The “ODB(x,c)” sheet of the “Tool_Output.xlsx” file.....	149
Figure 101 The “OD(x,c)” sheet of the “Tool_Output.xlsx” file.....	149

Figure 102 The “AD(x,c)” sheet of the “Tool_Output.xlsx” file.	150
Figure 103 The “Sheet_Description” sheet of “FDOT_HRX-project_2020.xlsx”.....	150
Figure 104 The “Data_Description” sheet of “FDOT_HRX-project_2020.xlsx”.....	151
Figure 105 The “p(x,c)” sheet of “FDOT_HRX-project_2020.xlsx”.....	152
Figure 106 The “EF(x,c)” sheet of “FDOT_HRX-project_2020.xlsx”.....	152
Figure 107 The “HS(x,s)” sheet of “FDOT_HRX-project_2020.xlsx”.....	153
Figure 108 The “W(s)” sheet of “FDOT_HRX-project_2020.xlsx”.....	153
Figure 109 The “CA(x,c)” sheet of “FDOT_HRX-project_2020.xlsx”.....	154
Figure 110 The “OD0(x)” sheet of “FDOT_HRX-project_2020.xlsx”.....	154
Figure 111 The “AD(x,c)” sheet of “FDOT_HRX-project_2020.xlsx”.....	155
Figure 112 The “TAB” sheet of “FDOT_HRX-project_2020.xlsx”.....	155
Figure 113 Specifying the index of highway-rail grade crossings and the index of countermeasures.....	157
Figure 114 Specifying the number of PF points.	159
Figure 115 The progress bar of “HRX Resource Allocation”.....	159
Figure 116 The results displayed on the user interface.....	160
Figure 117 The “PF Point #1” sheet of the “Resource Allocation.xlsx” file.....	162
Figure 118 The “PF Point #2” sheet of the “Resource Allocation.xlsx” file.....	162
Figure 119 The “PF Point #3” sheet of the “Resource Allocation.xlsx” file.....	163
Figure 120 The “PF Point #4” sheet of the “Resource Allocation.xlsx” file.....	163
Figure 121 The “PF Point #5” sheet of the “Resource Allocation.xlsx” file.....	163
Figure 122 The PFs generated for each budget availability scenario (the first 6 countermeasures are available for upgrading).	172
Figure 123 The PFs generated for each budget availability scenario (all 11 countermeasures are available for upgrading).	173
Figure 124 The average overall hazard severity over all the PF points for each budget availability scenario (the first 6 countermeasures are available for upgrading).	174
Figure 125 The average overall hazard severity over all the PF points for each budget availability scenario (all 11 countermeasures are available for upgrading).	174
Figure 126 The average overall traffic delay over all the PF points for each budget availability scenario (the first 6 countermeasures are available for upgrading).	175
Figure 127 The average overall traffic delay over all the PF points for each budget availability scenario (all 11 countermeasures are available for upgrading).	175
Figure 128 The average total number of highway-rail grade crossings selected for upgrading over all the PF points for each budget availability scenario (the first 6 countermeasures are available for upgrading).	176
Figure 129 The average total number of highway-rail grade crossings selected for upgrading over all the PF points for each budget availability scenario (all 11 countermeasures are available for upgrading).	177

Figure 130 The average installation cost of countermeasures implemented at highway-rail grade crossings selected for upgrading over all the PF points for each budget availability scenario (the first 6 countermeasures are available for upgrading).....	178
Figure 131 The average effectiveness of countermeasures implemented at highway-rail grade crossings selected for upgrading over all the PF points for each budget availability scenario (the first 6 countermeasures are available for upgrading).....	178
Figure 132 The average installation cost of countermeasures implemented at highway-rail grade crossings selected for upgrading over all the PF points for each budget availability scenario (all 11 countermeasures are available for upgrading).	179
Figure 133 The average effectiveness of countermeasures implemented at highway-rail grade crossings selected for upgrading over all the PF points for each budget availability scenario (all 11 countermeasures are available for upgrading).	180
Figure 134 The PFs generated for each countermeasure availability scenario.....	181
Figure 135 The average overall hazard severity over all the PF points for each countermeasure availability scenario.	182
Figure 136 The average overall traffic delay over all the PF points for each countermeasure availability scenario.	182
Figure 137 The average total number of highway-rail grade crossings selected for upgrading over all the PF points for each countermeasure availability scenario.....	183
Figure 138 The average installation cost of countermeasures implemented at highway-rail grade crossings selected for upgrading over all the PF points for each countermeasure availability scenario.	184
Figure 139 The average effectiveness of countermeasures implemented at highway-rail grade crossings selected for upgrading over all the PF points for each countermeasure availability scenario.	184
Figure 140 The PFs generated for each hazard severity weight scenario (the first 6 countermeasures are available for upgrading).	187
Figure 141 The PFs generated for each hazard severity weight scenario (all 11 countermeasures are available for upgrading).	188
Figure 142 The average overall hazard severity over all the PF points for each hazard severity weight scenario (the first 6 countermeasures are available for upgrading).	189
Figure 143 The average overall hazard severity over all the PF points for each hazard severity weight scenario (all 11 countermeasures are available for upgrading).....	189
Figure 144 The average overall traffic delay over all the PF points for each hazard severity weight scenario (the first 6 countermeasures are available for upgrading).	190
Figure 145 The average overall traffic delay over all the PF points for each hazard severity weight scenario (all 11 countermeasures are available for upgrading).....	190
Figure 146 The average total number of highway-rail grade crossings selected for upgrading over all the PF points for each hazard severity weight scenario (the first 6 countermeasures are available for upgrading).....	191

Figure 147 The average total number of highway-rail grade crossings selected for upgrading over all the PF points for each hazard severity weight scenario (all 11 countermeasures are available for upgrading).	191
Figure 148 The average installation cost of countermeasures implemented at highway-rail grade crossings selected for upgrading over all the PF points for each hazard severity weight scenario (the first 6 countermeasures are available for upgrading).	193
Figure 149 The average effectiveness of countermeasures implemented at highway-rail grade crossings selected for upgrading over all the PF points for each hazard severity weight scenario (the first 6 countermeasures are available for upgrading).	193
Figure 150 The average installation cost of countermeasures implemented at highway-rail grade crossings selected for upgrading over all the PF points for each hazard severity weight scenario (all 11 countermeasures are available for upgrading).	194
Figure 151 The average effectiveness of countermeasures implemented at highway-rail grade crossings selected for upgrading over all the PF points for each hazard severity weight scenario (all 11 countermeasures are available for upgrading).	194
Figure 152 The PFs generated for each crossing type scenario (the first 6 countermeasures are available for upgrading).	196
Figure 153 The PFs generated for each crossing type scenario (all 11 countermeasures are available for upgrading).	196
Figure 154 The average overall hazard severity over all the PF points for each crossing type scenario (the first 6 countermeasures are available for upgrading).	197
Figure 155 The average overall hazard severity over all the PF points for each crossing type scenario (all 11 countermeasures are available for upgrading).	197
Figure 156 The average overall traffic delay over all the PF points for each crossing type scenario (the first 6 countermeasures are available for upgrading).	198
Figure 157 The average overall traffic delay over all the PF points for each crossing type scenario (all 11 countermeasures are available for upgrading).	198
Figure 158 The average total number of highway-rail grade crossings selected for upgrading over all the PF points for each crossing type scenario (the first 6 countermeasures are available for upgrading).	199
Figure 159 The average total number of highway-rail grade crossings selected for upgrading over all the PF points for each crossing type scenario (all 11 countermeasures are available for upgrading).	200
Figure 160 The average installation cost of countermeasures implemented at highway-rail grade crossings selected for upgrading over all the PF points for each crossing type scenario (the first 6 countermeasures are available for upgrading).	201
Figure 161 The average effectiveness of countermeasures implemented at highway-rail grade crossings selected for upgrading over all the PF points for each crossing type scenario (the first 6 countermeasures are available for upgrading).	201

Figure 162 The average installation cost of countermeasures implemented at highway-rail grade crossings selected for upgrading over all the PF points for each crossing type scenario (all 11 countermeasures are available for upgrading).	202
Figure 163 The average effectiveness of countermeasures implemented at highway-rail grade crossings selected for upgrading over all the PF points for each crossing type scenario (all 11 countermeasures are available for upgrading).	203
Figure 164 Examples of LED signs near highway-rail grade crossings.	204
Figure 165 The PFs generated for each budget availability scenario (all 11 countermeasures are available for upgrading).	205
Figure 166 The PFs generated for each budget availability scenario (all 11 countermeasures and LED signs are available for upgrading).	206
Figure 167 The average overall hazard severity over all the PF points for each budget availability scenario (all 11 countermeasures are available for upgrading).	207
Figure 168 The average overall hazard severity over all the PF points for each budget availability scenario (all 11 countermeasures and LED signs are available for upgrading).	207
Figure 169 The average overall traffic delay over all the PF points for each budget availability scenario (all 11 countermeasures are available for upgrading).	208
Figure 170 The average overall traffic delay over all the PF points for each budget availability scenario (all 11 countermeasures and LED signs are available for upgrading).	208
Figure 171 The average total number of highway-rail grade crossings selected for upgrading over all the PF points for each budget availability scenario (all 11 countermeasures are available for upgrading).	209
Figure 172 The average total number of highway-rail grade crossings selected for upgrading over all the PF points for each budget availability scenario (all 11 countermeasures and LED signs are available for upgrading).	210
Figure 173 The average installation cost of countermeasures implemented at highway-rail grade crossings selected for upgrading over all the PF points for each budget availability scenario (all 11 countermeasures are available for upgrading).	211
Figure 174 The average installation cost of countermeasures implemented at highway-rail grade crossings selected for upgrading over all the PF points for each budget availability scenario (all 11 countermeasures and LED signs are available for upgrading).	211
Figure 175 The average effectiveness of countermeasures implemented at highway-rail grade crossings selected for upgrading over all the PF points for each budget availability scenario (all 11 countermeasures are available for upgrading).	212
Figure 176 The average effectiveness of countermeasures implemented at highway-rail grade crossings selected for upgrading over all the PF points for each budget availability scenario (all 11 countermeasures and LED signs are available for upgrading).	213

LIST OF TABLES

Table 1 Rail employment impact in Florida by industry.	3
Table 2 Distribution of Florida’s highway-rail grade crossings by warning device type.	6
Table 3 Distribution of Florida’s highway-rail grade crossings by crossing surface.	11
Table 4 Distribution of Florida’s highway-rail grade crossings that experienced accidents between 2015 and 2019 by warning device type.	15
Table 5 Distribution of Florida’s highway-rail grade crossings that experienced accidents between 2015 and 2019 by crossing surface.	20
Table 6 Features of various pavement markings.	36
Table 7 Features of regulatory and warning signs.	38
Table 8 Features of train warning signs.	45
Table 9 Features of crossing gate technologies.	48
Table 10 Features of detection technologies.	52
Table 11 Features of train detection devices.	56
Table 12 Features of ITS-based technologies.	64
Table 13 Features of other types of warning devices and advanced technology at highway-rail grade crossings.	69
Table 14 Detection methods used for vehicles approaching highway-rail grade crossings.	74
Table 15 Methods for quantifying traffic delays at highway-rail grade crossings.	85
Table 16 Advantages and disadvantages of traffic delay estimation methods.	88
Table 17 Key information for the default countermeasures considered.	110
Table 18 Feasibility of countermeasure implementation for the protection classes considered.	110
Table 19 The current delay time based on the existing protection.	112
Table 20 The additional delay time that is incurred on average at highway-rail grade crossings after implementation of different countermeasures.	112
Table 21 The average best overall hazard severity values returned by ECON for the generated scenarios.	115
Table 22 The average best overall hazard severity values returned by MPSDR for the generated scenarios.	115
Table 23 The average best overall hazard severity values returned by MESDR for the generated scenarios.	116
Table 24 The average best overall traffic delay values returned by ECON for the generated scenarios.	116
Table 25 The average best overall traffic delay values returned by MPSDR for the generated scenarios.	117
Table 26 The average best overall traffic delay values returned by MESDR for the generated scenarios.	117
Table 27 The average best overall hazard severity and traffic delay values returned by the candidate solution algorithms for the developed problem instances.	118
Table 28 The average computational time incurred by ECON for the generated scenarios.	122

Table 29	The average computational time incurred by MPSDR for the generated scenarios....	122
Table 30	The average computational time incurred by MESDR for the generated scenarios....	123
Table 31	The average and maximum computational times incurred by the candidate solution algorithms for the developed problem instances.	124
Table 32	Examples for inserting the index of highway-rail grade crossings.....	158
Table 33	Developed scenarios for hazard severity weight values.	185

1. INTRODUCTION

Some background information for this project is provided in this section of the report which includes (1) freight mobility in Florida; (2) role of rail transportation in Florida; (3) highway-rail grade crossings; (4) continuity of passenger and freight flows at highway-rail grade crossings; and (5) objectives of this project. The structure of the report will be also outlined in this section.

1.1. Freight Mobility in Florida

The standard of living in the United States (U.S.) has been improving over time. The Federal Highway Administration (FHWA) has reported that the average person in the U.S. generates and consumes 63 tons of freight per year (FDOT, 2020). As Florida is the third most populous state in the U.S., a substantial amount of freight is transported in Florida. Furthermore, residents from other states are now migrating to Florida, which is increasing the population in Florida at a greater rate as compared to other states of the U.S. This greater population growth rate is expected to further increase the amount of freight in Florida. Moreover, according to the U.S. Bureau of Economic Analysis, the Gross Domestic Product (GDP) of Florida has crossed the \$1 trillion mark, placing Florida as the 17th largest economy in the world (BEA, 2020; FDOT, 2020). Such a growing economy is significantly influenced by industries related to freight (e.g., manufacturing, trade, logistics, and construction). For instance, Florida has experienced an 80% increase in retail trade and a 40% increase in wholesale trade from the years of 2009 to 2019 (FDOT, 2020). When there is such a tremendous increase in trade, an increase in freight is also expected to occur.

A high volume of freight is handled every year in Florida. In the year 2017, 595.9 million tons of commodities were moved within Florida, while the amounts of freight imports and exports were 134.6 million tons and 55.8 million tons, respectively. According to the Florida Department of Transportation (FDOT), 68.1% of freight tonnage is exported by trucks in Florida, and 15.8% of freight tonnage is exported by rail (FDOT, 2020). This high volume of freight tonnage is expected to increase even further. For instance, the total freight tonnage in the U.S. (including domestic, imports, and exports) is expected to increase from 17.0 billion tons in 2012 to 25.3 billion tons in 2045 based on the baseline forecast scenario (FHWA, 2016). A sound infrastructure system is required to ensure a smooth mobility of such a high volume of freight.

1.2. Role of Rail Transportation in Florida

The rail system of Florida comprises 3,843 railroad miles, where mainlines (not including connectors, sidings, spurs, storages, and yard miles) comprises 2,742 miles (FDOT, 2018). The railroads in Florida are owned by several entities, and CSX Transportation owns around 53.5% of the railroads in Florida. Figure 1 presents a distribution of rail mileage in Florida, which demonstrates that after CSX Transportation, Short Lines is the second largest owner of the railroads in Florida with 819 miles of railroad, followed by Florida East Coast Railway with 561 miles of railroad (FDOT, 2018).

Rail transportation significantly affects the economy of Florida. If the freight user-impact activities and multiplier effects are considered, freight rail transportation-related employment in Florida would be 738,840 jobs (or 7.0% of the total 10.6 million jobs in Florida), with 4,990 direct employees (FDOT, 2018). Such an involvement resulted in an annual income of \$34.2

billion earned by these employees, which would cover 7.0% of the total statewide labor income in Florida. In addition, freight rail services and users created a combined value-added impact of \$57.9 billion, which comprised 7.3% of the Gross State Product of Florida. Other incomes were also associated with freight rail transportation in Florida, and its total economic output was \$121.0 billion, thus providing \$5.7 billion to the government in taxes (FDOT, 2018). Considering passenger rail user-impact activities and multiplier effects, passenger rail transportation created 9,420 jobs in Florida, with 970 direct employees (FDOT, 2018). Such an involvement resulted in an annual income of \$379.8 million earned by these employees. In addition, passenger rail services and users created a combined value-added impact of \$589.3 million (FDOT, 2018).

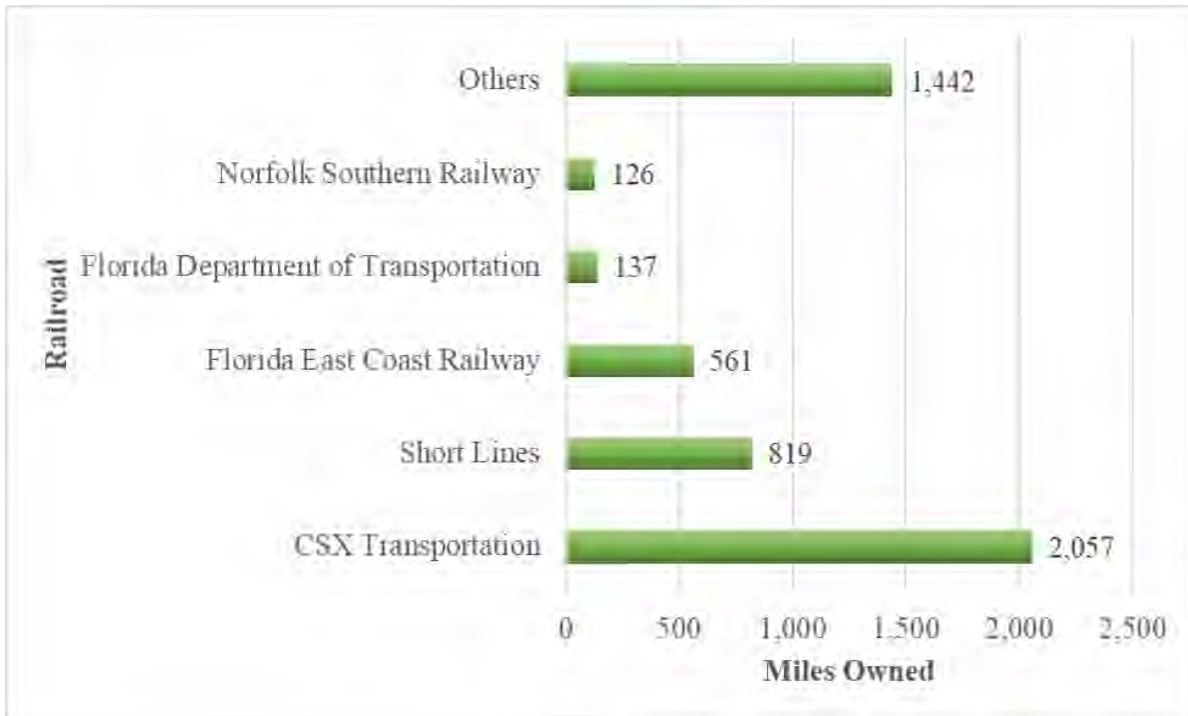


Figure 1 Rail mileage in Florida.

Notes: Others include switching, terminal, private operations, and the U.S. government

Rail transportation in Florida impacts a diverse array of industries. Table 1 highlights a distribution of rail employment impact in Florida by industry, which reveals that retail trade was the most impacted industry in Florida with 125,460 jobs (FDOT, 2018). The other industries, which are significantly impacted by rail transportation in Florida, are manufacturing (78,610 jobs), accommodation and food services (74,840 jobs), health and social services (69,220 jobs), and administrative and waste services (59,360 jobs).

Table 1 Rail employment impact in Florida by industry.

Industry	Jobs	Industry	Jobs
Retail Trade	125,460	Construction	29,130
Manufacturing	78,610	Wholesale Trade	25,990
Accommodation and Food Services	74,840	Agriculture, Forestry, Fish, and Hunting	24,040
Health and Social Services	69,220	Arts - Entertainment and Recreation	16,970
Administrative and Waste Services	59,360	Management of Companies	11,580
Other Services	42,930	Information	10,450
Professional - Scientific and Technological Services	40,960	Educational Services	9,990
Retail Estate and Rental	35,980	Government and Non NAICS	7,420
Transportation and Warehousing	34,740	Mining	3,870
Finance and Insurance	34,330	Utilities	2,980

1.3. Highway-Rail Grade Crossings

The primary focus of this project is the highway-rail grade crossings in Florida. The Federal Railroad Administration (FRA) crossing inventory database (FRA, 2020a), which was accessed in May 2020, indicated that Florida accommodated 9,607 crossings. According to the FRA crossing inventory database, there were 2,901 private crossings and 6,614 public crossings in Florida. The ownership information about the remaining 92 crossings was not specified in the FRA crossing inventory database. The locations of the private and public crossings in Florida are depicted in Figure 2. Note that the longitudes and latitudes of 2,735 crossings in Florida were not clearly provided in the FRA crossing inventory database. Therefore, those crossings are not depicted in Figure 2.

A distribution of Florida's crossings by crossing position is shown in Figure 3, which reveals that a substantial portion of Florida's crossings (a total of 9,607 crossings) were highway-rail grade crossings (i.e., at grade). In addition to the 9,090 highway-rail grade crossings in Florida, there were 447 underpasses (i.e., railroad under) and 70 overpasses (railroad over). Locations of these crossings are illustrated in Figure 4. As mentioned earlier, the longitudes and latitudes of 2,735 crossings in Florida were not specified in the FRA crossing inventory database. Therefore, those crossings are not depicted in Figure 4.



Figure 2 Locations of the private and public crossings in Florida.

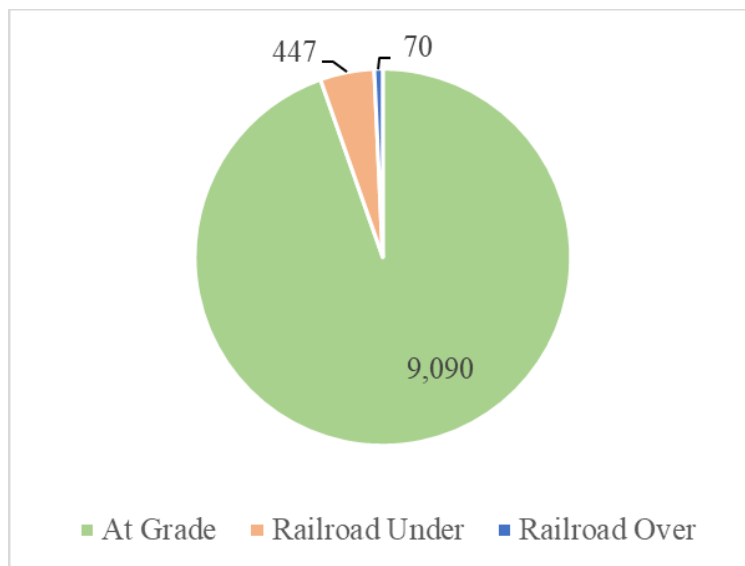


Figure 3 Distribution of Florida's crossings by crossing position.



Figure 4 Locations of different types of crossings in Florida.

1.3.1. Features of the Highway-Rail Grade Crossings in Florida

The FRA crossing inventory database (FRA, 2020a), which was accessed in May 2020, was used to report different features of the highway-rail grade crossings in Florida. A distribution of Florida’s highway-rail grade crossings by ownership type is presented in Figure 5. The FRA crossing inventory database revealed that among the 9,090 highway-rail grade crossings in Florida, 2,896 highway-rail grade crossings (or 31.9% of highway-rail grade crossings) were privately owned. The majority of the highway-rail grade crossings in Florida, however, were public highway-rail grade crossings, since 6,109 highway-rail grade crossings (or 67.2% of highway-rail grade crossings) were categorized as public. Moreover, the ownership information about 85 highway-rail grade crossings in Florida was not specified in the FRA crossing inventory database.

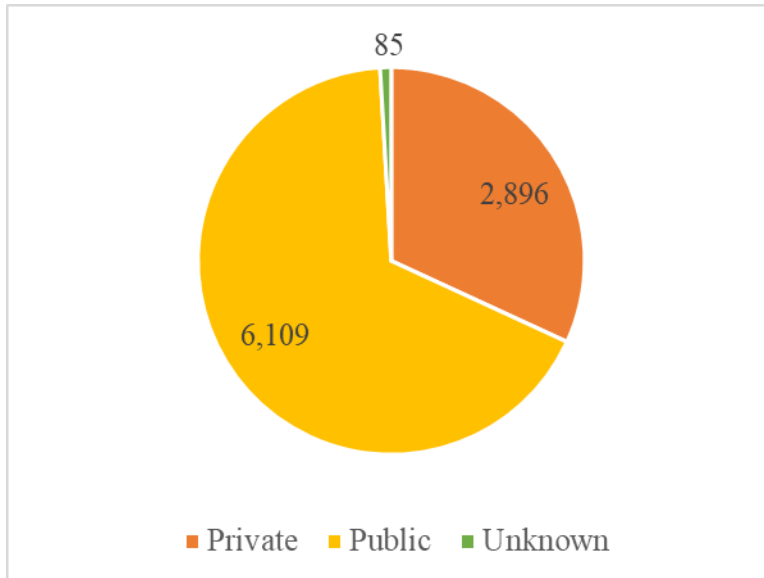


Figure 5 Distribution of Florida's highway-rail grade crossings by ownership type.

Table 2 presents a distribution of Florida's highway-rail grade crossings by warning device type. It was revealed that a total of 3,850 highway-rail grade crossings in Florida (or 42.4% of highway-rail grade crossings) was equipped with active warning devices (e.g., gates, flashing lights, highway traffic signals, wigwags, bells, or other active warning devices). On the other hand, a total of 2,161 highway-rail grade crossings in Florida (or 23.8% of highway-rail grade crossings) was equipped with passive warning devices (e.g., stop signs, crossbucks, or other signs or signals). No signs or signals were installed at 674 highway-rail grade crossings (or 7.4% of highway-rail grade crossings). Note that warning devices for 2,405 highway-rail grade crossings (or 26.5% of highway-rail grade crossings) were not specified in the FRA crossing inventory database. The term "unknown" will be used in this report when a given attribute of a highway-rail grade crossing is not specified in the FRA crossing inventory database by the reporting agency. The same issue can be applicable to other databases as well (e.g., the rail-highway crossing inventory [RHCI] database). The "unknown" crossing attributes could potentially fall under any or none of the listed categories.

Table 2 Distribution of Florida's highway-rail grade crossings by warning device type.

Warning Device Type	Number of Highway-Rail Grade Crossings
No Signs or Signals	674
Other Signs or Signals	8
Crossbucks	1,824
Stop Signs	329
Special Active Warning Devices	104
Highway Traffic Signals, Wigwags, Bells, or Other Activated	53
Flashing Lights	642
All Other Gates	2,952
Four Quad (Full Barrier Gates)	99
Unknown	2,405

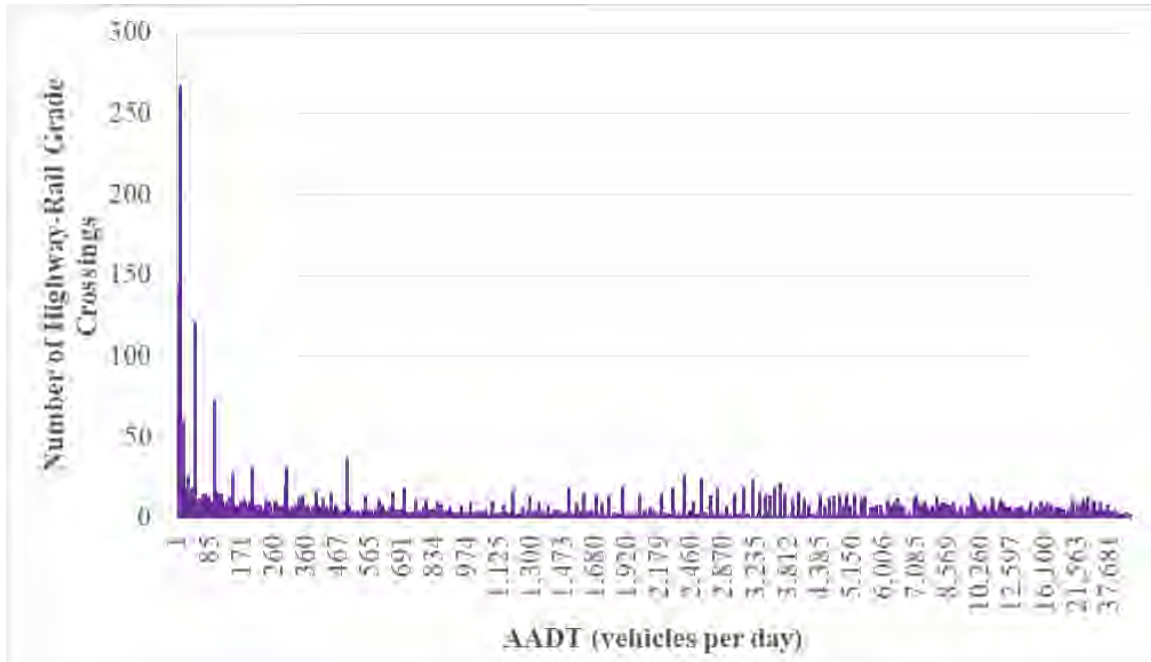


Figure 6 Distribution of Florida’s highway-rail grade crossings by AADT.

A distribution of Florida’s highway-rail grade crossings by Annual Average Daily Traffic (AADT) is presented in Figure 6. The FRA crossing inventory database revealed that 6,581 highway-rail grade crossings (or 72.4% of highway-rail grade crossings) in Florida had a positive AADT. Among the highway-rail grade crossings in Florida, the maximum AADT was 94,000 vehicles per day. AADT was zero (i.e., less than one vehicle per day) for a total of 84 highway-rail grade crossings (or 0.9% of highway-rail grade crossings). Note that AADT was not specified for 2,425 highway-rail grade crossings (or 26.7% of highway-rail grade crossings) in the FRA crossing inventory database. A distribution of Florida’s highway-rail grade crossings by total number of trains per day (i.e., sum of the day thru trains and the night thru trains) is presented in Figure 7. According to the FRA crossing inventory database, only 43.6% of the highway-rail grade crossings in Florida (or 3,966 highway-rail grade crossings) had a positive number of trains per day. The maximum number of trains per day at the highway-rail grade crossings in Florida was 159. The FRA crossing inventory database also indicated that 56.3% of the highway-rail grade crossings in Florida (or 5,118 highway-rail grade crossings) accommodated zero trains per day (i.e., less than one train per day). Furthermore, the train count was not specified for 6 highway-rail grade crossings in the FRA crossing inventory database.

A distribution of Florida’s highway-rail grade crossings by maximum timetable speed is shown in Figure 8, which reveals that the maximum and minimum values of the maximum timetable speed at the highway-rail grade crossings in Florida were 79 mph and 1 mph, respectively. For a significant portion of the highway-rail grade crossings in Florida (1,977 highway-rail grade crossings or 21.7% of highway-rail grade crossings), the maximum timetable speed was 10 mph. Furthermore, the maximum timetable speed was 25 mph and 40 mph at 859 highway-rail grade crossings (or 9.4% of highway-rail grade crossings) and 698 highway-rail grade crossings (or 7.7% of highway-rail grade crossings), respectively. Note that the FRA crossing inventory

database specified no maximum timetable speed for 1,469 highway-rail grade crossings (or 16.2% of highway-rail grade crossings) in Florida.

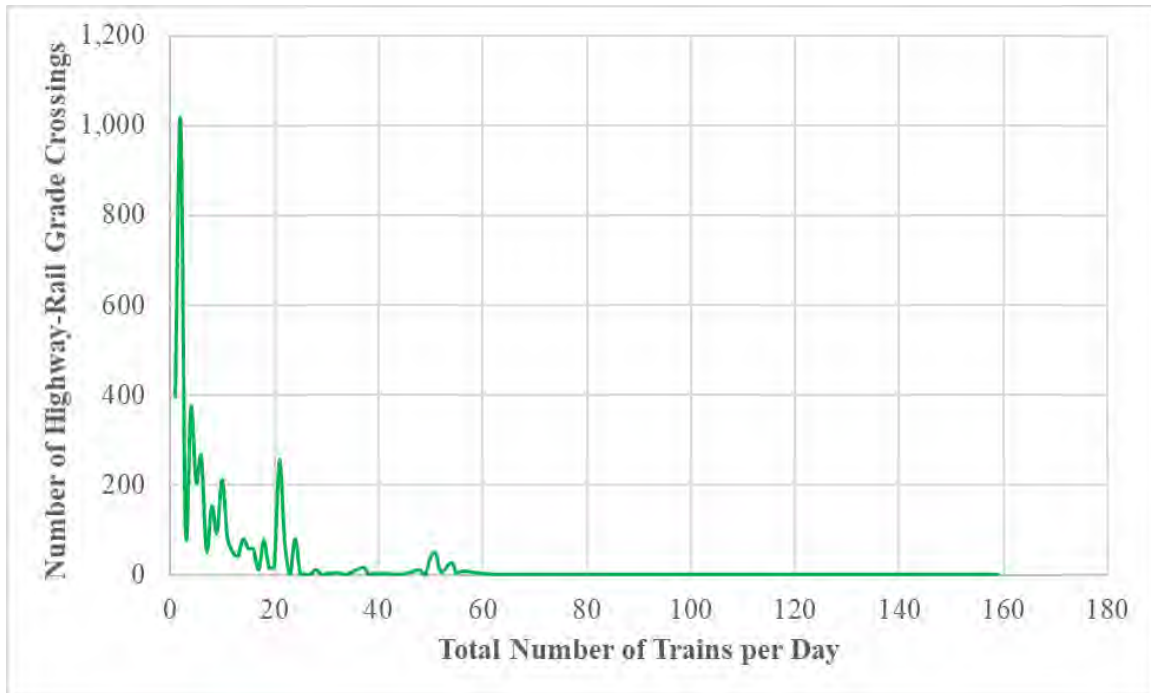


Figure 7 Distribution of Florida’s highway-rail grade crossings by total number of trains per day.

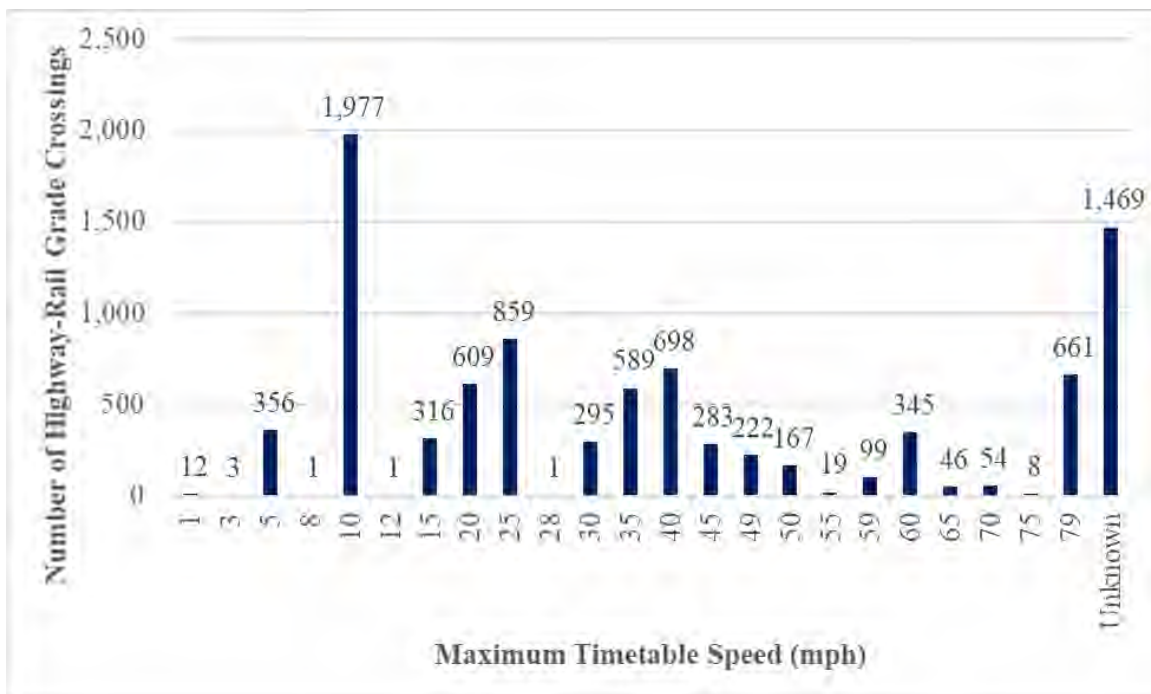


Figure 8 Distribution of Florida’s highway-rail grade crossings by maximum timetable speed.

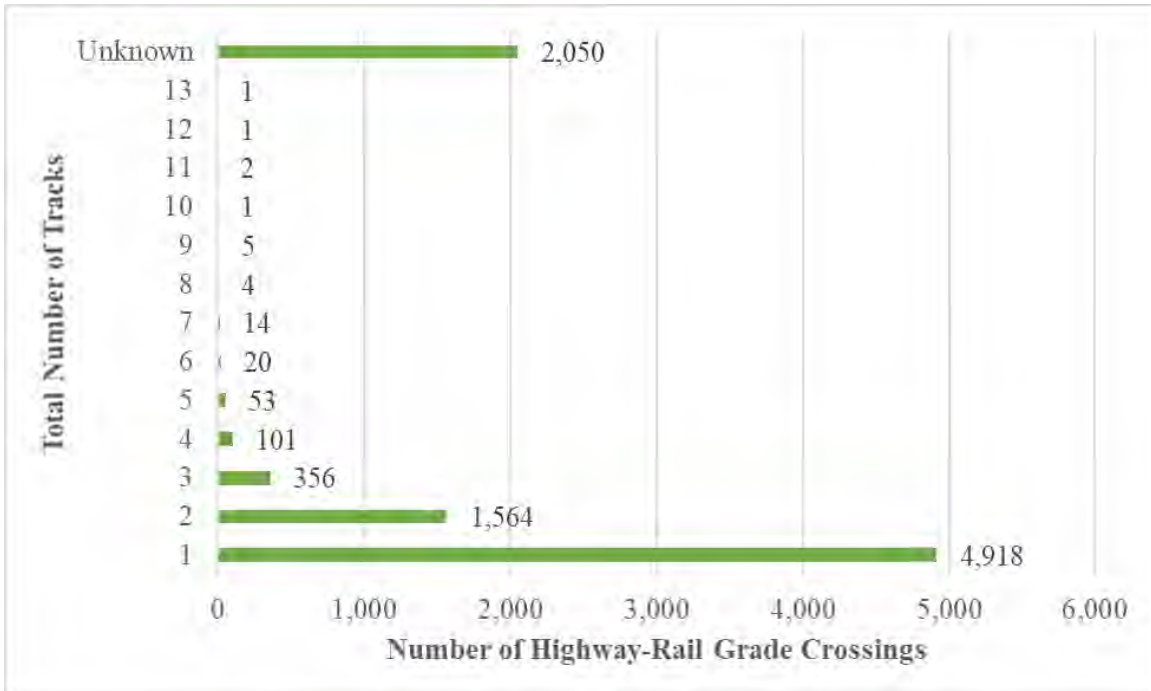


Figure 9 Distribution of Florida’s highway-rail grade crossings by total number of tracks.

Figure 9 presents a distribution of Florida’s highway-rail grade crossings by total number of tracks (i.e., sum of the main tracks and the other tracks). Among the highway-rail grade crossings in Florida, the minimum number of tracks was 1, and the maximum number of tracks was 13. According to the FRA crossing inventory database, the majority of the highway-rail grade crossings in Florida (4,918 highway-rail grade crossings or 54.1% of highway-rail grade crossings) had a single track. Furthermore, 1,564 highway-rail grade crossings (or 17.2% of highway-rail grade crossings) had 2 tracks, while 356 highway-rail grade crossings (or 3.9% of highway-rail grade crossings) had 3 tracks. A total of 202 highway-rail grade crossings (or 2.2% of highway-rail grade crossings) had 4 or more tracks. The number of tracks was not specified for 2,050 highway-rail grade crossings (or 22.6% of highway-rail grade crossings).

Figure 10 presents a distribution of Florida’s highway-rail grade crossings by roadway type. According to the FRA crossing inventory database, 5,639 highway-rail grade crossings in Florida (or 62.0% of highway-rail grade crossings) were paved, while 807 highway-rail grade crossings (or 8.9% of highway-rail grade crossings) were unpaved. The roadway type was not specified for 2,644 highway-rail grade crossings (or 29.1% of highway-rail grade crossings). A distribution of Florida’s highway-rail grade crossings by illumination type is shown in Figure 11. According to the FRA crossing inventory database, 1,682 highway-rail grade crossings in Florida (or 18.5% of highway-rail grade crossings) were illuminated, and 2,505 highway-rail grade crossings (or 27.6% of highway-rail grade crossings) were unilluminated. The illumination type was not specified for 4,903 highway-rail grade crossings (or 53.9% of highway-rail grade crossings).

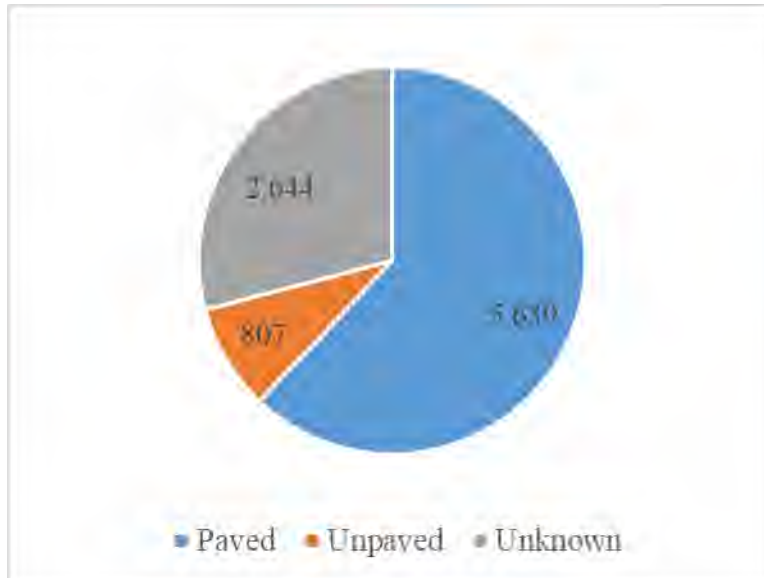


Figure 10 Distribution of Florida's highway-rail grade crossings by roadway type.

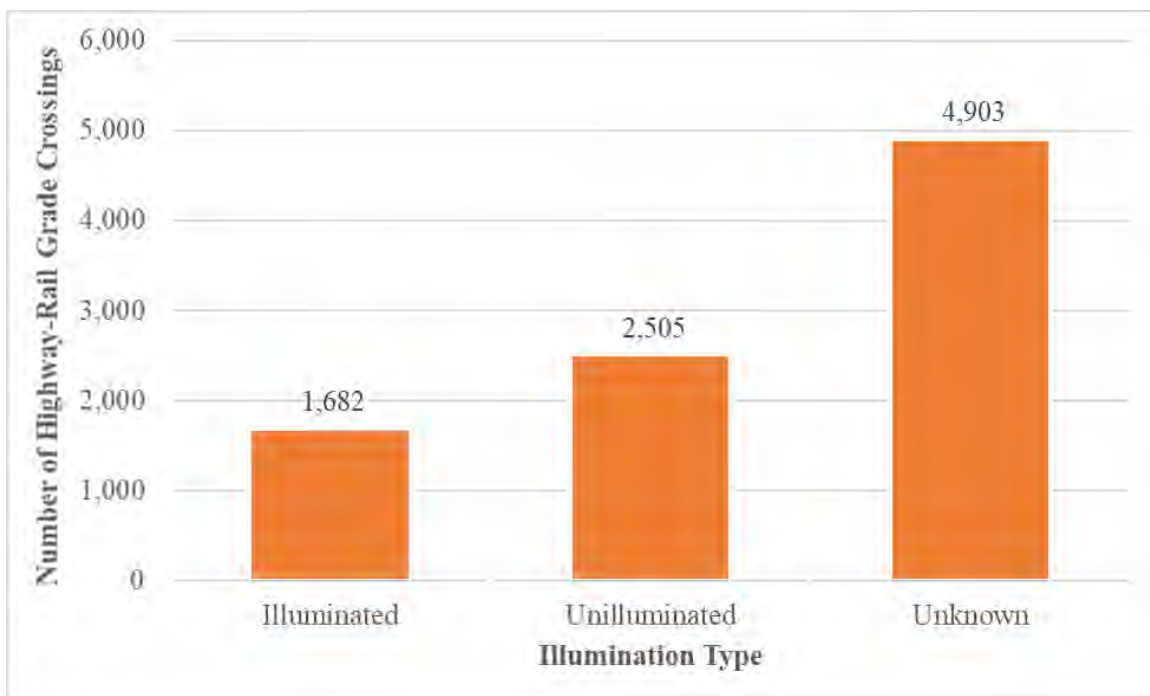


Figure 11 Distribution of Florida's highway-rail grade crossings by illumination type.

Table 3 presents a distribution of Florida's highway-rail grade crossings by crossing surface, where it can be observed that a significant portion of the highway-rail grade crossings in Florida had asphalt surfaces (2,690 highway-rail grade crossings or 29.6% of highway-rail grade crossings). A total of 1,627 highway-rail grade crossings (or 17.9% of highway-rail grade crossings) had surfaces made of asphalt and timber, while 1,398 highway-rail grade crossings (or 15.4% of highway-rail grade crossings) had concrete surfaces. Furthermore, a total of 351 highway-rail grade crossings (or 3.9% of highway-rail grade crossings) had unconsolidated surfaces, and 283 highway-rail grade crossings (or 3.1% of highway-rail grade crossings) had

surfaces made of timber. Other surface materials (e.g., rubber, metal) and combinations of surface materials (e.g., concrete and rubber; asphalt and concrete; asphalt, timber, and concrete; asphalt and rubber; asphalt and metal; asphalt, concrete, and rubber; timber and concrete) were found at 258 highway-rail grade crossings (or 2.8% of highway-rail grade crossings). The surface material information was not specified for 2,483 highway-rail grade crossings (or 27.3% of highway-rail grade crossings).

Table 3 Distribution of Florida’s highway-rail grade crossings by crossing surface.

Crossing Surface	Number of Highway-Rail Grade Crossings
Asphalt	2,690
Asphalt and Timber	1,627
Concrete	1,398
Unconsolidated	351
Timber	283
Rubber	163
Concrete and Rubber	18
Asphalt and Concrete	17
Asphalt, Timber, and Concrete	8
Asphalt and Rubber	6
Metal	3
Asphalt and Metal	1
Asphalt, Concrete, and Rubber	1
Timber and Concrete	1
Other	40
Unknown	2,483

A distribution of Florida’s highway-rail grade crossings by number of traffic lanes crossing railroad is shown in Figure 12. According to the FRA crossing inventory database, the highway-rail grade crossings in Florida were intersected by up to 9 traffic lanes. A total of 401 highway-rail grade crossings (or 4.4% of highway-rail grade crossings) was intersected by single traffic lanes, 5,079 highway-rail grade crossings (or 55.9% of highway-rail grade crossings) were crossed by 2 traffic lanes, and 194 highway-rail grade crossings (or 2.1% of highway-rail grade crossings) were intersected by 3 traffic lanes. Moreover, 507 highway-rail grade crossings (or 5.6% of highway-rail grade crossings) were intersected by 4 traffic lanes, 143 highway-rail grade crossings (or 1.6% of highway-rail grade crossings) were crossed by 5 traffic lanes, while 105 highway-rail grade crossings (or 1.2% of highway-rail grade crossings) were intersected by 6 traffic lanes. A total of 49 highway-rail grade crossings (or 0.5% of highway-rail grade crossings) was crossed by 7-9 traffic lanes. Note that the number of intersecting lanes was not specified for 2,612 highway-rail grade crossings (or 28.7% of highway-rail grade crossings).

A distribution of Florida’s highway-rail grade crossings by functional classification of road at crossing is shown in Figure 13. According to the FRA crossing inventory database, 2,174 roads at the highway-rail grade crossings in Florida (or 23.9% of roads) were categorized as rural roads. Furthermore, a total of 4,159 roads at the highway-rail grade crossings (or 45.8% of roads) was categorized as urban roads. Note that the functional classification of roads at 2,757 highway-

rail grade crossings (or 30.3% of highway-rail grade crossings) was not specified in the FRA crossing inventory database.

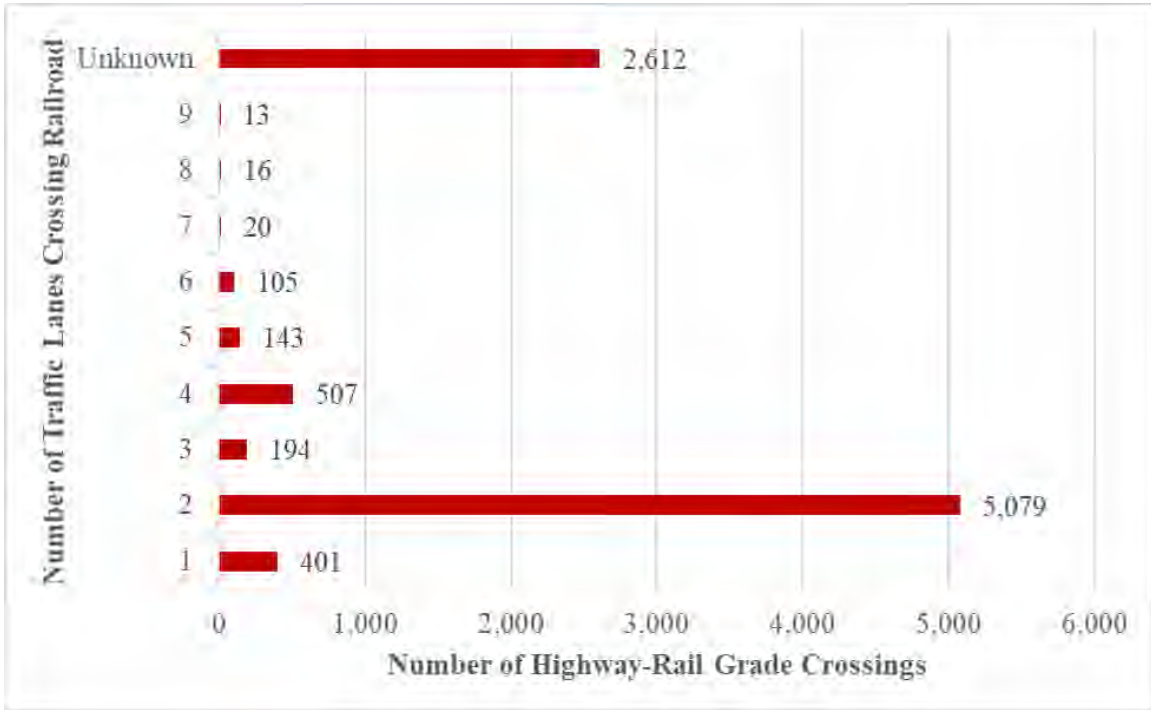


Figure 12 Distribution of Florida’s highway-rail grade crossings by number of traffic lanes crossing railroad.

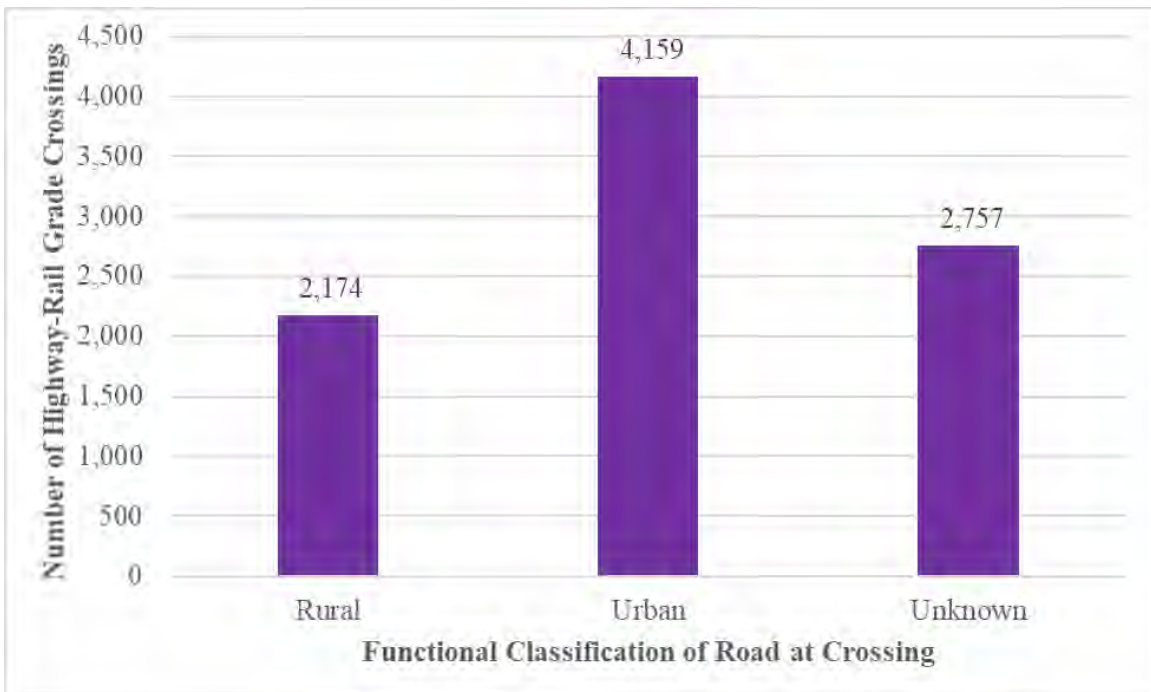


Figure 13 Distribution of Florida’s highway-rail grade crossings by functional classification of road at crossing.

1.3.2. Safety Issues at the Highway-Rail Grade Crossings in Florida

A highway-rail accident is defined as an impact between a highway user and a railroad user at a crossing site, which includes sidewalks, walkways, and so on (FDOT, 2010). Figure 14, which was created using the FRA highway-rail grade crossing accident database (FRA, 2020b), highlights the number of highway-rail grade crossing accidents/incidents, injuries, and fatalities in Florida between 2009 and 2019. Figure 14 reveals that a total of 889 highway-rail grade crossing accidents took place in Florida between 2009 and 2019, with an average of 80.82 accidents per year. Furthermore, these 889 highway-rail grade crossing accidents resulted in a total of 454 injuries and 156 fatalities. It can be observed that there has been an increase in the number of highway-rail grade crossing accidents in Florida over the last few years. For instance, a total of 135 highway-rail grade crossing accidents occurred in the year 2019, as compared to 51 highway-rail grade crossing accidents in the year 2009. Hence, safety issues at the highway-rail grade crossings in Florida should be examined and mitigated. Note that the accident statistics presented in Figure 14 could change because of updates in the FRA highway-rail grade crossing accident database.

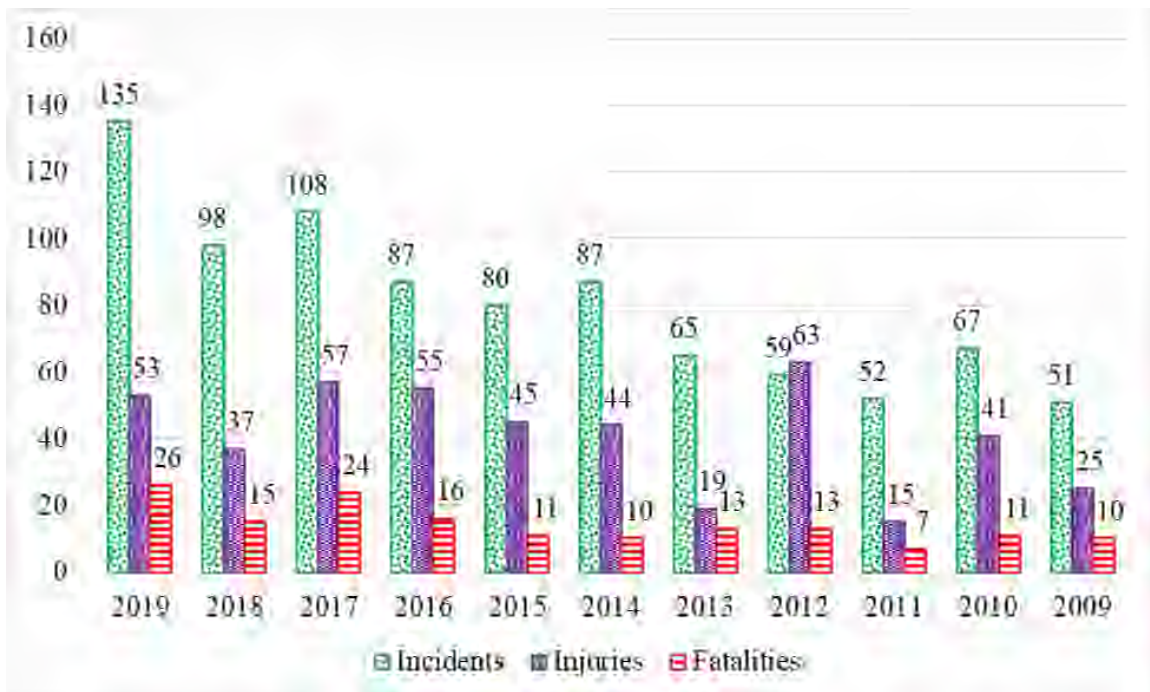


Figure 14 Highway-rail grade crossing accident statistics in Florida (2009 to 2019).

A statistical analysis was conducted to assess the features of the highway-rail grade crossings in Florida that experienced accidents within the last five years (i.e., the 2015-2019 time period). Such an analysis was carried out using the FRA crossing inventory database and the FRA highway-rail grade crossing accident database. It was found that a total of 377 highway-rail grade crossings in Florida experienced at least one accident within the 2015-2019 time period. The results from the statistical analysis are further highlighted. A distribution of Florida's highway-rail grade crossings that experienced accidents between 2015 and 2019 by ownership type is presented in Figure 15. The statistical analysis for ownership type revealed that among the 377 highway-rail grade crossings in Florida that experienced accidents within the 2015-2019 time period, 54 highway-rail grade crossings (or 14.3% of highway-rail grade crossings) were

privately owned. However, the majority of the highway-rail grade crossings in Florida that experienced accidents within the 2015-2019 time period were public highway-rail grade crossings, since 320 highway-rail grade crossings (or 84.9% of highway-rail grade crossings) were public. Moreover, the ownership information about 3 highway-rail grade crossings was not specified in the FRA crossing inventory database.

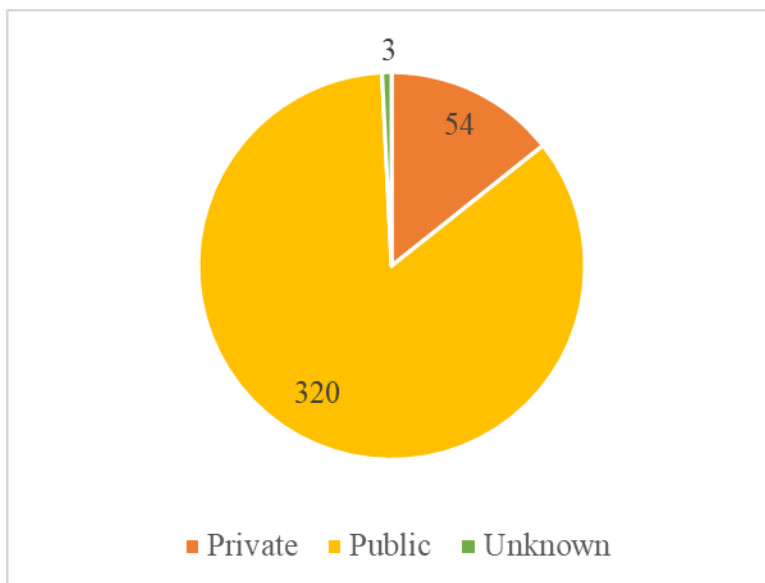


Figure 15 Distribution of Florida’s highway-rail grade crossings that experienced accidents between 2015 and 2019 by ownership type.

Table 4 presents a distribution of Florida’s highway-rail grade crossings that experienced accidents between 2015 and 2019 by warning device type. The statistical analysis for warning device type revealed that among the 377 highway-rail grade crossings in Florida that experienced accidents within the 2015-2019 time period, a total of 295 highway-rail grade crossings (or 78.2% of highway-rail grade crossings) was equipped with active warning devices (e.g., gates, flashing lights, highway traffic signals, wigwags, bells, or other active warning devices). On the other hand, a total of 26 highway-rail grade crossings (or 6.9% of highway-rail grade crossings) was equipped with passive warning devices (e.g., stop signs, crossbucks). No signs or signals were installed at 4 highway-rail grade crossings (or 1.1% of highway-rail grade crossings). Note that warning devices for 52 highway-rail grade crossings Florida (or 13.8% of highway-rail grade crossings) that experienced accidents within the 2015-2019 time period were not specified in the FRA crossing inventory database.

A distribution of Florida’s highway-rail grade crossings that experienced accidents between 2015 and 2019 by AADT is presented in Figure 16. The statistical analysis for AADT revealed that among the 377 highway-rail grade crossings in Florida that experienced accidents within the 2015-2019 time period, a total of 329 highway-rail grade crossings (or 87.3% of highway-rail grade crossings) had a positive AADT. Among these highway-rail grade crossings, the maximum AADT was found to be 63,000 vehicles per day. Furthermore, a zero AADT (i.e., less than one vehicle per day) was not specified in the FRA crossing inventory database for any of the highway-rail grade crossings in Florida that experienced accidents within the 2015-2019 time

period. Note that AADT was not specified for 48 highway-rail grade crossings (or 12.7% of highway-rail grade crossings) in the FRA crossing inventory database.

Table 4 Distribution of Florida’s highway-rail grade crossings that experienced accidents between 2015 and 2019 by warning device type.

Warning Device Type	Number of Highway-Rail Grade Crossings
No Signs or Signals	4
Crossbucks	23
Stop Signs	3
Highway Traffic Signals, Wigwags, Bells, or Other Activated	1
Flashing Lights	15
All Other Gates	241
Four Quad (Full Barrier Gates)	38
Unknown	52

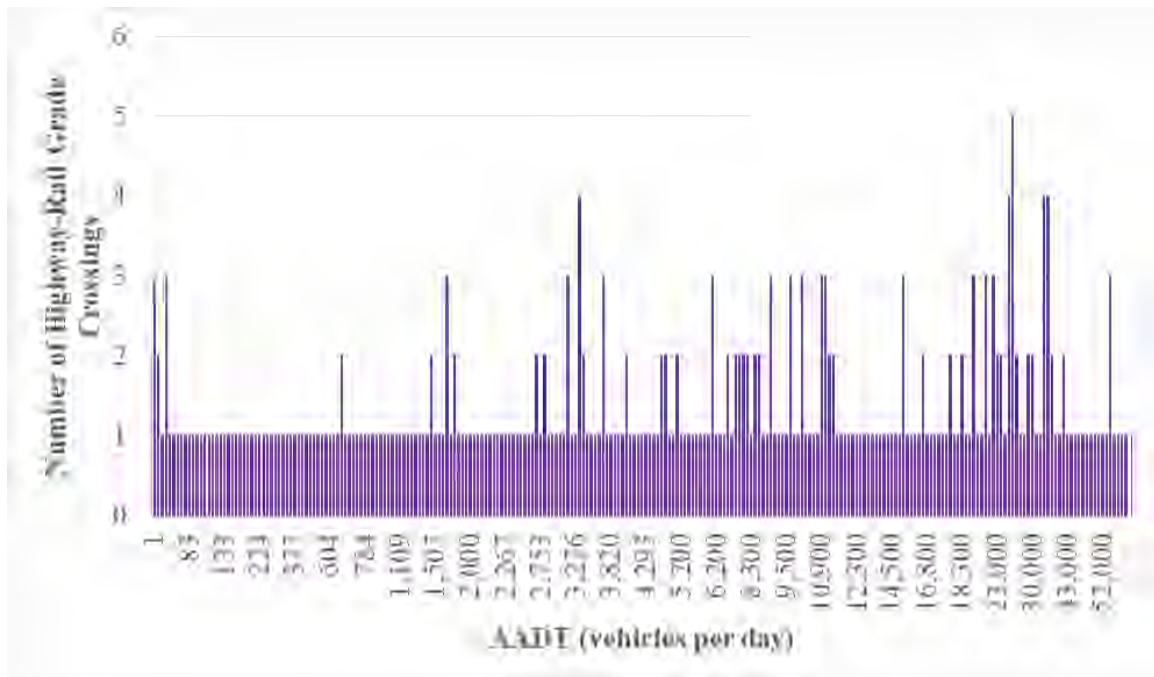


Figure 16 Distribution of Florida’s highway-rail grade crossings that experienced accidents between 2015 and 2019 by AADT.

A distribution of Florida’s highway-rail grade crossings that experienced accidents between 2015 and 2019 by total number of trains per day (i.e., sum of the day thru trains and the night thru trains) is presented in Figure 17. It was revealed that among the 377 highway-rail grade crossings in Florida that experienced accidents within the 2015-2019 time period, 301 highway-rail grade crossings (or 79.8% of highway-rail grade crossings) had a positive number of trains per day. The maximum number of trains per day at these highway-rail grade crossings was 56. Moreover, the train count was zero (i.e., less than one train per day) for 73 highway-rail grade crossings (or 19.4% of highway-rail grade crossings). Note that the train count was not specified in the FRA

crossing inventory database for 3 highway-rail grade crossings in Florida that experienced accidents within the 2015-2019 time period.

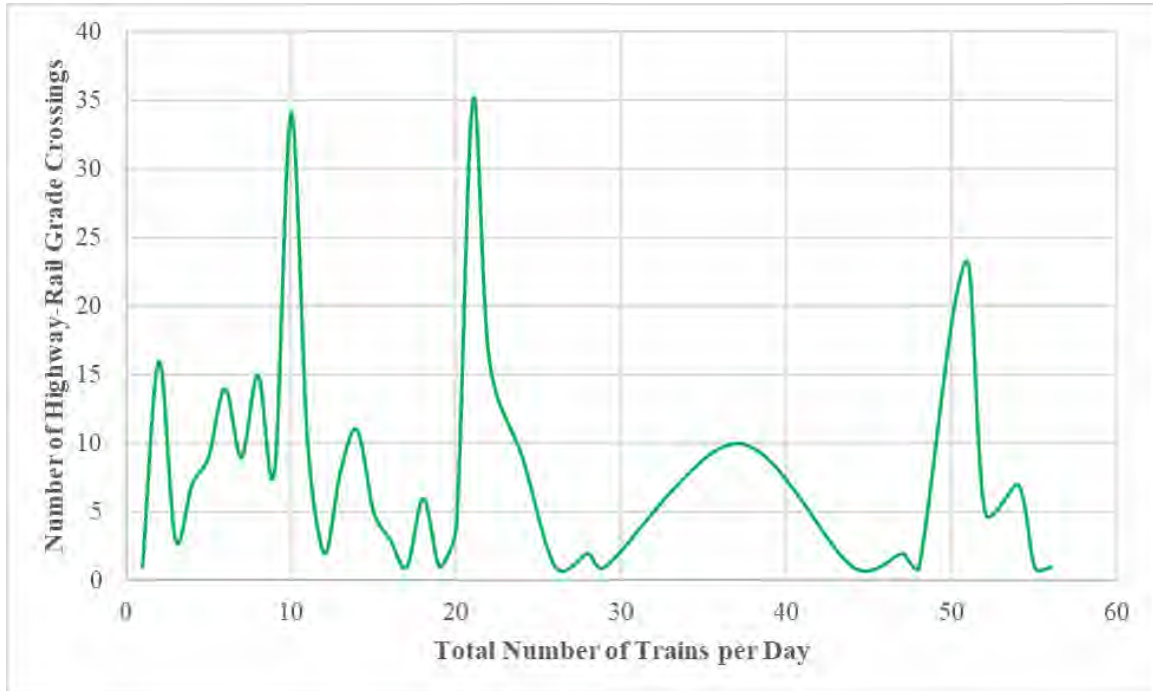


Figure 17 Distribution of Florida’s highway-rail grade crossings that experienced accidents between 2015 and 2019 by total number of trains per day.

A distribution of Florida’s highway-rail grade crossings that experienced accidents between 2015 and 2019 by maximum timetable speed is shown in Figure 18, which reveals that among the 377 highway-rail grade crossings in Florida that experienced accidents within the 2015-2019 time period, the maximum and minimum values of the maximum timetable speed were 79 mph and 10 mph, respectively. For a significant portion of the highway-rail grade crossings in Florida that experienced accidents within the 2015-2019 time period (114 highway-rail grade crossings or 30.2% of highway-rail grade crossings), the maximum timetable speed was 79 mph. Furthermore, the maximum timetable speed was 45 mph and 10 mph at 51 highway-rail grade crossings (or 13.5% of highway-rail grade crossings) and 42 highway-rail grade crossings (or 11.1% of highway-rail grade crossings), respectively. Note that the FRA crossing inventory database specified no maximum timetable speed for 9 highway-rail grade crossings (or 2.4% of highway-rail grade crossings) in Florida that experienced accidents within the 2015-2019 time period.

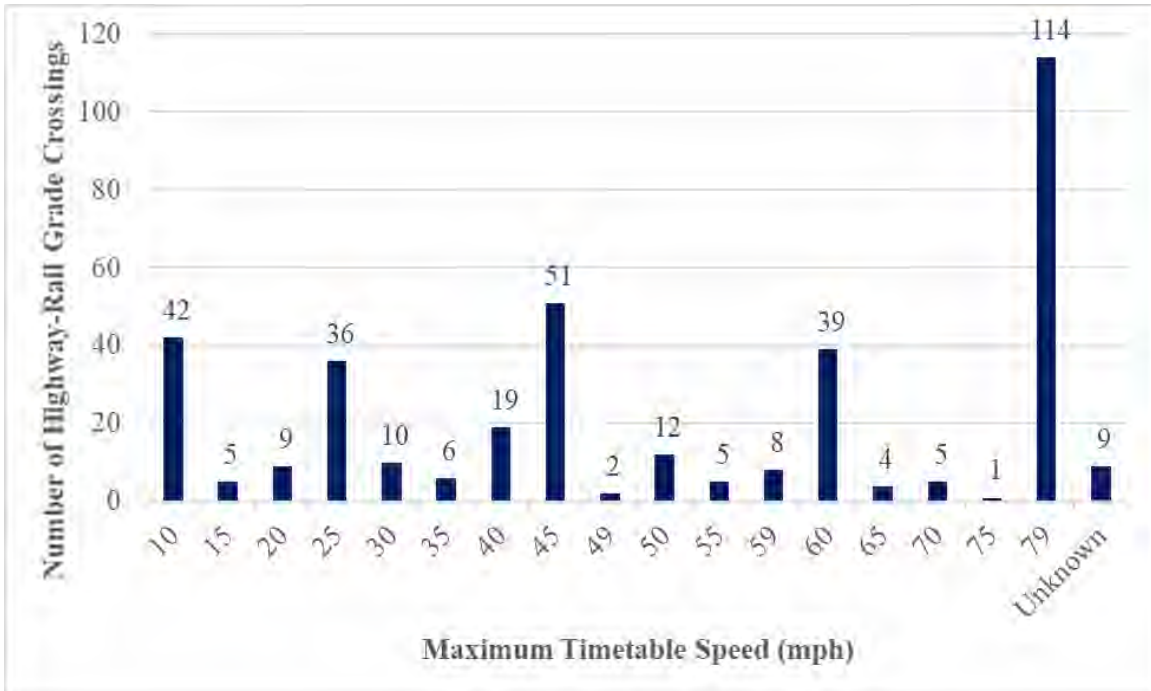


Figure 18 Distribution of Florida’s highway-rail grade crossings that experienced accidents between 2015 and 2019 by maximum timetable speed.

Figure 19 presents a distribution of Florida’s highway-rail grade crossings that experienced accidents between 2015 and 2019 by total number of tracks (i.e., sum of the main tracks and the other tracks). Among the 377 highway-rail grade crossings in Florida that experienced accidents within the 2015-2019 time period, the minimum number of tracks was 1, and the maximum number of tracks was 6. It was found that the majority of the highway-rail grade crossings in Florida that experienced accidents within the 2015-2019 time period had a single track (190 highway-rail grade crossings or 50.4% of highway-rail grade crossings). Furthermore, 118 highway-rail grade crossings (or 31.3% of highway-rail grade crossings) had 2 tracks, while 24 highway-rail grade crossings (or 6.4% of highway-rail grade crossings) had 3 tracks. A total of 10 highway-rail grade crossings (or 2.7% of highway-rail grade crossings) had 4 or more tracks. The number of tracks was not specified for 35 highway-rail grade crossings (or 9.3% of highway-rail grade crossings).

Figure 20 presents a distribution of Florida’s highway-rail grade crossings that experienced accidents between 2015 and 2019 by roadway type. The statistical analysis for roadway type revealed that among the 377 highway-rail grade crossings in Florida that experienced accidents within the 2015-2019 time period, a total of 318 highway-rail grade crossings (or 84.4% of highway-rail grade crossings) was paved, while 11 highway-rail grade crossings (or 2.9% of highway-rail grade crossings) were unpaved. Roadway type was not specified in the FRA crossing inventory database for 48 highway-rail grade crossings (or 12.7% of highway-rail grade crossings) in Florida that experienced accidents within the 2015-2019 time period.

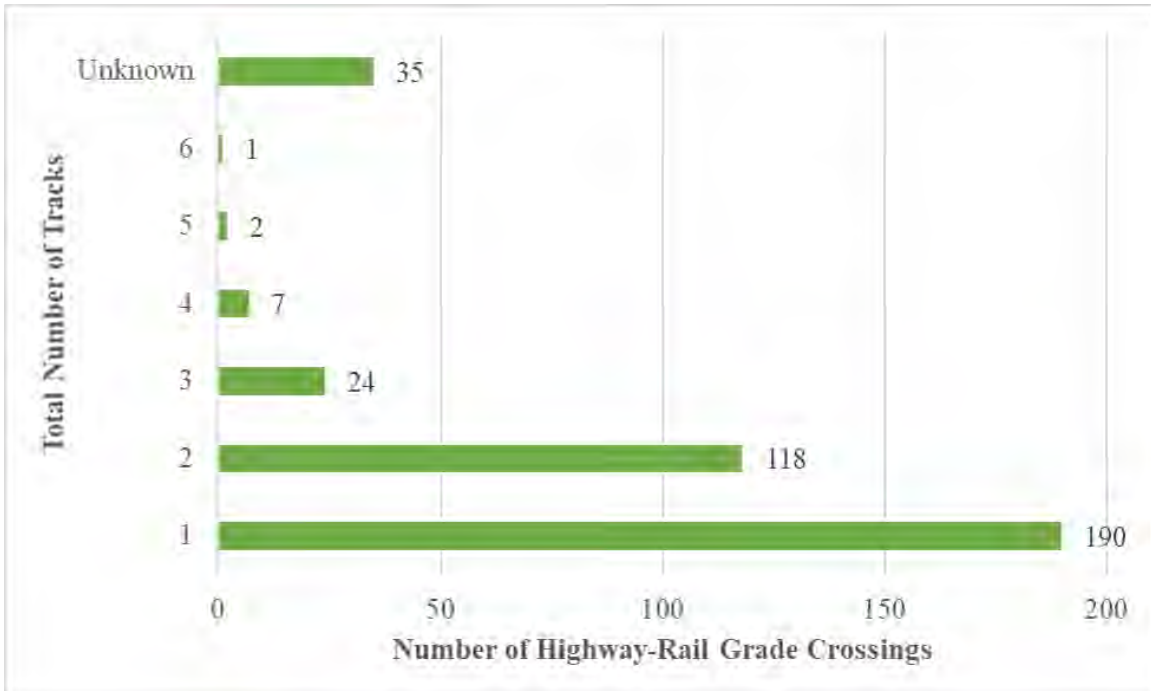


Figure 19 Distribution of Florida’s highway-rail grade crossings that experienced accidents between 2015 and 2019 by total number of tracks.

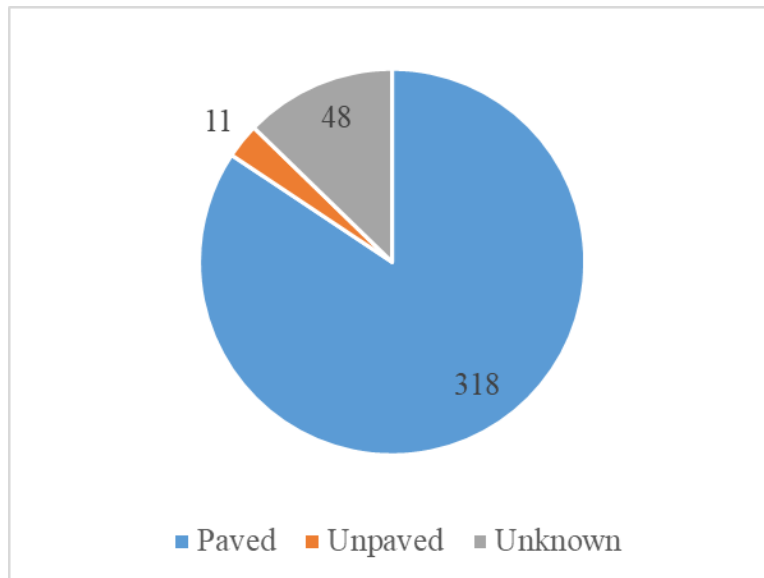


Figure 20 Distribution of Florida’s highway-rail grade crossings that experienced accidents between 2015 and 2019 by roadway type.

A distribution of Florida’s highway-rail grade crossings that experienced accidents between 2015 and 2019 by illumination type is shown in Figure 21. The statistical analysis for illumination type revealed that among the 377 highway-rail grade crossings in Florida that experienced accidents within the 2015-2019 time period, a total of 198 highway-rail grade crossings (or 52.5% of highway-rail grade crossings) was illuminated, and 151 highway-rail grade crossings (or 40.1% of highway-rail grade crossings) were unilluminated. Illumination type was not

specified in the FRA crossing inventory database for 28 highway-rail grade crossings (or 7.4% of highway-rail grade crossings) in Florida that experienced accidents within the 2015-2019 time period.

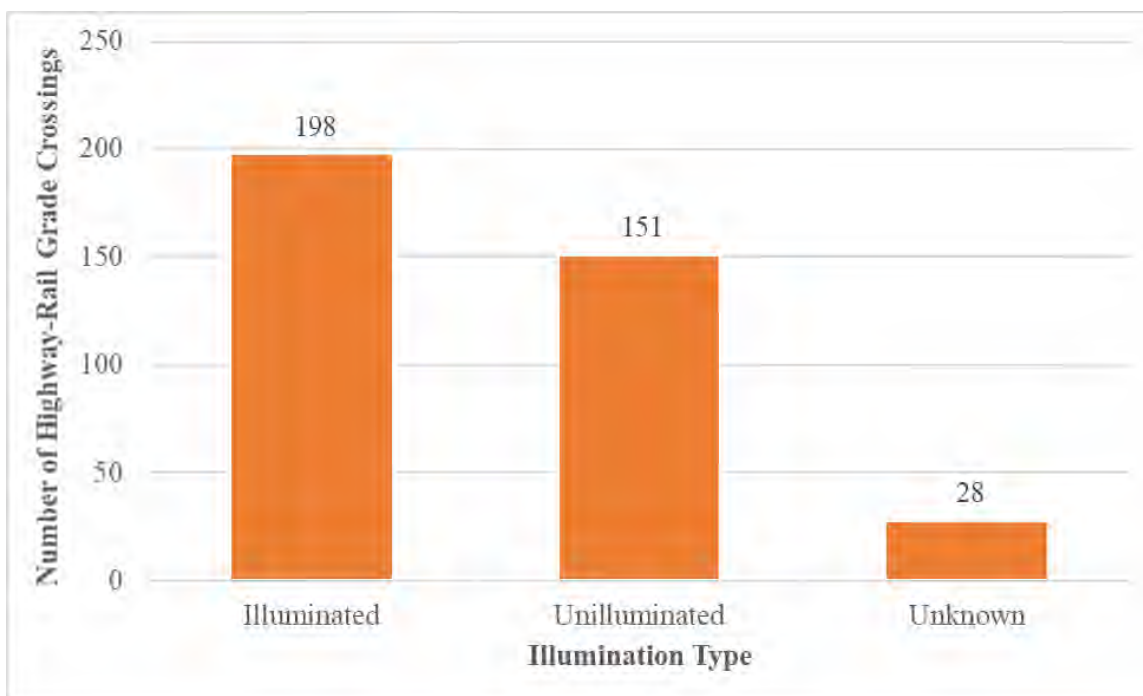


Figure 21 Distribution of Florida’s highway-rail grade crossings that experienced accidents between 2015 and 2019 by illumination type.

Table 5 presents a distribution of Florida’s highway-rail grade crossings that experienced accidents between 2015 and 2019 by crossing surface, where it can be observed that the majority of the highway-rail grade crossings in Florida that experienced accidents within the 2015-2019 time period had concrete surfaces (208 highway-rail grade crossings or 55.2% of highway-rail grade crossings). A total of 61 highway-rail grade crossings (or 16.2% of highway-rail grade crossings) had asphalt surfaces, while 59 highway-rail grade crossings (or 15.6% of highway-rail grade crossings) had surfaces made of asphalt and timber. Furthermore, a total of 8 highway-rail grade crossings (or 2.1% of highway-rail grade crossings) had rubber surfaces, 3 highway-rail grade crossings (or 0.8% of highway-rail grade crossings) had surfaces made of concrete and rubber, and 2 highway-rail grade crossings (or 0.5% of highway-rail grade crossings) included timber surfaces. Other combinations of surface materials (e.g., asphalt and concrete; asphalt and rubber) were found at 2 highway-rail grade crossings (or 0.5% of highway-rail grade crossings). The surface material information was not specified for 34 highway-rail grade crossings (or 9.0% of highway-rail grade crossings).

A distribution of Florida’s highway-rail grade crossings that experienced accidents between 2015 and 2019 by number of traffic lanes crossing railroad is shown in Figure 22. It was demonstrated that among the 377 highway-rail grade crossings in Florida that experienced accidents within the 2015-2019 time period, the highway-rail grade crossings in Florida were intersected by up to 9 traffic lanes. Among these highway-rail grade crossings, a total of 6 highway-rail grade crossings (or 1.6% of highway-rail grade crossings) was intersected by single traffic lanes, 179 highway-

rail grade crossings (or 47.5% of highway-rail grade crossings) were crossed by 2 traffic lanes, and 25 highway-rail grade crossings (or 6.6% of highway-rail grade crossings) were intersected by 3 traffic lanes. Moreover, 59 highway-rail grade crossings (or 15.6% of highway-rail grade crossings) were intersected by 4 traffic lanes, 29 highway-rail grade crossings (or 7.7% of highway-rail grade crossings) were crossed by 5 traffic lanes, while 13 highway-rail grade crossings (or 3.4% of highway-rail grade crossings) were intersected by 6 traffic lanes. A total of 19 highway-rail grade crossings (or 5.0% of highway-rail grade crossings) was crossed by 7-9 traffic lanes. Note that the number of intersecting lanes was not specified for 47 highway-rail grade crossings (or 12.5% of highway-rail grade crossings).

Table 5 Distribution of Florida’s highway-rail grade crossings that experienced accidents between 2015 and 2019 by crossing surface.

Crossing Surface	Number of Highway-Rail Grade Crossings
Concrete	208
Asphalt	61
Asphalt and Timber	59
Rubber	8
Concrete and Rubber	3
Timber	2
Asphalt and Concrete	1
Asphalt and Rubber	1
Unknown	34

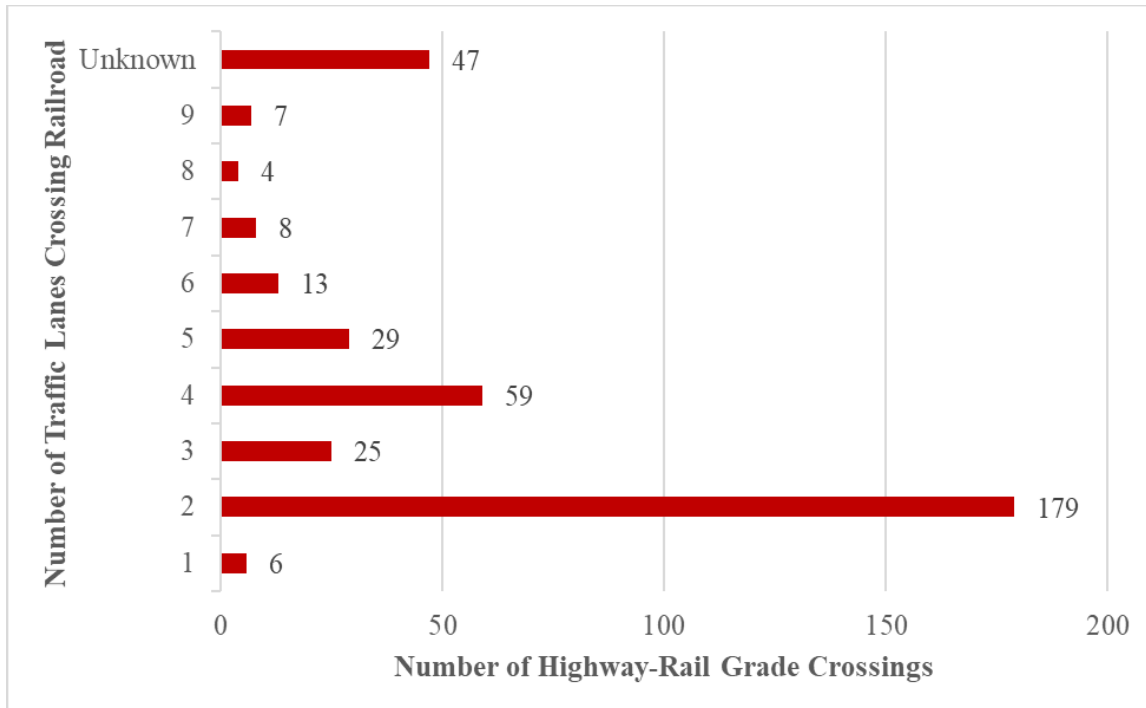


Figure 22 Distribution of Florida’s highway-rail grade crossings that experienced accidents between 2015 and 2019 by number of traffic lanes crossing railroad.

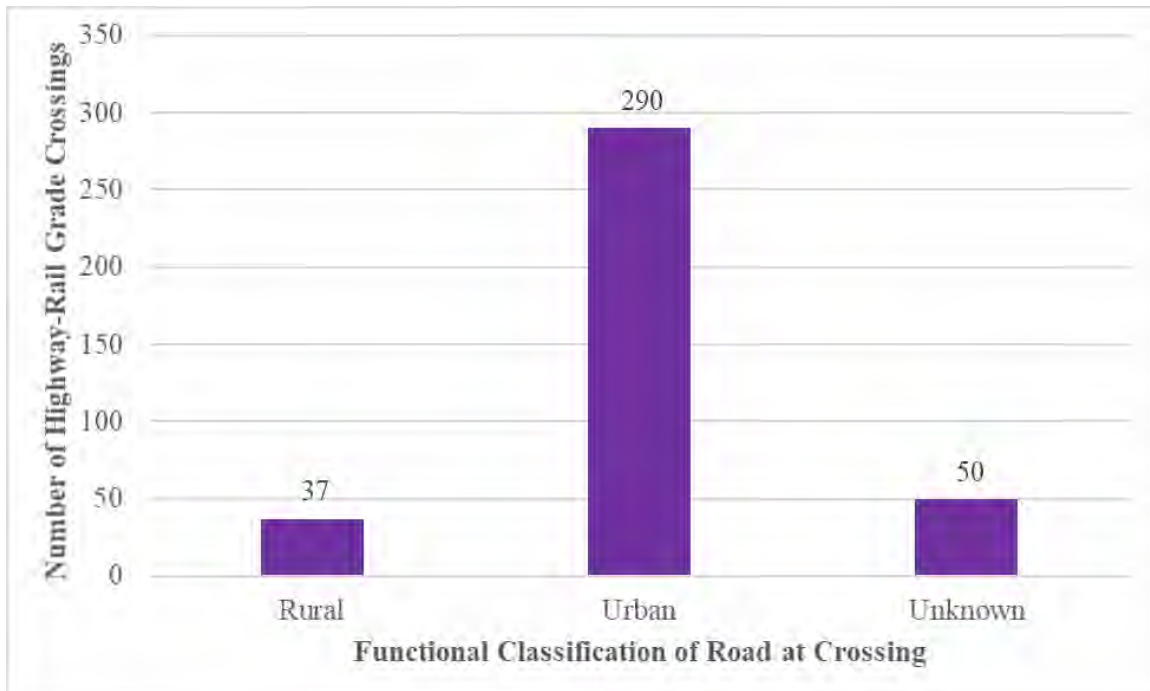


Figure 23 Distribution of Florida’s highway-rail grade crossings that experienced accidents between 2015 and 2019 by functional classification of road at crossing.

A distribution of Florida’s highway-rail grade crossings that experienced accidents between 2015 and 2019 by functional classification of road at crossing is shown in Figure 23. It was revealed that among the 377 highway-rail grade crossings in Florida that experienced accidents within the 2015-2019 time period, 37 roads at the highway-rail grade crossings (or 9.8% of roads) were categorized as rural roads. Furthermore, a total of 290 roads at the highway-rail grade crossings (or 76.9% of roads) was categorized as urban roads. Note that the FRA crossing inventory database did not specify any functional classification of roads at 50 highway-rail grade crossings (or 13.3% of highway-rail grade crossings) in Florida that experienced accidents within the 2015-2019 time period.

1.4. Continuity of Passenger and Freight Flows at Highway-Rail Grade Crossings

Rail transportation in the U.S. has been projected to increase significantly. For this reason, the number of rail vehicles, including both passenger and freight rail vehicles, has increased over the past years. Figure 24 showcases changes in the total rail fleet count in the U.S. from the year 2004 to the year 2014. Note that the total rail fleet count, specified in Figure 24, includes the following components: (i) commuter rail locomotives; (ii) commuter rail self-propelled passenger coaches; (iii) commuter rail passenger coaches; (iv) light rail; and (v) heavy rail. The total rail fleet count in the U.S. has increased by 11.4% from 2004 to 2014, and it is expected to increase even further (FHWA, 2019; p. 6-34).

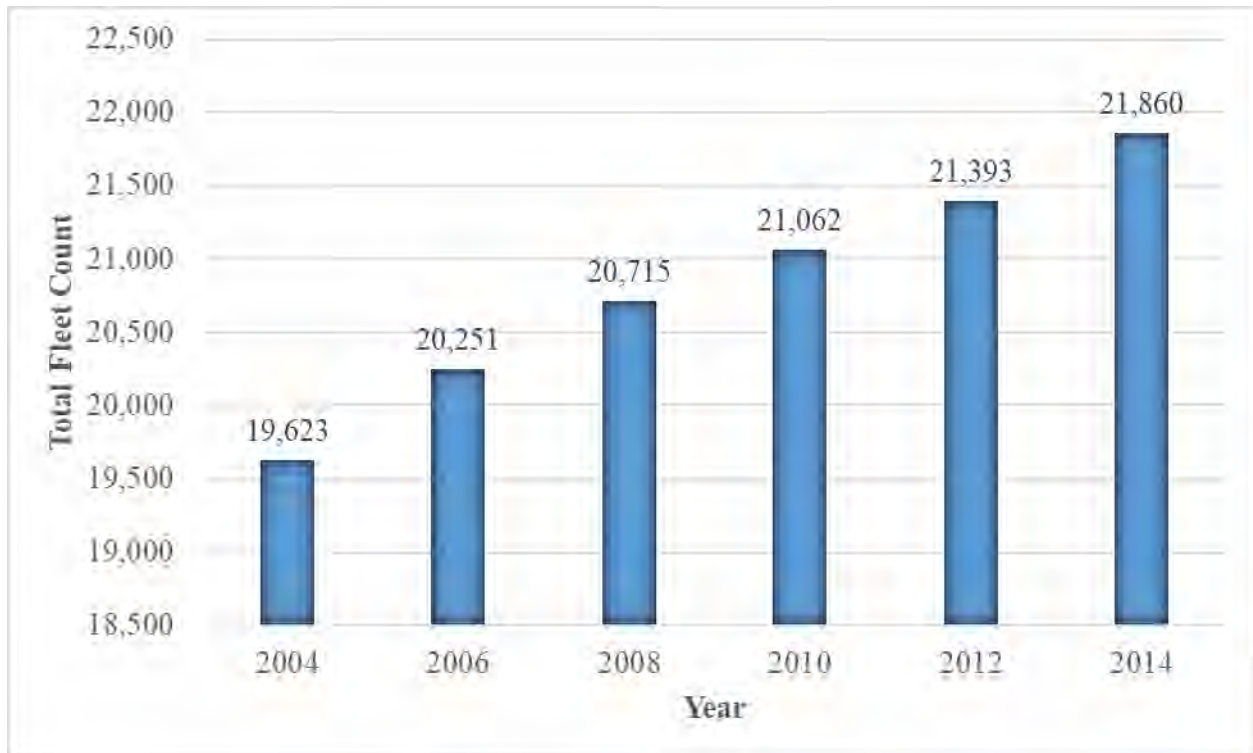


Figure 24 Total rail fleet count in the U.S. for 2004-2014.

Moreover, heavy rail vehicles, which are generally used for freight transportation, comprise most of the U.S. fleet of rail vehicles. The fleet of heavy rail vehicles has increased by 7.4% in the U.S. from 2004 to 2014 (see Figure 25) (FHWA, 2019; p. 6-34). This increase has caused an additional increase in highway traffic, as trucks and other vehicles are required to transport freight from railroad terminals to final destinations. Overall, the increase in the fleet of rail vehicles is likely to increase highway delays (e.g., delays to motorists and pedestrians), especially at/near highway-rail grade crossings, and could block emergency vehicles, increase inconvenience to residents, disrupt local economy, and create societal divisions. In 2002, FHWA reported that vehicular delays at/near highway-rail grade crossings for the next 20 years would amount approximately \$7.9 billion at 50% confidence level (FHWA, 2002). In fact, truck delays are likely to increase annually by 6.6 million hours, and annual auto delays are likely to increase annually by 123 million hours by the year 2022 (FHWA, 2002). These delays and the consequential congestion might also lead to highway system operation failures and intensify negative environmental externalities. As for the State of Florida, it has been observed that due to the migration of residents from different states amongst other reasons, rail transportation in Florida has been increasing at a rate higher than the U.S. average. Therefore, special attention should be given to mitigation of delays at the highway-rail grade crossings in the State Florida.

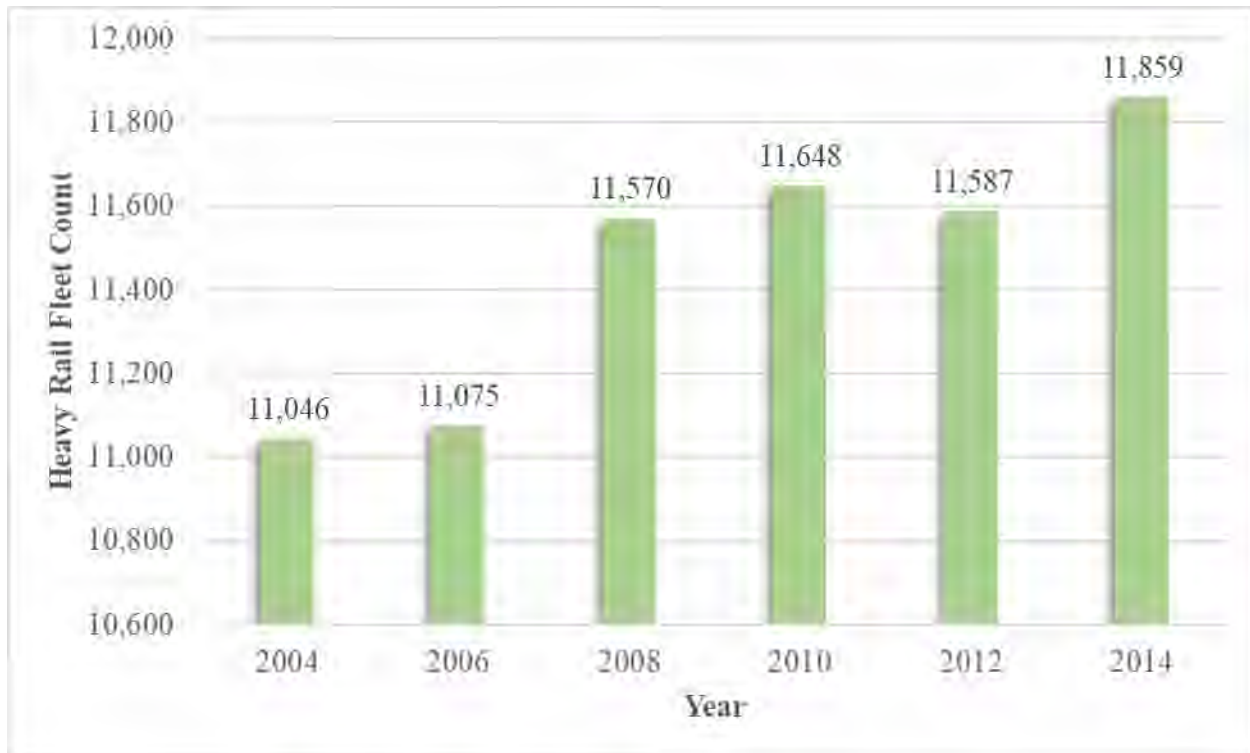


Figure 25 Heavy rail fleet count in the U.S. for 2004-2014.

Significant delays at highway-rail grade crossings can lead to violation of traffic rules at highway-rail grade crossings. Due to significant delays, vehicles might make unsafe maneuvers at highway-rail grade crossings, such as moving through a highway-rail grade crossing while gates are in motion or moving around closed gates so as to travel without delays (Rilett and Appiah, 2008; Khattak, 2014). Richards and Heathington (1990) stated that drivers started losing confidence in the existing traffic control system when warning times were in excess of 40 seconds at highway-rail grade crossings equipped with flashing lights and in excess of 60 seconds at highway-rail grade crossings equipped with gates. Abraham et al. (1998) conducted a survey of unsafe maneuvers at highway-rail grade crossings. Drivers, who made unsafe maneuvers, indicated their reasons for unsafe maneuvers as trains being stopped for unreasonable times and trains not being in sight, among others. Carlson and Fitzpatrick (1999) used logistic regression to show that higher warning times led to a higher chance of risky driver behavior at highway-rail grade crossings. Coleman and Venkataraman (2001) examined driver behavior at a highway-rail grade crossing and revealed that extensive warning times for advanced flashing lights increased the number of traffic rule violations. Such violations pose substantial safety issues and might result in loss of human lives and severe injuries.

1.5. Objectives of This Project

Rail transportation plays an important role for the economic development of the State of Florida, which is often impeded by highway-rail grade crossing accidents. Different types of countermeasures (e.g., upgrading the existing warning device, application of traffic preemption, grade separation) can be applied to reduce the number of accidents at highway-rail grade crossings. The installation of countermeasures, however, could result in increased traffic delays, and, therefore, hinder passenger and freight mobility. Hence, this project aims to develop a

multi-objective optimization model to identify highway-rail grade crossings for upgrades with appropriate countermeasures. The multi-objective optimization model will be used for resource allocation with two conflicting objectives: (1) to minimize the overall hazard severity at highway-rail grade crossings; and (2) to maximize passenger and freight flows (i.e., minimize delays). Afterwards, a standalone application will be developed to implement the aforementioned multi-objective optimization model with the primary goal of assisting the FDOT personnel with identification of highway-rail grade crossings for upgrades and selection of the appropriate countermeasures. Furthermore, using the standalone application, a set of case studies will be conducted to gain important managerial insights from resource allocation among the highway-rail grade crossings in Florida. Ultimately, this project is expected to improve safety at the highway-rail grade crossings in Florida. At the same time, ensuring continuity of passenger and freight flows, reducing delays at highway-rail grade crossings, and supporting economic development of the state are also envisioned.

1.6. Report Structure

This technical report is organized as follows. The second section provides a comprehensive review of the relevant studies and technologies, with focus on the following items: (1) approaches for quantifying continuity of passenger and freight flows at highway-rail grade crossings; (2) warning devices and advanced technology at highway-rail grade crossings; and (3) connected and autonomous vehicle applications at highway-rail grade crossings. The third section presents a multi-objective mathematical model for resource allocation among the highway-rail grade crossings, aiming to the overall hazard severity and the overall traffic delay at the considered highway-rail grade crossings. Furthermore, the third section describes the methods that will be used to quantify the overall hazard severity and the overall traffic delay at the considered highway-rail grade crossings. The fourth section provides a detailed description of the solution algorithms that were developed to solve the proposed multi-objective mathematical model.

The fifth section focuses on a comprehensive evaluation of the candidate solution algorithms in terms of various performance indicators. The sixth section describes the standalone application “HRX Safety Improvement” that was developed for multi-objective resource allocation among the most hazardous highway-rail grade crossings in Florida. The seventh section applies the developed multi-objective mathematical model for the highway-rail grade crossings in Florida and conducts a number of sensitivity analyses. Furthermore, the seventh section evaluates the impact of a low-cost effective alternative countermeasure (i.e., light-emitting diode [LED] signs) on the multi-objective resource allocation among highway-rail grade crossings. The eighth and the last section provides some concluding remarks and highlights the main future research needs.

2. REVIEW OF THE RELEVANT STUDIES AND TECHNOLOGIES

2.1. Approaches for Quantifying Continuity of Passenger and Freight Flows at Highway-Rail Grade Crossings

Highway traffic may experience significant delays due to the presence of a nearby highway-rail grade crossing. Halting highway traffic during a train's passage and installation of warning devices at a highway-rail grade crossing are some of the reasons behind these delays. The following sections underline some methodologies to quantify delays at/near highway-rail grade crossings.

2.1.1. Institute of Transportation Engineers (ITE)

In order to facilitate safe passage of a train, additional measures, such as traffic signal preemption near a highway-rail grade crossing, are sometimes adopted. Under traffic signal preemption, traffic signal control equipment is interconnected with the adjacent highway-rail grade crossing's signal control equipment. In case of an approaching train, normal traffic signal control operations at a highway intersection should be preempted to operate in a special mode (i.e., to prevent vehicles from driving towards an approaching train). Only highway traffic movements that do not conflict with railroad movements are allowed in the preemption mode. Some recommendations for traffic signal preemption near highway-rail grade crossings have been provided by the Institute of Transportation Engineers – ITE (ITE, 2006). Based on the ITE (2006) recommendations, presence of a highway-rail grade crossing near a highway intersection may be complemented by traffic signal preemption. Particularly, coordination between active warning devices at a highway-rail grade crossing and traffic signals at a highway intersection should be established if any of the two scenarios occur:

- Traffic queues starting from a highway intersection approach a highway-rail grade crossing (Figure 26).
- Traffic queues starting from a highway-rail grade crossing approach a highway intersection (Figure 27).

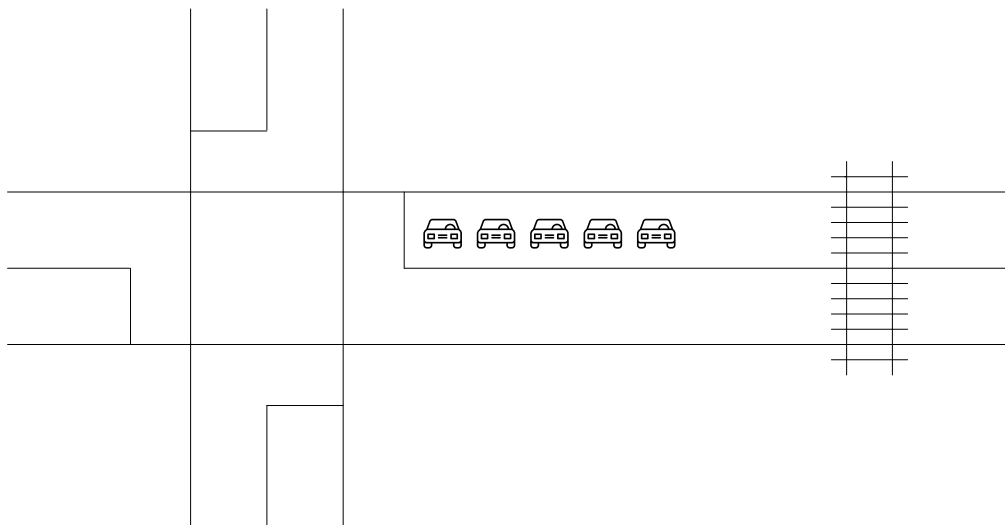


Figure 26 Traffic queues starting from a highway intersection approach a highway-rail grade crossing.

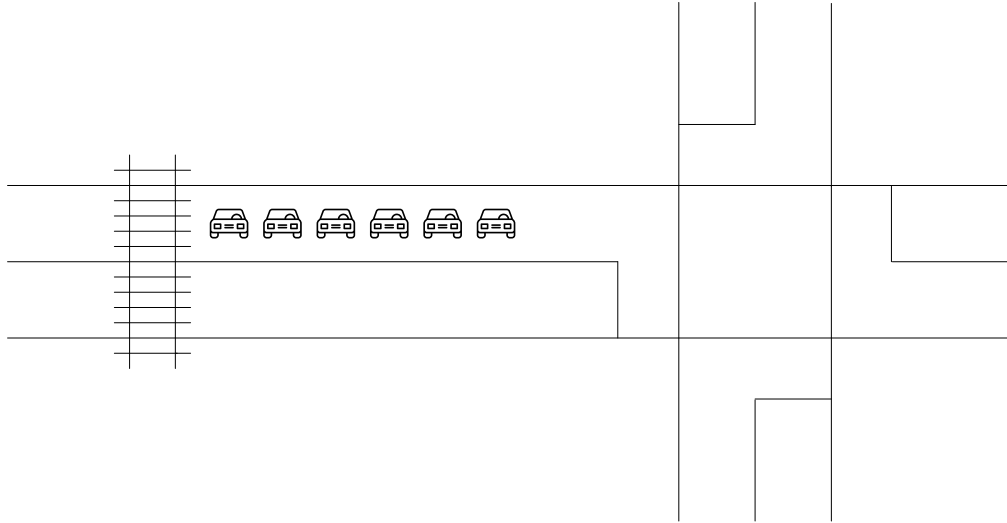


Figure 27 Traffic queues starting from a highway-rail grade crossing approach a highway intersection.

The Manual on Uniform Traffic Control Devices (MUTCD) specified that if some kind of coordination (e.g., omission of signal phases in case of queue detection, activation of variable message signs) is prevalent, then, a highway-rail grade crossing equipped with active warning devices and a signalized highway intersection should be placed at a minimum distance of 200 ft (ITE, 2006). Then, the 95th percentile queue length starting from a highway-rail grade crossing should not cross a highway intersection and vice versa. If the volume to capacity ratio (v/c) for a signalized highway intersection does not exceed 0.90, the 95th percentile queue length starting from a highway intersection and approaching a highway-rail grade crossing (see Figure 26) can be estimated as follows (ITE, 2006):

$$L = (2qr) \cdot (1 + p) \cdot (25) \quad (2.1)$$

where:

L – is the 95th percentile queue length (ft);

q – is the vehicle flow rate (vehicles/lane/second);

r – is the effective red time (i.e., the sum of red time and yellow time) (seconds);

p – is the portion of heavy vehicles (in decimal points);

25 – is the effective length of a passenger car (i.e., the sum of a passenger car's length and space between consecutive vehicles) (ft);

2 – is a random arrival factor.

The 95th percentile queue length starting from a highway-rail grade crossing can be calculated from the following equation, when the volume to capacity ratio for a signalized highway intersection is between 0.90 and 1.00 (ITE, 2006):

$$L = (2qr + \Delta x) \cdot (1 + p) \cdot (25) \quad (2.2)$$

$$\Delta x = 100(v/c - 0.90) \quad (2.3)$$

where:

v/c – is the volume of capacity ratio.

In case traffic queues start from a highway-rail grade crossing and approach a highway intersection (see Figure 27), the vehicle flow rate (q) used in equations (2.1) and (2.2) should include both through traffic as well as left/right turning traffic. Moreover, the symbol “ r ” should not necessarily denote the effective red time. Instead, it should represent the effective time during which a train blocks a highway-rail grade crossing, and it can be estimated using the following equation (ITE, 2006):

$$r = 35 + \frac{l}{1.47S} \quad (2.4)$$

where:

r – is the effective time during which a train blocks a highway-rail grade crossing (seconds);

l – is the train length (ft);

S – is the train speed (mph);

35 – is the amount of time during which gates block the highway-rail grade crossing (about 25 seconds before a train enters the highway-rail grade crossing and 10 seconds after the train exits the highway-rail grade crossing) (seconds).

Delays to highway traffic could be added at highway-rail grade crossings due to the queue lengths mentioned above. The methodologies for quantifying delays in time units from queue lengths recommended by the U.S. Department of Transportation (U.S. DOT) as well as other appropriate sources can be adopted for this purpose.

2.1.2. Highway-Rail Crossing Handbook

Different warning devices can cause additional delays at highway-rail grade crossings. The U.S. DOT Highway-Rail Crossing Handbook provides a collection of recommendations to quantify delays for different warning devices (U.S. DOT, 2019). For instance, the Code of Federal Regulations §234.225 (49 CFR 234.225) and MUTCD recommend a minimum of 20 seconds time to activate warning devices before a through train arrives at a highway-rail grade crossing (ITE, 2006; U.S. DOT, 2019 – page 53). Moreover, the American Railway Engineering and Maintenance-of-Way Association (AREMA) Communications and Signal Manual states that the minimum warning time to activate warning devices, before a through train arrives at a highway-rail grade crossing, should be the sum of a 20 seconds minimum time and a clearance time, which is 1 second for every 10 ft of additional highway-rail grade crossing length exceeding 35 ft (AREMA, 2004; ITE, 2006; U.S. DOT, 2019 – page 53). AREMA (2004) also recommends additional equipment response time (due to variations in equipment response), buffer time (due to variations in handling of trains), and advance preemption time (which can be added by the public agency to account for the advance preemption), if required. Moreover, the additional gate delay time, exit gate clearance time, and adjacent track clearance time should be accounted for (ITE, 2006).

Different warning devices could add different lengths of delay. For instance, automatic gates require a minimum of 3 seconds for their gate arms to start downward motion after flashing lights start operation (ITE, 2006; U.S. DOT, 2019 – page 64). According to the Code of Federal Regulations §234.223 (49 CFR 234.223), gate arms must reach their full horizontal position in not less than 5 seconds before a train arrives (ITE, 2006; U.S. DOT, 2019 – page 53). Note that gate arms typically require 8-12 seconds to reach their horizontal position (ITE, 2006). A

maximum of 12 seconds is required by gate arms to reach their initial vertical position after a train clears the highway-rail grade crossing, and, then, flashing lights as well as the lights on the gate arms stop operation (U.S. DOT, 2019; p. 64). Apart from automatic gates, wayside horns are required to sound at least 15 seconds before a train's arrival at a highway-rail grade crossing. In addition, they should include a 3 to 5 seconds delay before sounding, after flashing lights start operation (U.S. DOT, 2019; p. 63).

2.1.3. NCHRP Report 288

The National Cooperative Highway Research Program (NCHRP) Report 288 stated that replacing a deteriorated grade-separated crossing with a highway-rail grade crossing would cause additional delays to the associated highway traffic (NCHRP, 1987). In order to capture the changes in delays at different times of the day, the calculation of delay on an hourly basis was recommended. Based on the NCHRP Report 288, the total vehicular delay, caused by train operations, can be estimated as follows (NCHRP, 1987):

$$D = \frac{\left(\frac{T}{2} + 0.10\right) N + \left(\frac{N}{n}\right)^2}{60} \quad (2.5)$$

where:

D – is the total delay (minutes);

T – is the duration of highway-rail grade crossing closure (seconds); $(T/2)$ – is the average delay per vehicle as not all the vehicles will be delayed by the same amount of time (seconds);

N – is the number of delayed vehicles;

n – is the number of highway lanes;

0.10 – is the delay due to deceleration and acceleration along with the delay experienced while waiting for highway traffic to flow freely after the train has passed (seconds).

Note that equation (2.5) includes term $(N/n)^2$ that is used to account for the queue dissipation time after the train passes a given highway-rail grade crossing. Once the crossing gates are open, there will be a total of (N/n) vehicles in a queue in each highway lane. Assuming that the headway between two consecutive vehicles is 2 seconds, the total queue dissipation time for the first vehicle in each lane will be zero seconds, while the total queue dissipation time for the last vehicle in each lane will be $(2) \cdot (N/n)$ seconds. Then, the average queue dissipation time will be $(2) \cdot (N/n)/2$, and the total queue dissipation time will be $(2) \cdot (N/n)/2 \cdot (N/n) = (N/n)^2$ seconds (NCHRP, 1987). The duration of highway-rail grade crossing closure (T – minutes) due to a single train movement can be estimated as follows:

$$T = \frac{50 + \frac{0.682 \cdot L}{1.5S_e - S_x}}{60} \quad (2.6)$$

where:

L – is the train length (ft);

S_e – is the speed of the train when it enters the highway-rail grade crossing (mph);

S_x – is the speed of the train when it exits the highway-rail grade crossing (mph);

50 – is the duration of time when the warning devices are active before the train arrives and after the train leaves the highway-rail grade crossing (a constant warning time device is assumed) (seconds);

0.682 – is the conversion from mph to ft/second.

The probability of delay could be helpful to justify the delay estimates. The probability of delay can be determined as follows:

$$P = \frac{T}{m} \quad (2.7)$$

where:

P – is the probability of delay;

m – is the amount of time for the period under consideration (minutes).

The number of delayed vehicles (N) can be calculated as the product of the probability of delay (P) and the highway traffic volume passing through the highway-rail grade crossing throughout the given time period (V):

$$N = P \cdot V \quad (2.8)$$

2.1.4. Okitsu et al. (2010)

Okitsu et al. (2010) presented a straightforward methodology to estimate vehicular delays at highway-rail grade crossings. The following formula was used to estimate the total delay (Okitsu et al., 2010; Chicago Metropolitan Agency for Planning, 2015):

$$D = \frac{AR \cdot Q \cdot (B + LT)}{2} \quad (2.9)$$

where:

D – is the total delay (vehicle-hours);

AR – is the arrival rate (vehicles/hour);

Q – is the queue duration (hours);

B – is the duration of blockage event (hours);

LT – is the lost time (hours).

The queue duration (Q – hours) can be determined from the saturation flow rate ($SatFlowRate$ – vehicles/hour for lane group) as follows:

$$Q = \frac{B + LT}{AR \left(1 - \frac{AR}{SatFlowRate} \right)} \quad (2.10)$$

2.1.5. Southern California International Gateway Draft EIR

The Southern California International Gateway Draft EIR (2011) presented a methodology for computing vehicular delays for an isolated highway-rail grade crossing blockage. The number of

vehicle minutes of delay for an isolated blockage (V – minutes) can be estimated from the following equation (Southern California International Gateway Draft EIR, 2011):

$$V = \left(\frac{1}{2}\right) \left(\frac{qT_G^2}{1 - \frac{q}{d}}\right) \quad (2.11)$$

where:

q – is the arrival rate (vehicles/minute);

T_G – is the gate down time (minutes);

d – is the departure rate (vehicles/minute).

Equation (2.11) is applied for each train that arrives at the highway-rail grade crossing throughout the day. Note that delays are likely to differ at different times of the day due to changes in highway traffic volumes. Many vehicles arriving at the highway-rail grade crossing will not face delays due to train arrivals. Still, they are included for the estimation of the average delay. The hourly average delay per vehicle, on the other hand, is determined by dividing the total vehicular delay in one hour with the volume of vehicles that arrive at the highway-rail grade crossing over that time.

2.1.6. Center for Urban Transportation Research (CUTR), University of South Florida

The Center for Urban Transportation Research (CUTR) at the University of South Florida indicated that the delay at a highway-rail grade crossing due to a passing train could be estimated from the length and the speed of a train as follows (CUTR, 2014):

$$\text{Train Delay Time} = CWT + \frac{\text{Train Length}}{\text{Train Speed}} \quad (2.12)$$

where:

Train Delay Time – is the train delay time (seconds);

CWT – is the constant warning time, usually 20-25 seconds (seconds);

Train Length – is the train length (ft);

Train Speed – is the train speed (ft/second).

2.1.7. Surface Transportation Board (STB)

The Surface Transportation Board (STB), the federal agency that is responsible for economic regulation of different surface transportation modes (mostly freight rail), provided the methodology for estimating the total vehicular delay at highway-rail grade crossings. The traffic delay at a highway-rail grade crossing included the time required for a train to pass as well as the time required for warning devices to engage. It was assumed that the railroad traffic and highway traffic were uniform throughout the day. The total vehicular delay (D) was calculated as the product of the average delay per vehicle (D_V) and the number of vehicles delayed per day (N_V) (STB, 2020):

$$D = D_V \cdot N_V \quad (2.13)$$

The number of vehicles delayed per day (N_V) could be estimated from the following equation:

$$N_V = \frac{T}{24} \cdot N \cdot ADT \quad (2.14)$$

where:

T – is the gate down time per train event;

N – is the number of trains per day;

ADT – is the average daily traffic.

The gate down time per train event (T) was estimated as follows:

$$T = T_W + \frac{L}{V} \quad (2.15)$$

where:

T_W – is the gate warning time;

L – is the average train length estimated as the weighted average between freight and passenger trains;

V – is the average train speed estimated as the weighted average between freight and passenger trains.

The average delay per vehicle (D_V) during a 24-hour period was calculated as follows (STB, 2020):

$$D_V = \frac{N_V}{ADT} \cdot \frac{T \cdot \frac{R_D}{R_D - R_A}}{2} \quad (2.16)$$

where:

R_D – is the departure rate, 1,800 for highways, 1,400 for arterials, 900 for collectors, and 700 for local roads (vehicles/lane/hour);

R_A – is the arrival rate, average daily traffic converted to vehicles/lane/hour (vehicles/lane/hour);

2 – is used to indicate that vehicles do not wait for the entire time during which the train blocks the highway-rail grade crossing; the vehicles, on average, are assumed to arrive at the middle of the train crossing duration.

2.2. Warning Devices and Advanced Technology at Highway-Rail Grade Crossings

Various warning devices and new technologies have been installed at highway-rail grade crossing in the U.S. over the years, aiming to improve their safety. This section of the report provides a detailed review of different warning devices and advanced technologies that have been used at highway-rail grade crossings, including pavement markings, signage, conventional warning devices and technologies, train warning signs, crossing gate technologies, detection technologies (e.g., technologies for remote health monitoring of highway-rail grade crossings; vehicle detection technologies), train detection devices, intelligent transportation system (ITS)-based communication technologies, and others.

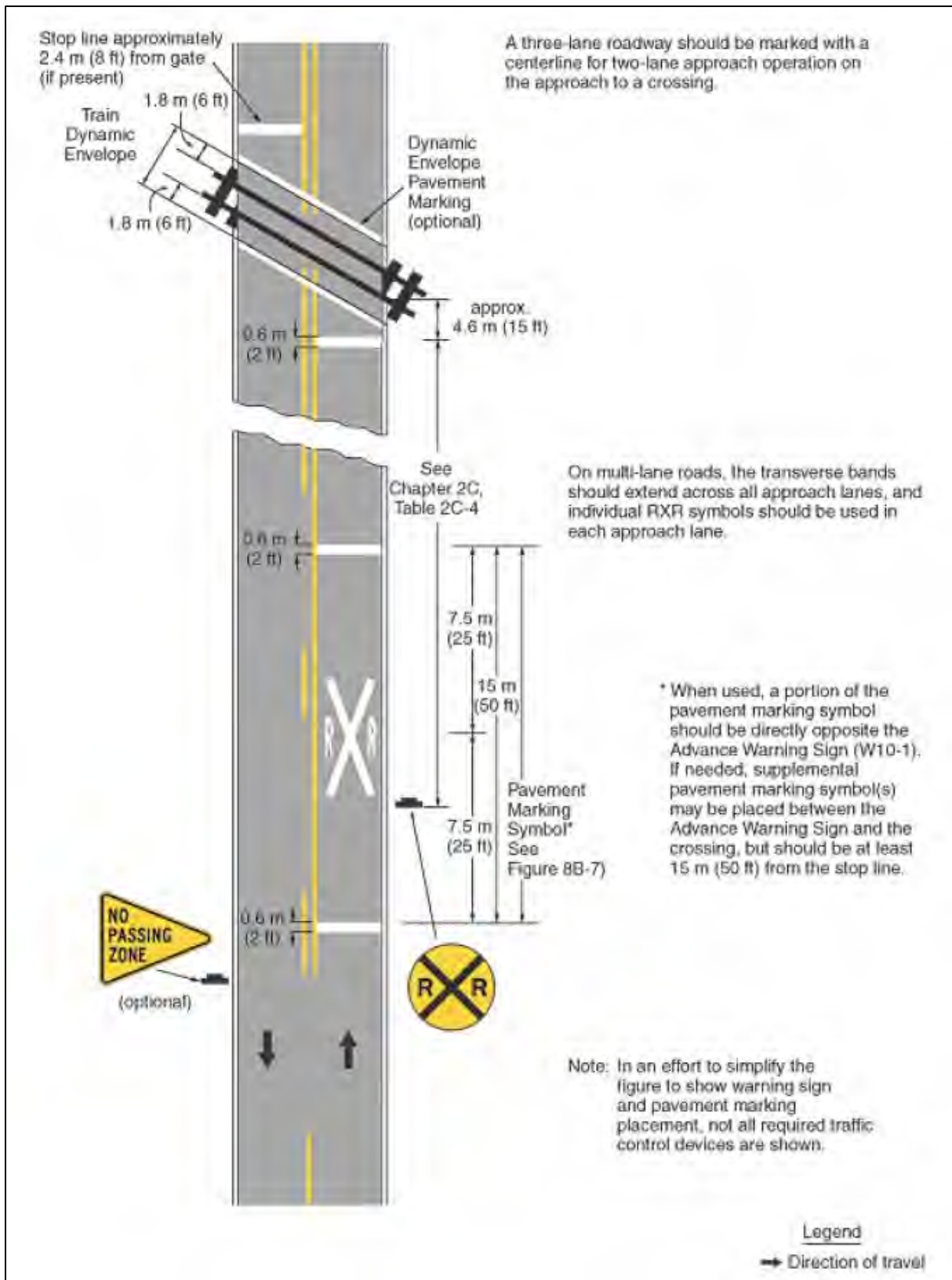


Figure 28 Regular pavement markings.

Source: U.S. DOT. (2019). *Highway-Rail Crossing Handbook* (Figure 16)

2.2.1. Pavement Markings

Pavement markings play a critical role in improving safety at highway-rail grade crossings, along with supplementary traffic control devices. There are certain disadvantages from using pavement markings. For example, pavement markings may not be visible when driving during inclement weather conditions (e.g., rain, fog, snow) and may not be durable for highways that are subject to heavy traffic loads. Figure 28 illustrates some of the typical pavement markings, including the letters “RR”, an “X”, the words “No Passing” on 2-lane, 2-way highways having centerline markings as well as certain transverse lines. Note that Figure 28 was prepared using the data reported by U.S. DOT (2019; p. 47). Such pavement markings are generally placed on all paved approaches of each approach lane of the highway-rail grade crossings that have signals and/or automatic gates as well as the highway-rail grade crossings, where the existing highway traffic speed is 40 mph at the minimum. Moreover, the aforementioned types of pavement marking are used at the highway-rail grade crossings, where there is a potential conflict between vehicles and trains, established based on the performed engineering studies. On the other hand, pavement markings are not necessary for minor highway-rail grade crossings in urban areas, where the existing traffic control devices provide an adequate control, established based on the performed engineering studies.

All pavement markings typically have white color. Only “No Passing” markings are colored in yellow in contrast with other types of pavement markings. The stop line must be 2 ft wide and stretch towards the approach lanes. At a given highway-rail grade crossing, the placement of the stop line must be at a right angle to the highway centerline and approximately 15 ft before the nearest rail. In case a given highway-rail grade crossing is equipped with automatic gates, the stop line has to be placed approximately 8 ft before the line, where the gate arm crosses the roadway surface (U.S. DOT, 2019).



Figure 29 Symbol and word pavement marking.

Source: TCRP-175. (2015). Guidebook on Pedestrian Crossings of Public Transit Rail Services (Figure 109)

Figure 29 illustrates a symbol and word pavement marking that was prepared using the data reported by TCRP-175 (2015; p. 120). These pavement markings have been prepared for providing guidance, warning, and traffic regulations. Symbol and word pavement markings can be used at rail tracks to alert pedestrians about restricted areas, where they should not enter.

Furthermore, the words “Not A Walk” can be provided on yellow striping. Figure 30 represents a diagonal exclusion zone pavement marking at a pre-signal location and was prepared using the data reported by U.S. DOT (2019; p. 49). Diagonal exclusion zone pavement markings are used on tracks, where there is a concern for vehicles queuing up near highway-rail grade crossings due to limited downstream storage space.

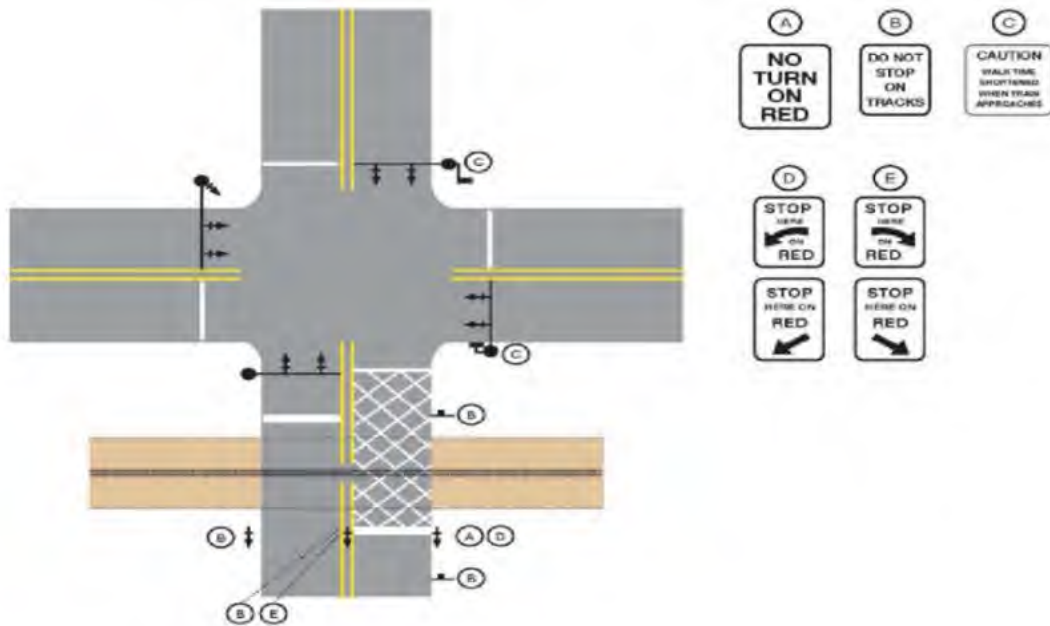


Figure 30 Diagonal exclusion zone pavement markings at pre-signal locations.
Source: U.S. DOT. (2019). Highway-Rail Crossing Handbook (Figure 17)

Figure 31 illustrates some of the alternate pavement markings, where the paint is used off the path of the wheel. Note that Figure 31 was prepared using the data reported by U.S. DOT (2007; p. 97) A supplementary “No Passing Zone” sign (W14-3) may be used at highway-rail grade crossings that have “No Passing” pavement markings. Such a sign is generally placed at the beginning of the no passing zone on the left side of the highway. The cost of pavement markings is \$1.50 to \$2.65 for tape and \$0.08 to \$0.10 for paint. The cost of pavement marking is based on the data provided by the Minnesota DOT (2000). Advantages, disadvantages, unit costs, as well as operation and maintenance (O&M) costs of different types of pavement markings at highway-rail grade crossings are further summarized in Table 6.

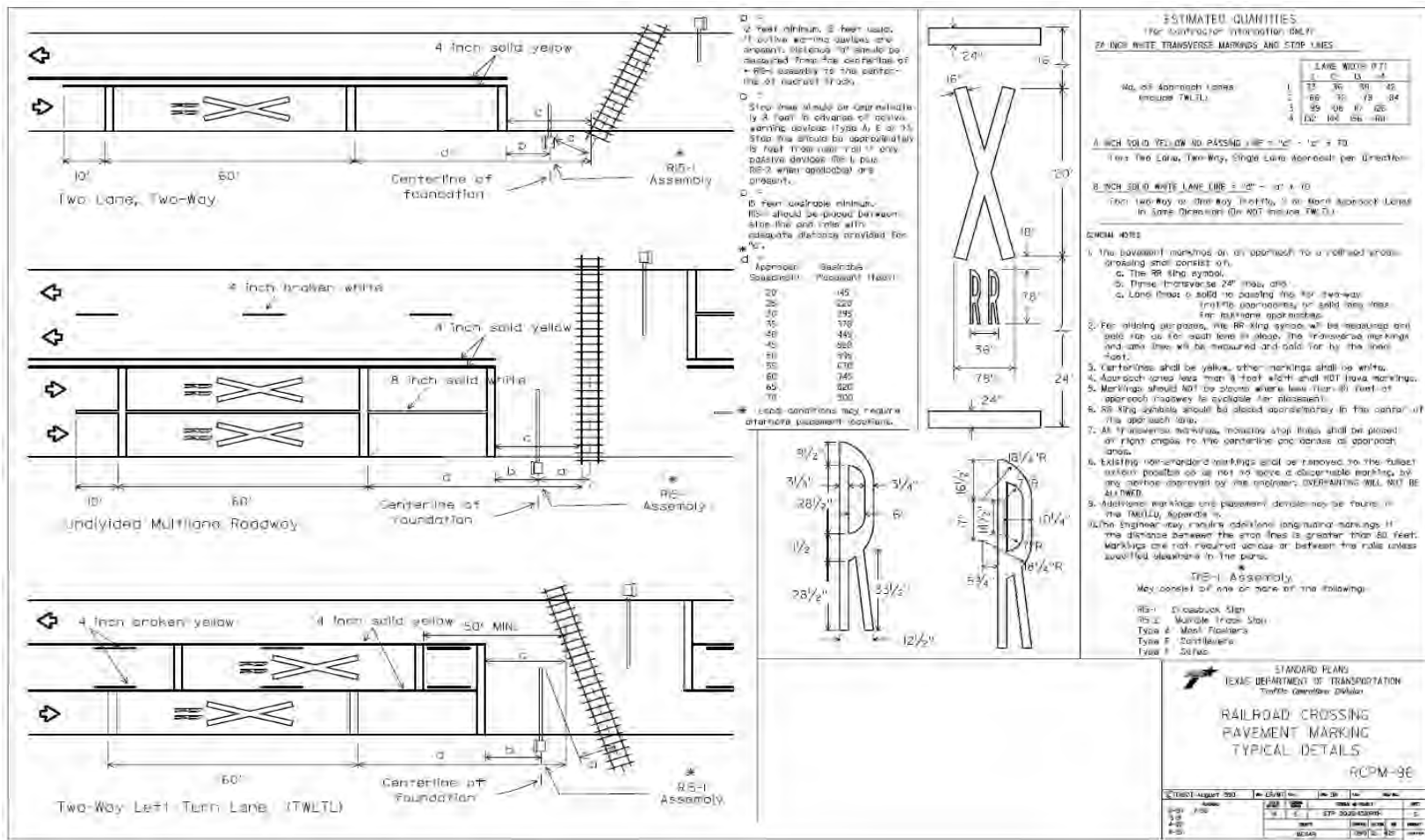


Figure 31 Alternative pavement markings at highway-rail grade crossings.
 Source: U.S. DOT. (2007). *Railroad-Highway Grade Crossing Handbook* (Figure 20)

Table 6 Features of various pavement markings.

Type of Marking	Advantages	Disadvantages	Unit Cost	O&M Cost
Regular pavement markings ^{1,2}	<p>Tape: (1) high quality of retro-reflectivity; (2) offer long life on roads with low to high volume; (3) useful in high traffic areas where wheels cross the markings; (4) beads are not needed; (5) longer life of tape reduces exposure of workers to road hazards.</p> <p>Paint: (1) less expensive; (2) fast-drying; (3) good for roads with low volume traffic only; (4) easy to apply, clean, and dispose; (5) there are no hazardous waste products used.</p>	<p>Tape: (1) expensive pavement marking; (2) works well on new road pavements and does not work well on older roads with poor pavement surface; (3) can be damaged in snowplow.</p> <p>Paint: (1) reduced life on roads with high volume; (2) can be damaged from surface abrasion; (3) need application of beads for reflection at night; (4) does not work well with concrete; (5) pavement should be warm for the paint to adhere.</p>	\$1.50 to \$2.65 per foot for tape and \$0.08 to \$0.10 per foot for paint	
Pedestrian crossing pavement marking symbols ³	(1) provides restricted area warning and information; (2) can be used for traffic regulation, guiding, and warning.	(1) there is not much help for roadway users with visual disability.	\$360.00 per symbol	
Diagonal exclusion zone pavement markings ^{1,2}	(1) same as regular pavement markings since both paint and tape can be used.	(1) same as regular pavement markings since both paint and tape can be used.	\$1.50 to \$2.65 per foot for tape and \$0.08 to \$0.10 per foot for paint	

Notes: 1 – U.S. DOT. (2019). Highway-Rail Crossing Handbook

2 – Minnesota DOT. (2000). Cost of Pavement Marking Materials

3 – TCRP-175. (2015). Guidebook on Pedestrian Crossings of Public Transit Rail Services

2.2.2. Signage

Various regulatory and warning signs along with plaques for highway-rail grade crossings are presented in Figure 32 and Figure 33, respectively. Some of these signs are used for general purposes, and the others are particular to highway-rail grade crossings. Highway-rail grade

crossing signs, such as “Do Not Stop on Tracks” (R8-8), “No Right (Left) Turn across Tracks” (R3-1a/R3-2a), blackout signs, “Stop Here” signs, etc., are generally used in combination with other devices (MUTCD, 2009). MUTCD (2009) provided some specific guidelines for the use of these signs. Different features of regulatory and warning signs are summarized in Table 7.



Figure 32 Regulatory signs and plaques for highway-rail grade crossings.
 Source: MUTCD. (2009). *Manual on Uniform Traffic Control Devices (Figure 8B-1)*

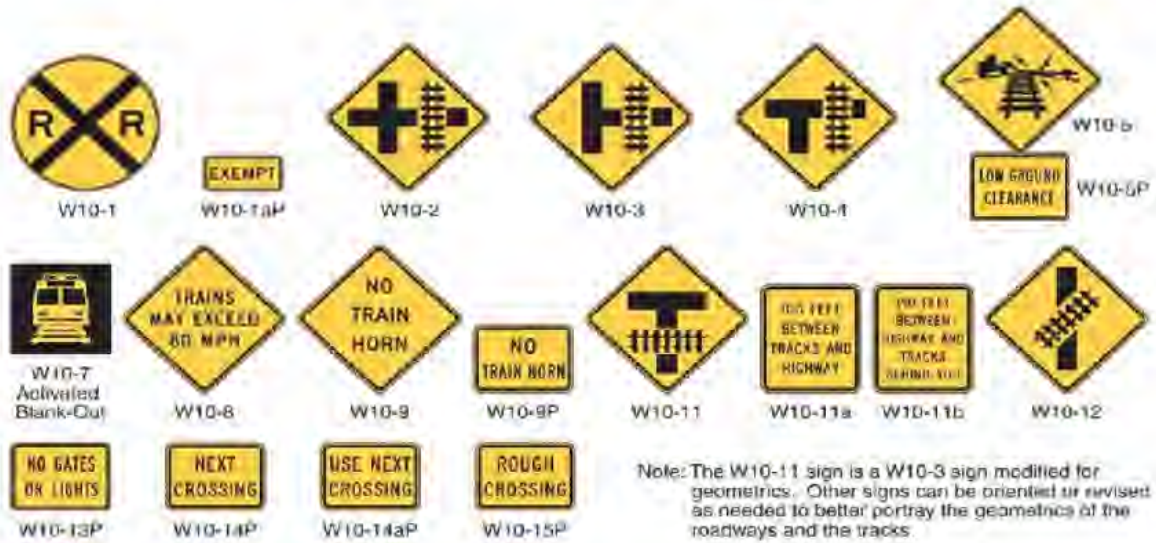


Figure 33 Warning signs and plaques for highway-rail grade crossings.

Source: MUTCD. (2009). *Manual on Uniform Traffic Control Devices (Figure 8B-4)*

Table 7 Features of regulatory and warning signs.

Type of Sign	Advantages	Disadvantages	Unit Cost	O&M Cost
Regulatory signs ^{1,2}	(1) required to comply with the law; (2) provide standard messages at approaches; (3) roadway users are required to take specific measures to avoid accidents.	(1) not useful for roadway users who cannot see properly or have vision impairment.	\$25-\$35 per square foot	
Warning signs ^{1,2}	(1) helpful for drawing attention to specific hazardous conditions; (2) benefit of using a sign depends on the type of signs; (3) can help reducing crashes and facilitate normal operations.	(1) not useful for roadway users who cannot see properly or have vision impairment.	\$25-\$35 per square foot	

Notes: 1 – MUTCD. (2009). *Manual on Uniform Traffic Control Devices*

2 – Moeur. (2019). *Manual of Traffic Signals*

2.2.3. Conventional Warning Devices and Technologies at Highway-Rail Grade Crossings

Conventional warning devices and technologies can be installed at multiple locations to alert drivers who drive across highway-rail grade crossings. Some of the basic conventional warning devices used at highway-rail grade crossings are stop signs, crossbucks, wigwags, crossing bells, flashing lights, and basic crossing gates. A concise description of the main conventional warning devices that have been used at highway-rail grade crossings is presented next.

Stop signs

Stop signs are used as a conventional traffic control device for a roadway user to delay the movement at passive and active highway-rail grade crossings when traffic control devices are activated. Stop signs can be used in combination with any other signs, crossbucks, flashing lights, crossing gates, and other technologies, when the roadway user is expected to make a complete stop before moving ahead. Figure 34 shows a typical stop sign.



Figure 34 An example of a stop sign.

Source: MUTCD. (2009). Manual on Uniform Traffic Control Devices

Crossbuck signs

Typically, the crossbuck sign shows “Railroad Crossing” on a white reflective sheeting and uses a black color font. The crossbuck sign is used as a standard practice on highway-rail grade crossings, except that its use is optional at light rail train crossings. It can be used either alone or with other devices. For the highway-rail grade crossings with two or more rail tracks, the supplementary plaque “Number of Tracks” (R15-2P) should be installed below the crossbuck sign (MUTCD, 2009). The location of the crossbuck sign should be close to the nearest track with the reference to the highway pavement. In case of any safety issue, engineering judgment should be applied for the placement of crossbuck signs. A typical crossbuck sign is shown in Figure 35.

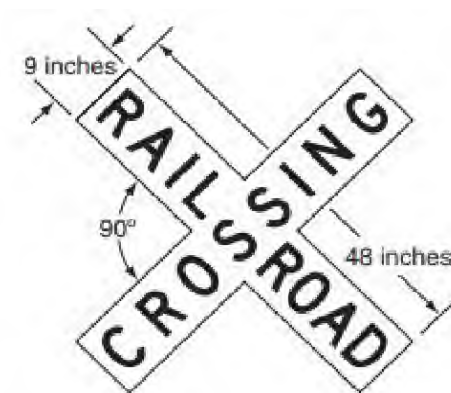


Figure 35 An example of a crossbuck sign.

Source: MUTCD. (2009). Manual on Uniform Traffic Control Devices

Wigwags

Wigwags serve as warning signals at highway-rail grade crossings. Wigwags are flashing light signals used in combination with crossbuck signs. The first wigwags were motor-driven. After years of its initial use, the magnetic flagman was installed and adopted as a standard in 1920s (Magnetic Signal Co., 2020). Typical wigwags are shown in Figure 36.



Figure 36 An example of wigwags.
Source: trainweb.org (2020)

Crossing bells

Crossing bells (or wayside horns) are installed as additional warning devices at highway-rail grade crossings and can be used in combination with gates, crossbucks, pedestrian gates, etc. Crossing bells are very useful for providing alerts to roadway users with visual disabilities. These bells can alert users about an incoming train. A typical crossing bell is shown in Figure 37.



Figure 37 An example of a crossing bell.
Source: U.S. DOT. (2019). Highway-Rail Crossing Handbook (Figure 26)

Flashing light signals

Flashing light signals can be installed with crossbucks mounted on a sign pole. Flashing light signals are used in combination with other warning devices as well, such as crossing bells, additional warning signs, etc. The two flashing lights mounted on a horizontal bar start to flash and alert roadway users regarding an approaching train (U.S. DOT, 2019). A typical flashing light signal assembly is shown in Figure 38.



Figure 38 An example of flashing light signals.
Source: Klassy. (2017). Railroad Crossing Lights



Figure 39 An example of basic gates.
Source: Whippany Railway Museum. (2020). Railroad Crossing Gates & Signals

Gates

Gates are typically painted with reflective materials. Gates could be operated manually or automatically. Manual gates are mostly not in use due to higher operating costs. Automatic gates are being used as barriers to protect roadway users from incoming trains. Gates are used in combination with flashing lights, wayside horns, crossbucks, and/or other warning devices that can provide additional alerts and warnings regarding the approaching trains (U.S. DOT, 2019). Three red lights are typically installed on the gate arm, where the light at the end stays steady and the other two flash. Figure 39 illustrates a set of basic gates.

2.2.4. Train Warning Signs

Light-emitting diode (LED) preemptive train warning signs

The light-emitting diode (LED) “commuter train approaching” signs have been used to enhance safety of pedestrians and motorists at light rail train crossings. Highway users approaching streetcar and commuter train traffic can be effectively alerted by LED safety signs. These signs can be installed at various transit stations, limited visibility areas, and mid-block highway-rail grade crossings to alert motorists and pedestrians regarding the approaching train traffic. These signs can be available with the input voltage of 100-240 VAC, 12-24 VDC, or others (Signal-Tech, 2020). Voice-activated speaker systems and third-party audio alarm systems can be engineered to interface with these signs. Design of the cabinets used for these signs are vandal- and weather-resistant. Moreover, messages can be displayed in flash or specific sequences (Signal-Tech, 2020). Typical LED preemptive train warning signs are shown in Figure 40. Dynamic LED blank-out signals can be engineered as single-sided or double-sided signs. The LED signs include “no right turn on tracks”, “another train coming”, “2nd train coming”, “2nd train approaching”, etc. The approximate cost of a LED preemptive train warning sign is \$1,800 to \$5,500 per sign (TCRP-175, 2015).



Figure 40 Examples of a LED preemptive train warning sign.

Source: Signal-Tech. (2020). LED Light Rail Train Crossing Signals and Pedestrian Warning Signs

LED blinker signs

A blinker sign gives necessary warning at dangerous highway-rail grade crossings, whether on tracks with LED stop signs or crossbucks or “do not stop on tracks” signs. The blinker signs capture drivers’ attention when passing highway-rail grade crossings. The main advantages of this sign are (TAPCO, 2020): (1) MUTCD-compliant signs; (2) visible from more than one-mile distance due to high-intensity LEDs and increases driver’s awareness in fog, rain, day, night, and snow; (3) easy to install on any signpost and easy to use; (4) the wiring is protected from weather

and vandalism; (5) brightness levels adjust automatically maintaining optimum battery life and LED output; (6) the optional blinker beam upgrade can be used to synchronize multiple signs at a given location; and (7) availability of both solar and alternating current (AC) power options, so the signs can work in any situation. Typical LED blinker signs are shown in Figure 41.



Figure 41 Examples of a LED blinker sign.

Source: TAPCO. (2020). Safe Travels

Variable message signs (VMSs)

Variable message signs (VMSs) provide real-time displays that are versatile and show drivers what they need to know. VMSs can display vehicle speed that is updated frequently and give instant alerts and messages. VMSs can be customized for text size, colors, power options, and responsive messaging. Some important features of VMSs are: (1) data collection; (2) choice of power supply; (3) integrated flashing speed violator strobe; (4) advance scheduling; (5) instant updates; (6) strobe activation/deactivation; (7) animated text/graphics; (8) dual color display; (9) customized messaging; (10) multiple mounting options; and others. The approximate capital cost of a small VMS could be around \$40K-\$45K, while the approximate capital cost of a large VMS could go up to \$90K (U.S. DOT, 2020). The approximate operating cost of labor and replacement parts is \$600 per portable unit. Each portable unit has an approximate lifetime of 7 years (U.S. DOT, 2020). Several types of VMSs are available, such as flip disk or flip dot displays, LED display boards, hybrid display boards, etc.

A system of square, rectangular, or circular disks is used in flip disk or flip dot displays. They flip or rotate to form the intended character and display the associated message (see Figure 42). The main advantages of flip disk or flip dot displays are (ALFAZETA, 2020; U.S. Access Board, 2020): (1) excellent visibility under different light conditions; (2) small operational costs and fairly high reliability; (3) small power consumption; (4) small number of components; (5) showing a lot of information in a short span of time; and (6) ability to operate in extreme weather conditions with the temperatures ranging from -40°C to $+75^{\circ}\text{C}$. The main disadvantages include the following (U.S. Access Board, 2020): (1) disk failure is common that causes partial or entire message failure; (2) problem of uniform night-time illumination; (3) problem of optimal legibility; (4) artificial fonts are made with low resolution; (5) effective for displaying uppercase letters and numerals only; (6) reduced luminescence over a period of time due to reflective disk fading; and (7) light is reflected from the protective plastic due to scratches and dirt that further degrades visibility.



Figure 42 An example of a flip disk or flip dot display.
Source: Wikimedia Commons. (2020). Flip-dots



Figure 43 An example of a LED display board.
Source: Photon Play. (2020). VMS signs & VMS boards

LED display boards employ such a technology, where a cluster of solid-state diodes that form a pixel, is used to display the message. Each diode cluster glows and displays a message, when it is connected with power. Figure 43 illustrates a typical LED display board. Upper-case letters are mostly displayed in LED display boards; however, they are capable of displaying both upper and lower-case letters. The main advantages of LED display boards are (U.S. Access Board, 2020): (1) desired heights of the letters can be attained; (2) cost-effective; (3) the design is flat cabinet and solid state; (4) capable of graphics and animation; (4) reduced consumption of power; (5) luminescence can be controlled; and (6) long life of LED elements. The main disadvantages of LED display boards are (U.S. Access Board, 2020): (1) direct light glare on sign face; and (2) reduced illumination due to large viewing angles (new LED technologies started addressing this issue).

Hybrid display boards use both LED and flip disks, with a minor difference in display technology. A hole in the fiber disk allows light to pass through it. The disk is flipped when the pixel is activated, and LED generates light. Light thus passes through the hole and displays the message, written with shining dots (Photon Play, 2020). The main advantage of hybrid display boards is that they can overcome various shortcomings associated with other VMS technologies. Different features of different train warning signs are further summarized in Table 8.

Table 8 Features of train warning signs.

Type of Sign	Advantages	Disadvantages	Unit Cost	O&M Cost
LED preemptive train warning signs ^{1,2}	(1) help improving traffic operations and safety; (2) help mellowing down pedestrian risky behavior; (3) can be seen from far and can improve line of sight; (4) can be used as warning signs for pedestrians, bicyclists, and motorists.	(1) always need a power source to function; (2) unclear message can confuse pedestrians and motorists.	\$1,800 to \$5,500	
LED blinker signs ³	(1) MUTCD-compliant; (2) visible from more than one-mile distance; (3) easy to install on any signpost; (4) the wiring is protected from weather and vandalism; (5) brightness levels adjust automatically; (6) the optional blinker beam upgrade can be used to synchronize multiple signs; (7) availability of both solar and AC power options.	(1) use of solar-enabled signs in areas with less sunlight can be a challenge.	\$1,500-\$2,000	
VMS ^{4,5}	(1) data collection; (2) choice of power supply; (3) integrated flashing speed violator strobe; (4) advance scheduling; (5) instant updates; (6) strobe activation/deactivation; (7) animated text/graphics; (8) dual color display; (9) customized messaging; (10) multiple mounting options.	(1) not useful for roadway users who cannot see properly or have vision impairment.	\$40K-\$45K (small) up to \$90K (large)	\$600 (portable)

Notes: 1 – Signal-Tech. (2020). LED Light Rail Train Crossing Signals and Pedestrian Warning Signs

2 – TCRP-175. (2015). Guidebook on Pedestrian Crossings of Public Transit Rail Services

3 – TAPCO. (2020). Safe Travels

4 – U.S. Access Board. (2020). Advancing Full Access and Inclusion for All

5 – U.S. DOT (2020). Costs Database. Intelligent Transportation Systems

Table 8 Features of train warning signs (cont'd).

Type of Sign	Advantages	Disadvantages	Unit Cost	O&M Cost
Flip disk or flip dot displays ⁴	(1) excellent visibility under different light conditions; (2) small operational costs and fairly high reliability; (3) small power consumption; (4) small number of components; (5) showing a lot of information in a short span of time; (6) ability to operate in extreme weather conditions.	(1) disk failure is common; (2) problem of uniform night-time illumination; (3) problem of optimal legibility; (4) artificial fonts are made with low resolution; (5) effective for uppercase letters and numerals only; (6) reduced luminescence over a period of time; (7) scratches and dirt further degrade visibility.		
LED display boards ⁴	(1) desired heights of the letters; (2) cost-effective; (3) the design is flat cabinet and solid state; (4) capable of graphics and animation; (4) reduced power consumption; (5) luminescence can be controlled; (6) long life of LED elements.	(1) direct light glare on sign face; (2) reduced illumination due to large viewing angles (new LED technologies started addressing this issue).		
Hybrid display boards ⁶	(1) it overcomes various disadvantages associated with other VMS technologies.			

Notes: 4 – U.S. Access Board. (2020). Advancing Full Access and Inclusion for All
6 – Photon Play. (2020). VMS signs & VMS boards

2.2.5. Crossing Gate Technologies

Two-quad gate technology

Two-quad gates are installed to protect highway-rail grade crossings and are a type of boom barriers. Two-quad gates are often used in combination with a channelizing device or a raised median. A channelizing device or a raised median are generally stretched back at least 60 feet from a highway-rail grade crossing (100 feet is preferable) in order to eliminate the possibility of roadway users driving around the gates that have their arms placed in a horizontal position. The installation cost of two-quad gates is approximately \$150K, while their O&M cost comprises approximately \$5K-\$10K (Village of Glendale, 2007). An example of two-quad gates with a raised median is presented in Figure 44.

Four-quad gate technology

Similar to two-quad gates, four-quad gates are considered as a type of boom barriers. Four-quad gates are used for both sides of tracks for both directions of traffic (see Figure 45). The

installation of gates may vary from one country to another. Consideration of the four-quad gate system at any location should be thoroughly evaluated by experts. The evaluation should be performed by studying the specific configurations of the considered highway-rail grade crossing, site characteristics, highway geometry, among other components. Moreover, there is a need to utilize magnetometers for additional testing of new technologies and their industry evaluation. The main advantages of four-quad gates are: (1) all roadway lanes are covered by gates; (2) provide more visual restrictions; (3) more effective traffic restriction when compared to two-quad gates; and (4) reduced risk of accidents (including quiet zones).



Figure 44 An example of two-quad gates with a raised median.
Source: Donahey. (2019). Council Evaluating Railroad 'Quiet Zones'



Figure 45 An example of four-quad gates.
Source: FDOT. (2013). Improved Traffic Control Measures to Prevent Incorrect Turns at Highway-Rail Grade Crossings (Figure 2-21)

The installation and O&M costs of four-quad gates may substantially vary from one highway-rail grade crossing location to another. On average, the unit cost of four-quad gates is approximately \$250K-\$280K, while their O&M cost comprises approximately \$5K-\$10K (Village of Glendale,

2007; U.S. DOT, 2014a). Different features of various crossing gate technologies are further summarized in Table 9.

Table 9 Features of crossing gate technologies.

Type of Technology	Advantages	Disadvantages	Unit Cost	O&M Cost
Two-quad gates ^{1,2}	(1) provide certain visual restrictions; (2) reduced risk of accidents in quiet zones.	(1) do not provide additional considerations for people with disabilities; (2) require installation of channelizing devices to prevent vehicles driving around the gates.	\$150K	\$5K- \$10K
Four-quad gates ^{1,2}	(1) all roadway lanes are covered by gates; (2) provide more visual restrictions; (3) reduced risk of accidents in quiet zones.	(1) do not provide additional considerations for people with disabilities	\$250K- \$280K	\$5K- \$10K

Notes: 1 – Village of Glendale. (2007). Quiet Zone

2 –U.S. DOT. (2014a). GradeDec.NET Reference Manual

2.2.6. Detection Technologies

Remote control health monitoring systems

The FRA regulations require highway-rail grade crossing warning devices (e.g., flashing lights, gates) to be tested, maintained, and inspected periodically. There are different types of technologies on the market that can be used for monitoring the condition of warning devices at highway-rail grade crossings. For example, Ansaldo STS USA offers two devices, called TransPortal® Remote Monitor and TransPortal® Network. These devices are designed for wireless monitoring of highway-rail grade crossing warning equipment (Progressive Railroading, 2009). The TransPortal® system supports features, such as event recorder, that can be used for detection and reporting of malfunctions or any anomalies related to standby battery power problems, warning time problems, power outages, and others. There are two major benefits of the TransPortal® system, which are: (1) ability to remotely monitor parameters with different types of wireless/wired communication systems; and (2) ability to establish communications with legacy systems (Progressive Railroading, 2009).

Intelligent Interpreter (I2)

Intelligent Interpreter (I2), a next-generation communication controller, was developed as an interface provider between communication devices, such as wayside communication devices, defect detector devices, crossing controllers, and other types of devices that require remote monitoring through a central office processor using systems (e.g., Supervisory Control and Data Acquisition or SCADA) (Progressive Railroading, 2009). The interfacing can be established by the controller either to microprocessor- or relay-based systems. In case of a primary path failure, I2 allows to backup and permit redundant communication channels as well as to imitate any

similar communication protocols. The I2 technology allows a given agency to monitor the equipment health information at various highway-rail grade crossing locations.

InterTest

A computer-based system, called as “InterTest”, has been tested for several years at several locations along with some demonstrations (Progressive Railroading, 2009). InterTest serves as an automated interlocking computed-based test system that features proprietary and commercial hardware. The InterTest control point interfaces have to be connected to a router that further collects the information and helps to identify the state of the interlocking (including track current and switch motors as well as lamp outages). Some of the main InterTest applications include the following: (a) read the information from multiple locations that have a system with some sort of communications (e.g., wide-area network, radio); and (b) conduct in-service tests for new cutovers and construction. Furthermore, InterTest can assist with automation of post-installation testing and Positive Train Control (PTC). Alternative interlocking monitoring systems have been also introduced over the years by different companies.

Sicas S7

Sicas S7, which is a wayside controller interlocking platform, is used for monitoring and diagnostics of wayside electronics and controlled equipment (Progressive Railroading, 2009). The Sicas S7 system can be also applied for crossing control functions, especially in a transit-rail domain that does not necessitate a constant warning time. The first Sicas S7 system that uses various monitor switches and signals connected on passing sidings has been installed on a CSX corporation railroad line near Jacksonville (Florida). Sicas S7 is able to provide a monitoring functionality as well as fairly extensive remote diagnostics. Moreover, Sicas S7 can remotely monitor coded track circuit ballast conditions, switch machine throw times, along with light outages. The Sicas S7 system can be accessed from any computer that is connected to a network using a software-based control panel. The users can also interact with Sicas S7 via their cellular service or radio. The signal cabinet contains the processor that has a push-button or touch-screen capability.

Railway Management System (RMS) Smartrain®

Railway Management System (RMS) Smartrain® is an attempt of a system upgrade to a remote monitoring system that can monitor and manage the movement of trains as well as interface with highway-rail grade equipment and signals (Progressive Railroading, 2009). Smartrain® is designed to collect and distribute real-time data and process the data from numerous devices that are active within a given network. The information becomes available immediately, so the appropriate personnel can schedule maintenance activities without any delays and continuously monitor the condition of different equipment units. Smartrain® can help railroad companies to avoid substantial disruptions in their operations. The Smartrain® system can be integrated into the existing infrastructure and serve as a top supervisory layer. Moreover, Smartrain® combines different state-of-the-art technologies that encompass the elements of communications-based train control and Positive Train Control (PTC).

Loop detectors

Hilleary and John (2011) stated that four-quad gate warning systems use vehicle detection at highway-rail grade crossings to influence exit gate behavior at high-speed rail corridors and quiet

zones as a supplemental safety measure. Detection of vehicles that are stored, disabled, or purposely left on railroad tracks near highway-rail grade crossings, is an important feature for the fully deployed Positive Train Control (PTC) infrastructure. Some of the radar-based detection technologies have a good potential for highway-rail grade crossing applications and provide substantial improvements in the canonical embedded vehicle detection technologies. In some cases, vehicle detection is considered as a key functional requirement.

Various embedded technologies (e.g., inductive loops, magnetometers, technologies that use video analytics, microwave, infrared lights) have been used for detecting vehicles with varying success rates (Hilleary and John, 2011). Among such technologies, loop detectors are advantageous because of the following reasons (FHWA, 2007): (1) flexible design; (2) well-understood technology; (3) provide the information regarding major traffic parameters; (4) insensitive to adverse weather conditions; (5) provide better accuracy when comparing to other technologies; and (6) deploy high-frequency excitation models. The main disadvantages of loop detectors are (FHWA, 2007): (1) they require pavement cut for installation; (2) reduced pavement life; (3) lane closure is needed for installation; (4) wire loop is affected by traffic and temperature; and (5) each location requires more than one loop detector. The approximate unit cost of loop detectors is \$2.7K. The unit cost is based on the 2019-dollar value (U.S. DOT, 2020).

Infrared and video detectors

Despite an advanced video system and analytical ability to differentiate and recognize vehicles, infrared and video systems lack reliability, especially in the cases with insufficient light levels (Hilleary and John, 2011). Nevertheless, the main advantages of infrared detectors include the following (FHWA, 2007): (1) accurate measurement of vehicle class, speed, and position; and (2) can be operated for multiple lanes. However, infrared detectors do not perform well under adverse weather conditions. Moreover, lane closure is required for installation and maintenance of infrared detectors. Infrared detectors are classified as passive and active. Passive detectors work great if a user would like to detect a general movement but do not provide additional information regarding the object (Cook, 2018).

On the other hand, the main advantages of video detectors include the following (FHWA, 2007): (1) monitor multiple lanes and zones; (2) easy to modify or add zones; (3) can be used to collect a rich array of data; and (4) the information can be linked between cameras. In the meantime, video detectors have several drawbacks, including the following (FHWA, 2007): (1) lane closure is required for installation and maintenance; (2) accuracy is affected by weather conditions; (3) camera mounting is required; and (4) lighting is required for an adequate night-time performance. The unit cost of an active infrared detector is approximately \$2.5K based on the 2013-dollar value, while the unit cost of a video detection system is approximately \$17.5K based on the 2009-dollar value (U.S. DOT, 2020).

Microwave radars

Ultra-wideband radar systems and microwave radar systems operate at gigahertz (GHz) wavelengths and have the edge of passing through snow, rain, and fog (Hilleary and John, 2011). Microwave radar systems do not rely on ambient light levels, visibility, and are not influenced by background sunlight. Multiple microwave radars are typically required in order to effectively

monitor a given highway-rail grade crossing location. The conventional solutions of microwave radar technology have become unsatisfactory because of their cost and associated complexity that restricted their use in railroad applications. In summary, the main advantages of microwave radar systems include the following (FHWA, 2007): (1) generally insensitive to adverse weather conditions; (2) enable direct speed measurement; and (3) can be operated for multiple lanes. The main drawbacks of microwave radar systems include the following (FHWA, 2007; Hilleary and John, 2011): (1) high installation and maintenance costs; and (2) cannot detect vehicles that are stopped. The approximate unit cost of microwave radars is \$11K. The unit cost is based on the 2019-dollar value (U.S. DOT, 2020). Figure 46 presents a typical microwave radar.



Figure 46 An example of a microwave radar.

Source: Elmore Group. (2020). Microwave Vehicle Detection

Buried detection technologies

Buried inductive loops and magnetometers operate based on fairly simple principles of physics, detecting any fluctuations in a magnetic field caused by an approaching vehicle that has a sufficient metallic content (Hilleary and John, 2011). The buried inductive loops are embedded in the roadway, which further leads to some challenges (e.g., additional costs that are associated with installation of such detectors; maintenance of such detectors would require lane or even entire roadway closure). Magnetometers communicate with a local concentrator, which further introduces complexity in a local wireless network and may potentially impact reliability of the collected data. Buried inductive loops have been used in highway-rail grade crossing applications. However, new types of technologies (e.g., radar-based systems) become more preferential due to lower life-cycle costs. The cost of a two-inch electrical conduit of buried plastic is around \$14.00/linear ft. The unit cost is based on the 2019-dollar value (U.S. DOT, 2020). Different features of various detection technologies are further summarized in Table 10.

Table 10 Features of detection technologies.

Type of Technology	Advantages	Disadvantages	Unit Cost	O&M Cost
Remote control health monitoring systems ¹	(1) ability to remotely monitor parameters with different types of wireless/wired communication systems; (2) ability to establish communications with legacy systems.			
I2 ¹	(1) provide interface between communication devices, such as wayside communication devices, defect detector devices, and crossing controllers; (2) provide flawless backup.			
InterTest ¹	(1) require no direct connections with devices; (2) capable to remotely identify the state of the interlocking; (3) read the information from multiple locations; (4) automation of post-installation testing and positive train control			
Sicas S7 ¹	(1) extensive remote monitoring and diagnostics of wayside electronics; (2) extensive remote monitoring of controlled equipment; (3) best applicable in a transit-rail domain that does not necessitate a constant warning time; (4) effective monitoring of track circuit ballast conditions and light outages.			
RMS Smartrain® ¹	(1) effective collection and distribution of the information from numerous devices within a network; (2) ability to schedule repairs without delays; (3) integration with a Positive Train Control and other technologies.			

Notes: 1 – Progressive Railroading. (2009). C&S Technology - Remote Monitoring Systems

Table 10 Features of detection technologies (cont'd).

Type of Technology	Advantages	Disadvantages	Unit Cost	O&M Cost
Loop detectors ^{2,3}	(1) flexible design; (2) well-understood technology; (3) provide the information regarding major traffic parameters; (4) insensitive to adverse weather conditions; (5) provide good accuracy; (6) deploy high-frequency excitation models.	(1) pavement cut for installation; (2) reduced pavement life; (3) lane closure is needed for installation; (4) wire loop is affected by traffic and temperature; (5) each location requires more than one loop detector.	\$2.7K	
Infrared detectors ^{2,3}	(1) accurate measurement of vehicle class, speed, and position; (2) can be operated for multiple lanes.	(1) lane closure is required for installation; (2) do not perform well under adverse weather conditions.	\$2.5K	
Video detectors ^{2,3}	(1) monitor multiple lanes and zones; (2) easy to modify or add zones; (3) can be used to collect a rich array of data; (4) the information can be linked between cameras.	(1) lane closure is required for installation and maintenance; (2) accuracy is affected by weather conditions; (3) camera mounting is required; (4) lighting is required for night-time monitoring.	\$17.5K	
Microwave radars ^{2,3,4}	(1) insensitive to adverse weather conditions; (2) enable direct speed measurement; (3) can be operated for multiple lanes.	(1) high installation and maintenance costs; (2) cannot detect vehicles that are stopped.	\$11K	
Buried detection technologies ^{3,4}	(1) safe from vandalism and tempering; (2) enable basic data collection.	(1) environmental stress limits their useful life; (2) any failure in a check loop requires its complete replacement; (3) additional financial burden.	\$14.00 per ft for two-inch electrical conduit (buried plastic)	

Notes: 2 – FHWA. (2007). A Summary of Vehicle Detection and Surveillance Technologies Used in Intelligent Transportation Systems

3 – U.S. DOT. (2020). Costs Database. Intelligent Transportation Systems.

4 – Hilleary and John. (2011). Development and Testing of a Radar-Based Non-Embedded Vehicle Detection System.

2.2.7. Train Detection Devices

A reliable train detection system assists pedestrians and motorists passing a highway-rail grade crossing by warning them about incoming trains on the tracks and, thus, enhances safety. Railroad circuits are used by automated train detection devices. Signals using train detection devices can be activated by railroad equipment or due to vandalism or due to broken rail, since the system is designed to be fail-safe (Siemens, 2020a). Several train detection devices being used at highway-rail grade crossings include wide band shunts, narrow band shunts, test shunts, motion-sensing devices, constant warning time devices, audible warning devices, among others.

Wide band shunts

Wide band shunts introduce high impedance to direct current energy and low impedance to all alternating current frequencies. Thus, wide band shunts allow proper termination of approach circuits (Siemens, 2020a). The unit cost of wide band shunts could range from \$438 to \$1,165. This cost is based on the data provided in the 2020 Siemens Rail Infrastructure Price Guide (Siemens, 2020b).

Narrow band shunts

Narrow band shunts introduce high impedance to direct and alternating current frequencies outside the selected band and low impedance to a selected narrow band of alternating current frequencies. Therefore, the approach circuit can be properly terminated by the end users. Narrow band shunts are designed for the use in high-power applications and have higher than normal impedance. Furthermore, they require no tuning (Siemens, 2020a). The unit cost of narrow band shunts could range from \$619 to \$2,354. This cost is based on the data provided in the 2020 Siemens Rail Infrastructure Price Guide (Siemens, 2020b).

Test shunts

Test shunt is another type of shunts that offers convenience with positive shunting. The shunts can be easily removed or attached to the ball or the base of the rail using toggle clamps. A positive grip with a release lever is provided by toggle clamps to enable easy removal. A better electrical contact is achieved through implementation of hardened steel points. Any size of rail can be accommodated by using adjustable jaws (Siemens, 2020a). The shunt has a compression-molded center block and high-impact plastic that allow withstanding harsh field use. The unit cost of test shunts may vary between \$264 and \$642. This cost is based on the data provided in the 2020 Siemens Rail Infrastructure Price Guide (Siemens, 2020b).

Motion-sensing devices

A motion-sensing device is a solid-state electrical device that is connected to tracks at a highway-rail grade crossing. A series of points over the rail provide a signal for train detection. A train movement towards an intersection will activate the signal and provide a minimum warning time of 20 seconds (Texas DOT, 1995). As long as the train moves towards the intersection, the signal will stay activated. The direction and speed of trains can be monitored by placing the sensor devices, called terminating shunts. Because of improved efficiency and safety of vehicular traffic flow through highway-rail grade crossings, motion-sensing devices are deployed in passenger rail terminal areas as well as freight switching zones (Texas DOT, 1995).

Constant warning time devices

Constant warning time devices are similar to motion-sensing devices. These are connected to rail tracks at highway-rail grade crossings. The main purpose of these devices is to provide a fixed signal activation time, regardless of an approaching train's speed (Texas DOT, 1995). Constant warning time devices are expected to transmit signals that will activate warning devices at a highway-rail grade crossing at least 20 seconds before the train reaches that highway-rail grade crossing. Constant warning time devices are often installed at railroad tracks that are shared by passenger and freight trains because of their capability of providing a constant warning time.

Audible warning devices

Audible warning devices (e.g., horns, bells, train whistles) enhance safety by providing warnings to pedestrians, motorists, and other highway and railroad users in case of an approaching train. Since the year 1980, the FRA requires every lead locomotive to be installed with audible warning devices that can produce a sound level of 96 decibels at 30.50 meters ahead of the locomotive (Texas DOT, 1995). Figure 47 illustrates a typical audible warning device. The main advantages of audible warning devices include: (1) helpful for visually impaired people; (2) can alert vehicles and pedestrians from far; and (3) can be used in combination with signals. A disadvantage of audible warning devices is that there is no concrete evidence of their effectiveness supported by studies. The unit cost of an audible warning device is \$385.00. This cost is based on the data provided in TCRP-175 (2015). Different features of various train detection devices are further summarized in Table 11.

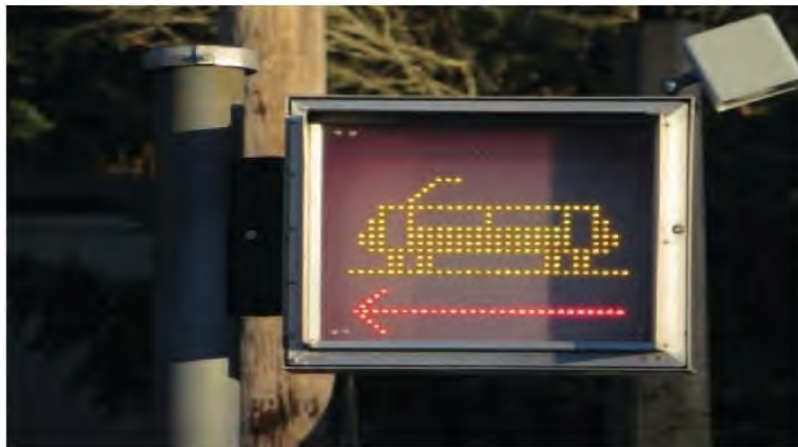


Figure 47 An audible warning device (upper right corner) near a blank-out sign.

Source: TCRP-175. (2015). Guidebook on Pedestrian Crossings of Public Transit Rail Services (Figure 118)

2.2.8. ITS-Based Communication Technologies

Dedicated Short-Range Communications (DSRC)

The use of existing technologies, such as the satellite Global Positioning System (GPS), could facilitate the communication between vehicles and trains (Singh et al., 2010). An implementation of the Dedicated Short-Range Communications (DSRC) further enables effective vehicle-to-infrastructure (V2I) and vehicle-to-vehicle (V2V) communications to facilitate the development of ITS and enhance safety at highway-rail grade crossings. The major potential benefits of the DSRC include mobility, safety, and a wide range of applications for commercial use.

Standardization and development of the DSRC technology could provide cost-effective solutions as well as offer various economic, social, and environmental benefits. The architecture of the DSRC is depicted in Figure 48.

Table 11 Features of train detection devices.

Type of Device	Advantages	Disadvantages	Unit Cost	O&M Cost
Wide band shunts ^{1,2}	(1) enable train detection.		\$438 to \$1,165	
Narrow band shunts ^{1,2}	(1) designed for the use in high-power applications; (2) have higher than normal impedance; (3) require no tuning.		\$619 to \$2,354	
Test shunts ^{1,2}	(1) convenience with positive shunting; (2) resistance to rust and scale; (3) allow withstanding harsh field use.		\$264 to \$642	
Motion-sensing devices ³	(1) can monitor a train's direction and speed; (2) offer efficiency and safety; (3) provide warning time in case of approaching trains.	(1) the installation can be costly.		
Constant warning time devices ³	(1) can monitor a train's direction and speed; (2) offer efficiency and safety; (3) provide warning time in case of approaching trains.	(1) the installation can be costly.		
Audible warning devices ⁴	(1) helpful for visually impaired people; (2) can alert vehicles and pedestrians from far; (3) can be used in combination with signals.	(1) there is no concrete evidence of effectiveness.	\$385	

Notes: 1 – Siemens. (2020a). Crossings – Train Detection

2 – Siemens. (2020b). 2020 Siemens Rail Infrastructure Price Guide

3 – Texas DOT. (1995). Enhanced Traffic Control Devices and Railroad Operations for Highway-Railroad Grade Crossings: First Year Activities

4 – TCRP-175. (2015). Guidebook on Pedestrian Crossings of Public Transit Rail Services

U.S. DOT (2015) described the DSRC as a short-range, reliable, high-speed two-way wireless radio service that can be used effectively for V2V and V2I communications. The DSRC permits and provides an efficient and robust environment for sharing the highway-rail grade crossing safety information. The situational information provided through the DSRC is updated regularly between connected vehicles, and its operations are done in a constant broadcast-receive mode. Evaluation of the information regarding a warning message to drivers to see if it is needed to be sent is done independently. A basic safety message (BSM) from vehicles equipped with the DSRC can be broadcast on a 5.9 GHz spectrum (U.S. DOT, 2015). Note that the vehicle

situational elements, including position, size, speed, heading direction, brake status, steering angle, etc., can be included in the BSM as well.

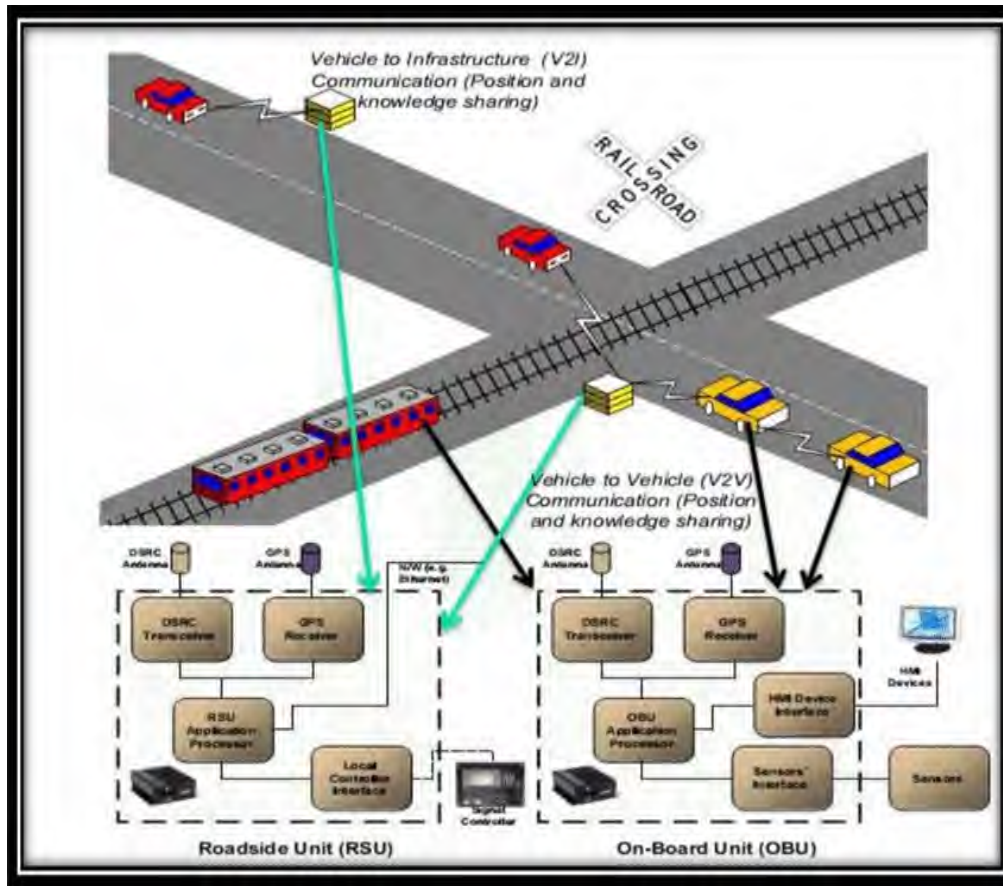


Figure 48 An architecture of the DSRC.

Source: Singh et al. (2010). Intelligent Transportation System to Improve Safety at Level Crossing

The DSRC is capable of broadcasting the BSM quite frequently (e.g., every 100 milliseconds). Some other communication technologies are not as efficient as the DSRC, since they rely on a one-to-one, not one-to-many, communication. The efficiency of other designs is reduced because of their need to establish one-to-one connections. One-to-one connections may result in substantial delays in the information flow between vehicles. When the DSRC is deployed, the recipient and the source do not have to be connected directly. Hence, the user privacy can be protected by establishing trust between the available parties (e.g., particular security credentials can be established in order to enable communication). The DSRC has been specifically developed for rapidly moving environments, where the receiver and the sender can be moving away from each other at speeds that are greater than 100 mph (U.S. DOT, 2015).

The DSRC has a number of advantages for effective V2V communications which include the following (U.S. DOT, 2015): (1) no network connection is needed to broadcast messages; (2) the messages are generally small enough and can be processed quickly and broadcast frequently; (3) secure and anonymous communication between vehicles; (4) provide communication capabilities

in a rapidly moving environment; and (5) strong performance during adverse weather conditions. The cost of DSRC technology is calculated on a per-site basis. The unit installation cost for the DSRC Roadside Unit (RSU) backhaul communications connection is approximately \$40K based on the 2016-dollar value (U.S. DOT, 2020), but may vary from one location to another. On the other hand, the unit installation cost for the DSRC onboard unit is \$1,500 based on the 2017-dollar value (U.S. DOT, 2020).

Aftermarket Safety Device (ASD)

Aftermarket Safety Devices (ASDs) are installed on a vehicle after its manufacturing is complete. As a V2V communication device, the ASD receives the location and speed information from other vehicles and can provide alerts to drivers (Safety Pilot, 2012). The level of V2V connection varies from one device to another. However, ASDs generally do not have a full integration with the vehicles. The cost of ASDs depends on the model and configurations. The expected costs of V2V communication (where ASDs serve as a component) range from \$341 to \$350 in 2020 but are expected to decrease to \$209 – \$227 in 2058 (U.S. DOT, 2020). A typical ASD is shown in Figure 49.



Figure 49 An example of an ASD.

Source: Safety Pilot. (2012). Technology

Retrofit Safety Device (RSD)

A Retrofit Safety Device (RSD) can be integrated into vehicles at the manufacturing stage. It is not limited to a particular type of vehicles. RSDs can be installed not only into the new vehicles, but into the older models as well, to ensure that different types of vehicles will benefit from the connected commercial vehicle applications. Figure 50 demonstrates some examples of the cues that can be provided by the RSD as a part of safety applications, including the following (U.S. DOT, 2014b): (1) Forward Collision Warning (FCW); (2) Emergency Electronic Brake Lights (EEBL); (3) Blind Spot Warning (BSW); (4) Curve Speed Warning (CSW); and (5) Intersection Movement Assist (IMA). Note that the FCW, EEBL, and IMA warnings could be accompanied with audible tones. An example of a truck that is equipped with the RSD hardware, RSD software, and DSRC antennas, is presented in Figure 51. The estimated consumer cost for an RSD is approximately \$300 based on the 2012-dollar value (U.S. DOT, 2020).










Safety Application	Inform	Warning (FCW, EEBL, and IMA were accompanied by audible tones.)
Forward Collision Warning (FCW)		
Emergency Electronic Brake Light (EEBL)		
Blind Spot Warning (BSW)		(There was no warn-level blind spot alert.)
Curve Speed Warning (CSW)		
Intersection Movement Assist (IMA)		

Figure 50 Example cues provided by an RSD.

Source: U.S. DOT. (2014b). *Connected Commercial Vehicles-Retrofit Safety Device Kit Project*



Figure 51 A truck equipped with the RSD device and DSRC antennas (pointed by an arrow).

Source: U.S. DOT. (2014b). *Connected Commercial Vehicles-Retrofit Safety Device Kit Project*

Vehicle Awareness Device (VAD)

The Vehicle Awareness Device (VAD) technology has a very simple design. As a V2V communication device, the VAD receives the location and speed information from other vehicles and can provide this information to the driver (Safety Pilot, 2012). However, it does not have the ability to provide any visual warnings to the driver due to the missing driver interface with safety applications (unlike RSD). The VAD is generally installed under the seat of a vehicle, while the GPS antenna is typically placed above the truck lid on a paint-protective film. Various businesses (e.g., private vehicles, rental agencies, and various fleet owners) can benefit from VADs. The estimated consumer cost for a VAD is approximately \$160 based on the 2012-dollar value (U.S. DOT, 2014c). A typical VAD is shown in Figure 52.



Figure 52 A typical VAD.

Source: Safety Pilot. (2012). Technology

Railroad Crossing Violation Warning System (RCVW)

The Railroad Crossing Violation Warning System (RCVW) is considered as a vehicle-to-infrastructure (V2I) application that combines features of certain previously developed connected vehicle technologies and components (U.S. DOT, 2017). The RCVW system includes two separate subsystems: (a) a roadside-based subsystem that is integrated with the roadside infrastructure near highway-rail grade crossings; and (b) a vehicle-based subsystem that is specifically installed inside connected vehicles. Both subsystems include the same software and hardware components, such as the computing platform, DSRC radios, and a GPS module. A vehicle-based subsystem is equipped with the driver visual interface that is able to provide warnings and visual alerts to the vehicle driver as needed. The RCVW system can also provide a real-time condition-based visual and audible warning to vehicle drivers regarding potential violations of other drivers at highway-rail grade crossings.

The main purpose of the RCVW system is to reduce the occurrence of accidents at highway-rail grade crossings as well as their severity. The RCVW is also expected to lead to the mobility-related operational improvements and a flexible design. The application concept of the RCVW is demonstrated in Figure 53. The main advantages of the RCVW system include the following (U.S. DOT, 2017): (1) reduction in the vehicle response time during an emergency; (2) improved routing and traffic flow efficiency; (3) energy consumption reduction; (4) air pollution reduction; and (5) reduction in the number of accidents.



Figure 53 The RCVW application concept.

Source: U.S. DOT. (2017). Vehicle to Infrastructure Prototype Rail Crossing Violation Warning Application (Page 11)

Other emerging ITS-based technologies

The ITS-based technologies at highway-rail grade crossings are used to provide efficiency, control, productivity, as well as communication with trains. There are five different functional areas for implementation of various ITS-based technologies at highway-rail grade crossings which include the following (Minnesota DOT, 2005): (1) in-vehicle warning system; (2) second train warning system; (3) use of crossing blockage data; (4) four-quad gates with an automatic train stop; and (5) a set of technologies that is known as the Intelligent Grade Crossing.

The HRI-2000 (Highway-Rail Intersection Active Warning System) is considered as one of the emerging ITS-based technologies that can be deployed at highway-rail grade crossings to improve operations and safety. The HRI-2000 system was developed by C3 Trans Systems in collaboration with a set of other organizations (FRA, FHWA, Minnesota DOT, and different consulting companies). This system initiates an additional active warning to roadway users along with the traditional equipment that is used at highway-rail grade crossings (e.g., flashing lights). The HRI-2000 relies on LED flashers to conserve power. An example of the HRI-2000 system installation at a highway-rail grade crossing is presented in Figure 54. Generally, there are four major subsystems: one on each advance warning sign and one on each crossbuck (i.e., master and slave). These subsystems can effectively communicate with each other (e.g., the information regarding the approaching train can be transferred from a master crossbuck to other signs). Multiple microcontrollers, GPS, and digital radios are used for a wide array of applications, including the following: (1) train detection; (2) flasher activation; (3) fault diagnostics; (4) automatic reporting; (5) data collection; and (6) in-locomotive warning. The flashers are primarily activated by using the radio.

The HRI-2000 system was developed with the main goal of providing a constant warning to roadway users regardless of the current train speed. The data exchange between the highway-rail grade crossing and the locomotive will begin via the beacon, once the train is approximately 5 kilometers away from the highway-rail grade crossing. Based on the train speed, travel direction,

and travel location, the warning devices at the highway-rail grade crossing will be activated using the pre-defined warning time and will remain activated until the train passes this crossing. The HRI-2000 system developers aimed to design a low-cost active warning ITS-based technology. The average HRI-2000 installation cost varies from \$10K to \$15K (Minnesota DOT, 2005). Installation cost savings as compared to other ITS-based technologies can be justified by the implementation of solar energy as a power source and a GPS system for train detection. Packaging and advanced electronic design also play an important role in achieving cost-effectiveness.

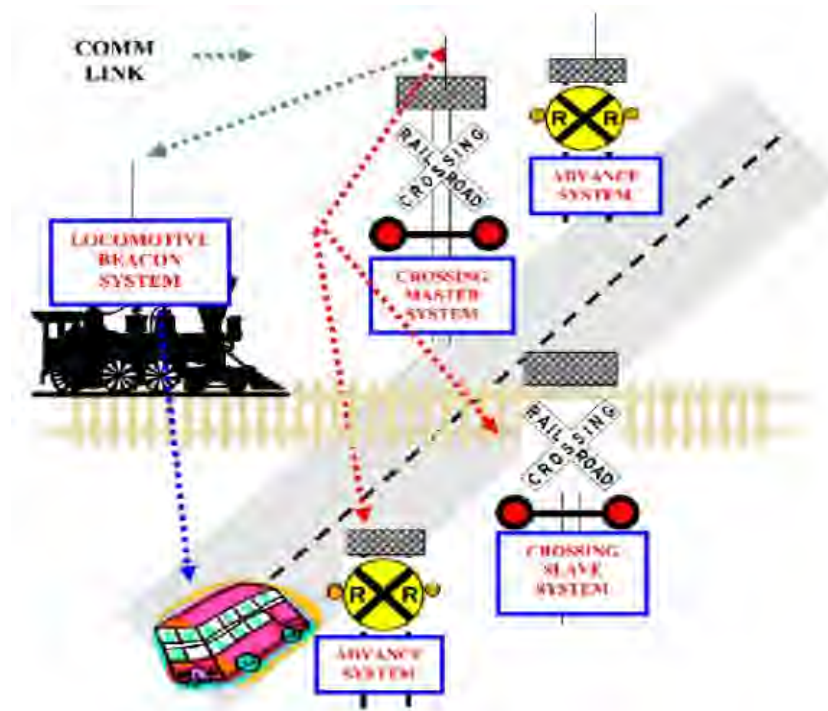


Figure 54 An example of the HRI-2000 system installation.

Source: Minnesota DOT. (2005). Low-Cost Highway-Rail Intersection Active Warning System Field Operational Test (Page 14)

Positive Train Control (PTC)

The Positive Train Control (PTC) technology has been devised as a rail safety system that breaks a train or automatically slows down a train in case it goes over the speed limit or misses a signal, thus reducing human errors (BNSF Railway, 2017). This system also reduces accidents that are caused by errors made by dispatchers or train operators. Moreover, it is suitable for wayside safety of rail workers, temporary speed restrictions, and collision avoidance by train separation. High-band radio transmission, GPS, and Wireless Fidelity (Wi-Fi) are used by the PTC to ensure that it determines the location of the train, and the train does not exceed the speed limit beyond the specified speed limit (see Figure 55). The PTC stops a moving train in case the train crew is unresponsive and checks unwarranted movement on new segments of the track. Two levels of PTCs were denoted by FRA (2004) that include the PTC Level A and the PTC Level B. The PTC Level A, or PTC A, is a lower-end system, and it does not replace the existing operation method. The approximate cost of PTC A is \$15K to \$25K per locomotive (FRA, 2004). On the other hand, the PTC Level B, or PTC B, is a higher-end, more extensive system. It is designed in

compliance with safety principles as a stand-alone system. The approximate cost of the PTC B is \$20K to \$35K per locomotive (FRA, 2004).

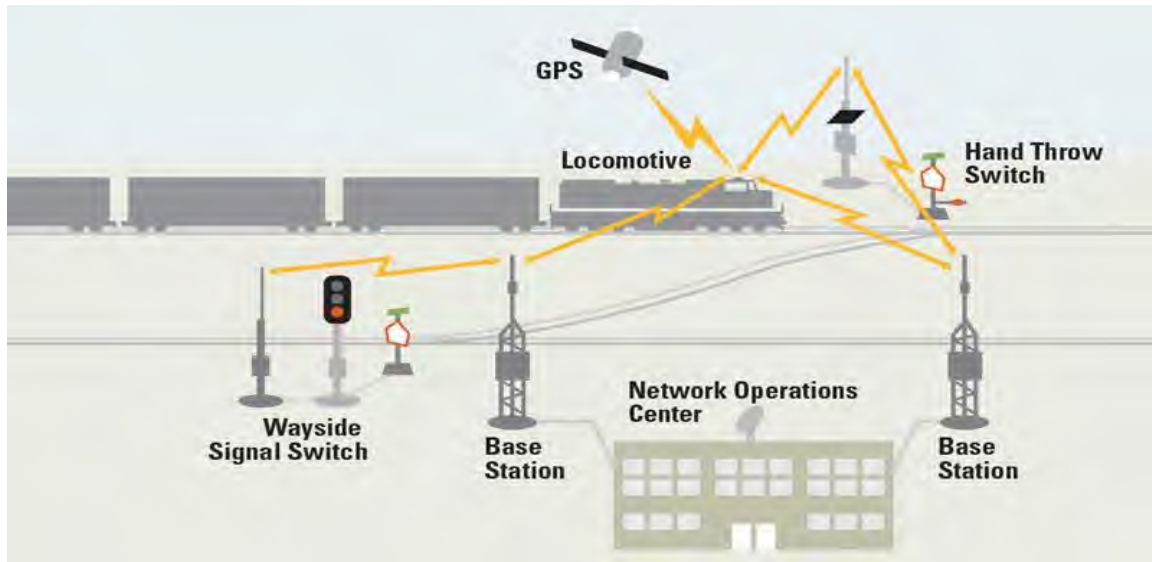


Figure 55 An example of the PTC technology.

Source: BNSF Railway. (2017). Positive Train Control and BNSF in the Pacific Northwest

Hartong et al. (2011) stated that extensive federal regulations and compliance governed the PTC system in the U.S. Before implementing the PTC system into a revenue stream on a railroad, a set of necessary regulations must be in place. The most critical component of these regulations is to undertake a detailed quantitative analysis to compare before- and after-risk in the installation of the PTC system. A quantitative analysis is an important functional requirement that is performed on a railroad. Like a conventional signal system, the main aim of the PTC system is to have a fail-safe operation if communication is lost. Unlike traditional railroad signals, leeway is allowed for the safety functionality of the first and the second order. The first-order safety functionalities are required to ensure a safe operation of a rail system. Unsafe system operations may occur due to the loss of first-order safety functionalities. On the other hand, the second-order safety functionalities are generally applied in conjunction with some other functions to ensure safe operations. Loss of one second-order function will not cause an inability to safely operate a given rail system, unless this loss is coupled with a loss of another second-order function (Hartong et al., 2011).

Resor et al. (2005) indicated that some major benefits of the PTC include: (1) improved reliability in service; (2) enhancement of line capacity; (3) faster running time over the road; (4) more efficient use of locomotives and cars based on real-time location information; (5) reduction in locomotive failure due to real-time diagnostics; (6) provide larger windows for maintenance workers to perform their responsibilities safely and conduct necessary railroad track repairs/checks; and (7) fuel savings. The PTC implementation cost is considered as one of the major drawbacks of this technology. Resor et al. (2005) mentioned that the PTC deployment on a Class I railroad network (with approximately 20,000 locomotives and 99,000 route miles) would range between \$2.3 billion and \$4.4 billion over a five-year time period. On the other hand, the annual benefits after the full PTC implementation were estimated to vary from \$2.2 billion to

\$3.8 billion. The internal rate of return for the PTC technology was found to range between 44% and 160% (Resor et al., 2005). Another challenge in the PTC implementation consists in the fact that it requires a wide range of technical components working cohesively, which may not be easy to achieve. Different features of various ITS-based technologies and devices are further summarized in Table 12.

Table 12 Features of ITS-based technologies.

Type of Technology	Advantages	Disadvantages	Unit Cost	O&M Cost
DSRC ^{1,2}	(1) no network connection is needed to broadcast messages; (2) the messages can be generally processed quickly; (3) secure and anonymous communication; (4) communication capabilities in a rapidly moving environment; (5) strong performance during adverse weather conditions.	(1) employed radios are expensive; (2) seamless connectivity is still a problem; (3) no ability to restrict incorrect information.	\$40K for the roadside unit and \$1.5K for the onboard unit	
ASD ^{2,3}	(1) ability to alert drivers through V2V communications; (2) fairly low-cost implementation.	(1) do not have a full integration with the vehicles; (2) do not provide visual alerts.	\$341 to \$350	
RSD ^{2,4}	(1) can support multiple applications; (2) robust performance because of access to quality data from integration; (3) fairly low-cost implementation.	(1) heavily dependent on other components (e.g., DSRC antenna, GPS)	\$300	
VAD ^{3,5}	(1) ability to transmit the location and speed information; (2) fairly low-cost implementation.	(1) do not have a full integration with the vehicles; (2) do not provide visual alerts.	\$160	

Notes: 1 – U.S. DOT. (2015). Status of the Dedicated Short-Range Communications Technology and Applications.

2 – U.S. DOT. (2020). Costs Database. Intelligent Transportation Systems.

3 – Safety Pilot. (2012). Technology.

4 – U.S. DOT. (2014b). Connected Commercial Vehicles-Retrofit Safety Device Kit Project

5 – U.S. DOT. (2014c). Vehicle-to-Vehicle Communications: Readiness of V2V Technology for Application

Table 12 Features of ITS-based technologies (cont'd).

Type of Technology	Advantages	Disadvantages	Unit Cost	O&M Cost
RCVW ⁶	(1) reduced emergency response time; (2) traffic flow improvements; (3) energy consumption reduction; (4) air pollution reduction; (5) improved safety.	(1) the system includes a lot of components that may be challenging to simultaneously operate; (2) audible warning may not be effective.		
HRI-2000 ⁷	(1) cost-effectiveness; (2) provide additional warning apart from traditional flashing lights; (3) provides a constant warning; (4) fault diagnostics; (5) data collection; (6) in-locomotive warning.	(1) the system is more beneficial at short lines and regional railroads than larger railroads; (2) difficulty to justify the cost-benefit ratio.	\$10K to \$15K	
PTC ^{8,9}	(1) improved reliability in service; (2) enhancement of line capacity; (3) faster running time over the road; (4) more efficient use of locomotives and cars based on real-time location information; (5) less frequent failures of locomotives; (6) larger windows for maintenance workers; (7) fuel savings.	(1) requirement of various technical components to work cohesively; (2) time-consuming testing of various components; (3) incomplete radio system requirements; (4) limitations in radio bandwidth; (5) fairly high-cost implementation.	\$15K to \$25K for PTC A and \$20K to \$35K for PTC B (per locomotive)	

Notes: 6 – U.S. DOT. (2017). Vehicle to Infrastructure Prototype Rail Crossing Violation Warning Application

7 – Minnesota DOT. (2005). Low-Cost Highway-Rail Intersection Active Warning System Field Operational Test.

8 – Resor et al. (2005). Positive Train Control (PTC): Calculating Benefits and Costs of a New Railroad Control Technology

9 – FRA. (2004). Benefits and Costs of Positive Train Control

2.2.9. Other Types of Warning Devices and Advanced Technology at Highway-Rail Grade Crossings

Channelization

Channelization is implemented at highway-rail grade crossings to avoid collisions through diversion from oncoming traffic. Channelization can help reducing the number of accidents at highway-rail grade crossings by restricting driver access to other lanes. Furthermore,

channelization is used as a safety tool at highway-rail grade crossings for directing pedestrians to a specific location by reducing conflicts between trains and pedestrians (TCRP-175, 2015). Types of channelization devices include raised wide medians, mountable raised curb systems (see Figure 56), barrier wall systems, among others (U.S. DOT, 2019). A barrier wall is considered as one of the most restrictive types of channelization. The approximate cost of installing a channelizing device is approximately \$334/linear ft and \$2,000 for 12 yellow delineators (TCRP-175, 2015).



Figure 56 An example of a mountable raised curb system.
Source: U.S. DOT. (2019). Highway-Rail Crossing Handbook (Figure 37)



Figure 57 An example of bollards.
Source: TCRP-175. (2015). Guidebook on Pedestrian Crossings of Public Transit Rail Services (Figure 158)

Bollards

Bollards are used as one of the methods to delineate the edge of a highway-rail grade crossing. Figure 57 demonstrates typical bollards. The main advantages of bollards are: (1) they are easy to notice; and (2) they are useful for people trying to access railroad stations or crossing roads. The approximate unit cost of bollards is \$730. This cost is based on the data provided in TCRP-175 (2015).

Dynamic envelope zone pavement markings and signage

Typical dynamic envelope zone pavement markings and signage are presented in Figure 58 and Figure 59, respectively. The main objective of adding dynamic envelope zone pavement markings and signage is to effectively guide roadway users approaching highway-rail grade crossings and decrease the number of roadway users stopping within the dynamic envelope zone (U.S. DOT, 2014d). A reduction in the number of roadway users stopping within the dynamic envelope zone is expected to decrease the number of accidents at highway-rail grade crossings and improve safety of vehicle passengers, train passengers, train crew, and other individuals involved. The implementation of the dynamic envelope zone pavement markings and signage has a potential of preventing roadway users from stopping near the dangerous zones (i.e., in a close proximity to railroad tracks). However, the dynamic envelope zone may not necessarily change actions of the roadway users who entered the dangerous zone (U.S. DOT, 2014d). In particular, some of the roadway users may not be willing to reverse after entering the dangerous zone despite the presence of a dynamic envelope zone.



Figure 58 An example of dynamic envelope zone pavement markings.

Source: U.S. DOT. (2014d). Effect of Dynamic Envelope Pavement Markings on Vehicle Driver Behavior at a Highway-Rail Grade Crossing (Page 11)

Additional field studies and engineering analyses are required before installing the dynamic envelope zone at a given highway-rail grade crossing to ensure that it will serve as an effective countermeasure against roadway user violations. The cost of pavement markings within the dynamic envelope zone is fairly low. The approximate cost for a 4-inch thermoplastic traffic stripe that is used for the dynamic envelope zone markings is \$0.49/linear ft. This cost is based on the data provided in TCRP-175 (2015).



Figure 59 An example of a dynamic envelope zone modified signage.

Source: U.S. DOT. (2014d). Effect of Dynamic Envelope Pavement Markings on Vehicle Driver Behavior at a Highway-Rail Grade Crossing (Page 11)

Wayside system

The wayside system is used to monitor the signals of tracks on a railroad and to communicate with a locomotive of an approaching train. The wayside system uses switches and track circuits. All the necessary information related to train operations and the rail network is stored by a back office. The authorization of train movements to operate on a new segment of tracks is transmitted by the server of the back office. The wayside system is considered as an integral part of the Positive Train Control (PTC) system and contains signals, defect detectors, track switches, and radio towers. The unit cost of a wayside system may vary from \$16K to \$24K based on the 2001-dollar value (Resor et al., 2005).

Video cameras

Video cameras can be used as an effective countermeasure for the highway-rail grade crossings that are equipped with gate assemblies. Some types of gates (e.g., two-quad gates) do not prevent roadway users driving around the gates that have their arms placed in a horizontal position. However, when roadway users approach a highway-rail grade crossing and notice that it is equipped with a video camera, they tend to avoid crossing gate violations (as their actions are recorded on a video camera). The installation cost of photo enforcement is approximately \$65K based on the 2014-dollar value, while the O&M cost is approximately \$25K (U.S. DOT, 2014a). Different features of other types of warning devices and advanced technology at highway-rail grade crossings are summarized in Table 13.

Table 13 Features of other types of warning devices and advanced technology at highway-rail grade crossings.

Type of devices	Advantages	Disadvantages	Unit Cost	O&M Cost
Channelization ^{1,2}	(1) minimizes conflict between trains, pedestrians, and bicyclists; (2) pedestrian movement can be controlled positively.	(1) not useful for roadway users who cannot see properly or have vision impairment.	\$334/linear ft and \$2,000 for 12 yellow delineators	
Bollards ²	(1) flexible; (2) easily noticeable; (3) useful for people trying to access rail stations or crossing roads.	(1) not useful for roadway users who cannot see properly or have vision impairment.	\$730	
Dynamic envelope zone pavement markings and signage ^{2,3}	(1) effective in guiding roadway users approaching a highway-rail grade crossing; (2) improved safety of roadway users.	(1) not useful for roadway users who cannot see properly or have vision impairment; (2) engineering studies are needed before implementation.	\$0.49/linear ft for 4-inch traffic stripe	
Wayside system ^{4,5}	(1) improved reliability in service; (2) enhancement of line capacity; (3) faster running time over the road; (4) more efficient use of locomotives and cars based on real-time location information; (5) less frequent failures of locomotives; (6) larger windows for maintenance workers; (7) fuel savings.	(1) requirement of various technical components to work cohesively; (2) time-consuming testing of various components; (3) incomplete radio system requirements; (4) limitations in radio bandwidth; (5) fairly high-cost implementation	\$16K to \$24K	

Notes: 1 – U.S. DOT. (2019). Highway-Rail Crossing Handbook

2 – TCRP-175. (2015). Guidebook on Pedestrian Crossings of Public Transit Rail Services

3 – U.S. DOT. (2014d). Effect of Dynamic Envelope Pavement Markings on Vehicle Driver Behavior at a Highway-Rail Grade Crossing

4 – Resor et al. (2005). Positive Train Control (PTC): Calculating Benefits and Costs of a New Railroad Control Technology

5 – FRA. (2004). Benefits and Costs of Positive Train Control

Table 13 Features of other types of warning devices and advanced technology at highway-rail grade crossings (cont'd).

Type of devices	Advantages	Disadvantages	Unit Cost	O&M Cost
Video cameras ⁶	(1) effective addition to gate assemblies; (2) simple installation; (3) recorded behavior of roadway users.	(1) do not provide any physical barriers; (2) fairly expensive countermeasure.	\$65K	\$25K

Notes: 6 – U.S. DOT. (2014d). GradeDec.NET Reference Manual

2.3. Connected and Autonomous Vehicle Applications at Highway-Rail Grade Crossings

Deployment of connected vehicles is expected to provide a high level of safety at highway-rail grade crossings. Innovation in wireless technologies, which facilitated advancements towards new connected vehicle technologies, has provided an opportunity to improve highway-rail grade crossing safety. Various DSRC technologies and devices discussed in the previous section of the report are being used for the connected vehicle technology. Elliott et al. (2019) highlighted five focus areas in the connected and autonomous vehicle (CAV) research that include the following: (1) inter-CAV communications; (2) security of CAVs; (3) CAV control at intersections using various technologies; (4) accident-free navigation of CAVs; and (5) ability to detect and protect pedestrians. The movement of CAVs and their success depend on the DSRC technologies (see section 2.2.8 for details) and 5th generation (5G) wireless cellular technology.



Figure 60 The CAV technology and highway-rail grade crossing communication.

Source: Zaouk and Ozdemir. (2017). *Implementing Connected Vehicle and Autonomous Vehicle Technologies at Highway-Rail Grade Crossings*

One of the most important aspects of connected vehicles is the vehicle-to-infrastructure (V2I) interaction. The V2I communication technology enables the transmission of data from a vehicle to the infrastructure and vice versa (see Figure 60). The data collected from the infrastructure is used to understand the pattern of vehicle groups and their behavior, including the speed and acceleration of vehicles passing a highway-rail grade crossing. The existing traffic conditions are being considered as well. Another important information used by vehicles about the

infrastructure is the condition of highway-rail grade crossings. CAVs use a combination of devices and technologies that need to work in synchronization with each other in order to enhance safety. Various BSMs are broadcast using different detection technologies, and smart signals are adjusted accordingly. These technologies alert the user through various warning devices when it is unsafe to enter a highway-rail grade crossing (Zaouk and Ozdemir, 2017). The following sections of the report elaborate more on different CAV technologies that have a potential of improving safety at highway-rail grade crossings.

2.3.1. Internet of Things (IoT)

The Internet of Things (IoT) is a next generation technology that uses high-speed internet technology and involves advanced wireless connectivity of various devices, systems, and applications. The IoT technology relies on advanced machine learning, big data, advanced sensors, cloud computing, and other futuristic applications that can be used to analyze data. This complex data analysis can help providing efficiency and safety in the system. For instance, the IoT technology can use advanced GPS applications to opt for different routes based on the current position of a train that is approaching a given highway-rail grade crossing (Figure 61).

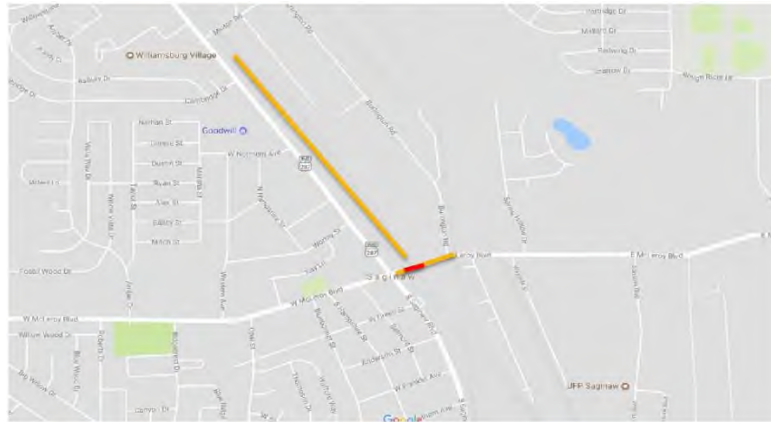


Figure 61 Alternate routing with the Internet of Things.

Source: Young. (2017). 2017 Grade Crossing Research Needs Conference

2.3.2. Autonomous Vehicle Technology

The autonomous vehicle (AV) technology is expected to play a major role in achieving a zero-accident vision at highway-rail grade crossings, along with the CAV technology. This technology has a great potential to enhance safety as well as efficiency at highway-rail grade crossings. A major issue regarding the AV technology is that its testing on real-world scenarios is restricted. Organizing field studies on the advantages and shortcomings of the AV technology at/near highway-rail grade crossings still remains a challenge. However, there are still some research attempts being made towards the integration of various connected vehicle technologies at highway-rail grade crossings for a safe and efficient AV movement. New technologies are providing great opportunities for the safety of users passing highway-rail grade crossings. Deployment of fully autonomous trains could eliminate human errors when vehicles would also use a fully automated technology. AVs at highway-rail grade crossings may substantially benefit from the future technologies that have the following features (Association of American Railroads, 2020): (1) ability to detect nearby highway-rail grade crossings using pavement markings and signs; (2) ability to detect approaching trains as well as locomotive devices (e.g.,

horns, bells, headlights); and (3) ability to avoid stopping on highway-rail grade crossing tracks due to traffic queues and other reasons and, therefore, reducing the risk of accidents.

AVs are equipped with the technologies that can comprehend the surrounding infrastructure and move with either no driver input or partial driver input, which depends on the level of automation achieved (see Figure 62). The SAE International's J3016 standards outlined a total of six levels of automation for AVs that are demonstrated in Figure 63 (SAE International, 2019). The levels of automation range from no automation to full automation. There is a sharp distinction between Level 2 and Level 3, which underlines a transition from the required driver inputs to auto pilot (i.e., the vehicle drives on its own).



Figure 62 An example of an autonomous vehicle.

Source: Zaouk and Ozdemir. (2017). Implementing Connected Vehicle and Autonomous Vehicle Technologies at Highway-Rail Grade Crossings

Substantial research efforts are currently being performed in the field of CAVs. Furthermore, significant development efforts are being made by several parties, such as vehicle manufacturers as well as suppliers of various devices and technologies. The level of automation is steadily moving towards Level 2 (especially, light passenger vehicles), where some important functions, such as acceleration, braking, movement of the steering wheel, adaptive cruise control, and lane centering, are handled by AVs. Efforts are continuously being made to move from a partial level of automation to a full-automation level. Present research and development efforts focus on the processing of onboard vehicle information and sensor fusion, with an aim to improve the driver assistance technology and driver acceptance (Zaouk and Ozdemir, 2017). However, a significant concern that is associated with the CAV technology is over-dependence on the technology aspect. There are many technology reliability issues regarding CAVs that have to be addressed before a full-automation level can be achieved. Although the system performance is expected to continuously improve, human attention may start declining. A decline in human attention may further lead to human errors (Zaouk and Ozdemir, 2017).

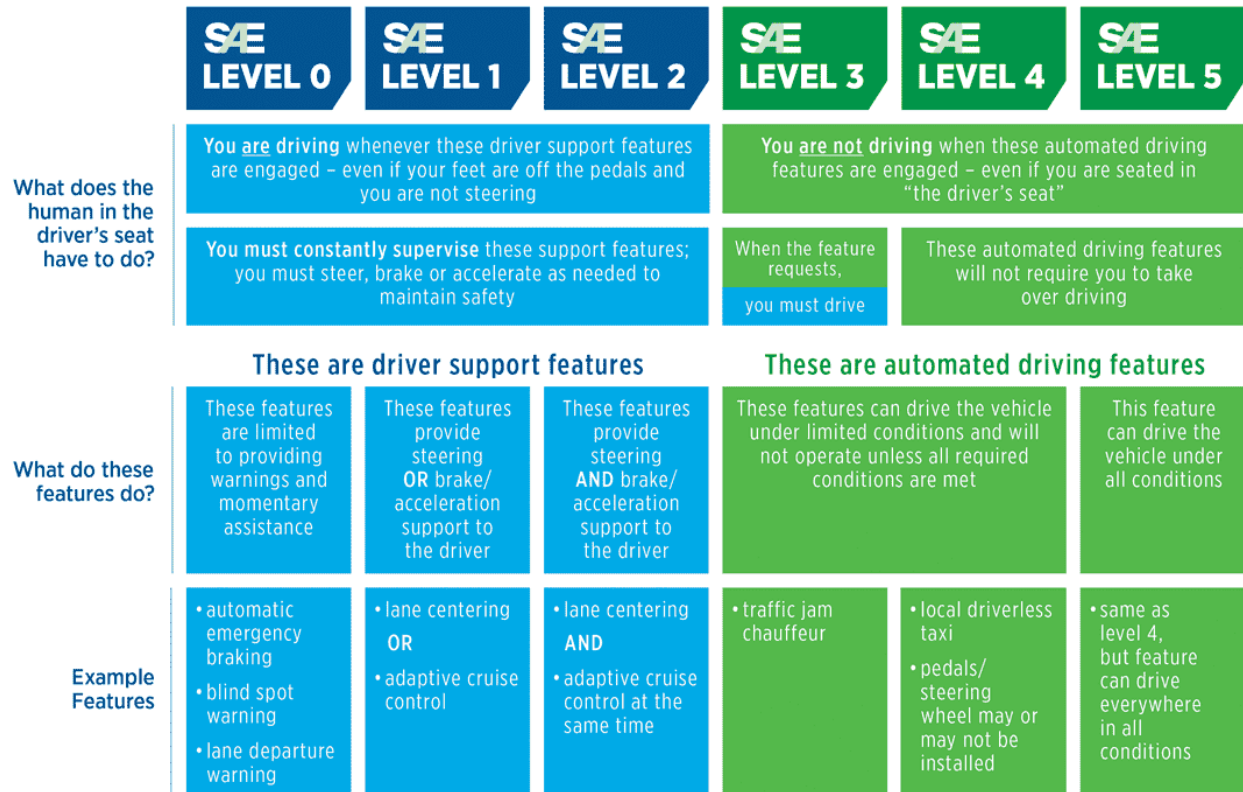


Figure 63 Levels of automation for autonomous vehicles.

Source: SAE International. (2019). SAE Standards News: J3016 Automated-Driving Graphic Update

U.S. DOT (2018) outlined a concept of operations and requirements for AVs at/near highway-rail grade crossings. One of the major goals was to understand and identify the requirements of AVs at highway-rail grade crossings to maneuver through them efficiently and safely. The framework of requirements was refined after investigating the existing AV and highway-rail grade crossing technologies as well as various inputs from experts. Table 14 presents different detection methods for various scenarios that may serve as a basis for vehicular communications at highway-rail grade crossings. The main information that is needed by AVs and CAVs includes location (i.e., where a given vehicle has to stop), train presence (i.e., occupying a given highway-rail grade crossing or approaching a given highway-rail grade crossing), and the information regarding the presence of queued vehicles at the highway-rail grade crossing. It can be observed that the detection method depends on the type of approaching vehicle (i.e., either AV or CAV), protection type (either active or passive), and availability of the data from queued vehicles (see Table 14).

Future research is needed in order to successfully implement the CAV technology at highway-rail grade crossings (Zaouk and Ozdemir, 2017). In particular, a variety of sensor technologies have to be developed to effectively detect and interpret the surrounding environment, including the following: (a) vision-based systems that can detect and interpret different roadway signs at highway-rail grade crossings; (b) stereo-based camera systems that are capable to emulate human binocular vision; and (c) deep learning models that can be further used for detecting of moving objects as well as recognition of approaching trains. Some of these technologies have already

demonstrated their potential for commercial motor vehicles and passenger vehicles, and they continue to evolve. For example, the sensor-based technologies that are installed in the vehicles with automation levels 2 and 3 have been quite successful with detecting the surrounding infrastructure (see Figure 64). Nevertheless, the viability of implementing new technologies at highway-rail grade crossings has to be further explored.

Table 14 Detection methods used for vehicles approaching highway-rail grade crossings.

ConOps Scenario #	Vehicle Type	Type of HRGC	Detection Method Used by Approaching Vehicle for:		
			Train	HRGC Stop Bar	Queued Vehicle(s)
1	AV	HRGC w AWD	No train approaching in range or occupying	Detection of stop bar pavement marking	Not Present
2	AV	HRGC w AWD	No train approaching in range or occupying	Detection of stop bar pavement marking	Detection of AV beyond HRGC
3	AV	HRGC w AWD	Detection of AWD flashing lights (train occupies HRGC)	Detection of stop bar pavement marking	Not Present
4	AV	HRGC w AWD	Detection of AWD flashing lights (train departs HRGC)	Detection of stop bar pavement marking	Not Present
5	CAV	HRGC w AWD	Receives communication from Connected HRGC (train occupies HRGC)	Receives communication from Connected HRGC	Not Present
6	CAV	HRGC w AWD	Receives communication from Connected HRGC (train departs HRGC)	Receives communication from Connected HRGC	Not Present
7	AV	HRGC w PWD	Detection of train presence (train occupies HRGC)	Detection of stop bar pavement marking	Not Present
8	AV	HRGC w PWD	Detection of train presence (train departs HRGC)	Detection of stop bar pavement marking	Not Present
9	CAV	HRGC w PWD	Receives communication from Connected Train (train occupies HRGC)	Detection of stop bar pavement marking	Not Present
10	CAV	HRGC w PWD	Receives communication from Connected Train (train departs HRGC)	Detection of stop bar pavement marking	Not Present
11	CAV	HRGC w PWD	No train approaching in range or occupying	Detection of stop bar pavement marking	Receives communication from CAV beyond HRGC

Source: U.S. DOT. (2018). *Automated Vehicles at Highway-Rail Grade Crossings*

Notes: HRGC – highway-rail grade crossing; AWD – Active Warning Device; PWD – Passive Warning Device.

2.3.3. Highway-Rail Interconnection

The existing regulations and recommendations that are provided by different organizations (e.g., FRA, FHWA, MUTCD) for highway-rail grade crossings may not be universally applied.

Reduction in the number of accidents at highway-rail grade crossings is considered as one of the main goals of different state and local agencies across the country. In order to achieve this goal,

safety requirements have to be implemented universally by traffic agencies. A unified vision of safety at highway-rail grade crossings and involvement of all the necessary parties is a major step towards “zero” accidents. A universal implementation of safety requirements by traffic agencies at highway-rail grade crossings is also referred to as “highway-rail interconnection” (Young, 2017).



Figure 64 An example of an autonomous vehicle with sensor-based technologies.

Source: Zaouk and Ozdemir. (2017). Implementing Connected Vehicle and Autonomous Vehicle Technologies at Highway-Rail Grade Crossings

About 14,800 highway-rail grade crossing accidents could have been avoided by implementing the connected vehicle (CV) technology, which could have saved about \$230 million per year (Zaouk and Ozdemir, 2017). To overcome the enormous cost of implementing the CV technology, there is a need to orient the efforts of the automobile industry and various governmental agencies. In the absence of these concerted efforts, it might be challenging to achieve automation by connected vehicles (i.e., advancement towards CAVs). The future development of CAVs and the goal to achieve full automation requires all the relevant stakeholders to work cohesively for a successful development, adoption, and implementation of future technologies. There is also a need for developing the next generation CAV technologies that can be directly implemented at highway-rail grade crossings.

2.3.4. Autonomous Trains

The rail system is quickly advancing forward by making significant technological advancements towards driverless trains that will eventually be fully autonomous. Autonomous trains use sophisticated technologies that include several devices, such as odometer, tachometer, radio set, camera, accelerometer, among others. Some advanced train technologies are demonstrated in Figure 65. The International Association of Public Transport outlined four grades of automation (GoAs) for trains which include the following (Harb, 2019):

- GoA1: All the operations, including starting, stopping, door operations, addressing emergency situations, and sudden diversions, are handled by the train driver.
- GoA2: The driver is still required, but certain operations can be handled by the train (e.g., starting, stopping, changing rail tracks).

- GoA3: This grade involves driverless train operations, but an onboard attendant has to take control in the event of an emergency.
- GoA4: At this grade, the train is fully automated with no onboard attendants/staff.

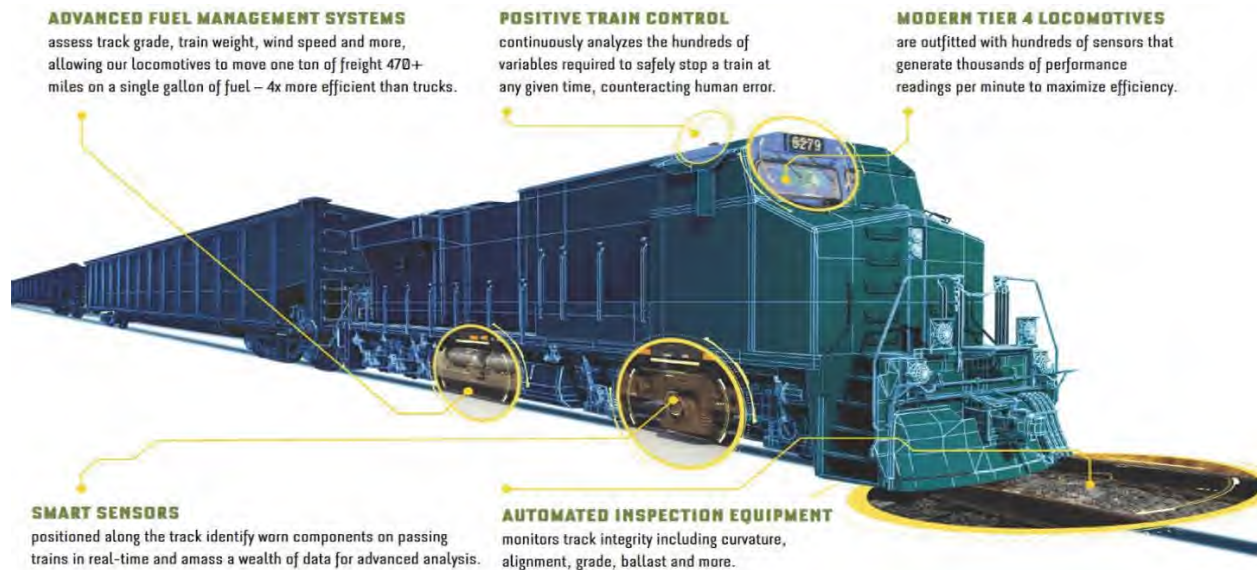


Figure 65 Advanced train technologies.

Source: California Short Line Railroad Association. (2019). Railroad Day in Sacramento

On 14 June 2019, Rio Tinto (Anglo-Australian second largest metals and mining corporation in the world) made a complete transition to fully automatic driverless operations of their heavy rail system in the Pilbara region (Western Australia). The rail network, where Rio Tinto executed fully automatic driverless operations, is considered as the first fully automated mainline rail network in the world (Briginshaw, 2019). The project took longer than was originally expected, and the project costs were higher than the originally planned costs. However, full automation is already providing some benefits to Rio Tinto, including the following: (a) short journey times; (b) lower operational costs; and (c) improved service reliability. All the aforementioned factors are critical for Rio Tinto in a highly competitive environment. Furthermore, full automation enhanced the scheduling efficiency and reduced the number of bottlenecks in the rail network. Similarly, French National Railways (SNCF) is extensively working towards automation of rail transportation and plans to develop a series of driverless freight and passenger train prototypes by 2022 (Briginshaw, 2019).

The Rio Tinto trains rely on the technologies that are similar to the Locomotive Engineer Assist / Display & Event Recorder (LEADER) used by New York Air Brake (see Figure 66). The trains that are equipped with the LEADER technology do not require train drivers and can be fully controlled by a computer. Moreover, the LEADER technology enables operations on different types of terrain, starting and stopping functions on downhill, uphill, as well as flat surfaces (Trains, 2019). Application of different artificial intelligence techniques within autonomous trains is expected to facilitate predictive maintenance and prevent accidents (Briginshaw, 2019).



Figure 66 LEADER controls by New York Air Brake.

Source: Trains. (2019). Computer Runs Train at Test Track, NYAB Announces

Autonomous trains face many challenges concerning the integration of various technologies, safety, and movement of trains. Some of these challenges include the following (Harb, 2019): (1) improving complex interactions between various train subsystems (e.g., monitoring the railroad track status, monitoring position of other trains, determining the space needed to safely brake); (2) railroad signaling is much more complex as compared to signalized highway intersections; (3) an autonomous system that can be applied to one type of trains may not be applicable to other train types; (4) many factors have to be considered when calculating the stopping sight distance for autonomous trains (e.g., weight of cargo, weight of a train, speed of a train, etc.); (5) improvements in reliability, security, and robustness are required before autonomous trains can be widely deployed and commercialized; and (6) accurate testing of autonomous trains will require access to the railroad infrastructure, which can be challenging. Various efforts are undertaken in order to improve operations and lead to better performance of future autonomous trains (Association of American Railroads, 2020).

Nokia has initiated the process of recognizing real-time highway-rail grade crossing issues using artificial intelligence technologies based on machine learning (FIERCE Telecom, 2020). Various trials of Nokia's SpaceTime scene analytics are conducted by Odakyu Electric Railway in Japan. These trials are intended to improve highway-rail grade crossing safety, and they have showed the ability of Nokia's SpaceTime scene analytics to detect unusual activities by applying artificial intelligence to camera images. The analysis of images captured by highway-rail grade crossing cameras can facilitate detection of possible issues before they arise (e.g., detection of heavy machinery in a position that can create a potential hazard to highway-rail grade crossing users). In case of restricted connectivity, Nokia's SpaceTime scene analytics can work using lower bandwidth in remote areas. This system can also initiate real-time warnings for any illegal entry in remote facilities (FIERCE Telecom, 2020).

Gebauer et al. (2012) assessed an autonomous train system prototype, named as autoBAHN. An overview of autoBAHN is illustrated in Figure 67. The concept of autoBAHN involves a digital

data radio system, an onboard computer system for supervision of train movements, central control station, and Global Navigation Satellite System (GNSS). The autoBAHN has an obstacle recognition system that relies on different sensor technologies. Based on the information received from sensors, the data fusion modules identify the obstacles in the vicinity of a given train. The train control system includes a digital data radio system, a central station, as well as an onboard-computer that can be effectively used for supervising the train. The individual components of the autoBAHN system are connected to the communication layer that ensures an efficient exchange of data between these components. The brake and engine control system receives the data from the train control system and manages the target train speed. Furthermore, the brake and engine control system is capable of autonomous actuation of the train engine. Given the interest of legal authorities and manufactures, the concept of autoBAHN is expected to be deployed on the existing railroads in the nearest future (Gebauer et al., 2012).

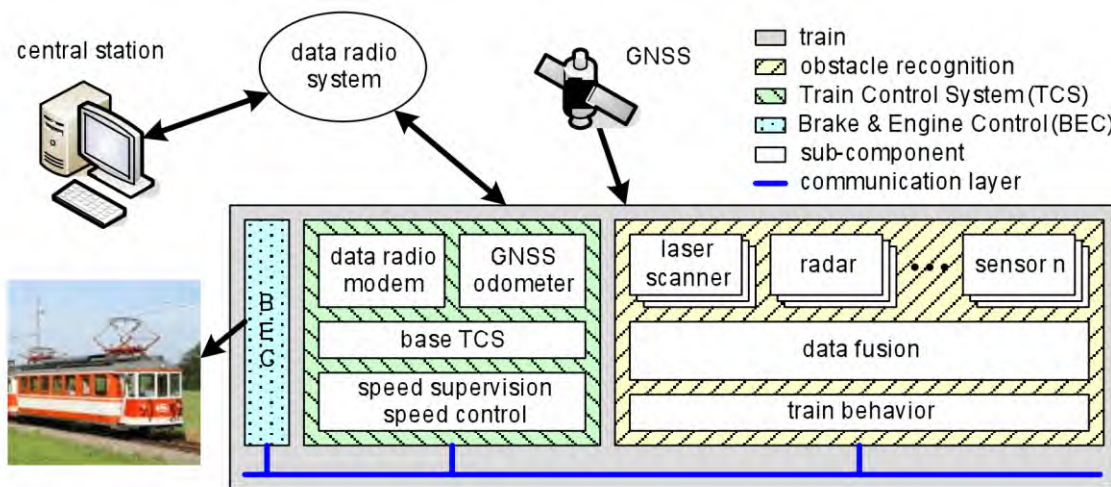


Figure 67 Overview of an autoBAHN.

Source: Gebauer et al. (2012). *Towards Autonomously Driving Trains on Tracks with Open Access*

3. MATHEMATICAL MODEL DEVELOPMENT

3.1. Problem Definition

This project tackles the resource allocation problem among the highway-rail grade crossings in Florida. Similar to every other state in the U.S., the State of Florida is provided with a limited budget to improve safety at the highway-rail grade crossings within the state. This limited budget is expected to be distributed in an efficient manner among the state's highway-rail grade crossings, so that the level of safety is improved with the application of proper countermeasures, while the other performance indicators (e.g., highway traffic delay) are not significantly impaired.

Let $X = \{1, \dots, n\}$ denote the highway-rail grade crossings, which are considered for upgrades. One established way to upgrade highway-rail grade crossings is to apply countermeasures (e.g., gates, flashing lights, wigwags). $C = \{1, \dots, m\}$ denotes the set of countermeasures, which are considered for the resource allocation process. One of the objectives of the proposed mathematical model is to minimize the overall hazard severity at the considered highway-rail grade crossings. The overall hazard severity can be determined from the overall hazard ($OH_x, x \in X$), which will be quantified using the Florida Priority Index Formula (see section 3.3 for details). The overall hazard can be divided into several severity categories, denoted by set $S = \{1, \dots, k\}$, which will be conducted using the methodology shown in the GradeDec.NET Reference Manual (U.S. DOT, 2014a). Thus, from OH_x , a hazard of severity s at highway-rail grade crossing x , which is denoted by $HS_{xs}, x \in X, s \in S$, will be estimated. Note that each severity category $s \in S$ is associated with a weight $W_s, s \in S$, which increases with the severity level. For instance, for a given highway-rail grade crossing, the fatality hazard usually has a higher weight than the injury hazard). The value of W_s varies from 0.0 to 1.0.

Based on certain physical and/or operational restrictions (e.g., existing traffic control devices), not all the countermeasures can be applied at a highway-rail grade crossing. In order to incorporate this practical consideration, parameter $p_{xc} \in \{0,1\} \forall x \in X, c \in C$ is introduced. If highway-rail grade crossing x is eligible for countermeasure c , the value of p_{xc} is 1. Otherwise, the value of p_{xc} is 0. When a countermeasure is applied at a highway-rail grade crossing, it is expected to reduce the potential hazard or hazard severity at that highway-rail grade crossing. The percentage reduction of a potential hazard or hazard severity at a given highway-rail grade crossing, due to the application of a given countermeasure, is represented by an effectiveness factor $EF_{xc}, x \in X, c \in C$. However, a countermeasure, applied at a highway-rail grade crossing, may also cause an additional delay to the associated highway traffic, which is denoted by $AD_{xc}, x \in X, c \in C$ (see section 3.4 for details). Each highway-rail grade crossing is assumed to have certain traffic delays with the existing warning devices ($OD_x^0, x \in X$ – hours) even before application of any countermeasures. Under one of the objectives of the proposed mathematical model, the overall traffic delay at the considered highway-rail grade crossings, due to the application of countermeasures, will be minimized. Finally, application of a given countermeasure at a highway-rail grade crossing is associated with a cost $CA_{xc}, x \in X, c \in C$ (USD). The total cost of applying the selected countermeasures at the considered highway-rail grade crossings should not exceed the total available budget (TAB – USD).

3.2. Proposed Mathematical Formulation

A detailed description of the main notations, which will be used throughout the development of the multi-objective optimization model for resource allocation among the highway-rail grade crossings in Florida, is provided in this section. Furthermore, the multi-objective optimization model, which has an integer programming formulation with the goal to minimize the overall hazard severity and to minimize the overall traffic delay at the highway-rail grade crossings in Florida, is shown in this section as well.

3.2.1. Main Notations

This section of the report explains the main notations of the proposed integer programming model, including sets, decision variable, and parameters.

Sets

$X = \{1, \dots, n\}$	set of highway-rail grade crossings (highway-rail grade crossings)
$C = \{1, \dots, m\}$	set of countermeasures (countermeasures)
$S = \{1, \dots, k\}$	set of severity categories (severity categories)

Decision Variable

$z_{xc} \in \mathbb{B} \forall x \in X, c \in C$	=1 if countermeasure c is applied at highway-rail grade crossing x (=0 otherwise)
--	--

Parameters

$n \in \mathbb{N}$	number of highway-rail grade crossings (highway-rail grade crossings)
$m \in \mathbb{N}$	number of countermeasures (countermeasures)
$k \in \mathbb{N}$	number of severity categories (severity categories)
$HS_{xs} \in \mathbb{R}^+ \forall x \in X, s \in S$	hazard of severity s at highway-rail grade crossing x (hazard severity units)
$W_s \in \mathbb{R}^+ \forall s \in S$	weight associated with severity s (varies from 0.0 to 1.0)
$p_{xc} \in \mathbb{B} \forall x \in X, c \in C$	=1 if countermeasure c can be applied at highway-rail grade crossing x (=0 otherwise)
$EF_{xc} \in \mathbb{R}^+ \forall x \in X, c \in C$	effectiveness factor for countermeasure c when applied at highway-rail grade crossing x (no units)
$OD_x^0 \in \mathbb{R}^+ \forall x \in X$	overall delay at highway-rail grade crossing x with the existing warning devices (hours)
$AD_{xc} \in \mathbb{R}^+ \forall x \in X, c \in C$	additional delay due to application of countermeasure c at highway-rail grade crossing x (hours)
$CA_{xc} \in \mathbb{R}^+ \forall x \in X, c \in C$	cost of applying countermeasure c at highway-rail grade crossing x (USD)
$TAB \in \mathbb{R}^+$	total available budget (USD)

3.2.2. Model Formulation

An integer programming formulation for the proposed Multi-Objective Resource Allocation Problem (**MORAP**) is presented in this section of the report.

MORAP:

$$\min F_1 = \sum_{x \in X} \sum_{s \in S} [1 - \sum_{c \in C} (EF_{xc} \cdot z_{xc})] \cdot W_s \cdot HS_{xs} \quad (3.1)$$

$$\min F_2 = \sum_{x \in X} [OD_x^0 + \sum_{c \in C} AD_{xc} \cdot z_{xc}] \quad (3.2)$$

Subject to:

$$\sum_{c \in C} z_{xc} \leq 1 \quad \forall x \in X \quad (3.3)$$

$$z_{xc} \leq p_{xc} \quad \forall x \in X, c \in C \quad (3.4)$$

$$\sum_{x \in X} \sum_{c \in C} CA_{xc} \cdot z_{xc} \leq TAB \quad (3.5)$$

$$z_{xc}, p_{xc} \in \{0,1\} \quad \forall x \in X, c \in C \quad (3.6)$$

$$HS_{xs}, W_s, EF_{xc}, OD_x^0, AD_{xc}, CA_{xc}, TAB \in \mathbb{R}^+ \quad \forall x \in X, c \in C, s \in S \quad (3.7)$$

The **MORAP** mathematical model comprises two objective functions. The objective function (3.1), denoted as F_1 , minimizes the overall hazard severity at the considered highway-rail grade crossings, while the objective function (3.2), denoted as F_2 , minimizes the overall traffic delay caused by the selected countermeasures at the considered highway-rail grade crossings.

Constraint set (3.3) indicates that a maximum of one countermeasure can be installed at a given highway-rail grade crossing. Constraint set (3.4) implies that a countermeasure can be applied only at those highway-rail grade crossings that are eligible for that countermeasure. Constraint set (3.5) ensures that the total cost of applying the selected countermeasures at the considered highway-rail grade crossings does not exceed the total available budget. Constraint sets (3.6) and (3.7) define the nature of the decision variable and various parameters of the **MORAP** mathematical model.

3.3. Estimation of the Overall Hazard Severity

This section of the report illustrates the estimation of the overall hazard severity, which will be derived from the overall hazard at a highway-rail grade crossing. In particular, the overall hazard will be differentiated into hazard severities of several categories.

The overall hazard at each highway-rail grade crossing ($OH_x, x \in X$) will be estimated from the Florida Priority Index Formula. The Florida Priority Index values obtained from the Florida Priority Index Formula will be used as the overall hazard at each highway-rail grade crossing. Dulebenets et al. (2020a) evaluated a number of accident and hazard prediction formulae selected from the highway-rail grade crossing safety literature for the highway-rail grade crossings in Florida. The evaluated accident prediction formulae included the following: (1) the Coleman-Stewart Model; (2) the NCHRP Report 50 Accident Prediction Formula; (3) the Peabody-Dimmick Formula; and (4) the U.S. DOT Accident Prediction Formula. Moreover, the evaluated hazard prediction formulae included the following: (1) the New Hampshire Formula; (2) the California Hazard Rating Formula; (3) the Connecticut Hazard Rating Formula; (4) the Illinois Hazard Index Formula; (5) the Michigan Hazard Index Formula; and (6) the Texas Priority Index Formula. In addition to the abovementioned formulae, the study developed and

evaluated modified versions of the California Hazard Rating Formula, the Connecticut Hazard Rating Formula, and the Texas Priority Index Formula.

In order to evaluate the candidate accident and hazard prediction formulae, 589 of the most hazardous highway-rail grade crossings in Florida, based on accident records and exposure, were selected. The study used a total of 3 approaches, which have been widely employed for the analysis of various accident and hazard prediction formulae. These approaches were: (1) chi-square formula; (2) grouping of highway-rail grade crossings based on the actual accident data; and (3) Spearman rank correlation coefficient. Note that the predicted number of accidents is required to perform the chi-square test; hence, the chi-square test was not conducted for the hazard prediction formulae. Based on the evaluative analysis, the modified version of the Texas Priority Index Formula, which was named the Florida Priority Index Formula, was recommended for ranking the highway-rail grade crossings in Florida for safety improvement projects.

The Florida Priority Index Formula estimates the potential hazard at a highway-rail grade crossing based on the average daily traffic volume, average daily train volume, train speed, protection factor, and an accident history parameter that is computed as the total number of accidents in the last 5 years or since the year of last improvement (when there was an upgrade). As discussed earlier, this project will consider the Florida Priority Index estimated for highway-rail grade crossing x ($FPI_x, x \in X$) as the overall hazard at that highway-rail grade crossing ($OH_x, x \in X$). The Florida Priority Index values can be estimated from the Florida Priority Index Formula as follows (Dulebenets et al., 2020a):

$$FPI_x = V_x \cdot T_x \cdot (0.1 \cdot S_x) \cdot PF_x \cdot (0.01 \cdot A_x^{1.15}) \quad (3.8)$$

where:

FPI_x – is the Florida Priority Index estimated for highway-rail grade crossing x (no units);

V_x – is the average daily traffic volume recorded for highway-rail grade crossing x (vehicles per day);

T_x – is the average daily train volume recorded for highway-rail grade crossing x (trains per day);

S_x – is the train speed recorded for highway-rail grade crossing x (mph);

PF_x – is the protection factor for highway-rail grade crossing x ($PF = 0.10$ for gates; $PF = 0.70$ for flashing lights; $PF = 1.00$ for passive);

A_x – is the accident history parameter for highway-rail grade crossing x (accidents); this parameter can be estimated as the total number of accidents in the last 5 years or since the year of last improvement (when there was an upgrade).

After obtaining the overall hazard from the Florida Priority Index Formula, the overall hazard will be differentiated into hazard severities of several categories. Highway-rail grade crossing accidents can be categorized into several groups based on severity. The methodology given in the GradeDec.NET Reference Manual (U.S. DOT, 2014a) categorizes highway-rail grade crossing accidents into the following classes:

- Fatality Accidents: These accidents involve at least one fatality.
- Casualty Accidents: These accidents involve at least one fatality or injury.
- Injury Accidents: These accidents involve at least one injury but no fatality.

- Property Damage Only Accidents: These accidents involve no fatalities or injuries. Only property damage is reported.

To the authors' knowledge, the existing highway-rail grade crossing safety literature mostly focuses on examining accident severity and does not report any methodologies for examining hazard severity. Hence, due to a lack of prediction methodologies for estimating hazard severity, this project will adopt the canonical severity prediction methodology outlined in the GradeDec.NET Reference Manual (U.S. DOT, 2014a), which was developed for quantifying accident severity at highway-rail grade crossings. Based on this methodology, the fatality hazard at a highway-rail grade crossing will be estimated from the overall hazard as follows:

$$FH_x = \frac{OH_x}{1 + KF \cdot MS_x^{FH} \cdot TT_x \cdot TS_x \cdot UR_x^{FH}} \quad \forall x \in X \quad (3.9)$$

$$KF = 440.9 \quad (3.10)$$

$$MS_x^{FH} = ms_x^{-0.9981} \quad \forall x \in X \quad (3.11)$$

$$TT_x = (thru_x + 1)^{-0.0872} \quad \forall x \in X \quad (3.12)$$

$$TS_x = (switch_x + 1)^{0.0872} \quad \forall x \in X \quad (3.13)$$

$$UR_x^{FH} = e^{0.3571 \cdot urban_x} \quad \forall x \in X \quad (3.14)$$

where:

FH_x – is the fatality hazard at highway-rail grade crossing x (no units);

OH_x – is the overall hazard at highway-rail grade crossing x (no units);

ms_x – is the maximum timetable train speed at highway-rail grade crossing x (miles per hour);

$ms_x = S_x \quad \forall x \in X$. Assume $ms_x = 1, x \in X$ when there are no data available.

$thru_x$ – is the number of through trains per day at highway-rail grade crossing x (trains per day).

Assume $thru_x = 1, x \in X$ when there are no data available.

$switch_x$ – is the number of switch trains per day at highway-rail grade crossing x (trains per day). Assume $switch_x = 1, x \in X$ when there are no data available.

$urban_x = 1$ if highway-rail grade crossing x is urban, else $urban_x = 0$. Assume $urban_x = 0, x \in X$ when there are no data available.

The casualty hazard at a highway-rail grade crossing will be estimated from the overall hazard as follows:

$$CH_x = \frac{OH_x}{1 + KC \cdot MS_x^{CH} \cdot TK_x \cdot UR_x^{CH}} \quad \forall x \in X \quad (3.15)$$

$$KC = 4.481 \quad (3.16)$$

$$MS_x^{CH} = ms_x^{-0.3430} \quad \forall x \in X \quad (3.17)$$

$$TK_x = e^{0.1153 \cdot tracks_x} \quad \forall x \in X \quad (3.18)$$

$$UR_x^{CH} = e^{0.2960 \cdot urban_x} \quad \forall x \in X \quad (3.19)$$

where:

CH_x – is the casualty hazard at highway-rail grade crossing x (no units);

$tracks_x$ – is the number of railroad tracks at highway-rail grade crossing x (tracks). Assume $tracks_x = 1, x \in X$ when there are no data available.

The injury hazard at a highway-rail grade crossing will be estimated as the difference between the casualty hazard and the fatality hazard at that highway-rail grade crossing using the following relationship:

$$IH_x = CH_x - FH_x \quad \forall x \in X \quad (3.20)$$

where:

IH_x – is the injury hazard at highway-rail grade crossing x (no units).

The property damage hazard at a highway-rail grade crossing will be estimated from the following relationship:

$$PH_x = OH_x - FH_x - IH_x \quad \forall x \in X \quad (3.21)$$

where:

PH_x – is the property damage hazard at highway-rail grade crossing x (no units).

The **MORAP** mathematical model includes a weight associated with each severity category ($W_s, s \in S$). This project will employ the data reported by the Iowa DOT (2020) for estimation of the weight values for the considered hazard severity categories. The Iowa DOT (2020) determined the societal costs of each fatal accident (FA), injury accident (IA), and property damage only accident (PDO) as \$4,500,000, \$650,000, and \$35,000, respectively. According to the aforementioned cost data, the weight of each severity category can be quantified as follows:

$$W_{FH} = \frac{\$4,500,000}{(\$4,500,000 + \$650,000 + \$35,000)} = 0.87 \quad (3.22)$$

$$W_{IH} = \frac{\$650,000}{(\$4,500,000 + \$650,000 + \$35,000)} = 0.12 \quad (3.23)$$

$$W_{PH} = \frac{\$35,000}{(\$4,500,000 + \$650,000 + \$35,000)} = 0.01 \quad (3.24)$$

where:

W_{FH} – is the weight of fatality hazard (fatality hazard severity units);

W_{IH} – is the weight of injury hazard (injury hazard severity units);

W_{PH} – is the weight of property damage hazard (property damage hazard severity units).

This project will set the base values for the weights of fatality hazard, injury hazard, and property damage hazard to $W_{FH} = 0.90$, $W_{IH} = 0.09$, and $W_{PH} = 0.01$, respectively, which are near the values suggested by the Iowa DOT (2020). Note that these weights can be tuned by the user if necessary (e.g., due to changes in societal costs). The representatives from the Florida Department of Transportation will be able to set the appropriate values depending on the societal costs of highway-rail grade crossing accidents across the state.

Table 15 Methods for quantifying traffic delays at highway-rail grade crossings.

a/a	Method	Formulation	Notes
1	Institute of Transportation Engineers (2006)	$L = (2qr) \cdot (1 + p) \cdot (25) \text{ if } v/c \leq 0.90$ $L = (2qr + \Delta x) \cdot (1 + p) \cdot (25) \text{ if } 0.90 < v/c \leq 1.00$ $\Delta x = 100(v/c - 0.90)$ where: v/c – is the volume to capacity ratio; L – is the 95th percentile queue length (ft); q – is the vehicle flow rate (vehicles/lane/second); through traffic and left/right turning traffic should be considered; r – is the effective time during which a train blocks a highway-rail grade crossing (seconds); $r = 35 + \frac{l}{1.47S}$; l – is the train length (ft); S – is the train speed (mph); 35 – is the amount of time during which gates block the highway-rail grade crossing (about 25 seconds before a train enters the highway-rail grade crossing and 10 seconds after the train exits the highway-rail grade crossing) (seconds); p – is the portion of heavy vehicles (in decimal points); 25 – is the effective length of a passenger car (i.e., the sum of a passenger car’s length and space between consecutive vehicles) (ft); 2 – is a random arrival factor.	This method provides estimation of the queue length and the crossing blockage time by a train. However, it does not estimate the overall delay experienced by vehicles due to crossing blockage (e.g., the first vehicle in the queue will experience the delay of r , while the last vehicle in the queue may arrive to the crossing when the train is leaving that crossing).
2	Highway-Rail Crossing Handbook (U.S. DOT, 2019)	Minimum warning time should be the sum of a 20 seconds minimum time and a clearance time, which is 1 second for every 10 ft of additional highway-rail grade crossing length exceeding 35 ft. Additional time can be included based on particular considerations for specific crossings (e.g., additional equipment response time, advance preemption time, buffer time due to variations in handling of trains).	This approach provides recommendations regarding the warning time. However, it does not estimate the overall delay experienced by vehicles due to crossing blockage.

Table 15 Methods for quantifying traffic delays at highway-rail grade crossings (cont'd).

a/a	Method	Formulation	Notes
3	NCHRP Report 288 (1987)	$D = \frac{\left(\frac{T}{2} + 0.10\right)N + \left(\frac{N}{n}\right)^2}{60}; T = \frac{50 + \frac{0.682 \cdot L}{1.5S_e - S_x}}{60}; N = V \cdot \frac{T}{m}$ <p>where: D – is the overall delay (minutes); T – is the duration of highway-rail grade crossing closure (minutes); $(T/2)$ – is the average delay per vehicle, as not all the vehicles will be delayed by the same amount of time (seconds); N – is the number of delayed vehicles; n – is the number of highway lanes; 0.10 – is the delay due to deceleration and acceleration along with the delay experienced while waiting for highway traffic to flow freely after the train has passed (seconds); L – is the train length (ft); S_e – is the speed of the train when it enters the highway-rail grade crossing (mph); S_x – is the speed of the train when it exits the highway-rail grade crossing (mph); 50 – is the duration of time when the warning devices are active before the train arrives and after the train leaves the highway-rail grade crossing (a constant warning time device is assumed) (seconds); 0.682 – is the conversion factor from mph to ft/second; V – is the traffic volume through the highway-rail grade crossing during the considered period of time; m – is the amount of time in the considered period (minutes).</p>	It can be challenging to obtain certain data for this method (e.g., the speed of the train when it enters the highway-rail grade crossing, the speed of the train when it exits the highway-rail grade crossing). The assumed constant warning time (i.e., 50 seconds) seems fairly large as compared to other recommendations (e.g., 20~35 seconds). The delay due to acceleration after the train has passed may be difficult to measure.
4	Okitsu et al. (2010)	$D = \frac{AR \cdot Q \cdot (B + LT)}{2}$ $Q = (B + LT) / (1 - AR / SatFlowRate)$ <p>where: D – is the overall delay (vehicle-hours); AR – is the arrival rate (vehicles/hour); Q – is the queue duration (hours); B – is the duration of blockage event (hours); LT – is the lost time (hours); $SatFlowRate$ – is the saturation flow rate (vehicles/hour for lane group).</p>	This method does not provide recommendations regarding the blockage event duration.

Table 15 Methods for quantifying traffic delays at highway-rail grade crossings (cont'd).

a/a	Method	Formulation	Notes
5	Southern California International Gateway Draft EIR (2011)	$V = \left(\frac{1}{2}\right) \left(\frac{qT_G^2}{1 - \frac{q}{d}}\right)$ <p>where: <i>V</i> – is the overall delay for an isolated blockage (minutes); <i>q</i> – is the arrival rate (vehicles/minute); <i>T_G</i> – is the gate down time (minutes); <i>d</i> – is the departure rate (vehicles/minute).</p>	This method does not explicitly capture the warning time (i.e., certain devices will be activated before gates start their downward movement).
6	Center for Urban Transportation Research (2014)	$\text{Train Delay Time} = \text{CWT} + \frac{\text{Train Length}}{\text{Train Speed}}$ <p>where: <i>Train Delay Time</i> – is the train delay time (seconds); <i>CWT</i> – is the constant warning time, usually 20-25 seconds (seconds); <i>Train Length</i> – is the train length (ft); <i>Train Speed</i> – is the train speed (ft/second).</p>	This method provides the total crossing blockage time but does not estimate the overall delay experienced by vehicles due to crossing blockage.
7	Surface Transportation Board (2020)	$N_V = \frac{T}{24} \cdot N \cdot \text{ADT}; T = T_W + \frac{L}{V}; D_V = \frac{N_V}{\text{ADT}} \cdot \frac{T \cdot R_D}{R_D - R_A}$ <p>where: <i>N_V</i> – is the number of vehicles delayed per day (vehicles); <i>T</i> – is the gate down time per train event; <i>N</i> – is the number of trains per day; <i>ADT</i> – is the average daily traffic; <i>T_W</i> – is the gate warning time; <i>L</i> – is the average train length estimated as the weighted average between freight and passenger trains; <i>V</i> – is the average train speed estimated as the weighted average between freight and passenger trains; <i>D_V</i> – is the average delay per vehicle in a 24-hour period; <i>R_D</i> – is the departure rate, 1,800 for highways, 1,400 for arterials, 900 for collectors, and 700 for local roads (vehicles/lane/hour); <i>R_A</i> – is the arrival rate, average daily traffic converted to vehicles/lane/hour (vehicles/lane/hour); 2 – is used to indicate that vehicles do not wait for the entire time during which the train blocks the highway-rail grade crossing; the vehicles, on average, are assumed to arrive at the middle of the train crossing duration.</p>	It can be challenging to obtain certain data for this method (e.g., length of every train passing the crossing, speed of every train passing the crossing, vehicle arrival and departure rates).

3.4. Estimation of the Overall Traffic Delay

This section of the report discusses different approaches that can be used for estimation of the overall traffic delay due to the presence of countermeasures at highway-rail grade crossings or halting of the associated highway traffic because of passing trains. Throughout this project, the research team identified a number of methods for quantifying traffic delays at highway-rail grade crossings. These methods were suggested by the following entities and sources:

- Institute of Transportation Engineers (2006)
- Highway-Rail Crossing Handbook (U.S. DOT, 2019)
- NCHRP Report 288 (1987)
- Okitsu et al. (2010)
- Southern California International Gateway Draft EIR (2011)
- Center for Urban Transportation Research (2014)
- Surface Transportation Board (2020)

The aforementioned methods for quantifying traffic delays at highway-rail grade crossings are presented in Table 15. Furthermore, various advantages and disadvantages of these traffic delay estimation methods are highlighted in Table 16.

Table 16 Advantages and disadvantages of traffic delay estimation methods.

a/a	Method	Advantages	Disadvantages
1	Institute of Transportation Engineers (2006)	(1) This method provides estimation of the queue length and the crossing blockage time by a train. (2) Queue lengths are estimated for multiple scenarios (e.g., traffic queues approach a highway-rail grade crossing; traffic queues approach a highway intersection).	(1) This method does not estimate the overall delay experienced by vehicles due to crossing blockage (e.g., the first vehicle in the queue will experience the delay of r , while the last vehicle in the queue may arrive at the crossing when the train is leaving that crossing).
2	Highway-Rail Crossing Handbook (U.S. DOT, 2019)	(1) This method provides recommendations regarding the warning time. (2) Different time periods required by several warning devices are recommended.	(1) This method does not estimate the overall delay experienced by vehicles due to crossing blockage.
3	NCHRP Report 288 (1987)	(1) This method accounts for the fact that not all the vehicles will be delayed by the same amount of time. (2) A queue dissipation time is included.	(1) It can be challenging to obtain certain data for this method (e.g., the speed of the train when it enters the highway-rail grade crossing, the speed of the train when it exits the highway-rail grade crossing). (2) The assumed constant warning time (i.e., 50 seconds) seems fairly large as compared to other recommendations (e.g., 20~35 seconds). (3) The delay due to acceleration after the train has passed may be difficult to measure.

Table 16 Advantages and disadvantages of traffic delay estimation methods (cont'd).

a/a	Method	Advantages	Disadvantages
4	Okitsu et al. (2010)	(1) This method estimates the queue duration along with the overall delay.	(1) This method does not provide recommendations regarding the blockage event duration.
5	Southern California International Gateway Draft EIR (2011)	(1) This method accounts for isolated blockages.	(1) This method does not explicitly capture the warning time (i.e., certain devices will be activated before gates start their downward movement). (2) Many vehicles arriving at the crossing may not face delays due to train arrivals. Still, they are included for the estimation of the average delay. (3) The railroad traffic and highway traffic are assumed to be uniform throughout the day.
6	Center for Urban Transportation Research (2014)	(1) This method provides a simple method for estimating the total crossing blockage time.	(1) This method does not estimate the overall delay experienced by vehicles due to crossing blockage.
7	Surface Transportation Board (2020)	(1) This method incorporates vehicle arrival rates and departure rates in the vehicle delay estimations.	(1) It can be challenging to obtain certain data for this method (e.g., length of every train passing the crossing, speed of every train passing the crossing, vehicle arrival and departure rates). (2) The railroad traffic and highway traffic are assumed to be uniform throughout the day.

Based on review of the identified methods for the traffic delay estimation at highway-rail grade crossings, it can be observed that many approaches provided calculations of the crossing blockage time without computing the overall delay experienced by vehicles. In reality, different vehicles are likely to experience different delays when arriving at a highway-rail grade crossing that is blocked by a train. In particular, the vehicles that arrived at the highway-rail grade crossing right before the closure of gates might experience longer delays as compared to the vehicles that arrived at the highway-rail grade crossing when the train just passed by. Furthermore, many of the existing methods do not account for the traffic delay due to queue dissipation after the train has passed the crossing and the gates have been moved to a vertical position.

Based on a detailed review of the relevant literature, this study will use the following approach for estimating traffic delays at highway-rail grade crossings. The effective time during which a train blocks highway-rail grade crossing x with the existing warning devices ($EBT_x^0, x \in X$ – seconds) can be estimated as follows (ITE, 2006; CUTR, 2014; STB, 2020):

$$EBT_x^0 = CCD_x^0 + \frac{L_x}{1.47 \cdot SC_x} \quad \forall x \in X \quad (3.25)$$

where:

$CCD_x^0, x \in X$ – is the current delay time for highway-rail grade crossing x with the existing warning devices (seconds);
 $L_x, x \in X$ – is the average train length for highway-rail grade crossing x (ft);
 $SC_x, x \in X$ – is the average train speed for highway-rail grade crossing x (mph);
 1.47 – is the conversion factor from mph to ft/second.

The maximum timetable train speed can be used as a starting value for the train speed when passing highway-rail grade crossings, as the maximum timetable train speed values are available in the FRA crossing inventory database. In the meantime, the upper and lower bounds will be imposed on the average train speed at highway-rail grade crossings to make sure that it remains within reasonable limits. The maximum average train speed at highway-rail grade crossings will be denoted as SC^{max} (mph), and the minimum average train speed at highway-rail grade crossings will be denoted as SC^{min} (mph). Hence, $SC^{min} \leq SC_x \leq SC^{max} \forall x \in X$.

Assume $T_x, x \in X$ is the average number of trains arriving at highway-rail grade crossing x per day. Assume $V_x, x \in X$ is the average number of vehicles arriving at highway-rail grade crossing x per day. If trains and vehicles are uniformly arriving at highway-rail grade crossing x throughout the day, which is a common assumption in the relevant literature (NCHRP, 1987; Okitsu et al., 2010; Chicago Metropolitan Agency for Planning, 2015; STB, 2020), there will be a total of T_x crossing blockage occurrences for a given day. The average number of vehicles queued at highway-rail grade crossing x with the existing warning devices during each blockage ($VQ_x^0, x \in X$ – vehicles) can be estimated based on a 15-min daily traffic volume and percentage of the 15-min time interval affected by the crossing blockage event as follows (NCHRP, 1987; Jusayan, 2015):

$$VQ_x^0 = \left(\frac{V_x}{24 \cdot 4} \right) \cdot \left(\frac{EBT_x^0}{900} \right) \forall x \in X \quad (3.26)$$

where:

$\left(\frac{V_x}{24 \cdot 4} \right), x \in X$ – is the 15-min daily traffic volume (vehicles);
 900 – is the number of seconds in a 15-min time interval.

Note that a 15-min daily traffic volume is used in the vehicle queue estimation, as it is highly unlikely that a substantial portion of vehicles (e.g., hourly volume) will experience the crossing blockage event (NCHRP, 1987; Jusayan, 2015). A total of $(VQ_x^0/2)$ vehicles will be queued in one direction, while the remaining $(VQ_x^0/2)$ vehicles will be queued in the opposite direction. The latter assumption can be modified if a directional distribution of vehicles is available for the considered highway-rail grade crossings. The overall delay experienced by queued vehicles during each blockage of highway-rail grade crossing x with the existing warning devices ($ODB_x^0, x \in X$ – seconds) with n highway lanes can be estimated as follows (NCHRP, 1987):

$$ODB_x^0 = \left(\frac{EBT_x^0}{2} \cdot VQ_x^0 \right) + \left(\frac{VQ_x^0}{2 \cdot n_x} \right)^2 \forall x \in X, c \in C \quad (3.27)$$

Note that the term $\left(\frac{vQ_x^0}{2 \cdot n_x}\right)^2$ is used to account for the queue dissipation time (QDT_x^0 , $x \in X$ – seconds) after the train passes highway-rail grade crossing x (see Figure 68): $QDT_x^0 = \left(\frac{vQ_x^0}{2 \cdot n_x}\right)^2 \forall x \in X$. Once the train passes the crossing, there will be a total of $\left(\frac{vQ_x^0}{2 \cdot n_x}\right)$ vehicles in a queue in each highway lane (n_x highway lanes will be available in one direction, and n highway lanes will be available in the opposite direction, which constitute to the term “ $2 \cdot n_x$ ” in the denominator). Assuming that the headway between two consecutive vehicles is 2 seconds (NCHRP, 1987), the total queue dissipation time for the first vehicle in each lane will be zero seconds, while the total queue dissipation time for the last vehicle in each lane will be $(2) \cdot \left(\frac{vQ_x^0}{2 \cdot n_x}\right)$ seconds. Then, the average queue dissipation time will be $(2) \cdot \left(\frac{vQ_x^0}{2 \cdot n_x}\right) / 2$, and the total queue dissipation time will be $(2) \cdot \left(\frac{vQ_x^0}{2 \cdot n_x}\right) / 2 \cdot \left(\frac{vQ_x^0}{2 \cdot n_x}\right) = \left(\frac{vQ_x^0}{2 \cdot n_x}\right)^2$ seconds (NCHRP, 1987). Furthermore, the term $(EBT_x^0 / 2)$ is used in equation (3.27) to account for the average effective blockage time per vehicle, as not all the vehicles will be delayed by the same amount of time.

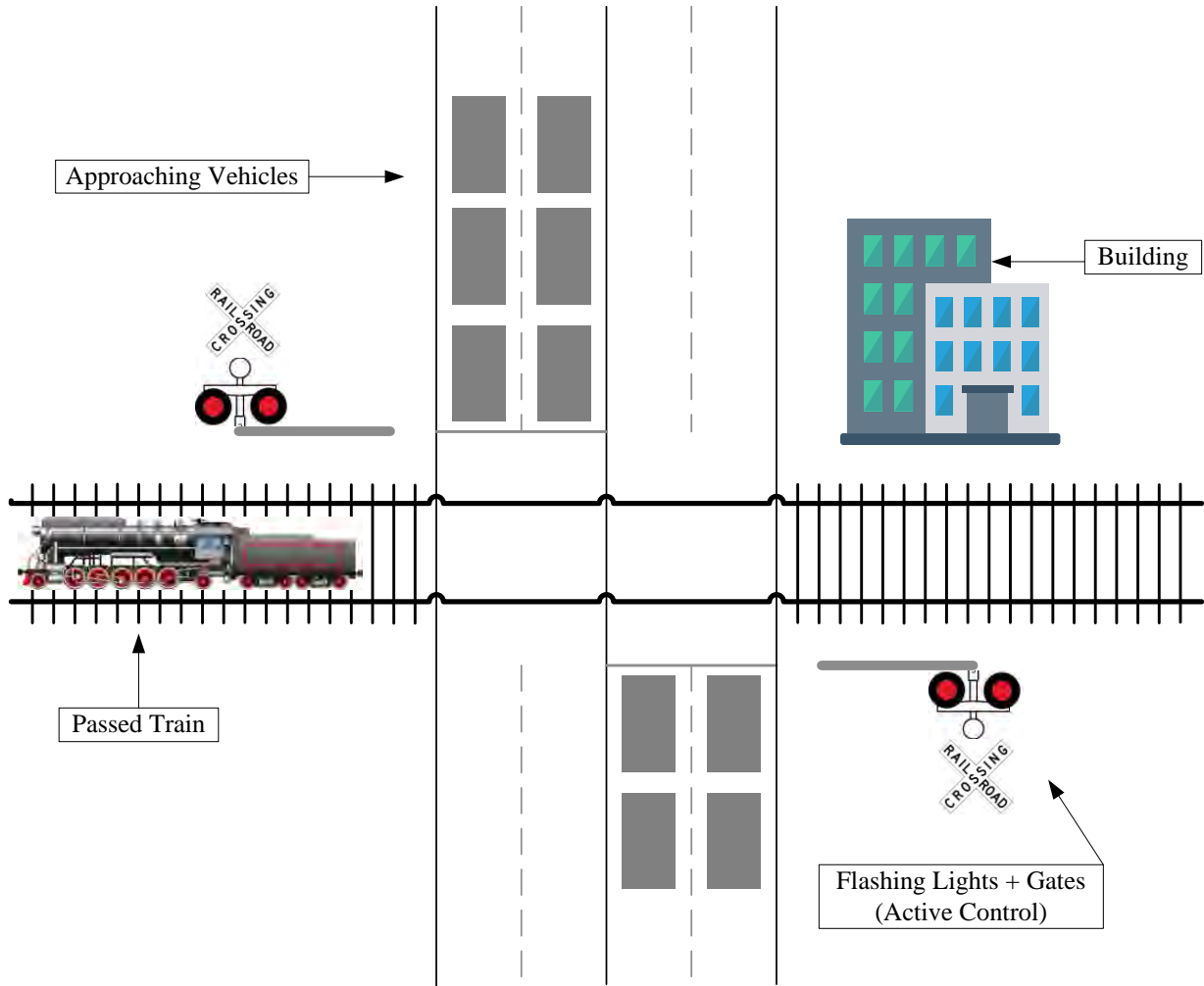


Figure 68 Queue dissipation time estimations.

The overall delay at highway-rail grade crossing x with the existing warning devices per day ($OD_x^0, x \in X$ – hours) can be estimated based on the number of blockage occurrences at that crossing per day ($T_x, x \in X$) and the overall delay experienced by queued vehicles during each blockage occurrence ($ODB_{xc}, x \in X$ – seconds) as follows:

$$\begin{aligned} OD_x^0 &= \frac{T_x \cdot ODB_x^0}{3600} = \left(\frac{T_x}{3600}\right) \cdot ODB_x^0 \\ &= \left(\frac{T_x}{3600}\right) \cdot \left[\left(\frac{CCD_x^0 + \frac{L_x}{1.47 \cdot SC_x} \cdot VQ_x^0}{2} \right) + \left(\frac{VQ_x^0}{2 \cdot n_x} \right)^2 \right] \forall x \in X \end{aligned} \quad (3.28)$$

Note that “3600” is used in equation (3.28) for converting seconds to hours. Considering the same assumptions, the overall delay for highway-rail grade crossing x after implementation of countermeasure c ($OD_{xc}, x \in X, c \in C$ – hours) can be estimated as follows:

$$\begin{aligned} OD_{xc} &= \frac{T_x \cdot ODB_{xc}}{3600} = \left(\frac{T_x}{3600}\right) \cdot ODB_{xc} \\ &= \left(\frac{T_x}{3600}\right) \cdot \left[\left(\frac{CCD_x^0 + ACD_c + \frac{L_x}{1.47 \cdot SC_x} \cdot VQ_{xc}}{2} \right) + \left(\frac{VQ_{xc}}{2 \cdot n_x} \right)^2 \right] \forall x \in X, c \in C \end{aligned} \quad (3.29)$$

where:

$ODB_{xc}, x \in X, c \in C$ – is overall delay experienced by queued vehicles during each blockage of highway-rail grade crossing x after implementation of countermeasure c (seconds);

$$ODB_{xc} = \left(\frac{EBT_{xc}}{2} \cdot VQ_{xc} \right) + \left(\frac{VQ_{xc}}{2 \cdot n_x} \right)^2 \forall x \in X, c \in C$$

$EBT_{xc}, x \in X, c \in C$ – is the effective time during which a train blocks highway-rail grade crossing x after implementation of countermeasure c (seconds);

$$EBT_{xc} = CCD_x^0 + ACD_c + \frac{L_x}{1.47 \cdot SC_x} \forall x \in X, c \in C$$

$ACD_c, c \in C$ – is the additional delay time that is incurred on average at highway-rail grade crossings after implementation of countermeasure c (seconds);

$VQ_{xc}, x \in X, c \in C$ – is the average number of vehicles queued at highway-rail grade crossing x after implementation of countermeasure c during each blockage (seconds);

$$VQ_{xc} = \left(\frac{V_x}{24 \cdot 4} \right) \cdot \left(\frac{EBT_{xc}}{900} \right) \forall x \in X, c \in C$$

Then, the additional delay due to application of countermeasure c at highway-rail grade crossing x ($AD_{xc}, x \in X, c \in C$ – hours) that is directly used in the **MORAP** mathematical model can be estimated as follows:

$$AD_{xc} = OD_{xc} - OD_x^0 \forall x \in X, c \in C \quad (3.30)$$

3.5. Model Complexity

The computational complexity of the **MORAP** model is analyzed in this section of the report. The computational complexity of an optimization model is important, since it plays a significant role in selection of the solution approach. Optimization models with high computational complexities require extensive computational times and are typically solved with heuristic or metaheuristic algorithms rather than exact optimization approaches. Exact optimization approaches may require a prohibitive computational time to solve optimization models with high computational complexities to global optimality (Cook, 2006).

3.5.1. Computational Complexity Classes

Based on computational complexity, optimization models can be categorized as follows (Van Leeuwen, 1990):

- **Polynomial (P)**: The computational time is a polynomial function of the problem size, and the problem can be solved relatively quickly.
- **Nondeterministic Polynomial Time (NP)**: The answer of the problem can be verified in a polynomial time. However, the problem cannot be solved quickly.
- **Nondeterministic Polynomial-Time Complete (NP-complete)**: The answer cannot be obtained in a polynomial time. However, it can be verified in a polynomial time. Among the problems of the NP class, NP-complete problems are considered as the most convoluted problems.
- **Nondeterministic Polynomial-Time Hard (NP-hard)**: Only a few problems in the NP-complete category can be verified in a polynomial time. However, none of them can be solved in a polynomial time.

The Euler diagram for the computational complexity classes is presented in Figure 69. Over the years, many research efforts have been carried out regarding the computational complexity classes. In spite of an announcement for a prize money of \$1 million, no researchers have been able to accomplish either of the following tasks (University of Hawaii, 2020):

- **Confirm that some problems in NP cannot be solved in a polynomial time** (indicating $P \neq NP$, illustrated in the left-hand side of Figure 69). The left-hand side of Figure 69 assumes that some common areas of the Euler diagram for the computational complexity classes are shared by problems of different complexity classes.
- **Obtain a polynomial time solution even for just one NP-complete problem** (indicating $P = NP\text{-complete}$, illustrated in the right-hand side of Figure 69). The right-hand side of Figure 69 assumes that P, NP, and NP-complete problems share the same computational complexity. Even some NP-hard problems are assumed to have the same computational complexity as P, NP, and NP-complete problems.

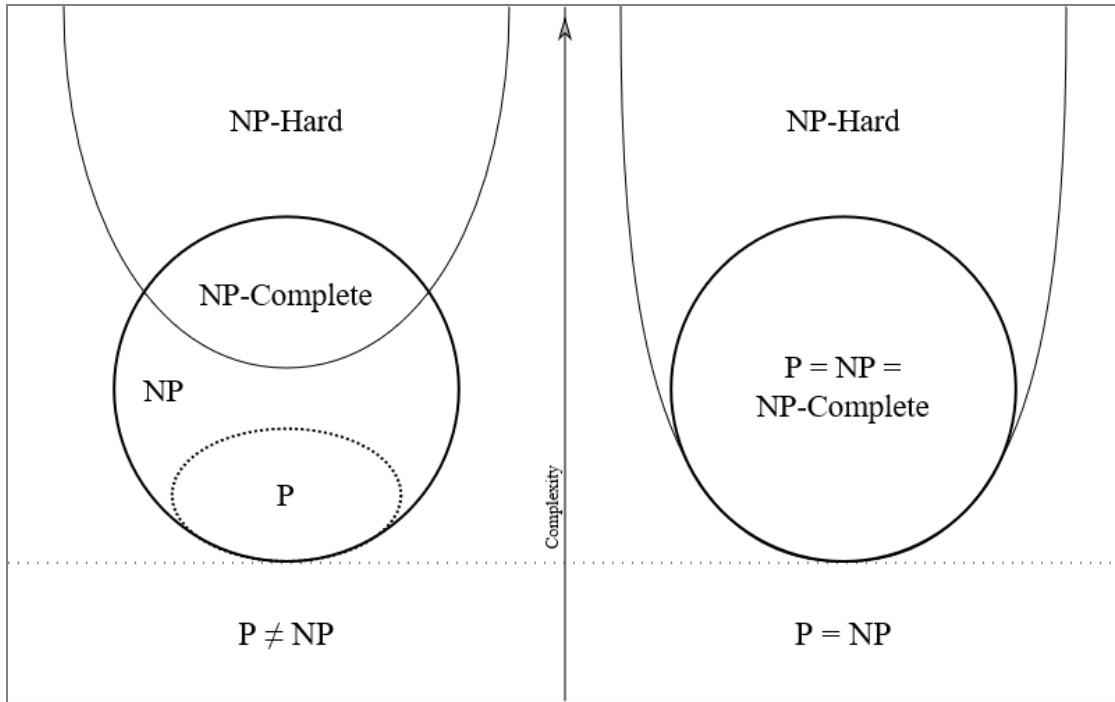


Figure 69 Euler diagram for computational complexity classes.
Source: University of Hawaii. (2020). ICS 311 #24: NP-Completeness

3.5.2. Complexity of the Proposed Model

Through the analysis of the features of the proposed **MORAP** mathematical model, it was found that the **MORAP** mathematical model has a significant level of resemblance with the knapsack problem. The knapsack problem, a combinatorial decision problem, aims to accommodate a collection of items with various weights and values into a knapsack. Maximization of the total value of items inside the knapsack, while not exceeding the carrying capacity of the knapsack, is the objective of the generic knapsack problem (Mathews, 1896). Figure 70 illustrates an example of the knapsack problem, which pertains to the railway industry. In this example, the front wagon of a train is considered as an equivalent of a knapsack, which has a limited capacity of 10 lbs. The front wagon can be equipped with one or more items from a list of five items, including a computer, a display, a phone, a radio, and a Wi-Fi connection. Each of the items has a specific weight along with a utility, which is estimated in dollars. The computer, for example, has a weight of 4 lbs and a utility of \$7. Note that the ratio of utility to weight is different for different items (e.g., 1.75 for the computer and 1.00 for the display). The railway authority has to decide which items to include in the front wagon in order to maximize the total utility. The main constraint here is that the maximum capacity of the front wagon (i.e., 10 lbs) must not be exceeded. The **MORAP** mathematical model, which resembles the knapsack problem, aims to minimize the overall hazard severity and the overall traffic delay at the highway-rail grade crossings in Florida with the application of appropriate countermeasures that have different implementation costs and effectiveness factors, taking into account the total available budget.

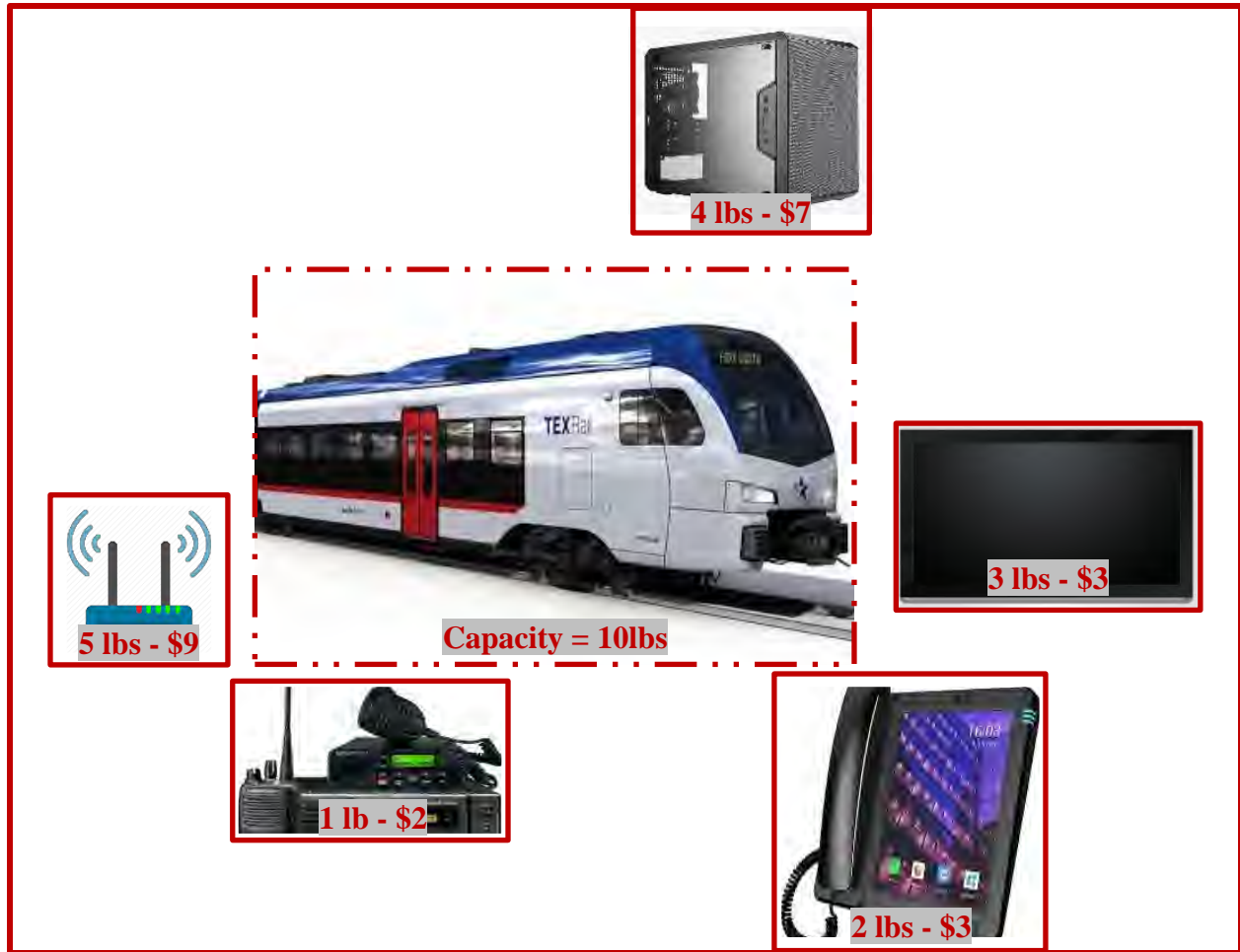


Figure 70 The knapsack problem prevailing in the railway industry.

3.5.3. Classes of the Knapsack Problem

The number and types of items to be accommodated in the knapsack or even the number of knapsacks might vary from one problem to another. The number of objectives of a problem (e.g., single objective, multiple objectives) might also be different. Several other features might vary as well. Therefore, based on the major assumptions and problem features, the knapsack problem can be divided into several classes, including the multi-objective knapsack problem, multi-dimensional knapsack problem, multiple knapsack problem, quadratic knapsack problem, subset-sum problem, and others (Khuri et al., 1994; Chang et al., 1995; Güntzer and Jungnickel, 2000; Fréville, 2004; Pisinger, 2007; Bazgan et al., 2009). Some of the well-known classes of the knapsack problem are discussed in the following sections.

Multi-Objective Knapsack Problem

The multi-objective knapsack problem includes more than one objective function. The **MORAP** mathematical model is very similar to the multi-objective knapsack problem, where the objective functions are to minimize the overall hazard severity and to minimize the overall traffic delay with the application of countermeasures. Application of a specific group of countermeasures at the considered highway-rail grade crossings may result in the lowest overall hazard severity possible, but that specific group of countermeasures may also lead to severe traffic delays. On

the other hand, application of another group of countermeasures at the considered highway-rail grade crossings may result in the lowest overall traffic delay, but that group of countermeasures may not be very effective in reducing the overall hazard severity. Therefore, the optimal solution should provide the best tradeoff between such objective functions for this kind of problem (Chang et al., 1995; Chang et al., 2000).

Multi-Dimensional Knapsack Problem

The multi-dimensional knapsack problem divides the knapsack into multiple sections with various capacities. The objective function of the multi-dimensional knapsack problem is maximization of the total value of items inside the knapsack. The uniqueness of this problem lies in the fact that the sum of weights inside each one of the sections of the knapsack must not exceed the capacity of the respective section (Fréville, 2004).

Multiple Knapsack Problem

As the name suggests, the multiple knapsack problem involves more than one knapsack. A major difference between the multiple knapsack problem and the generic knapsack problem is that the multiple knapsack problem can be tackled by a polynomial-time approximation scheme (Chekuri and Khanna, 2005).

Quadratic Knapsack Problem

The quadratic knapsack problem aims to maximize its quadratic objective function, and the quadratic objective function captures the total value of items inside the knapsack (Witzgall, 1975). Typically, the quadratic knapsack problem includes binary and/or linear capacity constraints. The quadratic knapsack problem has applications in several fields, such as telecommunication, transportation network, and others.

Subset-Sum Problem

The subset-sum problem, a special variant of the knapsack problem, dictates that the weight and the value of a given item should be the same. Therefore, inside the knapsack, the ratio of value to weight for each item should be one (Karp, 1972).

3.5.4. Solution Approaches for the Knapsack Problem

The knapsack problem can be solved with a number of exact solution approaches, heuristics, and metaheuristics. Gilmore and Gomory (1966) developed dynamic programming algorithms for the knapsack problem. Green (1967) suggested some extensions to Gilmore and Gomory's (1966) dynamic programming algorithms. To solve the multi-dimensional knapsack problem, Marsten and Morin (1976) integrated dynamic programming with a Branch-and-Bound approach. Isaka (1983) and Ibaraki (1987) removed irrelevant states, and, thus, improved a dynamic programming approach for the knapsack problem. However, exact optimization methods could require an extensive computational time to solve the knapsack problem. On the other hand, heuristic and metaheuristic algorithms could provide good-quality solutions within a significantly less time, especially for large-size problem instances (Kavoosi et al., 2019; Kavoosi et al., 2020a,b). A heuristic algorithm pertains to a specific problem. Several heuristic algorithms have been reported in the literature for solving the knapsack problem. Toyoda (1975) proposed a Greedy Algorithm, which was a recursive process involving a local optimum at every stage and aimed to obtain the global optimum during termination. Hanafi et al. (1996) designed a multi-

start algorithm that applied various heuristic processes with flexibility. For the multiple knapsack problem, Chekuri and Khanna (2005) presented a polynomial time approximation scheme.

Metaheuristics are applicable to a number of problems, and they effectively investigate the search space. A large number of metaheuristics have been tested for the knapsack problem. A Simulated Annealing algorithm was proposed by Drexl (1988) for the multi-dimensional knapsack problem. Dammeyer and Voss (1991) indicated that a dynamic version of the Tabu Search algorithm was more effective than the Simulated Annealing algorithm. For the knapsack problem, Khuri et al. (1994) employed a Genetic Algorithm that penalized the solutions that were infeasible. The **MORAP** mathematical model has more similarities with the multi-objective knapsack problem. The multi-objective knapsack problem can be solved with a number of metaheuristics, such as: (i) Non-dominated Sorting Genetic Algorithm II (NSGA-II); (ii) Multi-Objective Genetic Algorithm (MOGA); (iii) Pareto Archived Evolution Strategy (PAES); (iv) Multi-Objective Simulated Annealing (MOSA); (v) Multi-Objective Particle Swarm Optimization (MOPSO); among others.

4. DEVELOPMENT OF CANDIDATE SOLUTION ALGORITHMS

Single-objective optimization problems generally have one optimal solution, which has the best value of the objective function (Dulebenets et al., 2020a). On the other hand, multi-objective optimization problems (as the one that is represented by the **MORAP** mathematical model that was proposed in this project for multi-objective resource allocation among highway-rail grade crossings) do not have just one optimal solution, which has the best values for both objective functions. The latter phenomenon can be justified by the conflicting nature of the objective functions. For example, a decision maker can achieve the minimum overall hazard severity at the highway-rail grade crossings by applying a set of specific countermeasures but these countermeasures may result in traffic delays. In the meantime, a decision maker can achieve the minimum traffic delays at the highway-rail grade crossings by applying a set of specific countermeasures but these countermeasures may not yield the optimal safety performance. Therefore, instead of having just one optimal solution, multi-objective optimization problems with conflicting objectives have a set of optimal solutions that form a Pareto Front (PF). The PF can be further used to analyze tradeoffs between conflicting objectives.

A hypothetical example of a PF for conflicting resource allocation decisions at highway-rail grade crossings is presented in Figure 71. There are a total of 6 optimal solutions (i.e., resource allocation decisions) that form a PF. The PF points “1” and “6” are referred to as “corner” PF points. The corner point “1” associated with the first resource allocation decision has the best value of objective function F_1 (i.e., the overall hazard severity value of 20 hazard severity units) and the worst value of objective function F_2 (i.e., the overall traffic delay value of 45 hours). On the other hand, the corner point “6” associated with the sixth resource allocation decision has the best value of objective function F_2 (i.e., the overall traffic delay value of 5 hours) and the worst value of objective function F_1 (i.e., the overall hazard severity value of 180 hazard severity units).

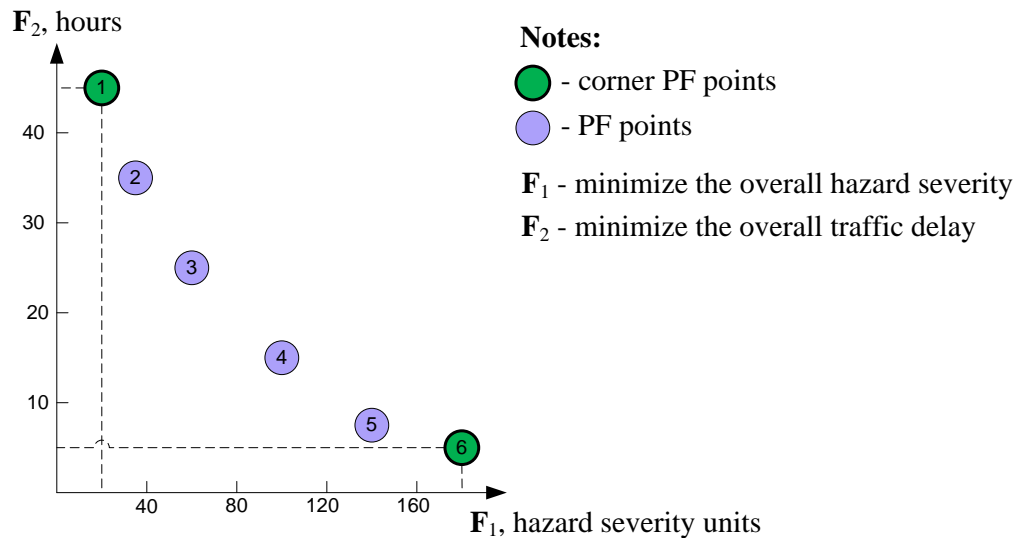


Figure 71 An illustrative example of a Pareto Front for the **MORAP** mathematical model.

This section of the report describes a set of solution algorithms for the proposed **MORAP** mathematical model. A total of three solution algorithms was developed and evaluated, including the following: (1) Epsilon-Constraint (ECON) method; (2) Multi-Objective Profitable Severity and Delay Reduction (MPSDR) heuristic; and (3) Multi-Objective Effective Severity and Delay Reduction (MESDR) heuristic. The ECON method is considered as one of the commonly used exact optimization methods for multi-objective problems (Dulebenets, 2018a; Dulebenets et al., 2020a,b; Pasha et al., 2021). The ECON method is able to provide an optimal PF for a given multi-objective optimization problem. Given the fact that the **MORAP** mathematical model has a lot of commonalities with the multi-objective knapsack problem (and, hence, has high computational complexity), finding an optimal PF may incur a substantial amount of computational time. Significant computational efforts required in order to conduct resource allocation among highway-rail grade crossings are not desirable from the practical perspective. Therefore, this project proposes two heuristic algorithms (i.e., the MPSDR and MESDR heuristics) that are expected to provide multi-objective resource allocation decisions in a timely manner. The following sections of the report provide more details regarding each one of the solution algorithms proposed in this project.

4.1. Epsilon-Constraint (ECON) Method

The first solution approach for the **MORAP** mathematical model is the Epsilon-Constraint (ECON) method. The ECON method constructs a PF iteratively by optimizing one of the objective functions (generally, the most important objective function from the practical perspective) and imposing constraint sets on the other objective function(s) to be optimized. Since safety at highway-rail grade crossings is of the utmost importance to the FDOT, the ECON method proposed in the project will minimize the overall hazard severity (denoted by function F_1) and impose an upper bound on the overall traffic delay (denoted by function F_2). The main steps of the ECON method are provided in Figure 72 and **Algorithm 1**.

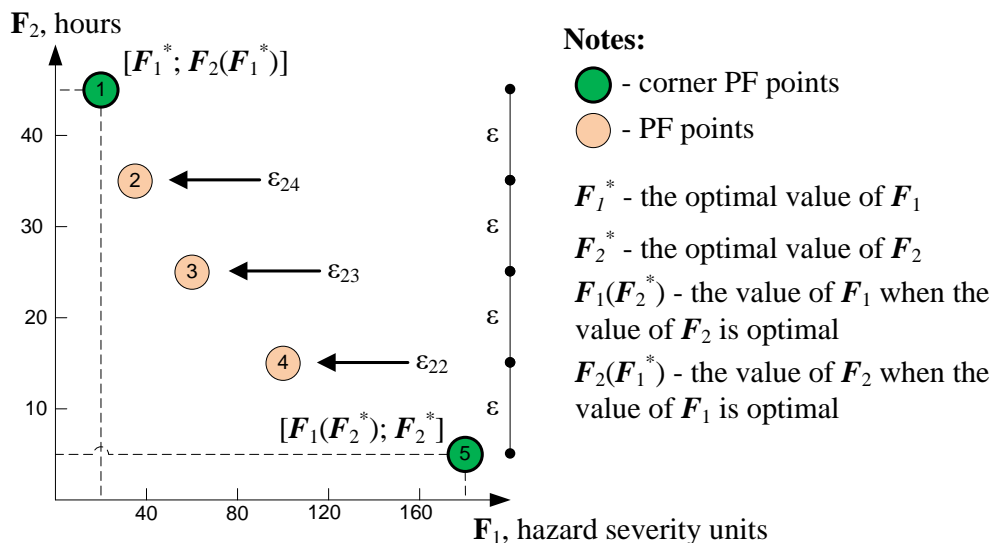


Figure 72 An illustrative example of the ECON method application.

Algorithm 1: The Epsilon-Constraint (ECON) Method

ECON($X, C, S, HS, W, p, EF, OD^0, AD, CA, TAB, PF^{size}, \varepsilon_1, \varepsilon_2$)

in: $X = \{1, \dots, n\}$ - set of crossings; $C = \{1, \dots, m\}$ - set of countermeasures; $S = \{1, \dots, k\}$ - set of severity categories; HS - hazard severity at each crossing; W - severity weights; p - crossing eligibility for upgrading; EF - effectiveness factors for countermeasures; OD^0 - overall delay with the existing warning devices; AD - additional delay due to application of each countermeasure; CA - cost of applying each countermeasure; TAB - total available budget; PF^{size} - PF size; ε_1 - upper bound on F_1 ; ε_2 - upper bound on F_2

out: PF - PF for the suggested resource allocation decisions

```
0:  $|PF| \leftarrow PF^{size}$  ◁ Initialization
1:  $[F_1^*; F_2(F_1^*)] \leftarrow \mathbf{MORAP-1}(X, C, S, HS, W, p, EF, OD^0, AD, CA, TAB, \varepsilon_2)$  ◁ Determine the  $F_1^*$  corner point
2:  $[F_1(F_2^*); F_2^*] \leftarrow \mathbf{MORAP-2}(X, C, S, HS, W, p, EF, OD^0, AD, CA, TAB, \varepsilon_1)$  ◁ Determine the  $F_2^*$  corner point
3:  $\varepsilon \leftarrow (F_2(F_1^*) - F_2^*) / (PF^{size} - 1)$  ◁ Calculate the upper bound interval for  $F_2$ 
4:  $iter \leftarrow 1$  ◁ Start the iteration counter
5:  $\varepsilon_{2(iter)} \leftarrow F_2^*$  ◁ Set the first upper bound on  $F_2$ 
6:  $PF \leftarrow PF \cup [F_1(F_2^*); F_2^*]$  ◁ Append the  $F_2^*$  corner point
7: while  $iter \leq (PF^{size} - 2)$  do
8:    $iter \leftarrow iter + 1$  ◁ Update the iteration counter
9:    $\varepsilon_{2(iter)} \leftarrow \varepsilon_{2(iter-1)} + \varepsilon$  ◁ Update the upper bound on  $F_2$ 
10:   $[F_{1(iter)}^*; F_2(F_{1(iter)}^*)] \leftarrow \mathbf{MORAP-1}(X, C, S, HS, W, p, EF, OD^0, AD, CA, TAB, \varepsilon_{2(iter)})$ 
11:   $PF \leftarrow PF \cup [F_{1(iter)}^*; F_2(F_{1(iter)}^*)]$  ◁ Append the newly generated PF point to the PF
12: end while
13:  $PF \leftarrow PF \cup [F_1^*; F_2(F_1^*)]$  ◁ Append the  $F_1^*$  corner point
14: return  $PF$ 
```

In step 0, the ECON method initializes a data structure for storing the PF for the suggested resource allocation decisions (PF). In step 1, the corner PF point with the best value of the objective function F_1 (i.e., the corner PF point $[F_1^*; F_2(F_1^*)]$ - see Figure 72) is determined by solving the **MORAP-1** mathematical model. The **MORAP-1** mathematical model presented in this section of the report aims to minimize the overall hazard severity F_1 , and an upper bound ε_2 is imposed on the overall traffic delay F_2 . In step 2, the corner PF point with the best value of the objective function F_2 (i.e., the corner PF point $[F_1(F_2^*); F_2^*]$ - see Figure 72) is determined by solving the **MORAP-2** mathematical model. The **MORAP-2** mathematical model presented in this section of the report aims to minimize the overall traffic delay F_2 , and an upper bound ε_1 is imposed on the overall hazard severity F_1 . In step 3, the ECON method calculates the upper bound interval ε for F_2 , as the PF will be constructed by minimizing F_1 and imposing an upper bound on F_2 . In step 4, the iteration counter ($iter$) is started. In step 5, the first upper bound on F_2 is set to F_2^* , assuming that the PF will be constructed starting from the F_2^* corner point. In step 6, the ECON method appends the F_2^* corner point to the PF data structure.

Then, the ECON method enters the main loop (steps 7 through 12), where the PF is constructed. In step 8, the iteration counter ($iter$) is updated. In step 9, the upper bound on F_2 for the current iteration $\varepsilon_{2(iter)}$ is updated by adding the upper bound interval ε to the upper bound on F_2 from the previous iteration $\varepsilon_{2(iter-1)}$. In step 10, the ECON method solves the **MORAP-1** mathematical model with an updated upper bound on F_2 and generates a new PF point

$[F_{1(iter)}^*; F_2(F_{1(iter)}^*)]$. In step 11, the newly generated PF point is appended to the PF data structure. Steps 7 through 12 are continuously repeated by the ECON method until the desired number of PF points (specified by the user) is generated. In step 13, the ECON method appends the F_1^* corner point to the PF data structure, which will be the last point in the PF. In step 14, the ECON method returns the PF for the suggested resource allocation decisions.

MORAP-1:

$$\min F_1 = \sum_{x \in X} \sum_{s \in S} [1 - \sum_{c \in C} (EF_{xc} \cdot z_{xc})] \cdot W_s \cdot HS_{xs} \quad (4.1)$$

Subject to:

$$\sum_{c \in C} z_{xc} \leq 1 \quad \forall x \in X \quad (4.2)$$

$$z_{xc} \leq p_{xc} \quad \forall x \in X, c \in C \quad (4.3)$$

$$\sum_{x \in X} \sum_{c \in C} CA_{xc} \cdot z_{xc} \leq TAB \quad (4.4)$$

$$F_2 = \sum_{x \in X} [OD_x^0 + \sum_{c \in C} AD_{xc} \cdot z_{xc}] \quad (4.5)$$

$$F_2 \leq \varepsilon_2 \quad (4.6)$$

$$z_{xc}, p_{xc} \in \{0,1\} \quad \forall x \in X, c \in C \quad (4.7)$$

$$HS_{xs}, W_s, EF_{xc}, OD_x^0, AD_{xc}, CA_{xc}, TAB, \varepsilon_2 \in \mathbb{R}^+ \quad \forall x \in X, c \in C, s \in S \quad (4.8)$$

MORAP-2:

$$\min F_2 = \sum_{x \in X} [OD_x^0 + \sum_{c \in C} AD_{xc} \cdot z_{xc}] \quad (4.9)$$

Subject to:

$$\sum_{c \in C} z_{xc} \leq 1 \quad \forall x \in X \quad (4.10)$$

$$z_{xc} \leq p_{xc} \quad \forall x \in X, c \in C \quad (4.11)$$

$$\sum_{x \in X} \sum_{c \in C} CA_{xc} \cdot z_{xc} \leq TAB \quad (4.12)$$

$$F_1 = \sum_{x \in X} \sum_{s \in S} [1 - \sum_{c \in C} (EF_{xc} \cdot z_{xc})] \cdot W_s \cdot HS_{xs} \quad (4.13)$$

$$F_1 \leq \varepsilon_1 \quad (4.14)$$

$$z_{xc}, p_{xc} \in \{0,1\} \quad \forall x \in X, c \in C \quad (4.15)$$

$$HS_{xs}, W_s, EF_{xc}, OD_x^0, AD_{xc}, CA_{xc}, TAB, \varepsilon_1 \in \mathbb{R}^+ \quad \forall x \in X, c \in C, s \in S \quad (4.16)$$

4.2. Multi-Objective Profitable Severity and Delay Reduction (MPSDR) Heuristic

The second solution approach for the **MORAP** mathematical model will be referred to as the Multi-Objective Profitable Severity and Delay Reduction (MPSDR) heuristic. The MPSDR heuristic constructs a PF iteratively by changing the priorities of the objectives that are used in the **MORAP** mathematical model (i.e., the priority to be assigned to the overall hazard severity

function F_1 and the priority to be assigned to the overall traffic delay function F_2). The main steps of the MPSDR heuristic are provided in **Algorithm 2**.

Algorithm 2: The Multi-Objective Profitable Severity and Delay Reduction (MPSDR) Heuristic

MPSDR($X, C, S, HS, W, p, EF, OD^0, AD, CA, TAB, PF^{size}$)
in: $X = \{1, \dots, n\}$ - set of crossings; $C = \{1, \dots, m\}$ - set of countermeasures; $S = \{1, \dots, k\}$ - set of severity categories; HS - hazard severity at each crossing; W - severity weights; p - crossing eligibility for upgrading; EF - effectiveness factors for countermeasures; OD^0 - overall delay with the existing warning devices; AD - additional delay due to application of each countermeasure; CA - cost of applying each countermeasure; TAB - total available budget; PF^{size} - PF size
out: PF - PF for the suggested resource allocation decisions

- 0: $|HSR| \leftarrow n \cdot m; |TDR| \leftarrow n \cdot m; |PF| \leftarrow PF^{size}$ ◁ Initialization
- 1: **for all** $x \in X$ **do**
- 2: **for all** $c \in C$ **do**
- 3: $HSR_{xc} \leftarrow (\sum_{s \in S} HS_{xs} \cdot W_s) \cdot EF_{xc}$ ◁ Estimate the hazard severity reduction
- 4: $TDR_{xc} \leftarrow \max_c(AD_{xc}) - AD_{xc}$ ◁ Estimate the traffic delay reduction
- 5: **end for**
- 6: **end for**
- 7: $\overline{HSR} \leftarrow HSR / \sum_{x \in X} \sum_{c \in C} HSR_{xc}; \overline{TDR} \leftarrow TDR / \sum_{x \in X} \sum_{c \in C} TDR_{xc}$ ◁ Normalize the HSR and TDR values
- 8: $iter \leftarrow 1$ ◁ Start the iteration counter
- 9: **while** $iter \leq PF^{size}$ **do**
- 10: $\Pi^{HS} \leftarrow 1.00 - (iter - 1) \cdot (1/[PF^{size} - 1]); \Pi^{TD} \leftarrow 1.00 - \Pi^{HS}$ ◁ Assign the objective priorities
- 11: $\Pi \leftarrow [\Pi^{HS}, \Pi^{TD}]$ ◁ Create a data structure for the objective priorities
- 12: $[F_1, F_2] \leftarrow \mathbf{PSDR}(X, C, S, HS, W, p, EF, OD^0, AD, CA, TAB, \Pi, \overline{HSR}, \overline{TDR})$ ◁ Apply the PSDR heuristic
- 13: $PF \leftarrow PF \cup [F_1, F_2]$ ◁ Append the newly generated PF point to the PF
- 14: $iter \leftarrow iter + 1$ ◁ Update the iteration counter
- 15: **end while**
- 16: **return** PF

In step 0, the MPSDR heuristic initializes several data structures for storing some of the variables that will be further used by the algorithm (i.e., the hazard severity reduction = HSR ; the traffic delay reduction = TDR ; the PF for the suggested resource allocation decisions = PF). Then, the MPSDR heuristic enters the first loop (steps 1 through 6), where the hazard severity reduction values and the traffic delay reduction values are estimated. Note that the hazard severity reduction for each crossing-countermeasure pair is estimated based of the predicted crossing hazard severities (i.e., fatality hazard, injury hazard, and property damage hazard), severity weights, and effectiveness factors of countermeasures. On the other hand, the traffic delay reduction due to application of a given countermeasure for a given highway-rail grade crossing is estimated as a difference between the maximum additional delay that could be potentially incurred due to application of one of the considered countermeasures and the additional delay due to application of a given countermeasure. For example, assume that there is highway-rail grade crossing x , and two types of countermeasures are considered for implementation at that crossing. The additional delay due to application of the first countermeasure is $AD_{x1} = 5$ seconds, while the additional delay due to application of the second countermeasure is $AD_{x2} = 30$ seconds. Hence, the potential traffic delay reduction due to application of the first

countermeasure for highway-rail grade crossing x will be $TDR_{x1} = \max(AD_{x1}, AD_{x2}) - AD_{x1} = \max(5,30) - 5 = 30 - 5 = 25$ seconds. On the other hand, the potential traffic delay reduction due to application of the second countermeasure for highway-rail grade crossing x will be $TDR_{x2} = \max(AD_{x1}, AD_{x2}) - AD_{x2} = \max(5,30) - 30 = 30 - 30 = 0$ seconds because the second countermeasure has the largest value of AD_{xc} .

After that, the MPSDR heuristic normalizes the HSR and TDR values (step 7). The purpose of normalizing the estimated values of the hazard severity reduction and the traffic delay reduction consists in the fact that these values may have different magnitudes (e.g., the hazard severity reduction may vary from 0.01 to 20,000 hazard severity units, while the traffic delay reduction may vary from 0.01 to 50.00 hours). After normalization, the sum of the hazard severity reduction values over all the crossing-countermeasure pairs will be equal to 1.00, and the sum of the traffic delay reduction values over all the crossing-countermeasure pairs will be equal to 1.00. Such a normalization procedure would be important when assigning priorities to the considered objectives (i.e., minimize the overall hazard severity vs. minimize the overall traffic delay).

Then, the MPSDR heuristic enters the second loop (steps 9 through 15), where the PF is constructed. In step 10, the priorities are updated for the overall hazard severity minimization objective and the overall traffic delay minimization objective (i.e., the values of Π^{HS} and Π^{TD} , respectively). Note that the objective priority values were assumed to vary from 0.00 to 1.00, such that $\Pi^{HS} + \Pi^{TD} = 1.00$ in each iteration of the MPSDR heuristic. It is assumed that the highest priority is assigned to the overall hazard severity minimization objective ($\Pi^{HS} = 1.00$), and the lowest priority is assigned to the overall traffic delay minimization objective ($\Pi^{TD} = 0.00$) in the first iteration. However, the priorities will be adjusted in the consecutive iterations of the MPSDR heuristic. In the last iteration, the highest priority will be assigned to the overall traffic delay minimization objective ($\Pi^{TD} = 1.00$), and the lowest priority will be assigned to the overall hazard severity minimization objective ($\Pi^{HS} = 0.00$). In step 12, the PSDR heuristic (that will be described later in this section of the report) is executed for the generated priority values to obtain a PF point characterized with the F_1 and F_2 values. In step 13, the newly generated PF point is appended to the PF data structure. In step 14, the iteration counter ($iter$) is updated. Steps 9 through 15 are continuously repeated by the MPSDR heuristic until the desired number of PF points (specified by the user) is generated. Note that a different PF point will be generated in each iteration of the MPSDR heuristic because different priorities will be assigned to the considered objectives.

The main steps of the PSDR heuristic, which is executed by the MPSDR heuristic in each iteration for generating a new PF point, are provided in **Algorithm 3**. In step 0, the PSDR heuristic initializes several data structures for storing some of the variables that will be further used by the algorithm (i.e., the assignment of countermeasures to crossings = \mathbf{z} ; the priority list of highway-rail grade crossings = $List$; the benefit-to-cost ratios = BCR ; and the remaining budget = RB). Then, the PSDR heuristic enters the first loop (steps 1 through 6), where the benefit-to-cost ratio is estimated for each crossing-countermeasure pair, and the priority list of highway-rail grade crossings is created. Note that the benefit-to-cost ratios are estimated for crossing-countermeasure pairs based on the normalized hazard severity reduction, normalized traffic delay reduction, associated objective priorities (i.e., the values of Π^{HS} and Π^{TD} ,

respectively) that were previously set by the MPSDR heuristic, and cost of applying countermeasures. In step 7, all the crossing-countermeasure pairs in the priority list are sorted in the descending order based on the BCR values. Furthermore, infeasible crossing-countermeasure pairs, where the highway-rail grade crossings are not eligible for certain countermeasures, are removed from the priority list in step 7.

Algorithm 3: The Profitable Severity and Delay Reduction (PSDR) Heuristic

PSDR($X, C, S, HS, W, p, EF, OD^0, AD, CA, TAB, \Pi, \overline{HSR}, \overline{TDR}$)
in: $X = \{1, \dots, n\}$ - set of crossings; $C = \{1, \dots, m\}$ - set of countermeasures; $S = \{1, \dots, k\}$ - set of severity categories; HS - hazard severity at each crossing; W - severity weights; p - crossing eligibility for upgrading; EF - effectiveness factors for countermeasures; OD^0 - overall delay with the existing warning devices; AD - additional delay due to application of each countermeasure; CA - cost of applying each countermeasure; TAB - total available budget; Π - priorities of objectives; \overline{HSR} - normalized hazard severity reduction; \overline{TDR} - normalized traffic delay reduction
out: F_1 - the overall hazard severity; F_2 - the overall traffic delay

```

0:  $|z| \leftarrow n \cdot m$ ;  $List \leftarrow \emptyset$ ;  $|BCR| \leftarrow n \cdot m$ ;  $RB \leftarrow TAB$                                  $\triangleleft$  Initialization
1: for all  $x \in X$  do
2:   for all  $c \in C$  do
3:      $BCR_{xc} \leftarrow ([\overline{HSR}_{xc} \cdot \Pi^{HS}] + [\overline{TDR}_{xc} \cdot \Pi^{TD}]) / CA_{xc}$                                  $\triangleleft$  Estimate the benefit-to-cost ratio
4:      $List \leftarrow List \cup \{x, c\}$                                                                  $\triangleleft$  Add a crossing-countermeasure pair to the list
5:   end for
6: end for
7:  $List \leftarrow \text{sort}(List, p, BCR)$                                                                  $\triangleleft$  Sort the list based on the benefit-to-cost ratios
8: while  $List \neq \emptyset$  and  $RB \geq \min(CA)$  do
9:    $x \leftarrow List_1^x$                                                                                  $\triangleleft$  Select the next crossing in the list
10:   $c \leftarrow List_1^c$                                                                                  $\triangleleft$  Select the next countermeasure in the list
11:  if  $RB \geq CA_{xc}$  do
12:     $z_{xc} \leftarrow 1$                                                                                  $\triangleleft$  Assign the countermeasure for the selected crossing
13:     $RB \leftarrow RB - CA_{xc}$                                                                          $\triangleleft$  Update the remaining budget
14:     $List \leftarrow List - \{x, : \}$                                                                  $\triangleleft$  Remove all the crossing-countermeasure pairs from the list
15:  else
16:     $List \leftarrow List - \{x, c\}$                                                                  $\triangleleft$  Remove the selected crossing-countermeasure pair from the list
17:  end if
18: end while
19:  $F_1 = \sum_{x \in X} \sum_{s \in S} [1 - \sum_{c \in C} (EF_{xc} \cdot z_{xc})] \cdot W_s \cdot HS_{xs}$ ;  $F_2 = \sum_{x \in X} [OD_x^0 + \sum_{c \in C} AD_{xc} \cdot z_{xc}]$ 
20: return  $[F_1, F_2]$ 

```

After that, the PSDR heuristic enters the second loop (steps 8 through 18). In steps 9 and 10, the next highway-rail grade crossing in the priority list along with the associated countermeasure is selected by the PSDR heuristic. In steps 11-17, the PSDR heuristic is checking whether the remaining budget is sufficient for application of a given countermeasure at the considered highway-rail grade crossing in the priority list. In case the remaining budget is sufficient, the following steps will be performed: (1) the selected countermeasure will be assigned to the considered highway-rail grade crossing (step 12); (2) the remaining budget will be updated (step 13); and (3) all the crossing-countermeasure pairs associated with the highway-rail grade crossing that was assigned for upgrading will be removed from the priority list (step 14). On the other hand, if the remaining budget is not sufficient for application of a given countermeasure at

the considered highway-rail grade crossing, the PSDR heuristic will remove the selected crossing-countermeasure pair from the priority list (step 16). However, the other crossing-countermeasure pairs associated with that highway-rail grade crossing may be still present in the priority list and further evaluated by the PSDR heuristic in later iterations. Steps 8 through 18 are continuously repeated by the PSDR heuristic until all the resource allocation decisions have been made for the considered highway-rail grade crossings (i.e., the value of decision variable \mathbf{z} has been set). In step 19, the values of the objective functions F_1 and F_2 are estimated based on the \mathbf{z} value. In step 20, a newly generated PF point, which is characterized with the F_1 and F_2 values, is returned to the MPSDR heuristic.

4.3. Multi-Objective Effective Severity and Delay Reduction (MESDR) Heuristic

The third solution approach for the **MORAP** mathematical model will be referred to as the Multi-Objective Effective Severity and Delay Reduction (MESDR) heuristic. Similar to the MPSDR heuristic, the MESDR heuristic constructs a PF iteratively by changing the priorities of the objectives that are used in the **MORAP** mathematical model (i.e., the priority to be assigned to the overall hazard severity function F_1 and the priority to be assigned to the overall traffic delay function F_2). The main steps of the MESDR heuristic are provided in **Algorithm 4**.

Algorithm 4: The Multi-Objective Effective Severity and Delay Reduction (MESDR) Heuristic

MESDR($X, C, S, HS, W, p, EF, OD^0, AD, CA, TAB, PF^{size}$)

in: $X = \{1, \dots, n\}$ - set of crossings; $C = \{1, \dots, m\}$ - set of countermeasures; $S = \{1, \dots, k\}$ - set of severity categories; HS - hazard severity at each crossing; W - severity weights; p - crossing eligibility for upgrading; EF - effectiveness factors for countermeasures; OD^0 - overall delay with the existing warning devices; AD - additional delay due to application of each countermeasure; CA - cost of applying each countermeasure; TAB - total available budget; PF^{size} - PF size

out: PF - PF for the suggested resource allocation decisions

```

0:  $|HSR| \leftarrow n \cdot m; |TDR| \leftarrow n \cdot m; |PF| \leftarrow PF^{size}$                                  $\triangleleft$  Initialization
1: for all  $x \in X$  do
2:   for all  $c \in C$  do
3:      $HSR_{xc} \leftarrow (\sum_{s \in S} HS_{xs} \cdot W_s) \cdot EF_{xc}$                                  $\triangleleft$  Estimate the hazard severity reduction
4:      $TDR_{xc} \leftarrow \max_c(AD_{xc}) - AD_{xc}$                                          $\triangleleft$  Estimate the traffic delay reduction
5:   end for
6: end for
7:  $\overline{HSR} \leftarrow HSR / \sum_{x \in X} \sum_{c \in C} HSR_{xc}; \overline{TDR} \leftarrow TDR / \sum_{x \in X} \sum_{c \in C} TDR_{xc}$    $\triangleleft$  Normalize the  $HSR$  and  $TDR$  values
8:  $iter \leftarrow 1$                                                                  $\triangleleft$  Start the iteration counter
9: while  $iter \leq PF^{size}$  do
10:   $\Pi^{HS} \leftarrow 1.00 - (iter - 1) \cdot (1/[PF^{size} - 1]); \Pi^{TD} \leftarrow 1.00 - \Pi^{HS}$    $\triangleleft$  Assign the objective priorities
11:   $\Pi \leftarrow [\Pi^{HS}, \Pi^{TD}]$                                                  $\triangleleft$  Create a data structure for the objective priorities
12:   $[F_1, F_2] \leftarrow \mathbf{ESDR}(X, C, S, HS, W, p, EF, OD^0, AD, CA, TAB, \Pi, \overline{HSR}, \overline{TDR})$    $\triangleleft$  Apply the ESDR heuristic
13:   $PF \leftarrow PF \cup [F_1, F_2]$                                                  $\triangleleft$  Append the newly generated PF point to the PF
14:   $iter \leftarrow iter + 1$                                                      $\triangleleft$  Update the iteration counter
15: end while
16: return  $PF$ 

```

In step 0, the MESDR heuristic initializes several data structures for storing some of the variables that will be further used by the algorithm (i.e., the hazard severity reduction = HSR ; the traffic delay reduction = TDR ; the PF for the suggested resource allocation decisions = PF). Then, the MESDR heuristic enters the first loop (steps 1 through 6), where the hazard severity reduction values and the traffic delay reduction values are estimated. After that, the MESDR heuristic normalizes the HSR and TDR values (step 7). Then, the MESDR heuristic enters the second loop (steps 9 through 15), where the PF is constructed. In step 10, the priorities are updated for the overall hazard severity minimization objective and the overall traffic delay minimization objective (i.e., the values of Π^{HS} and Π^{TD} , respectively). Note that the objective priority values were assumed to vary from 0.00 to 1.00, such that $\Pi^{HS} + \Pi^{TD} = 1.00$ in each iteration of the MESDR heuristic. It is assumed that the highest priority is assigned to the overall hazard severity minimization objective ($\Pi^{HS} = 1.00$), and the lowest priority is assigned to the overall traffic delay minimization objective ($\Pi^{TD} = 0.00$) in the first iteration. However, the priorities will be adjusted in the consecutive iterations of the MESDR heuristic. In the last iteration, the highest priority will be assigned to the overall traffic delay minimization objective ($\Pi^{TD} = 1.00$), and the lowest priority will be assigned to the overall hazard severity minimization objective ($\Pi^{HS} = 0.00$).

In step 12, the ESDR heuristic (that will be described later in this section of the report) is executed for the generated priority values to obtain a PF point characterized with the F_1 and F_2 values. In step 13, the newly generated PF point is appended to the PF data structure. In step 14, the iteration counter ($iter$) is updated. Steps 9 through 15 are continuously repeated by the MESDR heuristic until the desired number of PF points (specified by the user) is generated. Note that a different PF point will be generated in each iteration of the MESDR heuristic because different priorities will be assigned to the considered objectives.

The main steps of the ESDR heuristic, which is executed by the MESDR heuristic in each iteration for generating a new PF point, are provided in **Algorithm 5**. In step 0, the ESDR heuristic initializes several data structures for storing some of the variables that will be further used by the algorithm (i.e., the assignment of countermeasures to crossings = \mathbf{z} ; the priority list of highway-rail grade crossings = $List$; the hazard severity and traffic delay reduction values = SDR ; and the remaining budget = RB). Then, the ESDR heuristic enters the first loop (steps 1 through 6), where the hazard severity and traffic delay reduction value is estimated for each crossing-countermeasure pair, and the priority list of highway-rail grade crossings is created. Note that the hazard severity and traffic delay reduction values are estimated for the crossing-countermeasure pairs based on the normalized hazard severity reduction, normalized traffic delay reduction, and associated objective priorities (i.e., the values of Π^{HS} and Π^{TD} , respectively) that were previously set by the MESDR heuristic. In step 7, all the crossing-countermeasure pairs in the priority list are sorted in the descending order based on the SDR values (i.e., the cost of countermeasures is not considered by the ESDR heuristic when creating the priority list as opposed to the PSDR heuristic). Furthermore, infeasible crossing-countermeasure pairs, where the highway-rail grade crossings are not eligible for certain countermeasures, are removed from the priority list in step 7.

Algorithm 5: The Effective Severity and Delay Reduction (ESDR) Heuristic

ESDR($X, C, S, HS, W, p, EF, OD^0, AD, CA, TAB, \Pi, \overline{HSR}, \overline{TDR}$)
in: $X = \{1, \dots, n\}$ - set of crossings; $C = \{1, \dots, m\}$ - set of countermeasures; $S = \{1, \dots, k\}$ - set of severity categories; HS - hazard severity at each crossing; W - severity weights; p - crossing eligibility for upgrading; EF - effectiveness factors for countermeasures; OD^0 - overall delay with the existing warning devices; AD - additional delay due to application of each countermeasure; CA - cost of applying each countermeasure; TAB - total available budget; Π - priorities of objectives; \overline{HSR} - normalized hazard severity reduction; \overline{TDR} - normalized traffic delay reduction
out: F_1 - the overall hazard severity; F_2 - the overall traffic delay

- 0: $|z| \leftarrow n \cdot m$; $List \leftarrow \emptyset$; $|SDR| \leftarrow n \cdot m$; $RB \leftarrow TAB$ \triangleleft Initialization
- 1: **for all** $x \in X$ **do**
- 2: **for all** $c \in C$ **do**
- 3: $SDR_{xc} \leftarrow (\overline{HSR}_{xc} \cdot \Pi^{HS}) + [\overline{TDR}_{xc} \cdot \Pi^{TD}]$ \triangleleft Estimate the hazard severity and traffic delay reduction
- 4: $List \leftarrow List \cup \{x, c\}$ \triangleleft Add a crossing-countermeasure pair to the list
- 5: **end for**
- 6: **end for**
- 7: $List \leftarrow \text{sort}(List, p, SDR)$ \triangleleft Sort the list based on the hazard severity and traffic delay reduction
- 8: **while** $List \neq \emptyset$ **and** $RB \geq \min(CA)$ **do**
- 9: $x \leftarrow List_1^x$ \triangleleft Select the next crossing in the list
- 10: $c \leftarrow List_1^c$ \triangleleft Select the next countermeasure in the list
- 11: **if** $RB \geq CA_{xc}$ **do**
- 12: $z_{xc} \leftarrow 1$ \triangleleft Assign the countermeasure for the selected crossing
- 13: $RB \leftarrow RB - CA_{xc}$ \triangleleft Update the remaining budget
- 14: $List \leftarrow List - \{x, \cdot\}$ \triangleleft Remove all the crossing-countermeasure pairs from the list
- 15: **else**
- 16: $List \leftarrow List - \{x, c\}$ \triangleleft Remove the selected crossing-countermeasure pair from the list
- 17: **end if**
- 18: **end while**
- 19: $F_1 = \sum_{x \in X} \sum_{s \in S} [1 - \sum_{c \in C} (EF_{xc} \cdot z_{xc})] \cdot W_s \cdot HS_{xs}$; $F_2 = \sum_{x \in X} [OD_x^0 + \sum_{c \in C} AD_{xc} \cdot z_{xc}]$
- 20: **return** $[F_1, F_2]$

After that, the ESDR heuristic enters the second loop (steps 8 through 18). In steps 9 and 10, the next highway-rail grade crossing in the priority list along with the associated countermeasure is selected by the ESDR heuristic. In steps 11-17, the ESDR heuristic is checking whether the remaining budget is sufficient for application of a given countermeasure at the considered highway-rail grade crossing in the priority list. In case the remaining budget is sufficient, the following steps will be performed: (1) the selected countermeasure will be assigned to the considered highway-rail grade crossing (step 12); (2) the remaining budget will be updated (step 13); and (3) all the crossing-countermeasure pairs associated with the highway-rail grade crossing that was assigned for upgrading will be removed from the priority list (step 14). On the other hand, if the remaining budget is not sufficient for application of a given countermeasure at the considered highway-rail grade crossing, the ESDR heuristic will remove the selected crossing-countermeasure pair from the priority list (step 16). However, the other crossing-countermeasure pairs associated with that highway-rail grade crossing may be still present in the priority list and further evaluated by the ESDR heuristic in later iterations. Steps 8 through 18 are continuously repeated by the ESDR heuristic until all the resource allocation decisions have been

made for the considered highway-rail grade crossings (i.e., the value of decision variable \mathbf{z} has been set). In step 19, the values of the objective functions F_1 and F_2 are estimated based on the \mathbf{z} value. In step 20, a newly generated PF point, which is characterized with the F_1 and F_2 values, is returned to the MESDR heuristic.

5. EVALUATION OF SOLUTION ALGORITHMS

A set of candidate solution algorithms has to be carefully evaluated in terms of different performance indicators before they can be applied to a given problem of interest (Dulebenets, 2015; Dulebenets, 2018a-f). This section provides a detailed evaluation of the developed ECON, MPSDR, and MESDR solution algorithms. The following sections elaborate on the following aspects: (1) required input data; (2) CPU settings; (3) comparison of Pareto Fronts; (4) computational time; (5) solution algorithm recommendation; and (6) Pareto Front size effects.

5.1. Required Input Data

The input data for a given problem of interest have to be appropriately set to ensure an accurate evaluation of the candidate solution algorithms (Dulebenets, 2018g-i; Dulebenets, 2019a,b; Abioye et al., 2019; Abioye et al., 2020; Pasha et al., 2020a-c). This section provides details regarding the data that were used for the attributes of highway-rail grade crossings, attributes of countermeasures, hazard severity estimations, and traffic delay estimations. Furthermore, generation of problem instances and scenarios for evaluation of the candidate solution algorithms is discussed in this section as well.

5.1.1. Attributes of Highway-Rail Grade Crossings

The information regarding the major attributes of highway-rail grade crossings (e.g., average daily traffic volume, average daily train volume, train speed, protection class) will be retrieved from the FRA crossing inventory database (FRA, 2020a). The FRA crossing inventory database, which was accessed in May 2020, revealed that among the 9,090 highway-rail grade crossings in Florida, 2,896 highway-rail grade crossings (or 31.9% of highway-rail grade crossings) were privately owned. The majority of the highway-rail grade crossings in Florida, however, were public highway-rail grade crossings, since 6,109 highway-rail grade crossings (or 67.2% of highway-rail grade crossings) were categorized as public. The candidate solution algorithms will be evaluated for the public highway-rail grade crossings. The information from the FRA crossing inventory database will be required within the developed **MORAP** mathematical model in order to estimate the overall hazard at highway-rail grade crossings (based on the Florida Priority Index Formula) and further disaggregate the overall hazard into different severity categories (as discussed in section 5.1.3 of the report). Along with the major attributes of highway-rail grade crossings, the accident data will be required in order to estimate the overall hazard at highway-rail grade crossings. The FRA highway-rail grade crossing accident database (FRA, 2020b) will be used to estimate the 5-year accident history for each one of highway-rail grade crossings, which is necessary for the overall hazard calculations.

5.1.2. Attributes of Countermeasures

A set of countermeasures that is proposed in the GradeDec.NET Reference Manual (U.S. DOT, 2014a) will be adopted throughout this project in order to evaluate the candidate solution algorithms for the **MORAP** mathematical model. Table 17 presents the key information for the considered countermeasures, including the following: (1) effectiveness factors (EF_{xc} , $x \in X$, $c \in C$); and (2) installation costs (CA_{xc} , $x \in X$, $c \in C$). Furthermore, feasible countermeasure types that can be implemented for various protection classes of highway-rail grade crossings are specified in Table 18. Note that the protection classes were used from the FRA crossing inventory database (field “WdCode” – warning device code) – FRA (2020a). The adopted 11

countermeasures are recommended by the U.S. DOT and have been widely used across the U.S. for safety improvements at highway-rail grade crossings. Hence, these countermeasures will be used throughout evaluation of the candidate solution algorithms for the **MORAP** mathematical model. However, the solution algorithms developed in this project can be executed for the alternative types of countermeasures depending on the user needs.

Table 17 Key information for the default countermeasures considered.

a/a	Countermeasure	Effectiveness	Installation Cost
1	passive to flashing lights	0.57	\$74,800
2	passive to flashing lights and gates	0.78	\$180,900
3	flashing lights to gates	0.63	\$106,100
4	4 quadrant (no detection) - for gated crossings	0.82	\$244,000
5	4 quadrant (with detection) - for gated crossings	0.77	\$260,000
6	4 quadrant (with 60' medians) - for gated crossings	0.92	\$255,000
7	mountable curbs (with channelized devices) - for gated crossings	0.75	\$15,000
8	barrier curbs (with or without channelized devices) - for gated crossings	0.80	\$15,000
9	one-way street with gate - for gated crossings	0.82	\$5,000
10	photo enforcement - for gated crossings	0.78	\$65,000
11	grade separation	1.00	\$1,500,000

Table 18 Feasibility of countermeasure implementation for the protection classes considered.

a/a	Protection Class	Feasible Countermeasures
1	No signs or signals (WdCode = 1)	1, 2
2	Other signs or signals (WdCode = 2)	1, 2
3	Crossbucks (WdCode = 3)	1, 2
4	Stop signs (WdCode = 4)	1, 2
5	Special active warning devices (WdCode = 5)	1, 2
6	Highway traffic signals, wigwags, bells, or other activated (WdCode = 6)	1, 2
7	Flashing lights (WdCode = 7)	3
8	All other gates (WdCode = 8)	4, 5, 6, 7, 8, 9, 10, 11
9	Four quad (full barrier) gates (WdCode = 9)	5, 6, 7, 8, 9, 10, 11

5.1.3. Hazard Severity Data

As it was indicated earlier, the overall hazard (estimated based on the Florida Priority Index Formula in this project) will be differentiated into hazard severities of several categories. Based on the GradeDec.NET Reference Manual (U.S. DOT, 2014a), a total of three severity categories will be considered in this project, including the following: (1) fatality accidents – these accidents involve at least one fatality; (2) casualty accidents – these accidents involve at least one fatality or injury; and (3) property damage only accidents – these accidents involve no fatalities or injuries, and only property damage is reported. This project assumes the societal costs of each fatal accident (*FA*), injury accident (*IA*), and property damage only accident (*PDO*) to be

\$4,500,000, \$650,000, and \$35,000, respectively (Iowa DOT, 2020). Hence, the weight of each severity category will be quantified as follows:

$$W_{FH} = \frac{\$4,500,000}{(\$4,500,000 + \$650,000 + \$35,000)} = 0.87 \quad (5.1)$$

$$W_{IH} = \frac{\$650,000}{(\$4,500,000 + \$650,000 + \$35,000)} = 0.12 \quad (5.2)$$

$$W_{PH} = \frac{\$35,000}{(\$4,500,000 + \$650,000 + \$35,000)} = 0.01 \quad (5.3)$$

where:

W_{FH} = weight of fatality hazard (fatality hazard severity units);

W_{IH} = weight of injury hazard (injury hazard severity units);

W_{PH} = weight of property damage hazard (property damage hazard severity units).

This project will set the base values for the weights of fatality hazard, injury hazard, and property damage hazard to $W_{FH} = 0.90$, $W_{IH} = 0.09$, and $W_{PH} = 0.01$, respectively, which are near the values suggested by the Iowa DOT (2020). Note that these weights can be tuned by the user if necessary (e.g., due to changes in societal costs). The FDOT representatives will be able to set the appropriate values depending on the societal costs of highway-rail grade crossing accidents across the state.

5.1.4. Traffic Delay Data

As a part of this project, a new formula was developed for estimation of the overall traffic delay due to the presence of countermeasures (and implementation of countermeasures) at highway-rail grade crossings or halting of the associated highway traffic because of passing trains. A number of parameters will be required in order to estimate the overall traffic delay at highway-rail grade crossings. The effective time during which a train blocks highway-rail grade crossing x with the existing warning devices ($EBT_x^0, x \in X$) and the effective time during which a train blocks highway-rail grade crossing x after implementation of countermeasure c ($EBT_{xc}, x \in X, c \in C$) will require the following inputs: (1) the average train length for highway-rail grade crossing x ($L_x, x \in X$); (2) the average train speed for highway-rail grade crossing x ($SC_x, x \in X$); and (3) the current delay time for highway-rail grade crossing x with the existing warning devices ($CCD_x^0, x \in X$). The average train length at highway-rail grade crossings was set to 7,000 ft (GAO, 2019). The maximum timetable train speed was used as a starting value for the train speed when passing highway-rail grade crossings, as the maximum timetable train speed values are available in the FRA crossing inventory database. In the meantime, the upper and lower bounds were imposed on the average train speed at highway-rail grade crossings to make sure that it remains within reasonable limits: $SC^{min} \leq SC_x \leq SC^{max} \forall x \in X$ ($SC^{min} = 20$ mph and $SC^{max} = 49$ mph).

The current delay time for highway-rail grade crossing x with the existing warning devices was set based on the existing protection (see Table 19, where notation “CCDe” is used instead of “CCD” as the delay time values are based on the protection class). Furthermore, the effective time during which a train blocks highway-rail grade crossing x after implementation of countermeasure c ($EBT_{xc}, x \in X, c \in C$) will require the data for the additional delay time that is

incurred on average at highway-rail grade crossings after implementation of countermeasure c ($ACD_c, c \in C$). The values of $ACD_c, c \in C$ are provided in Table 20 for different types of countermeasures. It can be observed that the additional delay time values substantially vary depending on the countermeasure type. For example, the additional delay time that is incurred on average at highway-rail grade crossings with passive protection after installing flashing lights is $ACD_c = 5$ seconds. On the other hand, the additional delay time that is incurred on average at highway-rail grade crossings with passive protection after installing flashing lights and gates is $ACD_c = 30$ seconds. It is assumed that no delays will be incurred after implementing grade separation, since the highway traffic will not be interrupted by passing trains after application of grade separation (i.e., grade separation will have $ACD_c = 0$ seconds and $OD_{xc} = 0$ hours). For other countermeasures, $ACD_c, c \in C$ should be greater than 0 (i.e., at least 0.0001 sec).

Table 19 The current delay time based on the existing protection.

a/a	Protection Class	WdCode	CCDe, sec
1	no signs or signals	1	0.00
2	other signs or signals	2	5.00
3	crossbucks	3	5.00
4	stop signs	4	5.00
5	special active warning devices	5	10.00
6	highway traffic signals, wigwags, bells, or other activated	6	10.00
7	flashing lights	7	10.00
8	all other gates	8	35.00
9	four quad (full barrier) gates	9	40.00

Table 20 The additional delay time that is incurred on average at highway-rail grade crossings after implementation of different countermeasures.

a/a	Countermeasures	ACD(c), sec
1	passive to flashing lights	5.00
2	passive to flashing lights and gates	30.00
3	flashing lights to gates	25.00
4	4 quadrant (no detection) - for gated crossings	5.00
5	4 quadrant (with detection) - for gated crossings	5.00
6	4 quadrant (with 60' medians) - for gated crossings	7.50
7	mountable curbs (with channelized devices) - for gated crossings	7.50
8	barrier curbs (with or without channelized devices) - for gated crossings	7.50
9	one-way street with gate - for gated crossings	5.00
10	photo enforcement - for gated crossings	5.00
11	grade separation	0.00

The queue dissipation time after the train passes highway-rail grade crossing x with the existing warning devices ($QDT_x^0, x \in X$) and the queue dissipation time after the train passes highway-rail grade crossing x with implementation of countermeasure c ($QDT_{xc}, x \in X, c \in C$) will require the data for the number of traffic lanes at each highway-rail grade crossing, which will be adopted

from the FRA crossing inventory database (FRA, 2020a). In order to avoid abnormal queue dissipation time values at highway-rail grade crossings, this project assumes that the maximum queue length per lane at highway-rail grade crossings should not exceed $VQ^{max} = 8$ vehicles, and the maximum queue dissipation time at highway-rail grade crossings should not exceed $QDT^{max} = 60$ seconds. Note that the aforementioned parameters will be used for estimation of the overall traffic delay at highway-rail grade crossings throughout evaluation of the candidate solution algorithms in this project. The values of these parameters were set using the data reported in the available literature (AREMA, 2004; ITE, 2006; GAO, 2019; U.S. DOT, 2019; FRA, 2020a). However, without loss of generality, the FDOT representatives will be able to set the appropriate values for the overall traffic delay components if more specific data are available for the highway-rail grade crossings of interest.

5.1.5. Generation of Problem Instances and Scenarios

A total of 12 problem instances was developed in this project in order to evaluate the candidate solution algorithms for the **MORAP** mathematical model by changing the total available budget as follows: (1) problem instance 1 – $TAB = \$4.5M$; (2) problem instance 2 – $TAB = \$5.0M$; (3) problem instance 3 – $TAB = \$5.5M$; (4) problem instance 4 – $TAB = \$6.0M$; (5) problem instance 5 – $TAB = \$6.5M$; (6) problem instance 6 – $TAB = \$7.0M$; (7) problem instance 7 – $TAB = \$7.5M$; (8) problem instance 8 – $TAB = \$8.0M$; (9) problem instance 9 – $TAB = \$8.5M$; (10) problem instance 10 – $TAB = \$9.0M$; (11) problem instance 11 – $TAB = \$9.5M$; and (12) problem instance 12 – $TAB = \$10.0M$. Note that the adopted values for the total available budget were set based on the data reported by the Florida’s Highway-Rail Grade Crossing Safety Action Plan (FDOT, 2011; p. 10). Furthermore, a total of 121 different scenarios was generated for each problem instance by altering the number of public highway-rail grade crossings (i.e., cardinality of set $X - |X|$) and the number of available countermeasures (i.e., cardinality of set $C - |C|$). In particular, the following values for the number of public highway-rail grade crossings were considered: (1) $|X| = 3200$; (2) $|X| = 3500$; (3) $|X| = 3800$; (4) $|X| = 4100$; (5) $|X| = 4400$; (6) $|X| = 4700$; (7) $|X| = 5000$; (8) $|X| = 5300$; (9) $|X| = 5600$; (10) $|X| = 5900$; and (11) $|X| = 6109$. The number of available countermeasures, on the other hand, was altered from 1 to 11 with an increment of 1 countermeasure.

5.2. CPU Settings

All the numerical experiments in this project were executed on a CPU with Dell Intel(R) Core™ i7 Processor, 32 GB of RAM, and Operating System Windows 10. The ECON method was implemented within the MATLAB environment (MathWorks, 2020). CPLEX was used in each iteration of the ECON method to solve the **MORAP-1** mathematical model to global optimality. CPLEX was called via the General Algebraic Modeling System (GAMS, 2020). The target optimality for CPLEX was set to 1.00%. The MPSDR and MESDR heuristic algorithms were also implemented within the MATLAB environment (MathWorks, 2020).

5.3. Comparison of Pareto Fronts

While the ECON method is an exact optimization method, both MPSDR and MESDR heuristics are approximate solution algorithms and do not guarantee optimality of the PFs produced. The scope of this project included a detailed assessment of the PFs produced by the MPSDR and MESDR heuristics based on a comparative analysis against the PFs produced by the ECON method. Such a comparative analysis is essential, considering the importance of solution quality

for effective decision making (Dulebenets et al., 2018; Dulebenets et al., 2019). The ECON, MPSDR, and MESDR solution algorithms were launched to solve the **MORAP** mathematical model for all the generated scenarios of each problem instance. A total of 5 replications was performed for each one of the candidate solution algorithms in order to calculate the average computational time values. As the developed solution algorithms are deterministic in nature, the returned PFs did not change from one replication to another for each scenario of each problem instance. The PF size was set to 10 PF points for each one of the candidate solution algorithms.

The average best overall hazard severity values returned by the ECON, MPSDR, and MESDR solution algorithms over the developed problem instances are presented in Table 21, Table 22, and Table 23 for each one of the generated scenarios for the **MORAP** mathematical model. Moreover, the average best overall traffic delay values returned by the ECON, MPSDR, and MESDR solution algorithms over the developed problem instances are presented in Table 24, Table 25, and Table 26 for each one of the generated scenarios for the **MORAP** mathematical model. On the other hand, Table 27 shows the average best overall hazard severity and traffic delay values returned by the ECON, MPSDR, and MESDR solution algorithms over the generated scenarios for each one of the developed problem instances for the **MORAP** mathematical model.

Based on the conducted numerical experiments, the average best overall hazard severity values returned by the ECON, MPSDR, and MESDR solution algorithms comprised 204,523.5 hazard severity units, 206,663.8 hazard severity units, and 248,521.2 hazard severity units, respectively, over the generated scenarios and developed problem instances. On the other hand, the average best overall traffic delay values returned by the ECON, MPSDR, and MESDR solution algorithms comprised 14,525.5 hours, 14,786.7 hours, and 14,550.2 hours, respectively, over the generated scenarios and developed problem instances. Therefore, the ECON method produced the PFs with the best overall hazard severity values that were superior to the PFs that were produced by the MPSDR and MESDR heuristics on average by 1.05% and 21.51%, respectively. Furthermore, the ECON method produced the PFs with the best overall traffic delay values that were superior to the PFs that were produced by the MPSDR and MESDR heuristics on average by 1.80% and 0.17%, respectively. Hence, the MPSDR heuristic produced the PFs that were superior to the ones produced by the MESDR heuristic in terms of the best overall hazard severity values. In the meantime, the MESDR heuristic produced the PFs that were superior to the ones produced by the MPSDR heuristic in terms of the best overall traffic delay values.

Table 21 The average best overall hazard severity values returned by ECON for the generated scenarios.

 X / C 	1	2	3	4	5	6	7	8	9	10	11
3200	358149	357597	353317	246638	228074	211217	121295	109175	82194	82194	82194
3500	358784	358232	353952	247273	228709	211852	121930	109810	82829	82829	82829
3800	359251	358700	354421	247740	229176	212319	122398	110277	83296	83296	83296
4100	359611	359062	354782	248107	229559	212680	122758	110637	83657	83657	83657
4400	359883	359309	355050	248378	229830	212951	123030	110909	83928	83928	83928
4700	360074	359504	355240	248569	230021	213142	123220	111099	84119	84119	84119
5000	360211	359641	355377	248706	230158	213279	123357	111237	84256	84256	84256
5300	360299	359729	355465	248794	230246	213367	123445	111325	84344	84344	84344
5600	360348	359779	355514	248843	230295	213416	123495	111374	84393	84393	84393
5900	360366	359796	355533	248861	230313	213434	123512	111391	84411	84411	84411
6109	360368	359798	355535	248863	230315	213436	123514	111394	84413	84413	84413

Table 22 The average best overall hazard severity values returned by MPSDR for the generated scenarios.

 X / C 	1	2	3	4	5	6	7	8	9	10	11
3200	358321	358149	353865	246614	227947	210873	127096	111576	87053	87053	87053
3500	358956	358784	354500	247249	228582	211501	127731	112212	87688	87688	87688
3800	359424	359251	354968	247716	229049	211968	128198	112679	88156	88156	88156
4100	359784	359611	355328	248076	229410	212328	128559	113039	88516	88516	88516
4400	360056	359883	355600	248348	229682	212600	128830	113311	88788	88788	88788
4700	360246	360074	355790	248538	229872	212790	129021	113501	88978	88978	88978
5000	360383	360211	355927	248676	230009	212928	129158	113639	89115	89115	89115
5300	360471	360299	356015	248764	230097	213016	129246	113727	89204	89204	89204
5600	360521	360348	356065	248813	230146	213065	129295	113776	89253	89253	89253
5900	360538	360366	356082	248830	230164	213082	129313	113793	89270	89270	89270
6109	360540	360368	356084	248833	230166	213085	129315	113795	89272	89272	89272

Table 23 The average best overall hazard severity values returned by MESDR for the generated scenarios.

X / C	1	2	3	4	5	6	7	8	9	10	11
3200	358321	357758	353602	247120	228416	211000	199726	198879	169761	168993	222741
3500	358956	358393	354237	247755	229051	211635	200362	199515	170884	169629	223376
3800	359424	358859	354704	248222	229519	212103	200829	199982	170172	170341	223843
4100	359784	359219	355062	248582	229879	212463	201189	200342	170456	170702	224204
4400	360056	359491	355333	248854	230151	212735	201461	200614	170728	171043	224475
4700	360246	359681	355526	249045	230341	212925	201651	200765	170918	171234	224666
5000	360383	359818	355664	249182	230478	213062	201789	200902	171056	171371	224841
5300	360471	359906	355753	249270	230566	213150	201877	200990	171144	171459	224929
5600	360521	359955	355802	249319	230616	213200	201926	201039	171451	171420	224978
5900	360538	359971	355819	249336	230633	213217	201943	201057	171468	171438	224995
6109	360540	359972	355821	249339	230635	213219	201945	201059	171470	171440	224997

Table 24 The average best overall traffic delay values returned by ECON for the generated scenarios.

X / C	1	2	3	4	5	6	7	8	9	10	11
3200	13709	13708	13715	13818	13798	13819	13847	13847	13861	13845	13710
3500	13947	13947	13953	14056	14036	14057	14085	14110	14097	14082	13947
3800	14170	14170	14176	14279	14260	14280	14309	14309	14321	14313	14176
4100	14330	14330	14336	14439	14421	14440	14469	14494	14481	14489	14330
4400	14453	14455	14459	14563	14543	14563	14591	14591	14612	14612	14458
4700	14551	14553	14558	14661	14642	14661	14689	14689	14694	14694	14549
5000	14637	14639	14644	14747	14727	14747	14775	14775	14788	14781	14641
5300	14702	14705	14709	14813	14793	14812	14841	14841	14854	14854	14703
5600	14757	14760	14764	14868	14848	14867	14896	14896	14926	14927	14761
5900	14799	14802	14806	14910	14890	14909	14938	14938	14935	14935	14798
6109	14825	14827	14832	14935	14915	14935	14963	14963	14976	14976	14828

Table 25 The average best overall traffic delay values returned by MPSDR for the generated scenarios.

 X / C 	1	2	3	4	5	6	7	8	9	10	11
3200	13711	13709	13723	13828	13838	13855	14458	14459	14330	14330	14330
3500	13949	13947	13961	14066	14076	14093	14696	14697	14568	14568	14568
3800	14173	14170	14184	14290	14299	14316	14920	14920	14791	14791	14791
4100	14332	14330	14344	14450	14459	14476	15079	15080	14951	14951	14951
4400	14455	14453	14466	14572	14582	14598	15202	15203	15074	15074	15074
4700	14553	14551	14565	14670	14680	14697	15300	15301	15172	15172	15172
5000	14639	14637	14651	14756	14766	14783	15386	15387	15258	15258	15258
5300	14705	14702	14716	14822	14831	14848	15452	15452	15323	15323	15323
5600	14760	14757	14771	14877	14886	14903	15507	15507	15378	15378	15378
5900	14802	14799	14813	14919	14928	14945	15549	15549	15420	15420	15420
6109	14827	14825	14839	14944	14954	14971	15574	15575	15446	15446	15446

Table 26 The average best overall traffic delay values returned by MESDR for the generated scenarios.

 X / C 	1	2	3	4	5	6	7	8	9	10	11
3200	13711	13713	13730	13829	13839	13855	13885	13885	13902	13904	13717
3500	13949	13951	13968	14067	14077	14093	14123	14123	14140	14141	13955
3800	14173	14174	14191	14290	14300	14316	14347	14347	14365	14365	14178
4100	14332	14334	14351	14450	14460	14476	14506	14506	14525	14525	14338
4400	14455	14457	14474	14573	14583	14598	14629	14629	14647	14647	14460
4700	14553	14555	14572	14671	14681	14696	14727	14727	14745	14745	14558
5000	14639	14641	14658	14757	14767	14782	14813	14813	14831	14831	14644
5300	14705	14706	14723	14822	14832	14848	14879	14879	14897	14897	14710
5600	14760	14761	14778	14877	14887	14903	14934	14934	14952	14952	14765
5900	14802	14803	14820	14919	14929	14945	14975	14975	14994	14994	14807
6109	14827	14829	14846	14945	14955	14970	15001	15001	15019	15019	14832

Table 27 The average best overall hazard severity and traffic delay values returned by the candidate solution algorithms for the developed problem instances.

Instance	ECON		MPSDR		MESDR	
	$ave(F_1^*)$	$ave(F_2^*)$	$ave(F_1^*)$	$ave(F_2^*)$	$ave(F_1^*)$	$ave(F_2^*)$
1	216599.4	14480.3	217276.1	14743.6	268075.3	14506.1
2	213624.7	14483.5	214573.9	14752.9	253451.8	14513.2
3	211141.5	14494.8	212198.7	14763.5	250967.8	14522.2
4	208812.3	14498.6	210137.2	14771.5	259960.1	14523.7
5	206573.7	14499.7	208244.7	14779.1	246280.5	14531.2
6	204545.5	14538.4	206533.1	14786.3	244327.7	14565.3
7	202752.3	14537.8	204959.5	14793.1	254081.2	14563.7
8	201008.0	14536.0	203559.0	14798.8	241618.4	14557.4
9	199426.2	14551.6	202256.9	14805.3	240196.1	14575.0
10	197989.2	14556.9	201127.4	14810.4	249078.7	14576.6
11	196550.9	14562.4	200051.3	14815.2	237749.3	14580.9
12	195257.8	14566.3	199047.7	14820.1	236467.6	14587.1
Average:	204523.5	14525.5	206663.8	14786.7	248521.2	14550.2

Notes: $ave(F_1^)$ – is the average best overall hazard severity (hazard severity units); $ave(F_2^*)$ – is the average best overall traffic delay (hours).

A detailed evaluation of the generated scenarios indicates that the best overall hazard severity and traffic delay values returned by the MPSDR and MESDR heuristics were close for the scenarios with up to six countermeasures. The introduction of low-cost countermeasures (i.e. countermeasure “7”, “8”, “9”, and “10”) triggered substantial changes in multi-objective resource allocation decisions suggested by the MPSDR and MESDR heuristics. Such changes can be explained by nature of the heuristics. In particular, the MPSDR heuristic creates a priority list for highway-rail grade crossings based on the hazard severity reduction, traffic delay reduction, and cost of applying countermeasures. On the other hand, the MESDR heuristic creates a priority list for highway-rail grade crossings based on the hazard severity reduction and traffic delay reduction only and does not consider the cost of applying countermeasures. Therefore, after the introduction of low-cost countermeasures, the MESDR heuristic will prioritize the countermeasures with high effectiveness factors and low additional traffic delay due to their application (e.g., grade separation). On the contrary, the MPSDR heuristic will prioritize the countermeasures with high effectiveness factors and low additional traffic delay due to their application, considering the associated countermeasure implementation cost.

Figure 73 shows PFs for a total of six selected scenarios of problem instance “1” with $TAB = \$4.5M$ that have the following attributes: (1) $|X| = 3200$, $|C| = 3$; (2) $|X| = 6109$, $|C| = 3$; (3) $|X| = 3200$, $|C| = 6$; (4) $|X| = 6109$, $|C| = 6$; (5) $|X| = 3200$, $|C| = 11$; and (6) $|X| = 6109$, $|C| = 11$. A number of observations can be made based on the PFs produced by the ECON, MPSDR, and MESDR solution algorithms. First, the overall hazard severity and the overall traffic delay increased with increasing number of highway-rail grade crossings. Such a finding can be justified by the fact that the total available budget did not allow upgrading each one of the considered highway-rail grade crossings; therefore, increasing number of highway-rail grade crossings led to an increase of the overall hazard severity and the overall traffic delay.

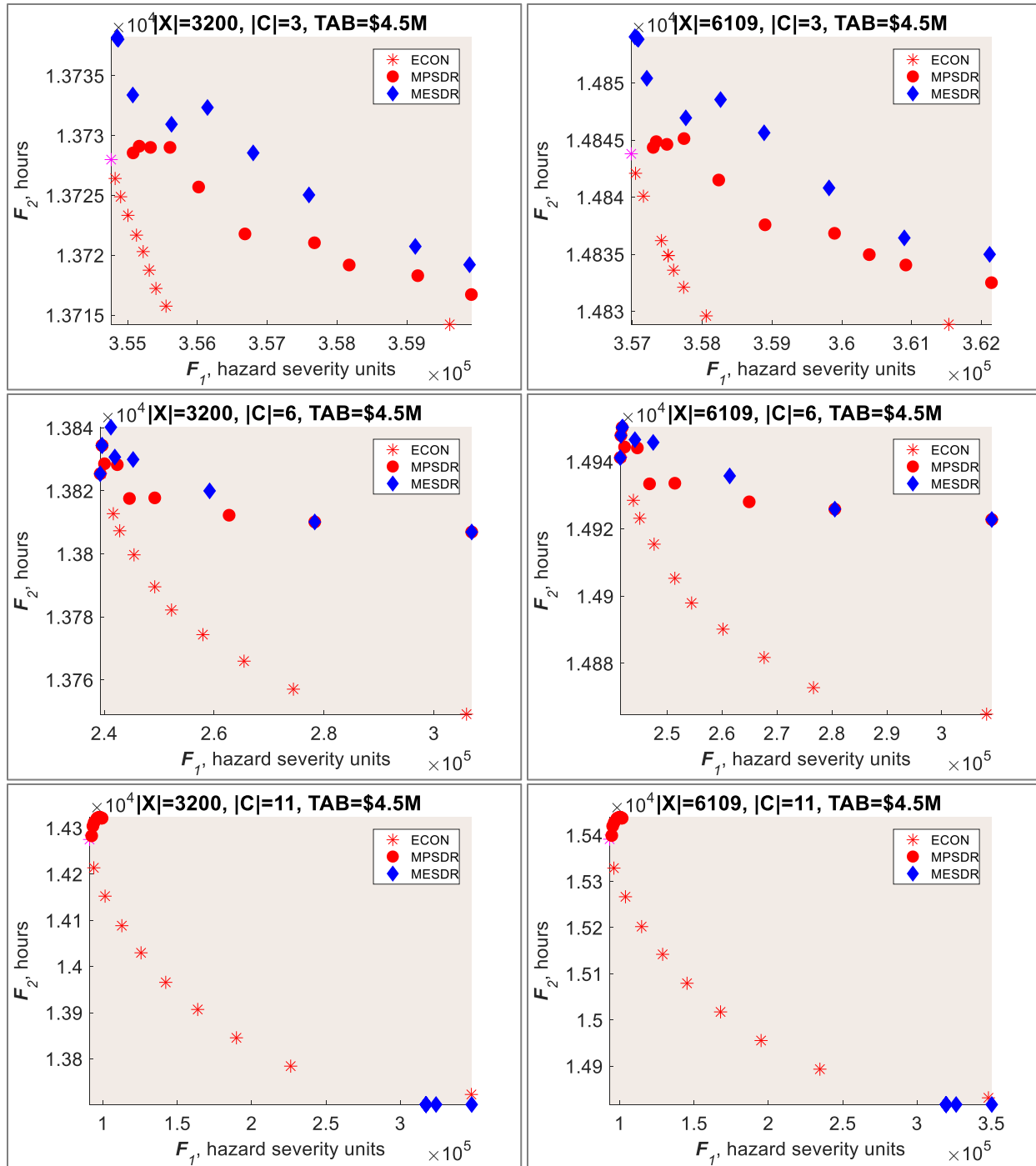


Figure 73 Pareto Fronts produced by ECON, MPSDR, and MESDR for the selected scenarios of problem instance with $TAB = \$4.5M$.

Second, it can be observed that for the scenarios with the first six countermeasures (i.e., $|C| = 1 \div 6$), the PFs produced by the MPSDR and MESDR heuristics did not have substantial differences and were close to the PFs produced by the ECON method (although the MESDR PFs were typically inferior to the MPSDR PFs). More specifically, the difference between the best overall hazard severity and traffic delay values returned by the MPSDR and MESDR heuristics

and the best overall hazard severity and traffic delay values returned by the ECON method did not exceed 0.50% for the scenarios with the first six countermeasures.

Third, for the scenario with grade separation (i.e., countermeasure “11”), the MESDR heuristic selected the most hazardous highway-rail grade crossings for upgrading and applied grade separation at those crossings, since grade separation has the highest effectiveness factor and the least additional traffic delay due to application of that countermeasure (i.e., the additional traffic delay due to application of grade separation was assumed to be zero in this project, since the highway traffic will not be interrupted by passing trains after application of grade separation). On the other hand, the MPSDR heuristic selected the most hazardous highway-rail grade crossings for upgrading and applied certain countermeasures, considering the associated implementation cost as well as the additional traffic delay due to application of those countermeasures. Since grade separation is the most expensive countermeasure with the total implementation cost of \$1.5M per highway-rail grade crossing, only a few highway-rail grade crossings could be upgraded by the MESDR heuristic.

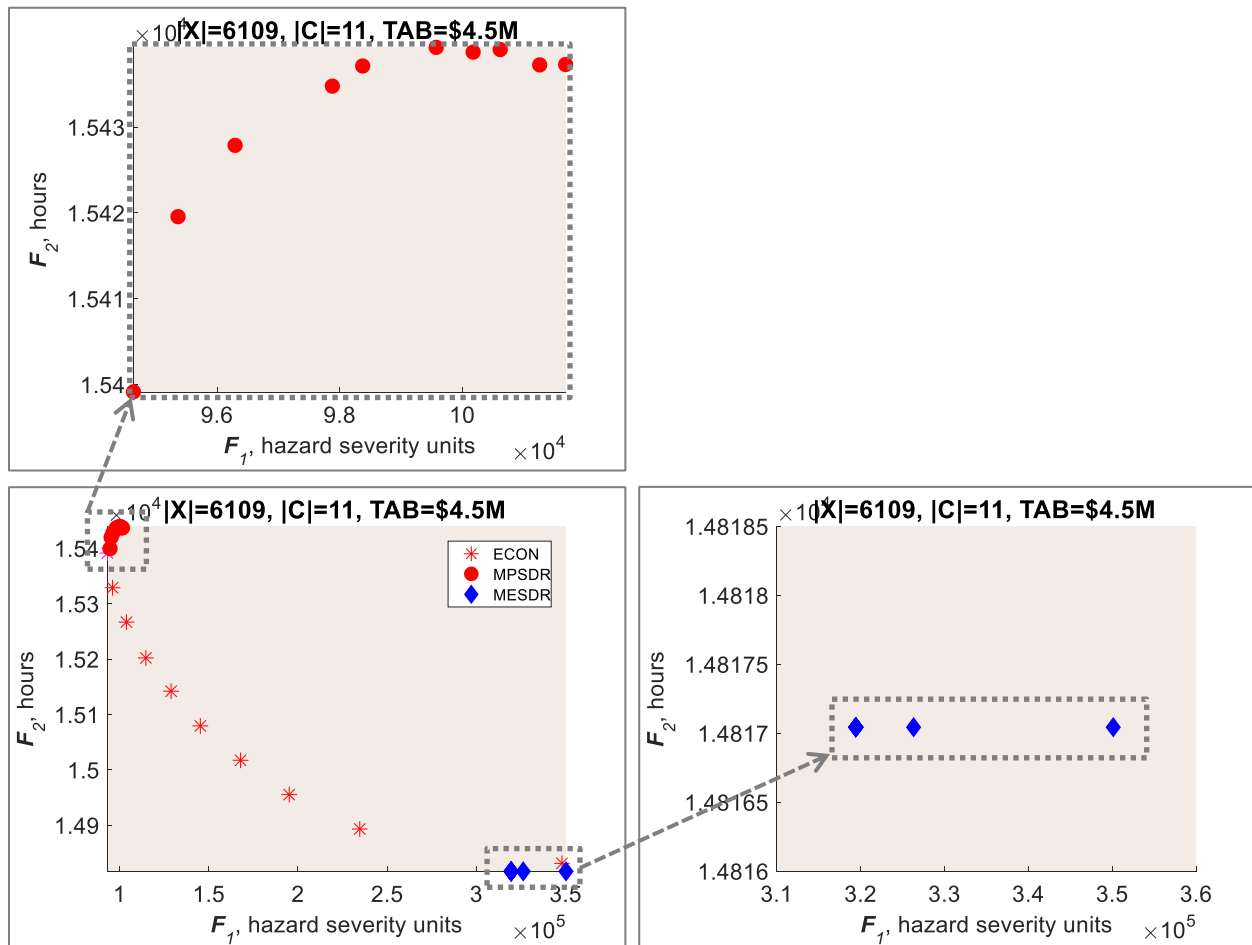


Figure 74 Detailed evaluation of Pareto Fronts produced by ECON, MPSDR, and MESDR for the problem instance with $|X| = 6109$, $|C| = 11$, and $TAB = \$4.5M$.

Hence, higher overall hazard severity values and lower overall traffic delay values were observed for the PFs produced by the MESDR heuristic as compared to the PFs produced by the MPSDR

heuristic. In particular, the best overall hazard severity for the scenario with 6109 highway-rail grade crossings and 11 countermeasures comprised 319,434.3 hazard severity units when MESDR was selected as a solution approach as compared to 94,633.8 hazard severity units when MPSDR was selected as a solution approach (see Figure 73 and Figure 74). In the meantime, the best overall traffic delay for the scenario with 6109 highway-rail grade crossings and 11 countermeasures comprised 14,817.0 hours when MESDR was selected as a solution approach as compared to 15,399.1 hours when MPSDR was selected as a solution approach (see Figure 73 and Figure 74).

Fourth, after the introduction of low-cost countermeasures, the MPSDR heuristic started selecting countermeasures that are effective in terms of reducing both the overall hazard severity and the overall traffic delay. Therefore, the PFs produced by the MPSDR heuristic for the scenarios with low-cost countermeasures generally do not show a conflicting nature of the overall hazard severity minimization objective and the overall traffic delay minimization objective (see Figure 74 as an example with the PFs produced by the MPSDR heuristic, where the selected countermeasures effectively reduce both the overall hazard severity and the overall traffic delay).

In conclusion, the MPSDR heuristic was found to be more promising as compared to the MESDR heuristic in terms of the overall hazard severity values. On the other hand, the MESDR heuristic was found to be more promising as compared to the MPSDR heuristic in terms of the overall traffic delay values. However, if we consider both overall hazard severity and traffic delay components, the MPSDR heuristic was found to be superior to the MESDR heuristic. In particular, the PFs produced by the MPSDR heuristic did not differ by more than 1.05% and 1.80% on average as compared to the optimal PFs produced by the ECON method in terms of the best overall hazard severity and traffic delay values, respectively. Therefore, the MPSDR performance can be viewed as acceptable in terms of both overall hazard severity and traffic delay components. On the contrary, the PFs produced by the MESDR heuristic differed by 21.51% and 0.17% on average as compared to the optimal PFs produced by the ECON method in terms of the best overall hazard severity and traffic delay values, respectively. Hence, the MESDR performance can be viewed as acceptable in terms of the overall traffic delay component only.

5.4. Computational Time

Since the ECON method is an exact optimization method, it can produce optimal PFs for different problem instances of the **MORAP** mathematical model. However, due to computational complexity of the **MORAP** mathematical model, finding an optimal PF may incur a substantial amount of computational time (as the **MORAP** mathematical model can be reduced to the multi-objective knapsack problem). Significant computational efforts required in order to conduct resource allocation among highway-rail grade crossings are not desirable from the practical perspective. The MPSDR and MESDR heuristics are expected to provide multi-objective resource allocation decisions in a timely manner. However, a detailed analysis of the computational time is required for the candidate solution algorithms before they can be implemented in practice. Along with solution quality, computational time serves as an important performance indicator as well, throughout evaluation of the candidate solution algorithms (Dulebenets, 2016; Dulebenets, 2020).

Table 28 The average computational time incurred by ECON for the generated scenarios.

$ X / C $	1	2	3	4	5	6	7	8	9	10	11
3200	88.768	91.767	95.792	100.462	104.201	108.900	113.800	118.758	121.979	125.575	131.984
3500	89.586	94.171	98.268	103.499	108.100	112.800	118.926	122.884	127.431	132.136	138.674
3800	91.181	96.863	101.822	107.545	112.758	118.034	124.112	129.799	133.327	138.926	146.056
4100	93.850	100.741	105.677	112.505	116.383	122.732	128.902	134.135	139.503	145.385	153.081
4400	96.762	103.305	108.905	115.239	120.984	128.018	135.668	141.720	146.282	151.839	159.779
4700	97.749	105.478	110.939	117.733	124.120	132.029	138.808	144.519	150.525	156.592	165.984
5000	100.868	108.606	114.299	121.313	128.319	136.705	144.567	151.019	156.893	162.541	172.326
5300	103.856	111.816	118.783	125.707	133.478	142.164	150.380	157.549	163.274	170.130	181.113
5600	106.453	115.174	122.286	129.962	137.577	147.267	155.868	162.407	168.162	176.054	187.938
5900	108.996	118.204	124.725	133.548	141.751	151.539	160.708	168.577	174.113	183.188	194.323
6109	111.328	120.282	128.017	137.061	145.889	156.497	164.520	172.830	179.151	188.444	200.822

Table 29 The average computational time incurred by MPSDR for the generated scenarios.

$ X / C $	1	2	3	4	5	6	7	8	9	10	11
3200	18.145	18.854	19.610	20.379	21.537	22.801	24.877	26.042	28.666	30.557	33.029
3500	18.407	19.145	20.140	21.191	22.581	23.659	25.773	27.829	30.607	33.169	35.479
3800	18.988	19.669	20.796	21.949	23.171	24.775	27.321	29.456	32.907	35.484	38.245
4100	19.140	20.019	21.314	22.722	24.384	26.079	28.941	31.573	35.449	38.242	45.679
4400	19.659	20.732	21.945	23.544	25.269	27.351	30.380	33.370	37.799	41.712	60.322
4700	20.017	21.262	22.691	24.416	26.309	28.854	32.492	35.739	40.402	54.876	75.591
5000	20.318	21.669	23.319	25.528	27.366	30.516	34.349	37.738	46.999	68.659	91.681
5300	21.642	23.293	24.999	27.186	29.736	33.021	37.072	41.302	59.818	83.404	109.672
5600	22.049	23.617	25.838	27.868	30.785	34.448	39.053	47.177	72.398	98.261	125.406
5900	22.536	24.087	26.649	31.594	32.323	36.131	41.188	57.750	85.027	113.089	143.562
6109	23.033	24.798	27.045	29.972	33.595	37.600	43.231	65.225	93.911	125.042	158.951

Table 30 The average computational time incurred by MESDR for the generated scenarios.

 X / C 	1	2	3	4	5	6	7	8	9	10	11
3200	18.703	19.426	20.199	20.985	22.174	23.469	25.565	26.749	29.407	31.329	33.843
3500	18.967	19.724	20.739	21.813	23.238	24.340	26.472	28.562	31.372	33.977	36.332
3800	19.555	20.257	21.399	22.582	23.843	25.472	28.043	30.217	33.711	36.333	39.134
4100	19.711	20.609	21.926	23.367	25.073	26.793	29.688	32.365	36.285	39.125	46.619
4400	20.232	21.329	22.569	24.212	25.970	28.087	31.153	34.200	38.676	42.631	61.399
4700	20.600	21.867	23.329	25.098	27.024	29.615	33.297	36.601	41.329	55.925	76.811
5000	20.909	22.284	23.969	26.229	28.103	31.301	35.190	38.635	47.973	69.814	93.055
5300	22.238	23.922	25.670	27.906	30.504	33.843	37.953	42.249	60.908	84.706	111.183
5600	22.653	24.256	26.520	28.610	31.576	35.302	39.969	48.167	73.599	99.709	127.083
5900	23.145	24.733	27.348	32.355	33.142	37.019	42.140	58.843	86.355	114.662	145.400
6109	23.642	25.449	27.751	30.748	34.425	38.506	44.216	66.389	95.325	126.714	160.935

The scope of this project included a detailed assessment of the computational time required by the ECON, MPSDR, and MESDR solution algorithms to solve the **MORAP** mathematical model for all the generated scenarios of each problem instance. The ECON, MPSDR, and MESDR solution algorithms were launched to solve the **MORAP** mathematical model for all the generated scenarios of each problem instance. A total of 5 replications was performed for each one of the candidate solution algorithms in order to calculate the average computational time values. The PF size was set to 10 PF points for each one of the candidate solution algorithms. The average computational times incurred by the ECON, MPSDR, and MESDR solution algorithms over the developed problem instances are presented in Table 28, Table 29, and Table 30 for each one of the generated scenarios for the **MORAP** mathematical model. On the other hand, Table 31 shows the average and maximum computational times incurred by the ECON, MPSDR, and MESDR solution algorithms over the generated scenarios for each one of the developed problem instances for the **MORAP** mathematical model.

Table 31 The average and maximum computational times incurred by the candidate solution algorithms for the developed problem instances.

Instance	Average CPU Time Values			Maximum CPU Time Values		
	ECON	MPSDR	MESDR	ECON	MPSDR	MESDR
1	83.1	22.1	22.5	140.6	137.5	139.2
2	96.2	26.6	27.2	168.8	142.3	144.1
3	114.6	30.5	31.2	182.5	153.7	155.7
4	137.1	23.8	24.3	213.5	142.3	144.1
5	158.4	28.3	28.9	228.9	148.1	150.0
6	180.9	32.4	33.1	253.9	154.5	156.5
7	83.0	36.9	37.7	154.1	154.1	156.0
8	105.0	41.2	42.1	172.1	159.9	161.9
9	125.6	46.1	47.2	193.7	167.1	169.2
10	144.4	51.6	52.8	209.1	178.7	180.9
11	166.8	56.4	57.6	239.4	177.0	179.2
12	190.0	61.8	63.2	253.4	192.1	194.5
Average:	132.1	38.1	39.0	200.8	159.0	160.9

Based on the conducted numerical experiments, the average computational time incurred by the ECON, MPSDR, and MESDR solution algorithms, comprised 132.1 seconds, 38.1 seconds, and 39.0 seconds, respectively, over the generated scenarios and developed problem instances. Moreover, the maximum computational time did not exceed 253.9 seconds, 192.1 seconds, and 194.5 seconds for the ECON, MPSDR, and MESDR solution algorithms, respectively, over the generated scenarios and developed problem instances. Generally, the computational time of the candidate solution algorithms increased with increasing number of highway-rail grade crossings, number of available countermeasures, and total available budget. It can be concluded that all the candidate solution algorithms demonstrated an acceptable performance in terms of the computational time required to solve different scenarios and problem instances of the **MORAP** mathematical model. However, the computational time of the ECON method may substantially increase after changing the input data for the **MORAP** mathematical model (e.g., increase the

number of highway-rail grade crossings considered, increase the number of available countermeasures) due to computational complexity of the model.

5.5. Solution Algorithm Recommendation

All the developed candidate algorithms were evaluated in terms of both solution quality and computational time criteria. The MPSDR heuristic was found to be superior to the MESDR heuristic when considering both overall hazard severity and traffic delay components. In particular, the PFs produced by the MPSDR heuristic did not differ by more than 1.05% and 1.80% on average as compared to the optimal PFs produced by the ECON method in terms of the best overall hazard severity and traffic delay values, respectively. Therefore, the MPSDR performance can be viewed as acceptable in terms of both overall hazard severity and traffic delay components. On the contrary, the PFs produced by the MESDR heuristic differed by 21.51% and 0.17% on average as compared to the optimal PFs produced by the ECON method in terms of the best overall hazard severity and traffic delay values, respectively. Hence, the MESDR performance can be viewed as acceptable in terms of the overall traffic delay component only.

As for the computational time, the maximum computational time did not exceed 253.9 seconds, 192.1 seconds, and 194.5 seconds for the ECON, MPSDR, and MESDR solution algorithms, respectively, over the generated scenarios and developed problem instances. Hence, all the candidate solution algorithms demonstrated an acceptable performance in terms of the computational time required to solve different scenarios and problem instances of the **MORAP** mathematical model. However, the computational time of the ECON method may substantially increase after changing the input data for the **MORAP** mathematical model (e.g., increase the number of highway-rail grade crossings considered, increase the number of available countermeasures) due to computational complexity of the model. Based on the analysis results, this project recommends the Multi-Objective Profitable Severity and Delay Reduction (MPSDR) heuristic as a solution approach for the **MORAP** mathematical model, as it demonstrated a competitive performance in terms of both solution quality and computational time criteria.

5.6. Pareto Front Size Effects

Another important parameter that directly affects the computational time of the MPSDR heuristic is the PF size. Increasing number of PF points provides more alternatives for the decision makers (e.g., there will be more resource allocation alternatives, and a more detailed analysis of tradeoffs between the overall hazard severity minimization and traffic delay minimization objectives could be conducted). However, increasing number of PF points also increases the number of iterations that have to be made by the MPSDR heuristic, which further increases the computational time required. The scope of this project included a detailed assessment of the PF size on the computational time required by the MPSDR heuristic. A total of 12 scenarios was developed by changing the PF size from 4 PF points to 26 PF points with an increment of 2 PF points. The problem instance with $|X| = 6109$, $|C| = 6$, and $TAB = \$10.0M$ was considered throughout the analysis. The MPSDR heuristic was launched to solve the **MORAP** mathematical model for all the generated PF size scenarios. A total of 5 replications was performed in order to calculate the average computational time values.

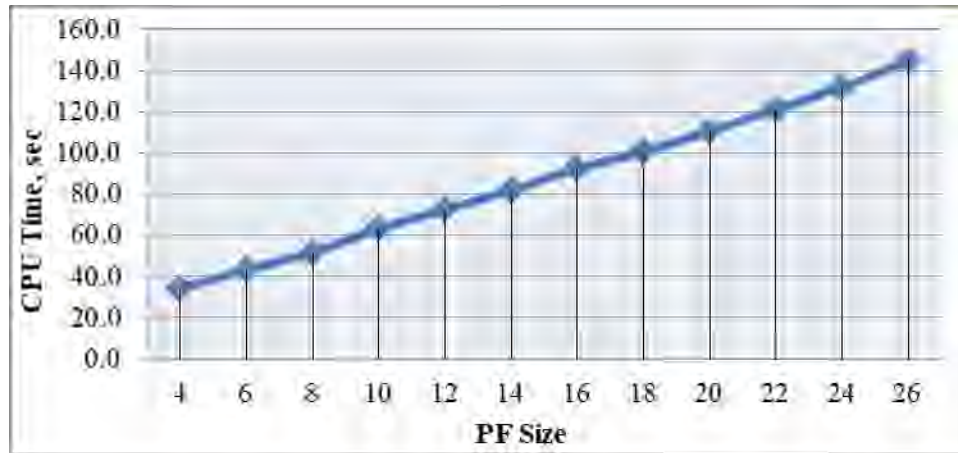


Figure 75 Relationship between the Pareto Front size and computational time required.

The results from conducted analysis are illustrated in Figure 75, where it can be observed that the computational time required by the MPSDR heuristic almost linearly increases with the PF size. The computational time comprised 33.8 seconds when the PF size was set to 4 PF points. On the other hand, the computational time increased to 145.0 seconds when the PF size was increased to 26 PF points. As indicated earlier, more dense PFs (i.e., the PFs that have more points) will enable decision makers with an effective evaluation of tradeoffs between conflicting objectives. Figure 76 shows the PFs that have 6 points, 12 points, 18 points, and 24 points for the problem instance with $|X| = 6109$, $|C| = 6$, and $TAB = \$10.0M$. A denser PF (i.e., the PF with 24 points) is expected to facilitate resource allocation decisions and assist with the selection of an alternative that will effectively compromise the overall hazard severity minimization and traffic delay minimization objectives. The computational time required by the MPSDR heuristic to produce the PF with 24 points comprised 131.9 seconds, which can be viewed as acceptable from the practical standpoint. However, increasing problem size is expected to increase the computational time even further (e.g., the MPSDR heuristic required 192.2 seconds to produce a PF with 10 points for the problem instance with $|X| = 6109$, $|C| = 11$, and $TAB = \$10.0M$).

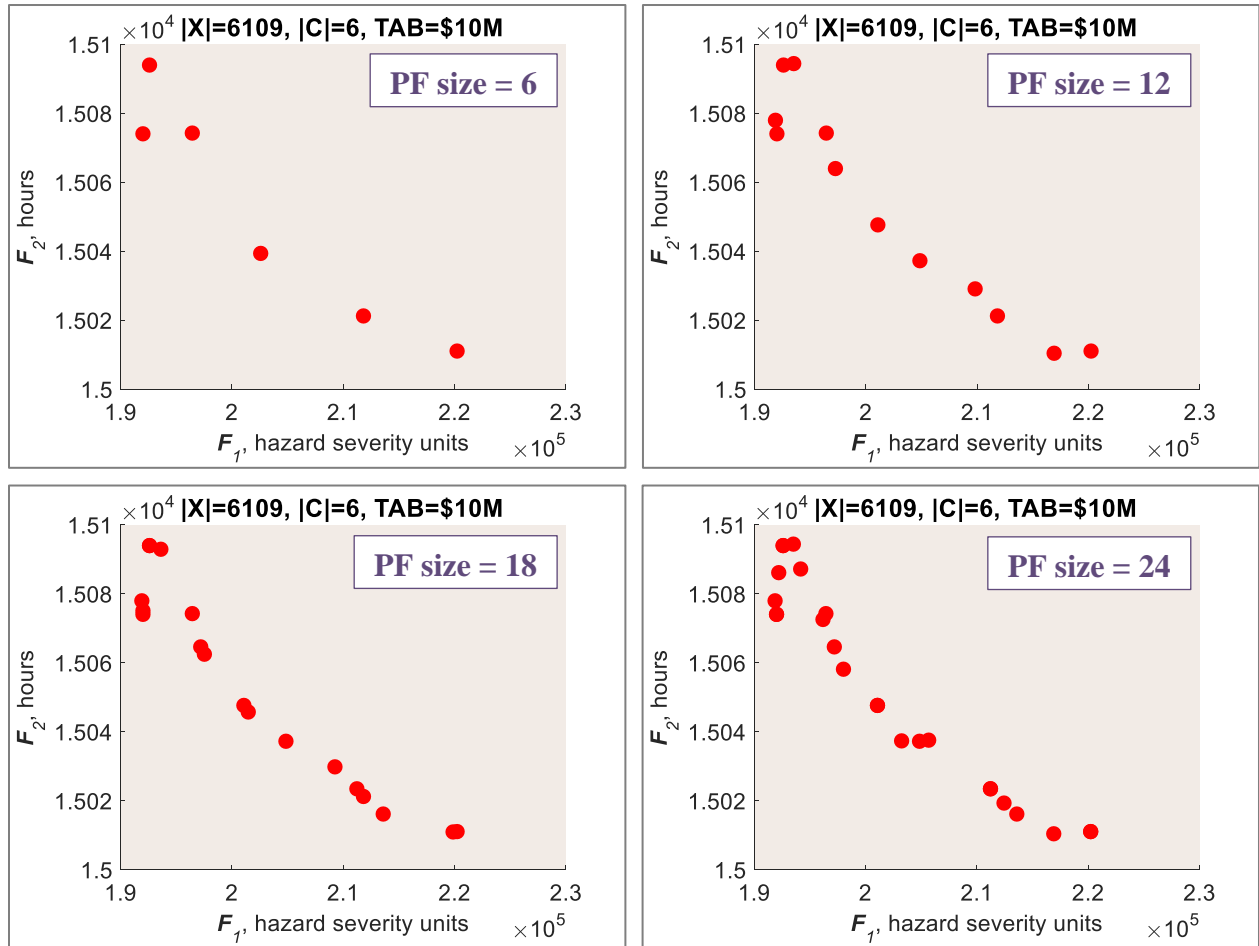


Figure 76 Examples of Pareto Fronts with different Pareto Front sizes.

6. DEVELOPMENT OF THE STANDALONE APPLICATION

Under this section of the report, the standalone application, named as “HRX Safety Improvement” (“HRX” stands for “highway-rail grade crossing”), is presented. The standalone application “HRX Safety Improvement” computes the overall hazard severity at the highway-rail grade crossings in Florida by employing the Florida Priority Index Formula and the severity prediction methodology outlined in the GradeDec.NET Reference Manual (U.S. DOT, 2014a). At the same time, it estimates the overall traffic delay due to application of the available countermeasures at the considered highway-rail grade crossings. Then, the standalone application distributes the available monetary resources among the chosen highway-rail grade crossings to upgrade them by implementing the available countermeasures, which were previously specified by the user. The purpose of the application, installation guidelines, and basic user guidelines are outlined in this section of the report.

6.1. Purpose of the Application

The State of Florida has been experiencing an increase in passenger and freight traffic volumes due to its population and economic growth. An increase in passenger and freight traffic volumes may have notable advantages; however, it has some disadvantages as well. A significant number of accidents between highway vehicles and passing trains have been observed in Florida over the past years. Accidents at highway-rail grade crossings could be mitigated with the application of appropriate countermeasures (e.g., flashing lights, wigwags). However, the application of a countermeasure at a highway-rail grade crossing may also add significant delays to the associated highway traffic. Moreover, upgrading all the highway-rail grade crossings in Florida is infeasible due to budget limitations. Hence, only a limited number of highway-rail grade crossings can be upgraded. In order to improve safety at the highway-rail grade crossings in Florida, it is imperative to reduce the highway-rail grade crossing hazard considering the limited financial resources, while not significantly increasing delays to the associated highway traffic. This study has developed a standalone application, named as “HRX Safety Improvement”, which can assist the FDOT personnel with selection of highway-rail grade crossings for upgrades using appropriate countermeasures. The standalone application “HRX Safety Improvement” assesses the highway-rail grade crossing hazard based on several factors, such as the average daily traffic volume, average daily train volume, train speed, protection factor, and accident history parameter (the total number of accidents in the last five years or since the year of last improvement in case there was an upgrade).

Furthermore, the standalone application estimates the overall traffic delay due to application of a countermeasure at a highway-rail grade crossing based on the number of blockage occurrences (i.e., number of trains) and the overall delay experienced by queued vehicles during each blockage. The overall delay experienced by queued vehicles during each blockage is computed based on the delay time for a given highway-rail grade crossing caused by the implemented countermeasure, average train length, average train speed, average number of vehicles arriving per day, and number of highway lanes. Finally, the developed standalone application “HRX Safety Improvement” can assist the FDOT personnel with assignment of the eligible countermeasures to the considered highway-rail grade crossings in order to conduct an efficient multi-objective resource allocation. In particular, the standalone application “HRX Safety Improvement” considers the available budget and assigns countermeasures to the considered

highway-rail grade crossings in order to minimize the overall hazard severity and to minimize the overall traffic delay.

6.2. Installation Guidelines

Before starting the installation process, the user should check and make sure to have the administrative rights on a given computer. If the user intends to install the tool on the office computer and does not have administrative rights, the appropriate IT Department should be contacted in advance to receive the required assistance with the installation process. In order to install the standalone application “HRX Safety Improvement” on a given PC, the following steps should be successfully completed:

1. It is assumed that the installation file will be placed to folder “C:\HRX_Safety_Improvement”. Open folder “C:\HRX_Safety_Improvement” (see Figure 77).



Figure 77 The folder containing the installation file.

2. Execute file “HRX_Safety_Improvement.exe” (see Figure 78). The installer will start running (see Figure 79). Click “Next”.

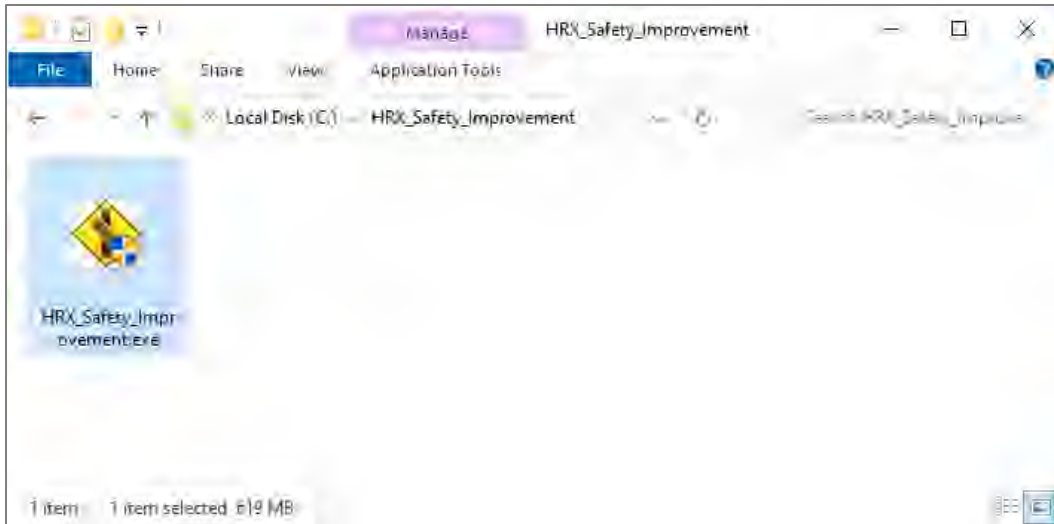


Figure 78 The installer of the standalone application “HRX Safety Improvement”.

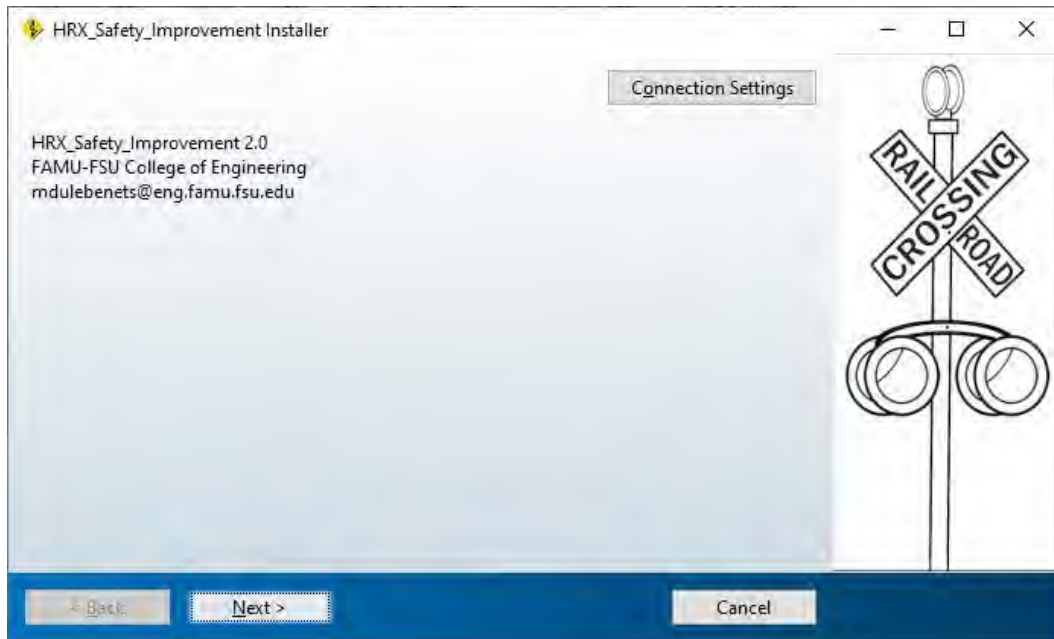


Figure 79 The installation window of the standalone application “HRX Safety Improvement”.

3. Select a directory, where the installation files of the standalone application “HRX Safety Improvement” will be placed (e.g., folder “**C:\Program Files\HRX_Safety_Improvement**” – see Figure 80). For convenience, “**Add a shortcut to the desktop**” option can be chosen.

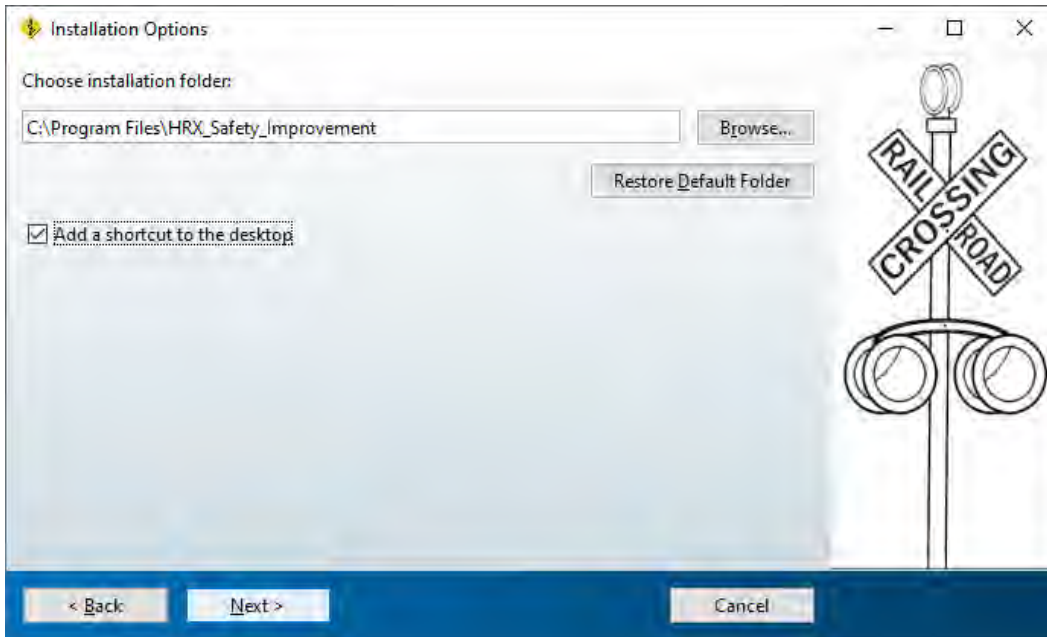


Figure 80 The installation directory of the standalone application “HRX Safety Improvement”.

4. MATLAB Runtime, a standalone set of shared libraries that is required to execute MATLAB components or applications without installing MATLAB, is essential to run the standalone application “HRX Safety Improvement”. MATLAB Runtime is included in the application package. However, the user needs to select a directory, where the installation files of MATLAB Runtime will be saved (e.g., folder “**C:\Program Files\MATLAB\MATLAB Runtime**” – see Figure 81).

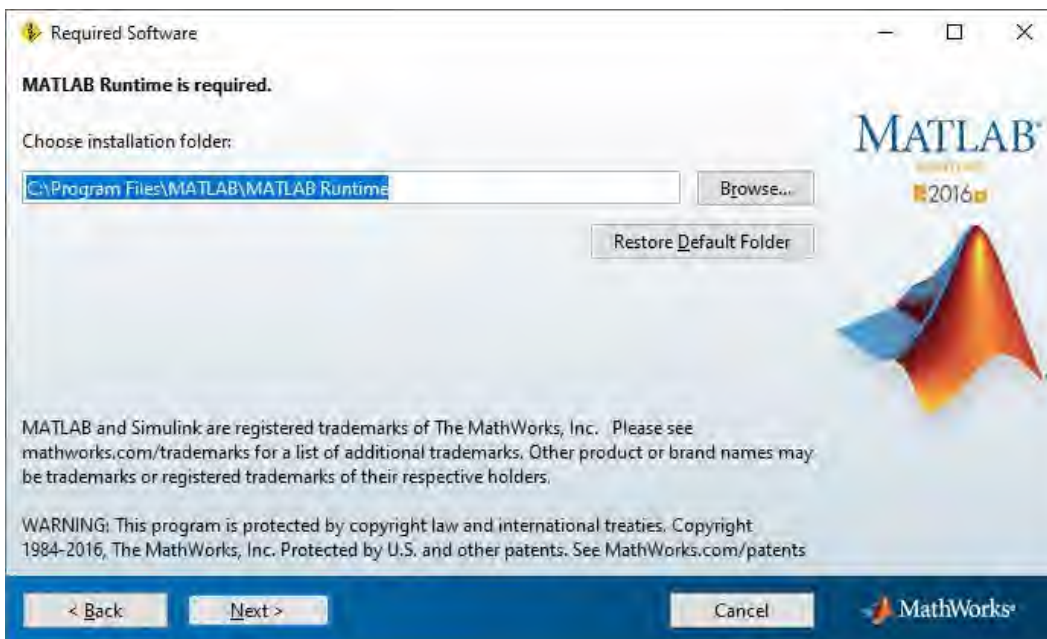


Figure 81 The installation directory of MATLAB Runtime.

5. Accept the terms of the license agreement and then click “Next” (see Figure 82).

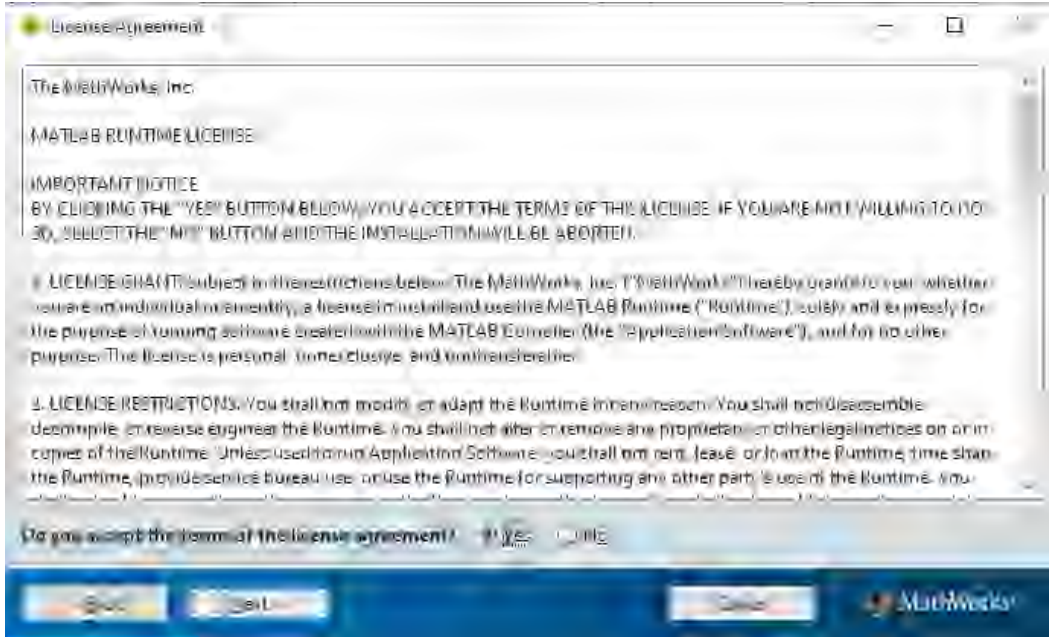


Figure 82 Accepting the terms of the license agreement.

6. A confirmation window showing the installation directories of the standalone application “HRX Safety Improvement” and MATLAB Runtime will pop up. Click “Install” on that window (see Figure 83).

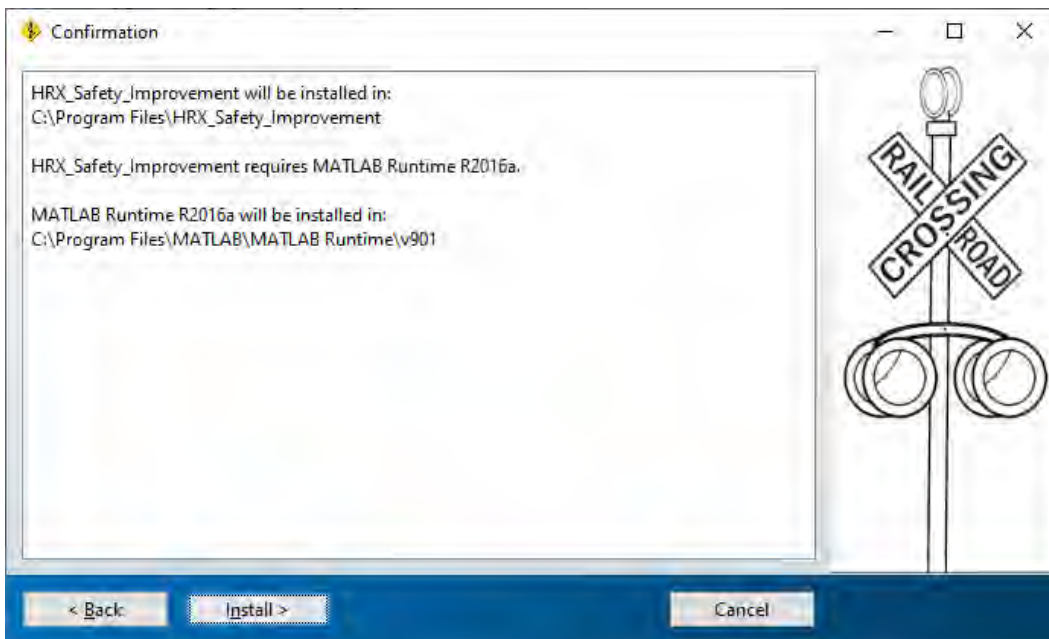


Figure 83 The confirmation window showing the installation directories.

7. When the installation starts running, a progress bar will appear (see Figure 84).

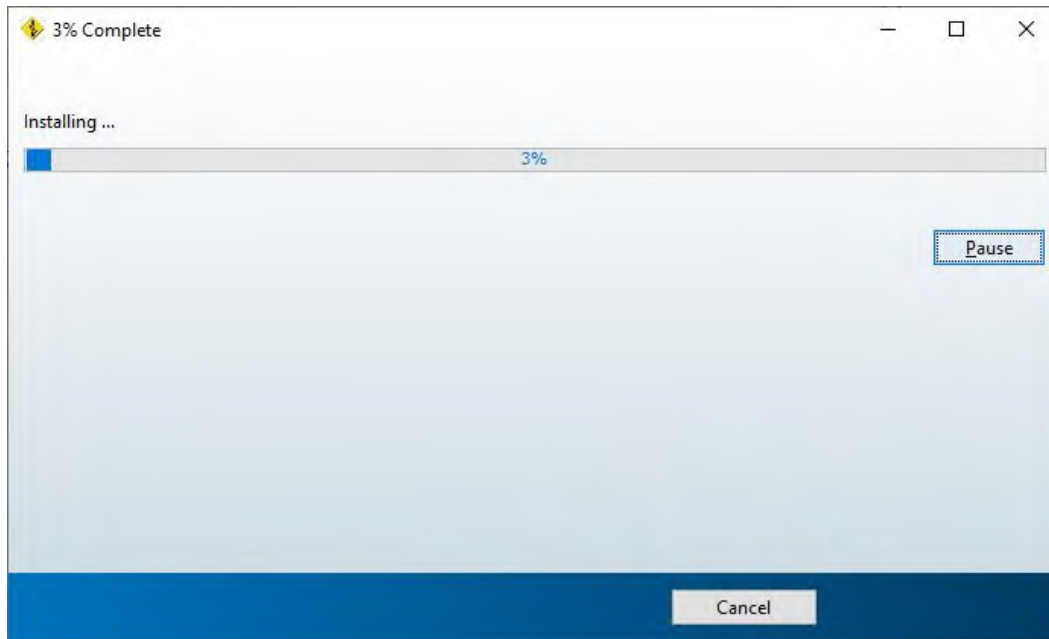


Figure 84 The installation progress.

8. When the installation is complete, a window confirming a successful completion will pop up (see Figure 85). Click "**Finish**" on that window.

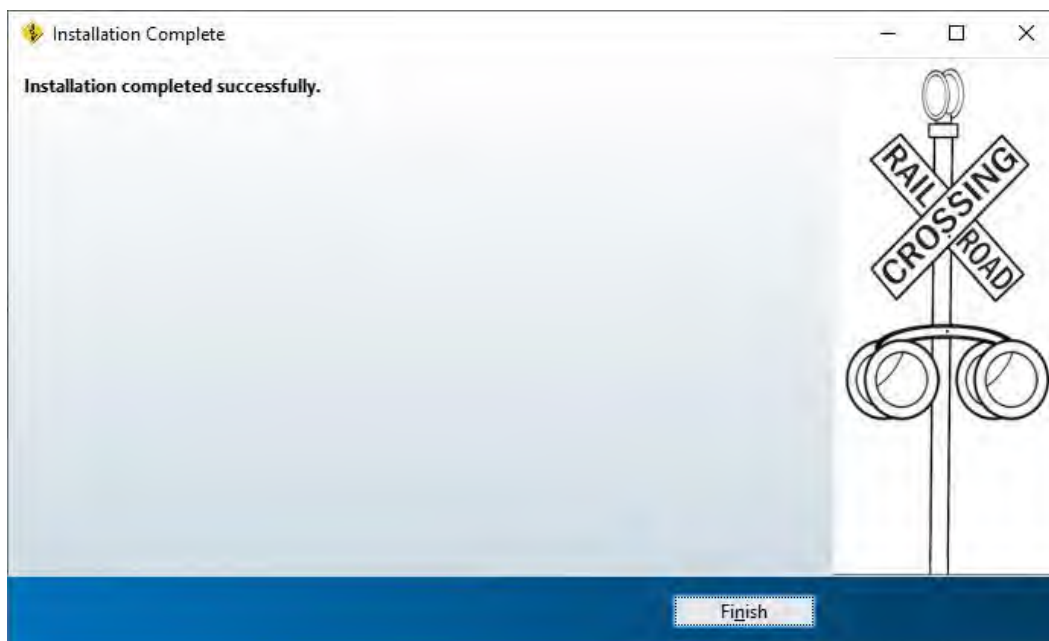


Figure 85 The installation completion.

6.3. User Guidelines

This section provides some basic user guidelines for the standalone application “HRX Safety Improvement”. Specifically, the following aspects are further discussed: (1) major assumptions; (2) user interface; (3) common inputs; (4) Florida Priority Index (FPI) and delay estimations; (5) HRX resource allocation; and (6) error messages.

6.3.1. Major Assumptions

The standalone application “HRX Safety Improvement” requires certain data from the Federal Railroad Administration (FRA) crossing inventory database and the FRA highway-rail grade crossing accident database in order to estimate the FPI values and delays for the considered highway-rail grade crossings. For the FPI estimations, the application requires the average daily traffic volume, average daily train volume, train speed, existing protection, and accident history for the last 5 years. The following assumptions have been used throughout estimation of the FPI values for the considered highway-rail grade crossings:

- 1) If no information regarding a given highway-rail grade crossing’s ownership (i.e., public or private) is available, the highway-rail grade crossing will be excluded from the analysis. The rationale behind such exclusion is that this highway-rail grade crossing could be abandoned or not controlled by the State of Florida. In the latter case, a private company may be responsible for application of countermeasures at the corresponding highway-rail grade crossings.
- 2) The values of certain predictors of the Florida Priority Index Formula will be assumed to be “1” for the cases when “zero” values or no values are reported in the FRA crossing inventory database. These predictors include the following: (1) annual average daily traffic (AADT); (2) total number of thru trains per day; (3) total number of switch trains per day; (4) maximum train timetable speed; and (5) number of main and other tracks. The latter assumption is necessary to ensure that the standalone application will not return any abnormal FPI values (e.g., “ $-\infty$ ”, “ $+\infty$ ”) for the considered highway-rail grade crossings.
- 3) If no protection is reported for a given highway-rail grade crossing, the worst-case protection factor value will be used in the analysis. The worst-case protection factor value is “1.00”, which is adopted for the highway-rail grade crossings with passive warning devices in the Florida Priority Index Formula. The same approach will be applied for highway-rail grade crossings with “zero” protection values. This approach will allow avoiding elimination of certain highway-rail grade crossings from the analysis due to the lack of protection information in the FRA crossing inventory database. Also, such an assumption will produce more conservative FPI values for the considered highway-rail grade crossings.
- 4) If no data are available regarding the classification of the roadway intersecting a railroad, the roadway will be assumed to be in a rural setting. Such an assumption will produce more conservative values of the hazard severity for the considered highway-rail grade crossings.
- 5) The prioritization or ranking of highway-rail grade crossings will be based on the FPI values (as the primary ranking criterion) and the exposure values (as the secondary ranking criterion). Note that the exposure is estimated as the product of AADT and the number of trains per day. If two highway-rail grade crossings have the same FPI value, a higher rank will be given to the highway-rail grade crossing with a higher exposure value.

In order to estimate the overall traffic delay due to application of a countermeasure at a highway-rail grade crossing, the standalone application “HRX Safety Improvement” requires the number of blockage occurrences (i.e., number of trains) and the overall delay experienced by queued vehicles during each blockage occurrence. In detail, the overall delay experienced by queued vehicles during each blockage occurrence is estimated from the delay time for a given highway-rail grade crossing equipped with a specific countermeasure (e.g., 35 seconds for gated highway-rail grade crossings), average train length, average train speed, average number of vehicles arriving per day, and number of highway lanes. In addition to the aforementioned assumptions (which have been used throughout the FPI estimations), another assumption has been used throughout estimation of the delay values at the considered highway-rail grade crossings. For the cases when “zero” values or no values for the number of traffic lanes crossing a railroad are reported in the FRA crossing inventory database, the number of traffic lanes crossing a railroad will be assumed to be “1”. The latter assumption is necessary to ensure that the standalone application will not return any abnormal delay values (e.g., “-∞”, “+∞”) for the considered highway-rail grade crossings.

As a part of this project, an optimization model, named the Multi-Objective Resource Allocation Problem (**MORAP**), was developed for resource allocation among the highway-rail grade crossings in Florida. This multi-objective optimization model has two objective functions, which are to minimize the overall hazard severity and to minimize the overall traffic delay at the highway-rail grade crossings in Florida. As discussed earlier, a total of three solution algorithms was developed to solve the **MORAP** model which include: (1) Epsilon-Constraint (ECON) method; (2) Multi-Objective Profitable Severity and Delay Reduction (MPSDR) heuristic; and (3) Multi-Objective Effective Severity and Delay Reduction (MESDR) heuristic. The previously conducted numerical experiments demonstrated that the MPSDR heuristic was the most promising solution approach for the **MORAP** model. Hence, the developed standalone application “HRX Safety Improvement” allocates resources using the MPSDR heuristic. The following assumptions have been followed throughout resource allocation (i.e., assignment of countermeasures) among the considered highway-rail grade crossings:

- 1) The MPSDR heuristic constructs a Pareto Front (PF) iteratively by changing the priorities of the objectives that are used in the **MORAP** mathematical model (i.e., the priority to be assigned to the overall hazard severity function F_1 and the priority to be assigned to the overall traffic delay function F_2). For each PF point, a priority list of highway-rail grade crossing-countermeasure pairs is generated and sorted by the benefit-to-cost ratios. The benefit-to-cost ratios are estimated for crossing-countermeasure pairs based on the normalized hazard severity reduction, normalized traffic delay reduction, associated objective priorities, and cost of applying countermeasures. Then, as long as there is enough budget available, the countermeasure with the highest benefit-to-cost ratio is assigned to each highway-rail grade crossing (considering the eligibility of highway-rail grade crossings for the countermeasures specified by the user).
- 2) A total of 11 countermeasures, discussed in the GradeDec.Net Reference Manual (U.S. DOT, 2014a), was considered in this project. However, not all of the countermeasures can be implemented at every single highway-rail grade crossing. The feasibility of implementation of each countermeasure at a given highway-rail grade crossing was considered based on the existing protection of highway-rail grade crossings (see section 5.1.2 for more details).

- 3) The values of the effectiveness factors of the countermeasures were adopted from the Highway-Rail Crossing Handbook (U.S. DOT, 2019) and the GradeDec.Net Reference Manual (U.S. DOT, 2014a, pages 25-26). If more than one value was available for a given countermeasure, the lowest value was adopted.
- 4) The installation costs of the considered countermeasures at highway-rail grade crossings were adopted from the GradeDec.Net Reference Manual (U.S. DOT, 2014a, pages 59-60).
- 5) As discussed earlier, the FPI values and the GradeDec severity prediction methodology were adopted in this project to assess the hazard severity of a given highway-rail grade crossing due to the lack of prediction methodologies for quantifying the hazard severity.
- 6) The weight values of the hazard severity categories for the **MORAP** model were adopted using the report by the Iowa DOT (2020) and were further set at $W_{FH} = 0.90$ for fatality hazard, $W_{IH} = 0.09$ for injury hazard, and $W_{PH} = 0.01$ for property damage hazard, which are near the values suggested by the Iowa DOT (2020).

6.3.2. User Interface

The user interface of the standalone application “HRX Safety Improvement” is presented in Figure 86. The user interface has three sections: (1) “**Common Inputs**”, which is located at the top of the interface; (2) “**FPI and Delay Estimation**”, which is located in the middle of the interface; and (3) “**HRX Resource Allocation**”, which is located at the bottom of the interface. The following color coding was adopted for the application interface: (1) yellow color was used for the fields where the user has to specify the path or select one of the available options from a drop-down menu; and (2) magenta color was used for the fields where the user has to type the values manually.



Figure 86 The user interface of the standalone application “HRX Safety Improvement”.

In the “**Common Inputs**” section, there are two buttons, named as “**HRX Database**” and “**Exports Results**”. The button “**HRX Database**” is used to provide the location (i.e., path) to the Excel database, which contains the information that will be further used throughout resource allocation among the highway-rail grade crossings. The button “**Export Results**” is utilized to provide the location (i.e., path) in the Windows Operating System and save the results in the Excel format. The message windows on the right side of the aforementioned buttons show the locations specified by the user. The “**FPI and Delay Estimation**” section has two buttons on the left, named as “**FL HRX Inventory**” and “**FL Accident Data**”. These buttons can load the highway-rail grade crossings inventory file and five accident data files, respectively. There is a message window on the right side of the “**FL HRX Inventory**” button that shows the location of the crossing inventory file. Similarly, a message window on the right side of the “**FL Accident Data**” button shows the path of the accident data files. The “**FPI and Delay Estimation**” section includes a pop-up menu, named as “**Crossing Type**”, which allows the user to select different types of highway-rail grade crossings for the analysis, including the following: (1) “**Public Only**”, (2) “**Private Only**”, and (3) “**Both**”. There is also a text box, named as “**Prediction Year**”. The year, for which the FPI values and delays are to be estimated, should be entered into

the “**Prediction Year**” textbox. At the bottom-right corner of the “**FPI and Delay Estimation**” section, there is a button, named as “**Estimate FPI and Delay**”. After pressing the “**Estimate FPI and Delay**” button, the standalone application starts estimating the FPI values and delay values for highway-rail grade crossings and exports the FPI values and delay values along with the associated data to an Excel file.

In the third section of the standalone application “HRX Safety Improvement”, which is “**HRX Resource Allocation**”, two textboxes, named as “**Index of Crossings**” and “**Index of Countermeasures**”, have been provided to insert the index of the highway-rail grade crossings to be considered throughout resource allocation and the index of the countermeasures to be considered throughout resource allocation, respectively. Another textbox, named as “**Number of PF Points**”, has been provided to insert the number of PF points for multi-objective resource allocation. When all the aforementioned input data are successfully set, the user should press the “**HRX Resource Allocation**” button at the bottom-right corner of the user interface, so that the standalone application “HRX Safety Improvement” can start assigning the available countermeasures to the specified highway-rail grade crossings for each PF point, based on the budget available. After a successful execution, the PF generated from multi-objective resource allocation will appear in the graph of the “**HRX Resource Allocation**” section. Moreover, the budget information will be shown in three textboxes, named as: (1) “**Total Budget Available**”; (2) “**Maximum Remaining Budget**”; and (3) “**Minimum Remaining Budget**” (see the bottom of the user interface in Figure 86).

6.3.3. Common Inputs

In order to estimate the FPI values and delays for the highway-rail grade crossings in Florida and perform resource allocation among the highway-rail grade crossings, the user has to provide certain common input data. Specifically, the standalone application “HRX Safety Improvement” requires the user to load the database with the information regarding the considered highway-rail grade crossings and the available countermeasures by pressing the button “**HRX Database**” (see Figure 87). By default, the user can work with the database “**FDOT_HRX-project_2020.xlsx**”, which was developed by the research team as a part of this project. The HRX database contains the information that will be further used throughout resource allocation among the highway-rail grade crossings. As it will be discussed in section 6.3.4 of this report, the standalone application “HRX Safety Improvement” will be automatically updating the HRX database based on the user input (e.g., if the user requests estimating the FPI values and delays for both private and public highway-rail grade crossings, the standalone application “HRX Safety Improvement” will calculate the FPI values and delays for both private and public highway-rail grade crossings and will paste the required data into the HRX database – i.e., the user will not be required to paste any values manually). However, the user will be able to make appropriate changes in the HRX database before conducting resource allocation (e.g., add another countermeasure, update the default installation costs of the available countermeasures, adjust the FPI values and/or delays for certain highway-rail grade crossings, etc.). Once the HRX database is loaded, the message window on the right side of the “**HRX Database**” button will show the location (i.e., path) of the selected file (see Figure 87).



Figure 87 Loading the database with highway-rail grade crossings and countermeasures.

Moreover, the standalone application “HRX Safety Improvement” requires the user to specify the path, where the output Excel files (generated after estimation of the FPI values and delays as well as performing resource allocation) will be exported. The “**Export Results**” button on the user interface allows specifying the location for the output Excel files (see Figure 88). Once the user specifies the export location (i.e., path) for the output Excel files, the message window on the right side of the “**Export Results**” button will show that export location in the Windows Operating System.



Figure 88 Specifying the location to export the results.

6.3.4. FPI and Delay Estimations

The section “**FPI and Delay Estimation**” of the standalone application “HRX Safety Improvement” ranks the highway-rail grade crossings based on the FPI values using the Florida Priority Index Formula. If two highway-rail grade crossings have the same FPI value, the highway-rail grade crossing with a higher exposure value will be assigned a higher rank. Note that the exposure of a given highway-rail grade crossing is estimated as a product of AADT and the number of trains per day. The traffic delays at the highway-rail grade crossings are estimated in this section as well.



Figure 89 Loading the crossing inventory data.

In order to estimate the FPI values and delays for the highway-rail grade crossings, the user has to load the Florida crossing inventory data in the Excel format. The Florida crossing inventory data can be downloaded from the FRA crossing inventory database. After downloading, the crossing inventory file can be named as **“Florida_Crossings.xls”** (or other appropriate names set by the user). The **“FL HRX Inventory”** button on the user interface allows loading the crossing inventory file. Once the file is loaded, the message window on the right side of the **“FL HRX Inventory”** button will show the location of the crossing inventory file (see Figure 89).

The year, for which the FPI values and delays are to be estimated, should be inserted in the **“Prediction Year”** textbox (see Figure 90). Furthermore, the user should load the Florida accident data for five years before the prediction year in the Excel format (e.g., the 2019-2015 accident data are required for the prediction year 2020). The accident data can be downloaded from the FRA highway-rail grade crossing accident database. However, the accident data should be downloaded for each single year. Therefore, there will be five files for five years of the accident data. Note that a specific naming convention must be followed for the accident data files to keep a correct order of the files. For example, if the prediction year is 2020, the accident data

file for the 1st year before 2020 (the year 2019) should be named as “**Florida Accident Data - 1st Year.xls**”; the accident data file for the 2nd year before 2020 (the year 2018) should be named as “**Florida Accident Data - 2nd Year.xls**”; the accident data file for the 3rd year before 2020 (the year 2017) should be named as “**Florida Accident Data - 3rd Year.xls**”; the accident data file for the 4th year before 2020 (the year 2016) should be named as “**Florida Accident Data - 4th Year.xls**”; and the accident data file for the 5th year before 2020 (the year 2015) should be named as “**Florida Accident Data - 5th Year.xls**”. Note that the authorized users may not be required to download any files from the FRA databases and will be instructed to retrieve the required files (including the tool installation file) from a cloud-based “master folder” managed by the FDOT Freight & Multimodal Operations Office.



Figure 90 Specifying the prediction year and loading the accident data.

Note that this report primarily relies on the term “accident”, which is consistent with the highway-rail grade crossing safety literature. However, other stakeholders (e.g., railroad companies) primarily rely on the term “incident”. Without loss of generality, the naming convention for the accident data files can be adjusted, as long as the order of files is kept based on the reporting year (e.g., “**Florida Accident Data - 1st Year**” can be renamed as “**Florida**

Incident Data - 1st Year” – the standalone application “HRX Safety Improvement” will not return any errors). The “**FL Accident Data**” button on the user interface allows loading the five accident data files. Once the files are loaded, the message window on the right side of the “**FL Accident Data**” button will show the location (i.e., path) of the five accident data files (see Figure 90). Note that the five files must be loaded at once.



Figure 91 Selection of the crossing type.

The standalone application “HRX Safety Improvement” can distinguish between public and private highway-rail grade crossings. Using the “**Crossing Type**” pop-up menu, the user can direct the standalone application to estimate the FPI values and delays for the following types of highway-rail grade crossings: (1) “**Public Only**”; (2) “**Private Only**”; and (3) “**Both**” (see Figure 91). However, if no crossing type is selected, the standalone application will choose public highway-rail grade crossings as default.

After successfully completing the previous steps, the user can execute the “**FPI and Delay Estimation**” section of the standalone application “HRX Safety Improvement” to estimate the FPI values and delays for the selected type(s) of highway-rail grade crossings by pressing the

“**Estimate FPI and Delay**” button. When the “**Estimate FPI and Delay**” button is pressed, a progress bar which states “**Estimating Florida Priority Index and Delay...**”, will pop up (see Figure 92). Once the FPI values and delays are successfully estimated, the progress bar will disappear.

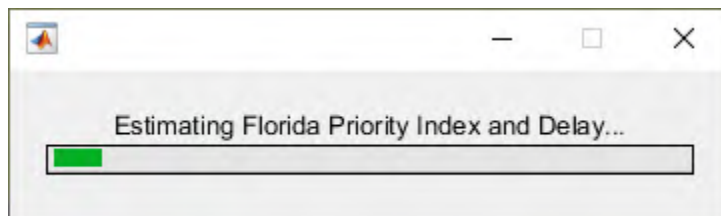


Figure 92 The progress bar of “**FPI and Delay Estimation**”.

Note: There is a certain condition which can interrupt a successful execution of the standalone application “HRX Safety Improvement”. Specifically, the standalone application “HRX Safety Improvement” cannot delete or modify an open Excel file. If the user has already executed the “**FPI and Delay Estimation**” section of the application successfully, opened some of the Excel files (e.g., “**FDOT_HRX-project_2020.xlsx**”, “**Tool_Output.xlsx**”, or other Excel files), and tries to run the application again, the application may not run successfully (i.e., “freeze”), even if the Excel files have been closed by the user (as the Windows Operating System may still have the Excel application invoked). If the standalone application “HRX Safety Improvement” gets frozen due to the Excel data exchange issues, the progress bar will not appear anymore after pressing the button “**Estimate FPI and Delay**” or the button “**HRX Resource Allocation**”. However, if the user closes the application and restarts it, the application will resume working normally again. Therefore, it is recommended for users to determine the analysis types they would like to conduct before executing the standalone application “HRX Safety Improvement”. Also, it is recommended for users to keep the Excel application closed, while performing certain procedures with the standalone application “HRX Safety Improvement”, to ensure that the standalone application “HRX Safety Improvement” works normally. In order to prevent the “freezing” issue, the latest version of the standalone application “HRX Safety Improvement” automatically closes open Excel files after pressing the button “**Estimate FPI and Delay**” or the button “**HRX Resource Allocation**”.

FPI Estimation Outputs

The standalone application “HRX Safety Improvement” exports the FPI values for the considered highway-rail grade crossings and the associated data to the previously specified location in the Excel format (i.e., XLSX). The Excel file is named as “**Tool_Output.xlsx**”. The FPI estimation outputs are shown in the “**Output_FPI**” sheet of the file “**Tool_Output.xlsx**”. A certain number of fields (i.e., columns) are shown in the “**Output_FPI**” sheet. Each row in the “**Output_FPI**” sheet represents a highway-rail grade crossing. Figure 93 presents an example showing the “**Output_FPI**” sheet of the “**Tool_Output.xlsx**” file for the public highway-rail grade crossings in Florida. This example showcases the data for 6,109 highway-rail grade crossings, as 6,109 public highway-rail grade crossings in Florida are presented in the latest crossing inventory file downloaded from the FRA crossing inventory database (as of May of 2020).

FPI_ID	CrossingID	Aadt	TotalTrains	MaxTtSpd	WdCode	PF	AH5	AwdIDate	A	FPI	ThruTrain	TotalSWT	HwyClass	TotTracks
1	628191E	56000	56	79	8	0.1	0	0	A	122009.5	52	A	1	2
2	628177F	56000	55	79	8	0.1	4	0	A	119824.8	51	A	1	2
3	628188J	50500	52	79	8	0.1	3	0	3	73385.67	48	A	1	2
4	628168G	59400	55	79	9	0.1	2	82009	2	56888.74	51	A	1	2
5	628169V	56000	55	79	8	0.1	2	0	2	53996.09	51	A	1	2
6	628163X	53000	52	79	8	0.1	2	0	2	48315.98	51	1	1	2
7	628146G	32000	52	79	9	0.1	3	0	3	46501.81	51	1	1	1
8	628187L	29000	56	79	8	0.1	3	0	3	45383.98	51	5	1	2
9	272596P	31300	51	79	8	0.1	3	0	3	44609.88	50	1	1	2
10	628139W	47500	52	79	8	0.1	2	0	2	43302.06	51	1	1	1

Figure 93 The “Output_FPI” sheet of the “Tool_Output.xlsx” file.

Variable	Description
FPI_ID	rank/index of a highway-rail grade crossing
CrossingID	crossing inventory number
Aadt	annual average daily traffic (AADT) count
TotalTrains	total number of trains (daylight through + night time through + switching) (trains)
MaxTtSpd	maximum timetable speed (mph)
WdCode	warning device code (1 = no signs or signals; 2 = other signs or signals; 3 = crossbucks; 4 = stop signs; 5 = special active warning devices; 6 = highway traffic signals, wigwags, bells, or other activated; 7 = flashing lights; 8 = all other gates; 9 = four quad (full barrier) gates)
PF	protection factor (1.00 for passive; 0.70 for flashing lights; 0.10 for gates)
AH5	5-year accident history (accidents)
AwdIDate	installation date of current active warning devices
A	accident history parameter (accidents)

Figure 94 The “Legend_FPI” sheet of the “Tool_Output.xlsx” file.

The explanation of all the headings in the “Output_FPI” sheet of the “Tool_Output.xlsx” file, which denote different features of the considered highway-rail grade crossings that were used for estimating the FPI values for these highway-rail grade crossings, is provided in the “Legend_FPI” sheet (see Figure 94). These features include the following:

- FPI_ID – rank/index of a highway-rail grade crossing;
- CrossingID – crossing inventory number;
- Aadt – annual average daily traffic (AADT) count;
- TotalTrains – total number of trains (daylight through + night time through + switching) (trains);
- MaxTtSpd – maximum timetable speed (mph);
- WdCode – warning device code (1 = no signs or signals; 2 = other signs or signals; 3 = crossbucks; 4 = stop signs; 5 = special active warning devices; 6 = highway traffic signals, wigwags, bells, or other activated; 7 = flashing lights; 8 = all other gates; 9 = four quad (full barrier) gates);
- PF – protection factor (1.00 for passive; 0.70 for flashing lights; 0.10 for gates);
- AH5 – 5-year accident history (accidents);
- AwdIDate – installation date of current active warning devices;
- A – accident history parameter (accidents);

- FPI – the Florida Priority Index;
- ThruTrains – total number of through trains (daylight through + night time through) (trains);
- TotalSwT – total number of switching trains (trains);
- HwyClassCD – functional classification of road at crossing (0 = rural; 1 = urban);
- TotTracks – number of main and other tracks (tracks);
- OverallHaz – overall hazard at a highway-rail grade crossing;
- FatHaz – fatality hazard at a highway-rail grade crossing;
- CasHaz – casualty hazard at a highway-rail grade crossing;
- InjHaz – injury hazard at a highway-rail grade crossing;
- PropHaz – property damage hazard at a highway-rail grade crossing;
- TypeXing – crossing type (2 = private; 3 = public)
- HwynrSig – does nearby highway intersection have traffic signals? (1 = yes; 2 = no);
- MonitorDev – highway monitoring devices (0 = none; 1 = yes-photo/video recording; 2 = yes-vehicle presence detection);
- PaveMrkIDs – pavement markings (0 = none; 1 = stop lines; 2 = railroad crossing symbols; 3 = dynamic envelope);
- PrempType – highway traffic signal preemption (1 = simultaneous; 2 = advance);
- DevelTypID – type of land use (11 = open space; 12 = residential; 13 = commercial; 14 = industrial; 15 = institutional; 16 = farm; 17 = recreational; 18 = railroad yard);
- TypeTrnSrvIDs – type of train service (11 = freight; 12 = intercity passenger; 13 = commuter; 14 = transit; 15 = shared use transit; 16 = tourist/other);
- Whistban – quiet zone (0 = no; 1 = 24 hour; 2 = partial; 3 = Chicago excused);
- HwyNear – intersecting roadway within 500 feet? (1 = yes; 2 = no);
- HwyPved – is roadway/pathway paved? (1 = yes; 2 = no);
- Illumina – is crossing illuminated? (1 = yes; 2 = no);
- TraficLn – number of traffic lanes crossing railroad (lanes);
- XAngle – smallest crossing angle (1 = 0° – 29°; 2 = 30° – 59°; 3 = 60° – 90°);
- XSurfaceIDs – crossing surface (11 = timber; 12 = asphalt; 13 = asphalt and timber; 14 = concrete; 15 = concrete and rubber; 16 = rubber; 17 = metal; 18 = unconsolidated; 19 = composite; 20 = other [specify]);
- HwySpeed – highway speed limit (mph);
- PctTruk – estimated percent trucks; and
- SchlBsCnt – average number of school bus count per day (busses).

Delay Estimation Outputs

The standalone application “HRX Safety Improvement” exports the delay estimation outputs for the considered highway-rail grade crossings and the associated data to the “**Tool_Output.xlsx**” file as well. The delay estimation outputs are shown in the “**Output_Delay**”, “**EBT(x,c)**”, “**VQ(x,c)**”, “**QDT(x,c)**”, “**ODB(x,c)**”, “**OD(x,c)**”, and “**AD(x,c)**” sheets of the file “**Tool_Output.xlsx**”. A certain number of fields (i.e., columns), which underline different features of the considered highway-rail grade crossings that were used for estimating the overall delay at these highway-rail grade crossings with the existing warning devices per day, are shown in the “**Output_Delay**” sheet. Each row in the “**Output_Delay**” sheet represents a highway-rail grade crossing. Figure 95 presents an example showing the “**Output_Delay**” sheet of the

“**Tool_Output.xlsx**” file for the public highway-rail grade crossings in Florida. This example showcases the data for 6,109 highway-rail grade crossings, as 6,109 public highway-rail grade crossings in Florida are presented in the latest crossing inventory file downloaded from the FRA crossing inventory database (as of May of 2020).

FPI_ID	CrossingID	V	T	CCD0	L	SC	ESTD	VQD	n	DDM	DDB	QDQ
1 628191B	56000	56	35	7000	49	132.1817	86	6	60	5743.834	89.34822	
2 628177F	56000	56	35	7000	49	132.1817	86	6	60	5743.834	87.73272	
3 628183J	50200	52	35	7000	49	132.1817	77	9	60	5148.997	74.1744	
4 628168G	59000	55	40	7000	49	137.1817	94	6	60	6507.541	99.42077	
5 628189N	56000	55	35	7000	49	132.1817	86	7	60	5743.834	87.75272	
6 628163M	53000	52	35	7000	49	132.1817	81	9	60	5413.36	78.19298	
7 628146G	32000	52	40	7000	49	137.1817	51	8	60	3558.134	51.39527	
8 628187L	29000	56	35	7000	49	132.1817	44	7	60	2967.998	46.16886	
9 272956P	31800	51	35	7000	49	132.1817	48	8	60	3282.362	45.79179	
10 628139W	47500	52	35	7000	49	132.1817	73	8	60	4884.633	70.55581	

Figure 95 The “**Output_Delay**” sheet of the “**Tool_Output.xlsx**” file.

Variable	Description
FPI_ID	rank/index of a highway-rail grade crossing
CrossingID	crossing inventory number
V	average number of vehicles arriving at a highway-rail grade crossing per day (vehicles)
T	average number of trains arriving at a highway-rail grade crossing per day (trains)
CCD0	current delay time for a highway-rail grade crossing with the existing warning devices (seconds)
L	average train length for a highway-rail grade crossing (feet)
SC	average train speed for a highway-rail grade crossing (mph)
ESTD	effective time during which a train blocks a highway-rail grade crossing with the existing warning devices (seconds)
VQD	average number of vehicles queued at a highway-rail grade crossing with the existing warning devices during each blockage (vehicles)
n	number of traffic lanes crossing railroad (lanes)

Figure 96 The “**Legend_Delay**” sheet of the “**Tool_Output.xlsx**” file.

The explanation of all the headings in the “**Output_Delay**” sheet of the “**Tool_Output.xlsx**” file, which denote different features of the considered highway-rail grade crossings that were used for estimating the overall delay at these highway-rail grade crossings with the existing warning devices per day, is provided in the “**Legend_Delay**” sheet (see Figure 96). These features include the following:

- FPI_ID – rank/index of a highway-rail grade crossing;
- CrossingID – crossing inventory number;
- V – average number of vehicles arriving at a highway-rail grade crossing per day (vehicles);
- T – average number of trains arriving at a highway-rail grade crossing per day (trains);
- CCD0 – current delay time for a highway-rail grade crossing with the existing warning devices (seconds);
- L – average train length for a highway-rail grade crossing (feet);
- SC – average train speed for a highway-rail grade crossing (mph);

- EBT0 – effective time during which a train blocks a highway-rail grade crossing with the existing warning devices (seconds);
- VQ0 – average number of vehicles queued at a highway-rail grade crossing with the existing warning devices during each blockage (vehicles);
- n – number of traffic lanes crossing railroad (lanes);
- QDT0 – queue dissipation time after a train passes a highway-rail grade crossing with the existing warning devices (seconds);
- ODB0 – overall delay experienced by queued vehicles during each blockage of a highway-rail grade crossing with the existing warning devices (seconds); and
- OD0 – overall delay at a highway-rail grade crossing with the existing warning devices per day (hours).

Along with the “**Output_Delay**” sheet, the “**Tool_Output.xlsx**” file contains the following sheets that are associated with delay estimations at the considered highway-rail grade crossings after implementation of different countermeasures:

- “**EBT(x,c)**” – effective time during which a train blocks highway-rail grade crossing x after implementation of countermeasure c (seconds) (see Figure 97);
- “**VQ(x,c)**” – average number of vehicles queued at highway-rail grade crossing x after implementation of countermeasure c during each blockage (vehicles) (see Figure 98);
- “**QDT(x,c)**” – queue dissipation time once a train passes highway-rail grade crossing x after implementation of countermeasure c (seconds) (see Figure 99);
- “**ODB(x,c)**” – overall delay experienced by queued vehicles during each blockage of highway-rail grade crossing x after implementation of countermeasure c (seconds) (see Figure 100);
- “**OD(x,c)**” – overall delay at highway-rail grade crossing x per day after implementation of countermeasure c (hours) (see Figure 101); and
- “**AD(x,c)**” – additional delay due to application of countermeasure c at highway-rail grade crossing x (hours) (see Figure 102).

Crossing\Countermeasure	1	2	3	4	5	6	7	8	9	10	11
1	137.1817	152.1817	137.1817	137.1817	137.1817	139.6817	139.6817	139.6817	137.1817	137.1817	132.1817
2	137.1817	152.1817	137.1817	137.1817	137.1817	139.6817	139.6817	139.6817	137.1817	137.1817	132.1817
3	137.1817	152.1817	137.1817	137.1817	137.1817	139.6817	139.6817	139.6817	137.1817	137.1817	132.1817
4	142.1817	157.1817	152.1817	142.1817	142.1817	144.6817	144.6817	144.6817	142.1817	142.1817	137.1817
5	137.1817	152.1817	137.1817	137.1817	137.1817	139.6817	139.6817	139.6817	137.1817	137.1817	132.1817

Figure 97 The “**EBT(x,c)**” sheet of the “**Tool_Output.xlsx**” file.



Figure 98 The “VQ(x,c)” sheet of the “Tool_Output.xlsx” file.

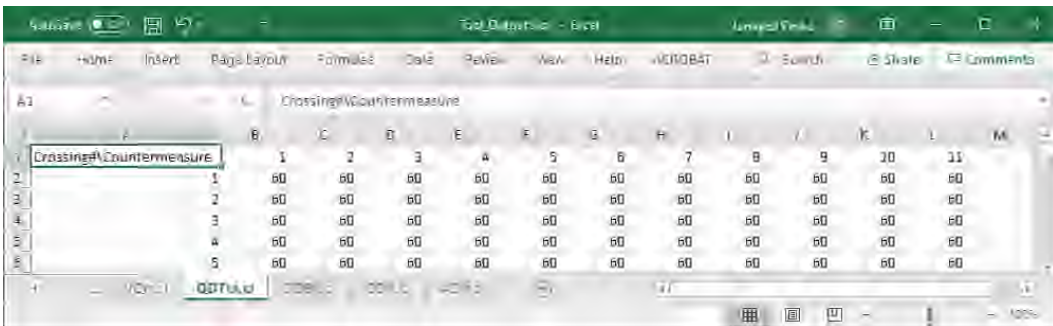


Figure 99 The “QDT(x,c)” sheet of the “Tool_Output.xlsx” file.

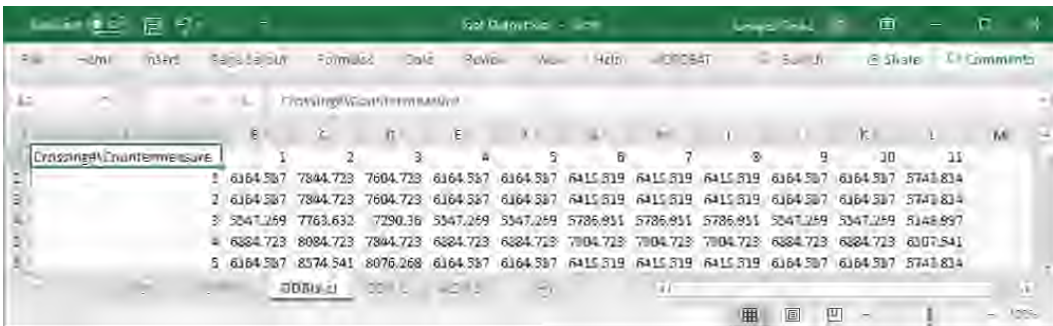


Figure 100 The “ODB(x,c)” sheet of the “Tool_Output.xlsx” file.



Figure 101 The “OD(x,c)” sheet of the “Tool_Output.xlsx” file.



Figure 102 The “AD(x,c)” sheet of the “Tool_Output.xlsx” file.

HRX Database Updates

The highway-rail grade crossing information required for resource allocation (e.g., hazard severity values, delay values) will be transferred by the standalone application “HRX Safety Improvement” into the HRX database, which is named as “**FDOT_HRX-project_2020.xlsx**” (however, the users can rename the HRX database as appropriate). The HRX database contains 10 sheets, namely: (1) “**Sheet_Description**”; (2) “**Data_Description**”; (3) “**p(x,c)**”; (4) “**EF(x,c)**”; (5) “**HS(x,s)**”; (6) “**W(s)**”; (7) “**CA(x,c)**”; (8) “**OD0(x)**”; (9) “**AD(x,c)**”; and (10) “**TAB**”. A description of the information provided in these 10 sheets is presented below.

- 1) **Sheet_Description**: This sheet explains the information provided in different sheets of the HRX database, which is directly used by the standalone application “HRX Safety Improvement” (see Figure 103).

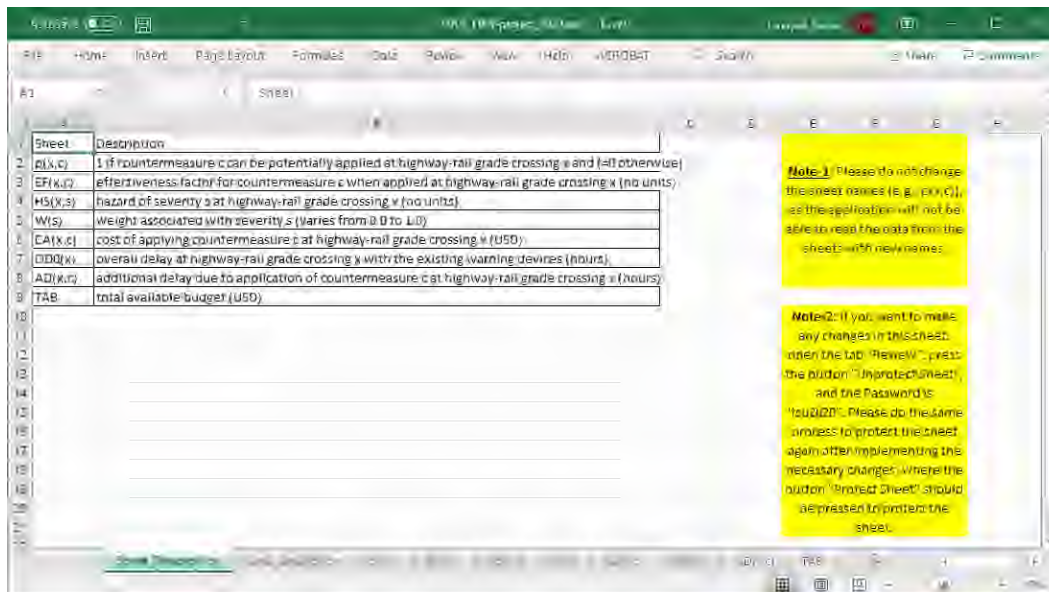


Figure 103 The “Sheet_Description” sheet of “FDOT_HRX-project_2020.xlsx”.

- 2) **Data_Description**: This sheet presents the information regarding a number of parameters. The default effectiveness factors for the considered countermeasures (as suggested by the GradeDec.Net Reference Manual – U.S. DOT, 2014a), the default installation costs for the considered countermeasures (as suggested by the GradeDec.Net Reference Manual – U.S. DOT, 2014a), the severity categories considered, and the total available budget are presented

in this sheet (see Figure 104). In addition, the data needed for delay estimations are provided in this sheet, which include the warning device codes for different protection classes (FRA, 2016), the current delay time at highway-rail grade crossings for different protection classes (i.e., the CCDe value will be used by the application to set the CCD0 value for each highway-rail grade crossing based on its protection type), the additional delay time that is incurred on average at highway-rail grade crossings after implementation of the considered countermeasures, the average train length, the maximum average train speed at highway-rail grade crossings, the minimum average train speed at highway-rail grade crossings, the maximum queue length per lane at highway-rail grade crossings (i.e., an upper bound on $\frac{VQ_x^0}{2 \cdot n_x}$ and $\frac{VQ_{xc}}{2 \cdot n_x}$), and the maximum queue dissipation time at highway-rail grade crossings (i.e., an upper bound on QDT_x^0 and QDT_{xc}). Note that the values of the aforementioned parameters can be adjusted by the user. For example, if the user changes the installation cost for countermeasure “1” (“passive to flashing lights”) from \$74,800 to \$50,000, the standalone application “HRX Safety Improvement” will be using the updated installation cost of \$50,000 for countermeasure “1” and all the considered highway-rail grade crossings when preparing the necessary cost data (sheet “CA(x,c)”).

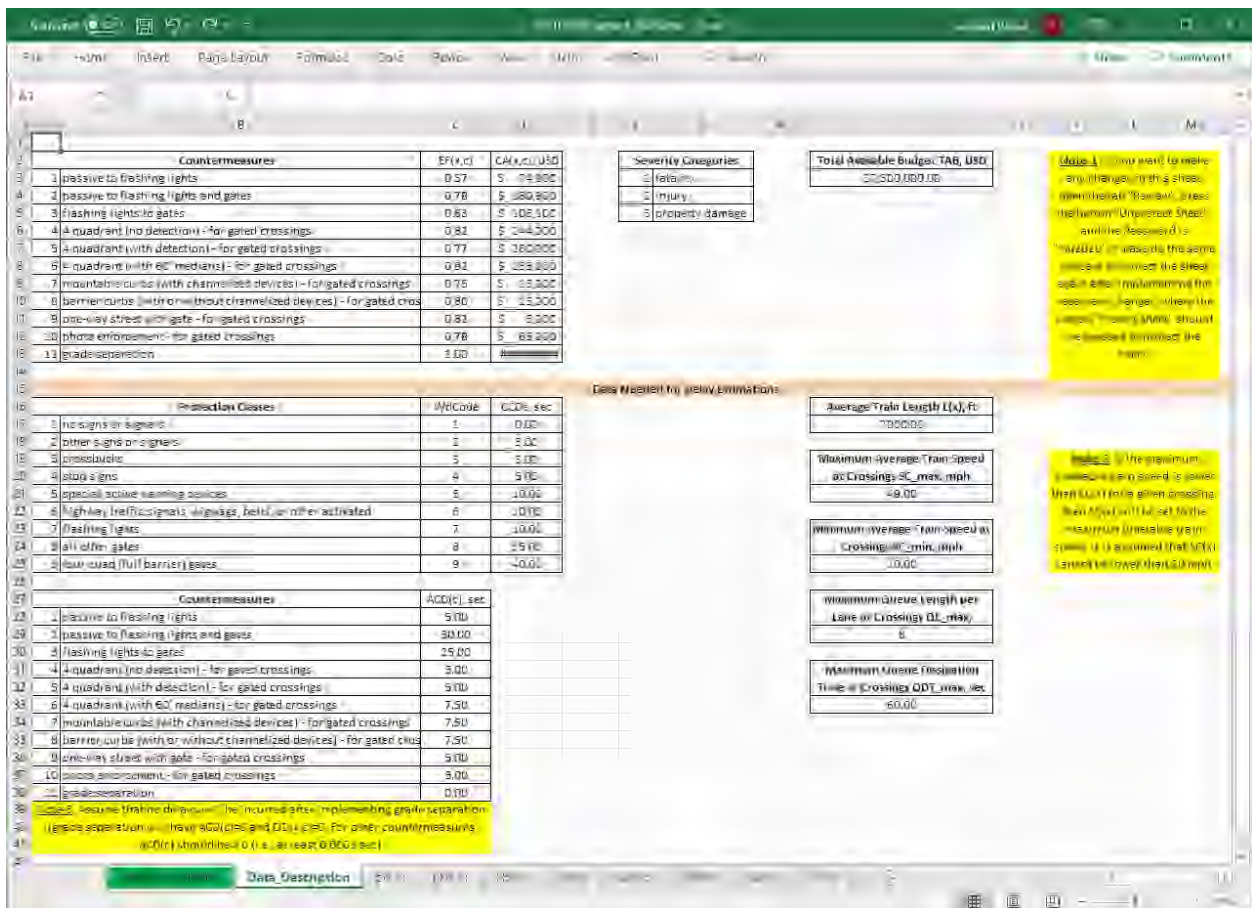


Figure 104 The “Data_Description” sheet of “FDOT_HRX-project_2020.xlsx”.

- 3) **p(x,c)**: This sheet specifies the eligibility of all the considered highway-rail grade crossings for the available countermeasures. Particularly, there is a matrix in this sheet, whose number of rows and columns are equal to the number of highway-rail grade crossings and countermeasures, respectively (see Figure 105). A cell value of “1” in this matrix denotes that the corresponding highway-rail grade crossing is eligible for the corresponding countermeasure. In case of ineligibility, the cell value is “0”. The default countermeasure eligibility values (as suggested by the GradeDec.Net Reference Manual – U.S. DOT, 2014a) will be inserted for the considered highway-rail grade crossings by the standalone application “HRX Safety Improvement” into the sheet “**p(x,c)**”. For example, passive highway-rail grade crossings are eligible for the two default countermeasures suggested by the GradeDec.Net Reference Manual (U.S. DOT, 2014a), including the following: (a) “passive to flashing lights”; and (b) “passive to flashing lights and gates”.

Crossing\Countermeasure	1	2	3	4	5	6	7	8	9	10	11
1	1	0	0	0	1	1	1	1	1	1	1
2	1	0	0	0	1	1	1	1	1	1	1
3	1	0	0	0	1	1	1	1	1	1	1
4	1	0	0	0	1	1	1	1	1	1	1
5	1	0	0	0	1	1	1	1	1	1	1

Figure 105 The “**p(x,c)**” sheet of “**FDOT_HRX-project_2020.xlsx**”.

- 4) **EF(x,c)**: This sheet specifies the effectiveness values of the available countermeasures at each highway-rail grade crossing. This sheet includes a matrix, whose number of rows and columns are equal to the number of highway-rail grade crossings and countermeasures, respectively (see Figure 106). Each cell in the matrix specifies the effectiveness value of a given countermeasure (corresponding to the column of the matrix) at a given highway-rail grade crossing (corresponding to the row of the matrix). The default effectiveness values of the available countermeasures will be copied by the standalone application “HRX Safety Improvement” from the sheet “**Data_Description**” and pasted into the sheet “**EF(x,c)**”.

Crossing\Countermeasure	1	2	3	4	5	6	7	8	9	10	11
1	0.57	0.78	0.63	0.82	0.77	0.92	0.75	0.8	0.82	0.78	1
2	0.57	0.78	0.63	0.82	0.77	0.92	0.75	0.8	0.82	0.78	1
3	0.57	0.78	0.63	0.82	0.77	0.92	0.75	0.8	0.82	0.78	1
4	0.57	0.78	0.63	0.82	0.77	0.92	0.75	0.8	0.82	0.78	1
5	0.57	0.78	0.63	0.82	0.77	0.92	0.75	0.8	0.82	0.78	1

Figure 106 The “**EF(x,c)**” sheet of “**FDOT_HRX-project_2020.xlsx**”.

- 5) **HS(x,s)**: This sheet specifies the hazard value for each severity category at each highway-rail grade crossing. In particular, each highway-rail grade crossing is assigned a row with four cells (see Figure 107). From the left, the first cell denotes the highway-rail grade crossing

number (i.e., rank/index of a highway-rail grade crossing based on its FPI value). The second, third, and fourth cells from the left specify fatality hazard severity, injury hazard severity, and property damage hazard severity at a given highway-rail grade crossing, respectively. The estimated hazard severity values for the considered highway-rail grade crossings will be copied by the standalone application “HRX Safety Improvement” from the sheet “**Output_FPI**” of the “**Tool_Output.xlsx**” file and pasted into the sheet “**HS(x,s)**”.

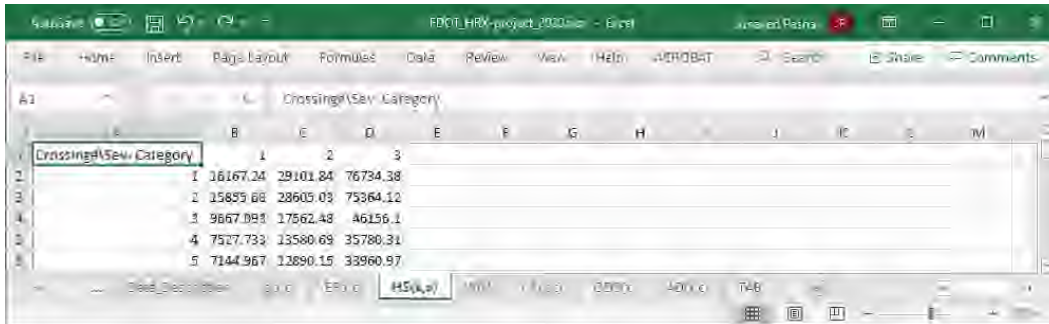


Figure 107 The “**HS(x,s)**” sheet of “**FDOT_HRX-project_2020.xlsx**”.

- 6) **W(s)**: This sheet shows the severity weight values considered for fatality hazard severity (the default value is set to 0.90), injury hazard severity (the default value is set to 0.09), and property damage hazard severity (the default value is set to 0.01) (see Figure 108).

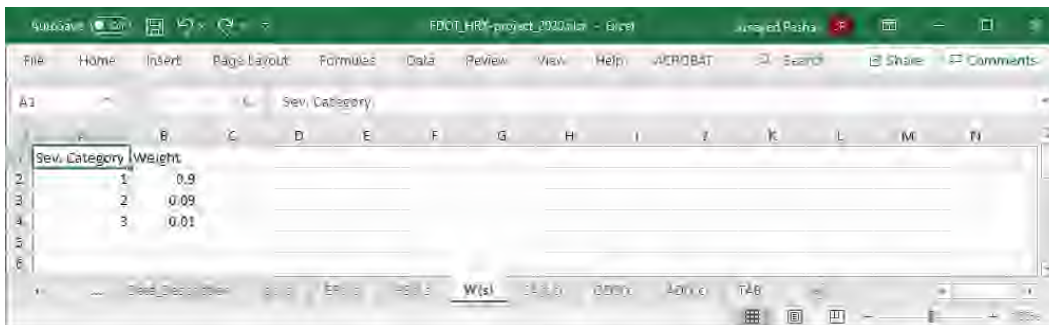


Figure 108 The “**W(s)**” sheet of “**FDOT_HRX-project_2020.xlsx**”.

- 7) **CA(x,c)**: This sheet provides the installation costs of the available countermeasures at all the highway-rail grade crossings considered for safety improvement projects. Specifically, there is a matrix in this sheet, whose number of rows and columns are equal to the number of highway-rail grade crossings and countermeasures, respectively (see Figure 109). Each cell in the matrix specifies the cost to implement a given countermeasure (corresponding to the column of the matrix) at a given highway-rail grade crossing (corresponding to the row of the matrix). The default installation cost values of the available countermeasures will be copied by the standalone application “HRX Safety Improvement” from the sheet “**Data_Description**” and pasted into the sheet “**CA(x,c)**”.



Figure 109 The “CA(x,c)” sheet of “FDOT_HRX-project_2020.xlsx”.

- 8) **OD0(x)**: This sheet shows the overall delay at each highway-rail grade crossing with the existing countermeasures. In particular, each highway-rail grade crossing is assigned a row with two cells, where the cell on the left side denotes the highway-rail grade crossing number (i.e., rank/index of a highway-rail grade crossing based on its FPI value), and the cell on the right side specifies the overall delay at that highway-rail grade crossing with the existing countermeasures (see Figure 110). The overall delay values at the considered highway-rail grade crossings with the existing countermeasures will be copied by the standalone application “HRX Safety Improvement” from the sheet “Output_Delay” of the “Tool_Output.xlsx” file and pasted into the sheet “OD0(x)”.

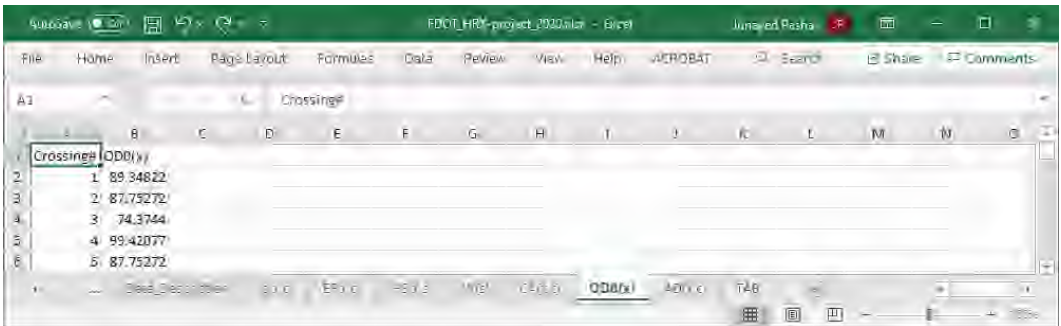


Figure 110 The “OD0(x)” sheet of “FDOT_HRX-project_2020.xlsx”.

- 9) **AD(x,c)**: This sheet presents the additional delays due to application of the available countermeasures at each highway-rail grade crossing. Specifically, there is a matrix in this sheet, whose number of rows and columns are equal to the number of highway-rail grade crossings and countermeasures, respectively (see Figure 111). Each cell in the matrix specifies the additional delay due to application of a given countermeasure (corresponding to the column of the matrix) at a given highway-rail grade crossing (corresponding to the row of the matrix). The estimated additional delay values due to application of the available countermeasures at the considered highway-rail grade crossings will be copied by the standalone application “HRX Safety Improvement” from the sheet “AD(x,c)” of the “Tool_Output.xlsx” file and pasted into the sheet “AD(x,c)” of the HRX database (i.e., the “FDOT_HRX-project_2020.xlsx” file).

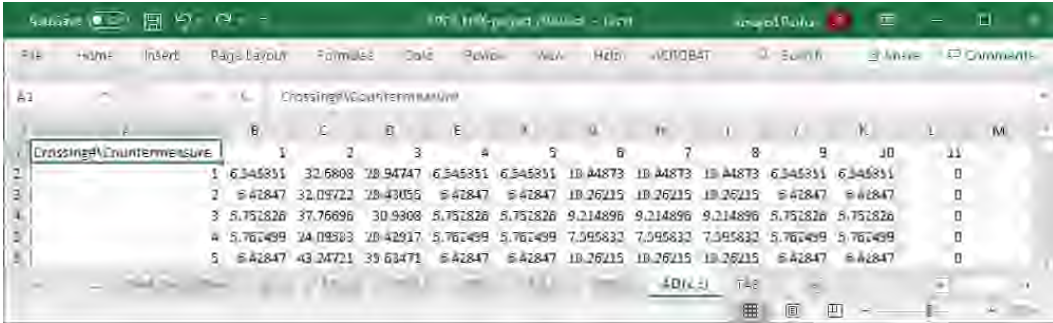


Figure 111 The “AD(x,c)” sheet of “FDOT_HRX-project_2020.xlsx”.

- 10) **TAB**: This sheet shows the value of the total available budget (TAB) that will be used for safety improvement projects at the considered highway-rail grade crossings (see Figure 112). The default total available budget will be copied by the standalone application “HRX Safety Improvement” from the sheet “Data_Description” and pasted into the sheet “TAB”.

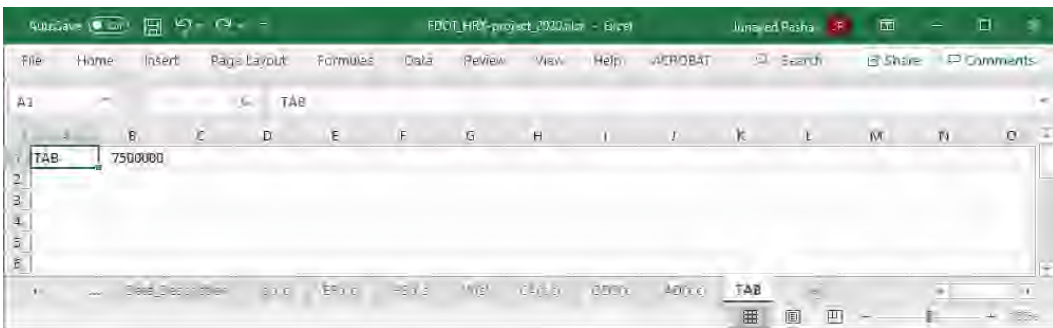


Figure 112 The “TAB” sheet of “FDOT_HRX-project_2020.xlsx”.

The first two sheets of the HRX database (i.e., “Sheet_Description” and “Data_Description”) play very important roles in the standalone application “HRX Safety Improvement”; hence, they are protected by a password to avoid any unwanted and unintentional changes. Specifically, the standalone application “HRX Safety Improvement” reads the respective data from these two sheets based on the location of the cells in the sheets. For example, the “FPI and Delay Estimation” section of the standalone application “HRX Safety Improvement” reads the effectiveness values of countermeasures from the cells “C3” to “C13” in the second sheet (i.e., “Data_Description”), and if these data are relocated to any other cells, the application will not be able to retrieve the correct data from the sheet. Therefore, the user must avoid any relocation of the data related to the effectiveness values in the second sheet. The same applies to all the information included in the “Data_Description” sheet of the HRX database. In order to edit the data in the sheets “Sheet_Description” and “Data_Description”, the user should open the “Review” tab in the respective sheet(s), press the “Unprotect Sheet” button, and type the password, which is “fsu2020”. The password can be changed by the users as needed. After implementing the necessary changes, the user should repeat the latter process to password-protect the edited sheet(s) using the “Protect Sheet” button (instead of using the “Unprotect Sheet” button). The instructions on how to protect and unprotect the first two sheets are provided in first two sheets of the HRX database as well.

As mentioned earlier, the standalone application “HRX Safety Improvement” is composed of three sections, including “**Common Inputs**”, “**FPI and Delay Estimation**”, and “**HRX Resource Allocation**”. Each section utilizes the HRX database for a particular purpose. The “**Common Inputs**” section receives the path to the HRX database and transfers it to the “**FPI and Delay Estimation**” section and the “**HRX Resource Allocation**” section without making any changes in the HRX database. The “**FPI and Delay Estimation**” section receives the path to the HRX database and makes necessary changes in the file (e.g., change the type of highway-rail grade crossings based on the user’s choice and, therefore, modify the number of rows in certain sheets; change the FPI values and delays; etc.), which can be further used in the “**HRX Resource Allocation**” section. In particular, the “**FPI and Delay Estimation**” section reads data from the second sheet (i.e., “**Data_Description**”) and rewrites the last eight sheets (i.e., “**p(x,c)**”, “**EF(x,c)**”, “**HS(x,s)**”, “**W(s)**”, “**CA(x,c)**”, “**OD0(x)**”, “**AD(x,c)**”, and “**TAB**”). If the user would like to manually edit some data in the “**Data_Description**” sheet of the HRX database, the editing must be completed before execution of the “**FPI and Delay Estimation**” section. On the other hand, if the user would like to manually make some changes in the last eight sheets (i.e., “**p(x,c)**”, “**EF(x,c)**”, “**HS(x,s)**”, “**W(s)**”, “**CA(x,c)**”, “**OD0(x)**”, “**AD(x,c)**”, and “**TAB**”) of the HRX database (e.g., change the installation cost or the effectiveness of a countermeasure at a highway-rail grade crossing, change the eligibility of a highway-rail grade crossing for a countermeasure, etc.) due to practical considerations, the changes must be made after execution of the “**FPI and Delay Estimation**” section (otherwise, the application will re-write the values inserted by the user and paste the default values from the “**Data_Description**” sheet after pressing the button “**Estimate FPI and Delay**”). Moreover, if the user does not want to execute the “**FPI and Delay Estimation**” section, the changes in the HRX database can be made before or after uploading the Excel file in the “**Common Inputs**” section (as the “**Common Inputs**” section just provides the path of the HRX database to the “**FPI and Delay Estimation**” section and the “**HRX Resource Allocation**” section). However, all modifications to the HRX database must be done before performing resource allocation among highway-rail grade crossings using the “**HRX Resource Allocation**” section of the standalone application “HRX Safety Improvement”.

Note: If the user would like to adopt the default values for all 11 countermeasures (i.e., default effectiveness factors and installation costs), as suggested by the GradeDec.Net Reference Manual (U.S. DOT, 2014a), throughout resource allocation among highway-rail grade crossings, no manual changes will be required in the HRX database. The standalone application “HRX Safety Improvement” will prepare the required data for the HRX database based on the options selected by the user on the application interface.

6.3.5. HRX Resource Allocation

The “**HRX Resource Allocation**” section of the standalone application “HRX Safety Improvement” allocates the available countermeasures to the considered highway-rail grade crossings. In the “**HRX Resource Allocation**” section, the first input data that the user should provide are the “**Index of Crossings**” and the “**Index of Countermeasures**” (see Figure 113). In particular, the indices of the selected highway-rail grade crossings and the chosen countermeasures should be inserted in the “**Index of Crossings**” textbox and the “**Index of Countermeasures**” textbox, respectively. Note that the index of highway-rail grade crossings

can be found in the outmost left column of the “**Output_FPI**” sheet or the “**Output_Delay**” sheet in the Excel file “**Tool_Output.xlsx**” (the heading of the column is named as “**FPI_ID**”).



Figure 113 Specifying the index of highway-rail grade crossings and the index of countermeasures.

Several alternatives have been provided for the user to insert the indices of highway-rail grade crossings and countermeasures. In particular, the user must use the characters defined below to specify the list of highway-rail grade crossings and countermeasures:

- Numbers: all the digits (i.e., 0, 1, 2, 3, 4, 5, 6, 7, 8, and 9) are allowed;
- Delimiters: two characters, including comma “,” and semicolon “;” are allowed to be used as delimiters; and
- Ranges: two characters, including hyphen “-” and colon “:” are allowed to define a range of highway-rail grade crossings and/or countermeasures.

Note that inserting any other character in the fields “**Index of Crossings**” and “**Index of Countermeasures**” will result in an error message generated by the application.

Table 32 Examples for inserting the index of highway-rail grade crossings.

Example	Index of Crossings	Insertion Alternative 1	Insertion Alternative 2	Insertion Alternative 3
1	1, 2, 3, 4, 5, 6, 7, 8	8	1-8	1,2,3,4,5,6,7,8
2	35, 36, 37, 38, 39, 40, 41	N/A	35-41	35,36,37,38,39,40, 41
3	8, 9, 10, 11, 12, 23, 24, 25, 26, 27	N/A	8-12,23-27	8,9,10,11,12,23,24,25, 26,27
4	8, 9, 10, 11, 12, 17, 19, 23, 24, 25, 26, 27	N/A	8-12,17,19,23-27	8,9,10,11,12,17,19,23, 24,25,26,27

Table 32 illustrates different alternatives that the user can select to insert the index of highway-rail grade crossings. In example 1, the first 8 consecutive highway-rail grade crossings are considered for upgrading, and the user can insert just the total number of highway-rail grade crossings to specify the index of crossings in the application (i.e., insertion alternative “1”). In example 2, the index of the first crossing, which is considered for upgrading, is not “1”. Hence, the user is not allowed to insert just the total number of highway-rail grade crossings in the application. The second insertion alternative (i.e., “35-41”) becomes the most convenient one for example 2. In example 3, there are two ranges of highway-rail grade crossing indices, where the first range comprises the highway-rail grade crossings ranked from 8th to 12th, while the second range includes the highway-rail grade crossings ranked from 23rd to 27th. As the two aforementioned ranges in example 3 are separate ranges, the user cannot insert the index of highway-rail grade crossings as “8-27”. Hence, the second insertion alternative (i.e., “8-12,23-27”) becomes the most convenient one for example 3. In example 4, there is a combination of ranges of highway-rail grade crossings and single highway-rail grade crossings, which are considered for upgrading. Therefore, the user cannot insert the index of highway-rail grade crossings as “8-27”. The second insertion alternative (i.e., “8-12,17,19,23-27”) can be considered as the most convenient one for example 4. The third insertion alternative is fairly straightforward, as the indices of highway-rail grade crossings are inserted one by one, and this alternative is applicable for all the examples. Note that the user is not required to insert the index of crossings in any specific order (e.g., ascending or descending). Furthermore, the user is not required to insert ranges or single highway-rail grade crossings in any order, as the application can handle all the possible insertion orders. Note that the user is not allowed to use any spacing between the characters inserted in the field of “**Index of Crossings**”. Furthermore, all the aforementioned instructions, which are applicable for the field of “**Index of Crossings**”, will be valid for the field of “**Index of Countermeasures**”.

The next input data, which the user should provide, is the “**Number of PF Points**” (see Figure 114). Note that the number of PF points inserted by the user should not be less than two. Otherwise, the standalone application will generate an error message. After successfully completing the previous steps, the user can execute the standalone application “HRX Safety Improvement” to perform resource allocation among the considered highway-rail grade crossings by pressing the “**HRX Resource Allocation**” button. Once the “**HRX Resource Allocation**” button is pressed, a progress bar which states “**Resource allocation is in process...**”, will pop up

(see Figure 115). The progress bar will disappear after a successful completion of the resource allocation process.



Figure 114 Specifying the number of PF points.

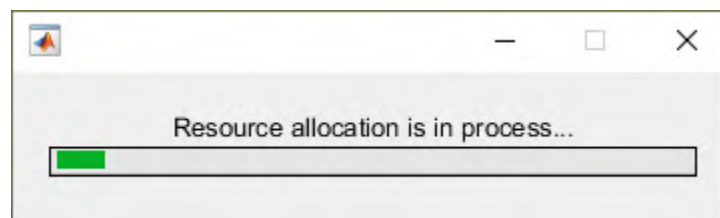


Figure 115 The progress bar of “**HRX Resource Allocation**”.

Note: There is a certain condition which can interrupt a successful execution of the standalone application “HRX Safety Improvement”. Specifically, the standalone application “HRX Safety Improvement” cannot delete or modify an open Excel file. If the user has already executed the “**HRX Resource Allocation**” section of the application successfully, opened some of the Excel files (e.g., “**Resource Allocation.xlsx**” or other Excel files), and tries to run the application

again, the application may not run successfully (i.e., “freeze”), even if the Excel files have been closed by the user (as the Windows Operating System may still have the Excel application invoked). In case if the standalone application “HRX Safety Improvement” gets frozen due to the Excel data exchange issues, the progress bar will not appear anymore after pressing the button “**Estimate FPI and Delay**” or the button “**HRX Resource Allocation**”. However, if the user closes the application and restarts it, the application will resume working normally again. Therefore, it is recommended for users to determine the analysis types they would like to conduct before executing the standalone application “HRX Safety Improvement”. Also, it is recommended for users to keep the Excel application closed, while performing certain procedures with the standalone application “HRX Safety Improvement”, to ensure that the standalone application “HRX Safety Improvement” works normally. In order to prevent the “freezing” issue, the latest version of the standalone application “HRX Safety Improvement” automatically closes open Excel files after pressing the button “**Estimate FPI and Delay**” or the button “**HRX Resource Allocation**”.

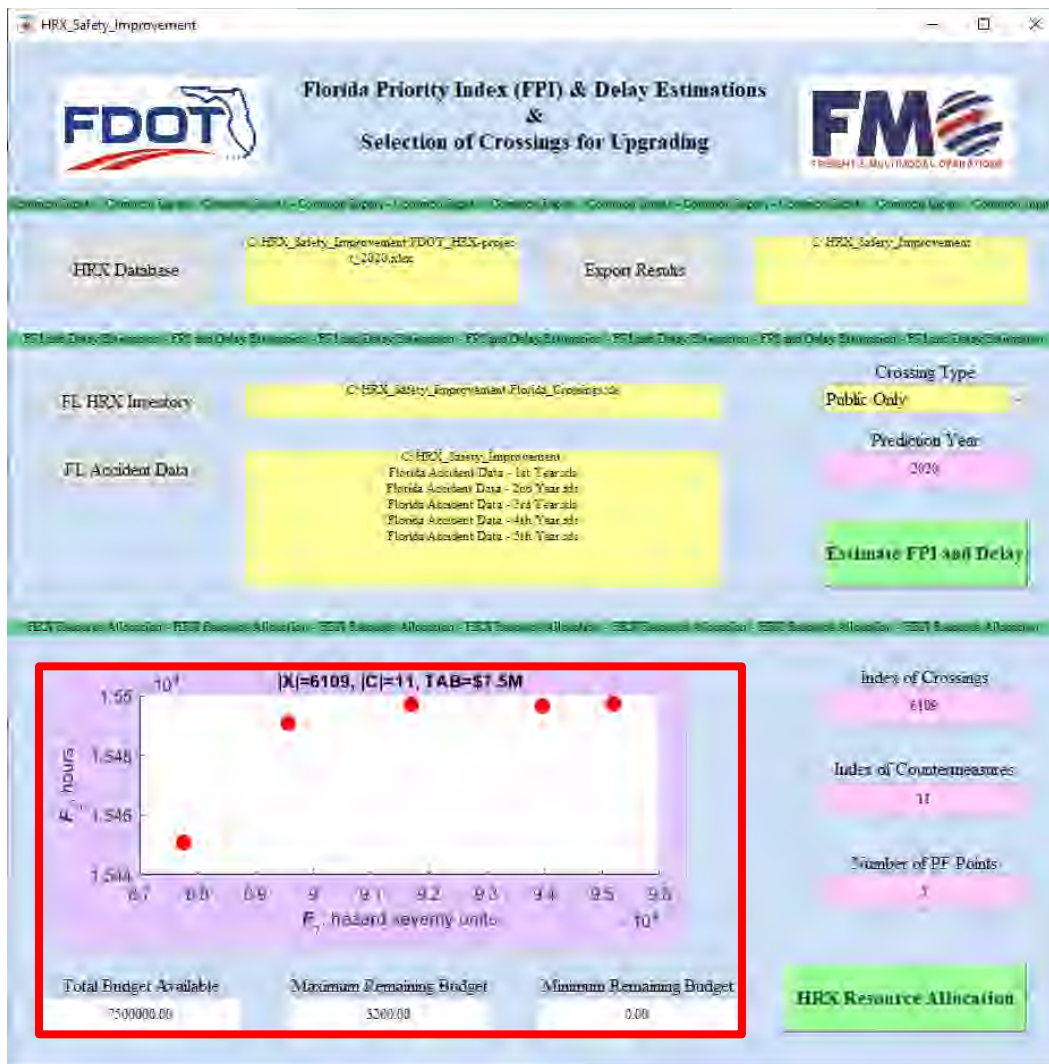


Figure 116 The results displayed on the user interface.

HRX Resource Allocation Outputs

Upon completing the resource allocation, the graph on the user interface will show the PF generated from multi-objective resource allocation (see Figure 116). The title of the graph highlights three parameters which are: (1) “**X**” – number of highway-rail grade crossings selected for resource allocation; (2) “**C**” – number of countermeasures chosen for resource allocation; and (3) “**TAB**” – total available budget. The graph has two axes. The horizontal axis is labeled “**F₁, hazard severity units**” and denotes the overall hazard severity at the considered highway-rail grade crossings. The vertical axis is labeled “**F₂, hours**” and represents the overall traffic delay caused by the selected countermeasures at the considered highway-rail grade crossings. In the presented example, the number of PF points is five. Hence, five red circles are plotted in the graph, and each of them represents a PF point (see Figure 116). In addition, there are three fields at the bottom of the user interface, which show the financial information related to resource allocation, including the following data: (1) “**Total Budget Available**”; (2) “**Maximum Remaining Budget**”; and (3) “**Minimum Remaining Budget**” (see Figure 116). Here, the “**Maximum Remaining Budget**” indicates the maximum value among the remaining budgets for the PF points. Similarly, the “**Minimum Remaining Budget**” indicates the minimum value among the remaining budgets for the PF points.

Moreover, the standalone application “HRX Safety Improvement” exports the resource allocation results to the previously specified location in the Excel format (i.e., XLSX). The Excel file is named as “**Resource Allocation.xlsx**”. The number of sheets in the “**Resource Allocation.xlsx**” file and their names are based on the number of PF points inserted by the user. Since there are five PF points in the presented example, the “**Resource Allocation.xlsx**” file includes a total of five sheets, named as “**PF Point #1**”, “**PF Point #2**”, “**PF Point #3**”, “**PF Point #4**”, and “**PF Point #5**”. These sheets display a summary of the results along with the detailed results for the respective PF points (see Figure 117, Figure 118, Figure 119, Figure 120, and Figure 121). In each of these sheets, a summary of the resource allocation results for the respective PF point is presented in the first five rows, including the PF point number, overall hazard severity, overall traffic delay, total budget available, and total remaining budget. After the first five rows, specifically from the eighth row, the detailed resource allocation results for the respective PF point are shown. In particular, the following information is provided:

- Crossing – rank/index of a highway-rail grade crossing;
- Countermeasure – index of the countermeasure assigned to a highway-rail grade crossing;
- Effectiveness Factor – effectiveness factor of the assigned countermeasure;
- Cost – cost to implement a given countermeasure at a highway-rail grade crossing (USD);
- Fatality Hazard Before – fatality hazard of a highway-rail grade crossing before implementing a given countermeasure;
- Fatality Hazard After – fatality hazard of a highway-rail grade crossing after implementing a given countermeasure;
- Injury Hazard Before – injury hazard of a highway-rail grade crossing before implementing a given countermeasure;
- Injury Hazard After – injury hazard of a highway-rail grade crossing after implementing a given countermeasure;

- Property Damage Hazard Before – property damage hazard of a highway-rail grade crossing before implementing a given countermeasure;
- Property Damage Hazard After – property damage hazard of a highway-rail grade crossing after implementing a given countermeasure;
- Overall Delay Before – overall delay at a highway-rail grade crossing with the existing warning devices per day (hours);
- Additional Delay – additional delay due to application of a given countermeasure at a highway-rail grade crossing (hours); and
- Overall Delay After – overall delay at a highway-rail grade crossing per day after implementation of a given countermeasure (hours).

Counter	Effectiveness	Cost	Fatality H	Fatality H	Injury Haz	Injury Haz	Property (Property (Overall D	Additional	Overall Delay	After
1	0.82	5000	16167.24	2910.103	29101.84	5238.331	76734.38	13812.19	89.34822	6.545351	95.89358	
2	0.82	5000	15855.68	2854.022	28605.03	5148.905	70364.12	13565.54	87.75272	6.42847	94.18119	
3	0.82	5000	9667.093	1740.077	17562.48	3161.246	-46156.1	8308.098	74.3744	5.752826	80.12722	
4	0.82	5000	7527.733	1354.992	13580.69	2444.524	35780.31	6440.456	99.42077	5.762499	105.1833	
5	0.82	5000	7144.967	1286.094	12890.15	2320.226	33960.97	6112.975	87.75272	6.42847	94.18119	

Figure 117 The “PF Point #1” sheet of the “Resource Allocation.xlsx” file.

Counter	Effectiveness	Cost	Fatality H	Fatality H	Injury Haz	Injury Haz	Property (Property (Overall D	Additional	Overall Delay	After
1	0.82	5000	16167.24	2910.103	29101.84	5238.331	76734.38	13812.19	89.34822	6.545351	95.89358	
2	0.82	5000	15855.68	2854.022	28605.03	5148.905	70364.12	13565.54	87.75272	6.42847	94.18119	
3	0.82	5000	9667.093	1740.077	17562.48	3161.246	-46156.1	8308.098	74.3744	5.752826	80.12722	
5	0.82	5000	7144.967	1286.094	12890.15	2320.226	33960.97	6112.975	87.75272	6.42847	94.18119	
4	0.82	5000	7527.733	1354.992	13580.69	2444.524	35780.31	6440.456	99.42077	5.762499	105.1833	

Figure 118 The “PF Point #2” sheet of the “Resource Allocation.xlsx” file.

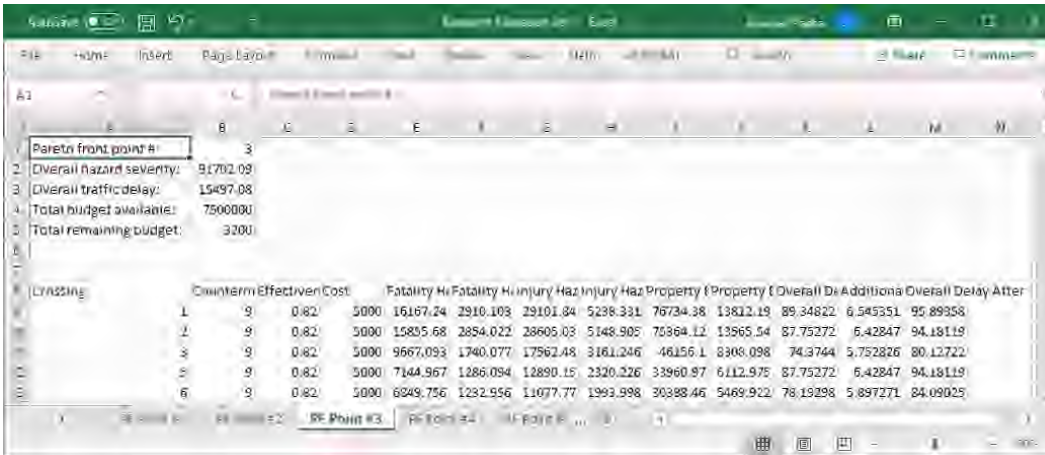


Figure 119 The “PF Point #3” sheet of the “Resource Allocation.xlsx” file.

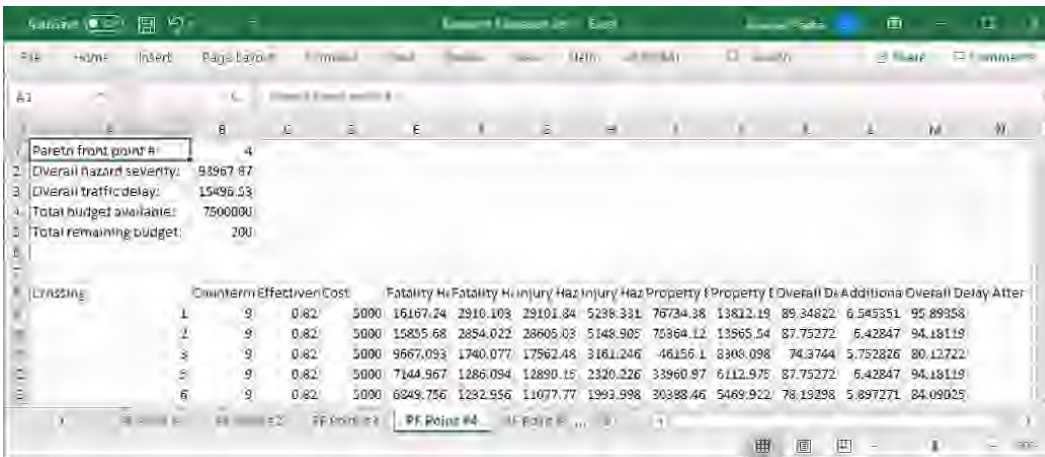


Figure 120 The “PF Point #4” sheet of the “Resource Allocation.xlsx” file.

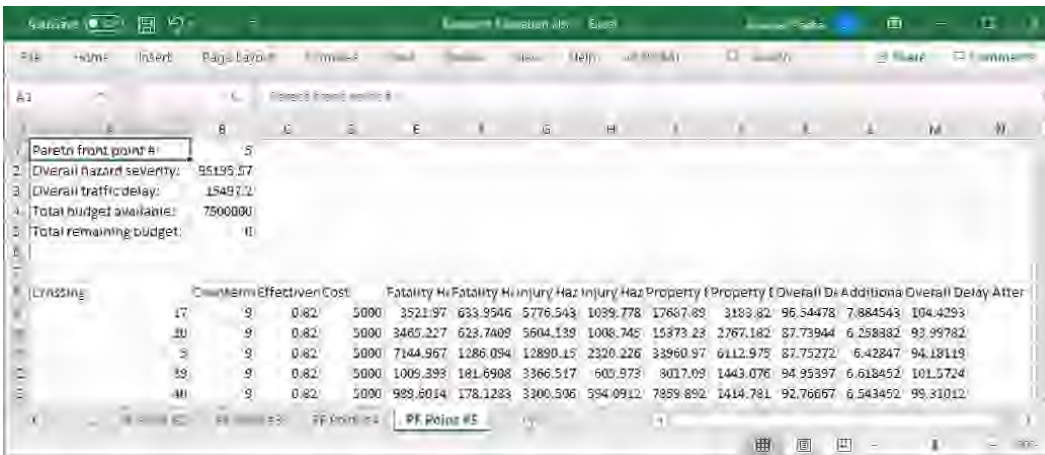
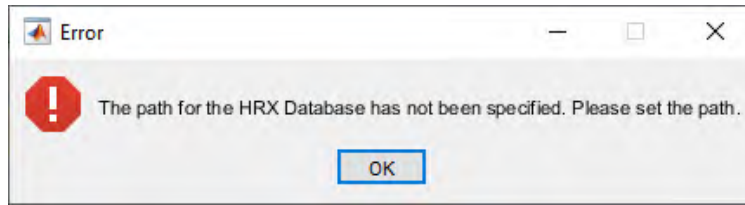


Figure 121 The “PF Point #5” sheet of the “Resource Allocation.xlsx” file.

6.3.6. Error Messages

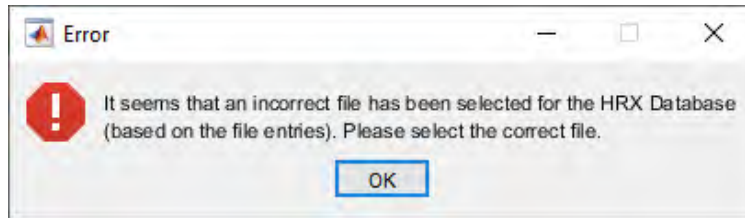
The following error messages may appear while executing the standalone application “HRX Safety Improvement”:

- (a) In case if the user has not specified the path for the HRX Database, the standalone application “HRX Safety Improvement” will return the following error message (see figure below): “The path for the HRX Database has not been specified. Please set the path.”



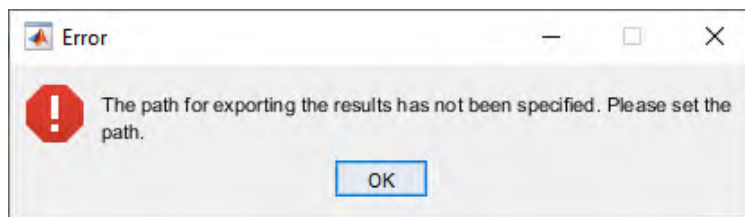
(a) The path for the HRX Database has not been specified.

- (b) In case if the user has selected an incorrect file for the HRX Database (based on the file entries), the standalone application “HRX Safety Improvement” will return the following error message (see figure below): “It seems that an incorrect file has been selected for the HRX Database (based on the file entries). Please select the correct file.”



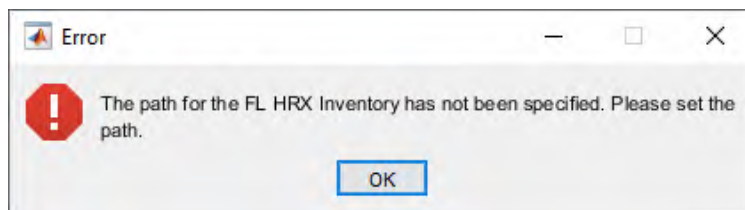
(b) An incorrect file has been selected for the HRX Database.

- (c) In case if the user has not specified the path for exporting the results, the standalone application “HRX Safety Improvement” will return the following error message (see figure below): “The path for exporting the results has not been specified. Please set the path.”



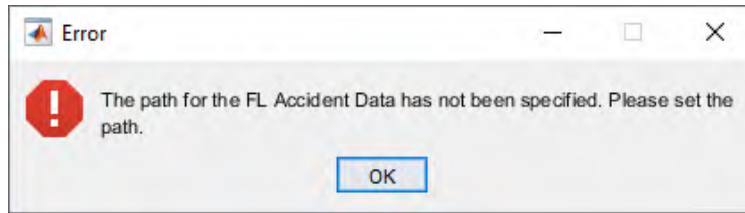
(c) The path for exporting the results has not been specified.

- (d) In case if the user has not specified the path for the FL HRX Inventory, the standalone application “HRX Safety Improvement” will return the following error message (see figure below): “The path for the FL HRX Inventory has not been specified. Please set the path.”



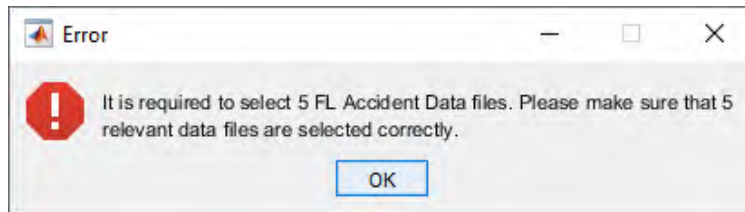
(d) The path for the crossing inventory data has not been specified.

- (e) In case if the user has not specified the path for the FL Accident Data, the standalone application “HRX Safety Improvement” will return the following error message (see figure below): “The path for the FL Accident Data has not been specified. Please set the path.”



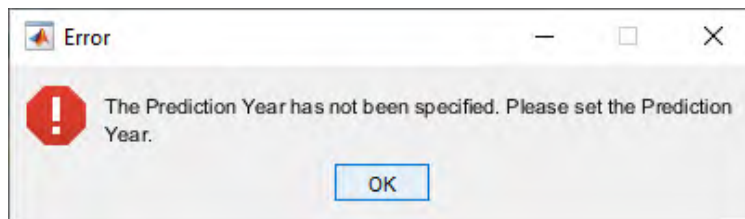
(e) The path for the accident data has not been specified.

- (f) In case if the user has not selected the 5 FL Accident Data files (i.e., the accident data for 5 years before the prediction year), the standalone application “HRX Safety Improvement” will return the following error message (see figure below): “It is required to select 5 FL Accident Data files. Please make sure that 5 relevant data files are selected correctly.”



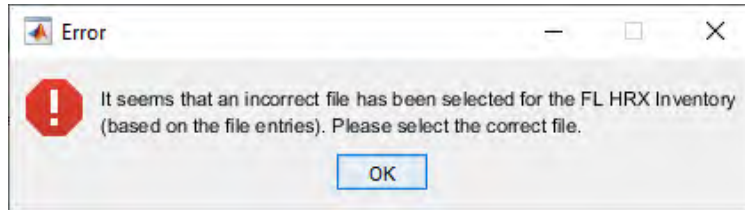
(f) The 5 accident data files have not been selected.

- (g) In case if the user has not specified the prediction year, the standalone application “HRX Safety Improvement” will return the following error message (see figure below): “The Prediction Year has not been specified. Please set the Prediction Year.”



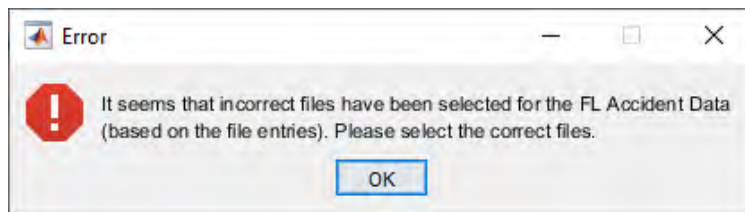
(g) The prediction year has not been specified.

- (h) In case if the user has selected an incorrect file for the FL HRX Inventory (based on the file entries), the standalone application “HRX Safety Improvement” will return the following error message (see figure below): “It seems that an incorrect file has been selected for the FL HRX Inventory (based on the file entries). Please select the correct file.”



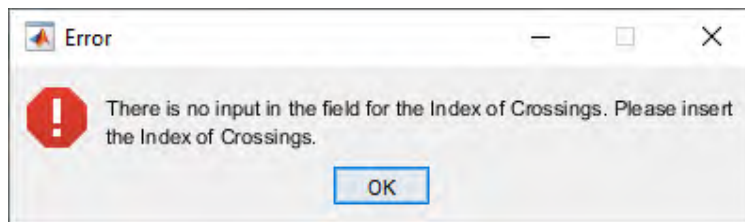
(h) Incorrect file has been selected for the crossing inventory data.

- (i) In case if the user has selected incorrect files for the FL Accident Data (based on the file entries), the standalone application “HRX Safety Improvement” will return the following error message (see figure below): “It seems that incorrect files have been selected for the FL Accident Data (based on the file entries). Please select the correct files.”



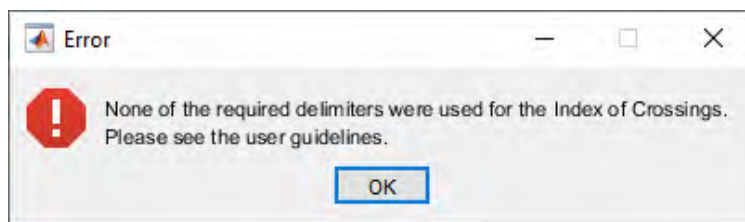
(i) Incorrect files have been selected for the accident data.

- (j) In case if the user has not inserted the Index of Crossings, the standalone application “HRX Safety Improvement” will return the following error message (see figure below): “There is no input in the field for the Index of Crossings. Please insert the Index of Crossings.”



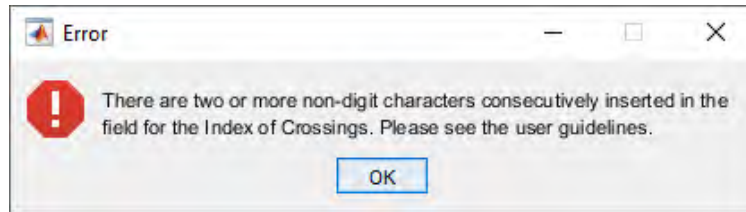
(j) The Index of Crossings has not been specified.

- (k) In case if none of the required delimiters (see section 6.3.5) have been inserted by the user in the field for the Index of Crossings, the standalone application “HRX Safety Improvement” will return the following error message (see figure below): “None of the required delimiters were used for the Index of Crossings. Please see the user guidelines.”



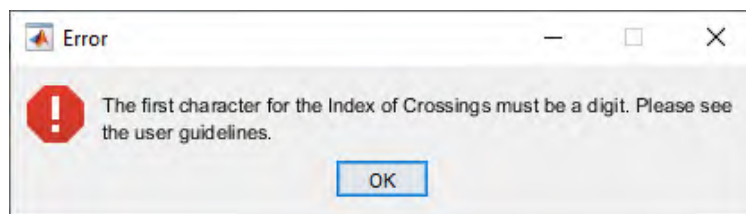
(k) None of the required delimiters have been inserted by the user for the Index of Crossings.

- (l) In case if the user has inserted two or more allowed non-digit characters (i.e., comma, semicolon, hyphen, and colon) in the field for the Index of Crossings consecutively, the standalone application “HRX Safety Improvement” will return the following error message (see figure below): “There are two or more non-digit characters consecutively inserted in the field for the Index of Crossings. Please see the user guidelines.”



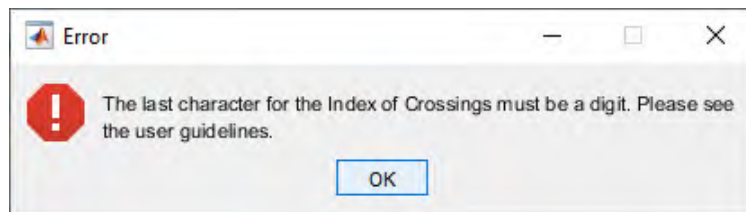
- (l) Two or more allowed non-digit characters have been consecutively inserted in the field for the Index of Crossings.

- (m) In case if the user has inserted a wrong character as the first character in the field for the Index of Crossings, which is not among the allowed characters (see section 6.3.5), the standalone application “HRX Safety Improvement” will return the following error message (see figure below): “The first character for the Index of Crossings must be a digit. Please see the user guidelines.”



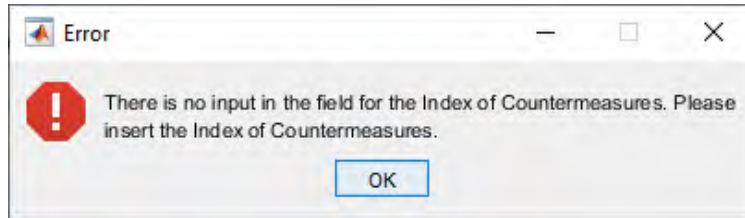
- (m) A wrong character has been inserted by the user for the first character of Index of Crossings.

- (n) In case if the user has inserted a wrong character as the last character in the field for the Index of Crossings, which is not among the allowed characters (see section 6.3.5), the standalone application “HRX Safety Improvement” will return the following error message (see figure below): “The last character for the Index of Crossings must be a digit. Please see the user guidelines.”



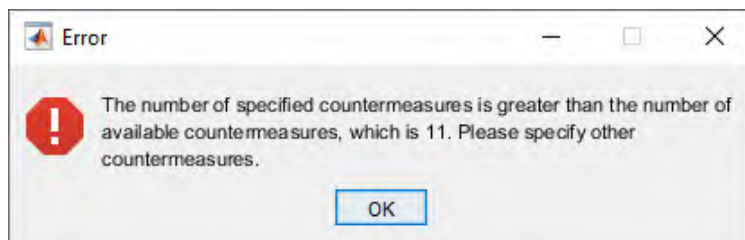
- (n) A wrong character has been inserted by the user for the last character of Index of Crossings.

- (o) In case if the user has not inserted the Index of Countermeasures, the standalone application “HRX Safety Improvement” will return the following error message (see figure below): “There is no input in the field for the Index of Countermeasures. Please insert the Index of Countermeasures.”



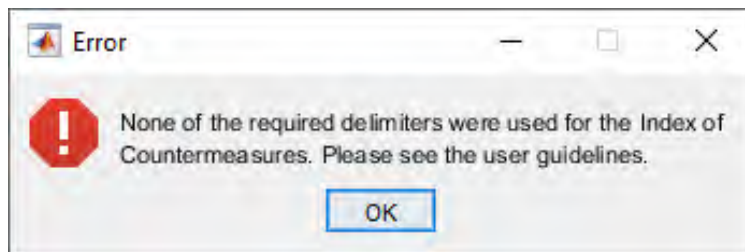
- (o) The Index of Countermeasures has not been specified.

- (p) In case if the user has specified the number of countermeasures, which is greater than the number of countermeasures available in the HRX Database, the standalone application “HRX Safety Improvement” will return the following error message (see figure below): “The number of specified countermeasures is greater than the number of available countermeasures, which is (11). Please specify other countermeasures.”



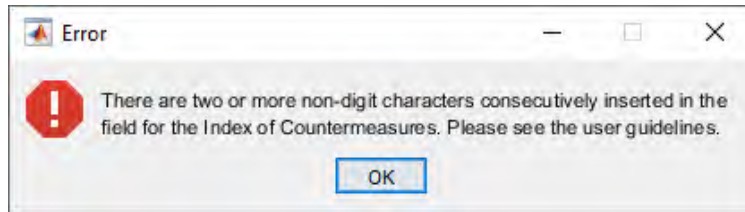
- (p) The number of specified countermeasures is greater than the number of available countermeasures.

- (q) In case if none of the required delimiters (see section 6.3.5) have been inserted by the user in the field for the Index of Countermeasures, the standalone application “HRX Safety Improvement” will return the following error message (see figure below): “None of the required delimiters were used for the Index of Countermeasures. Please see the user guidelines.”

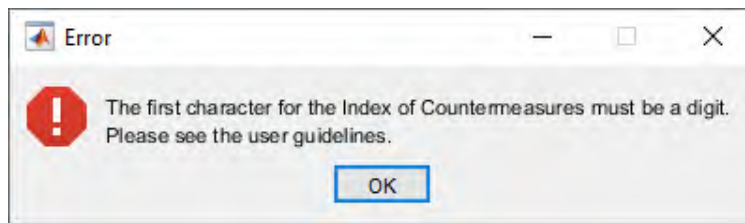


- (q) None of the required delimiters have been inserted by the user for the Index of Countermeasures.

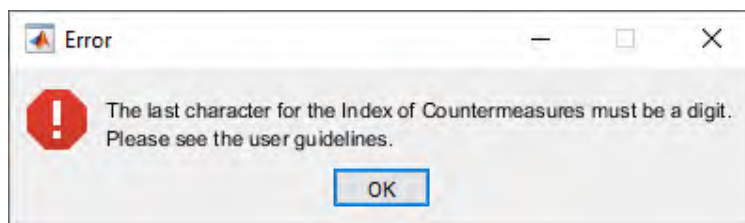
- (r) In case if the user has inserted two or more allowed non-digit characters (i.e., comma, semicolon, hyphen, and colon) in the field for the Index of Countermeasures consecutively, the standalone application “HRX Safety Improvement” will return the following error message (see figure below): “There are two or more non-digit characters consecutively inserted in the field for the Index of Countermeasures. Please see the user guidelines.”



- (r) Two or more allowed non-digit characters have been consecutively inserted in the field for the Index of Countermeasures.
- (s) In case if the user has inserted a wrong character as the first character in the field for the Index of Countermeasures, which is not among the allowed characters (see section 6.3.5), the standalone application “HRX Safety Improvement” will return the following error message (see figure below): “The first character for the Index of Countermeasures must be a digit. Please see the user guidelines.”

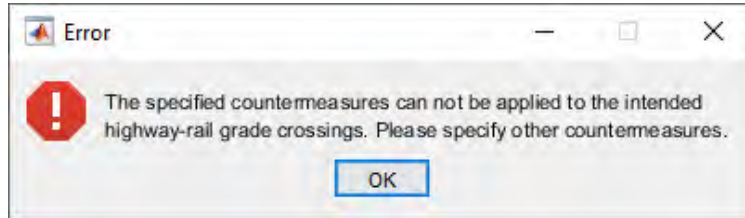


- (s) A wrong character has been inserted by the user for the first character of Index of Countermeasures.
- (t) In case if the user has inserted a wrong character as the last character in the field for the Index of Countermeasures, which is not among the allowed characters (see section 6.3.5), the standalone application “HRX Safety Improvement” will return the following error message (see figure below): “The last character for the Index of Countermeasures must be a digit. Please see the user guidelines.”



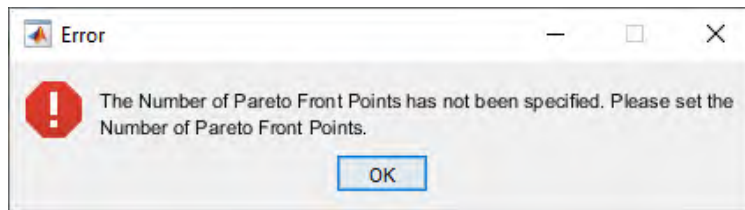
- (t) A wrong character has been inserted by the user for the last character of Index of Countermeasures.

- (u) In case if none of the specified countermeasures can be applied to the intended highway-rail grade crossings (due to certain physical and/or operational characteristics of the highway-rail grade crossings), the standalone application “HRX Safety Improvement” will return the following error message (see figure below): “The specified countermeasures cannot be applied to the intended highway-rail grade crossings. Please specify other countermeasures.”



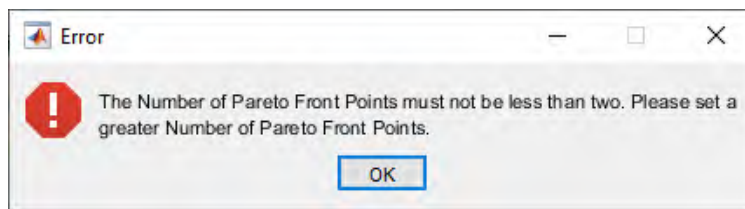
- (u) None of the specified countermeasures can be applied to the intended highway-rail grade crossings.

- (v) In case if the user has not specified the number of PF points, the standalone application “HRX Safety Improvement” will return the following error message (see figure below): “The Number of Pareto Front Points has not been specified. Please set the Number of Pareto Front Points.”



- (v) The number of PF points has not been specified.

- (w) In case if the user has specified the number of PF points, which is less than two, the standalone application “HRX Safety Improvement” will return the following error message (see figure below): “The Number of Pareto Front Points must not be less than two. Please set a greater Number of Pareto Front Points.”



- (w) The number PF points is less than two.

7. METHODOLOGY APPLICATION

A set of computational experiments was performed to illustrate applicability of the proposed methodology for conducting multi-objective resource allocation in order to minimize the overall hazard severity and to minimize the overall traffic delay at the existing highway-rail grade crossings in Florida. A comprehensive description of the computational experiments is presented in this section of the report. Specifically, this section presents the following analyses: (1) sensitivity analysis for the total available budget; (2) sensitivity analysis for the number of available countermeasures; (3) sensitivity analysis for the hazard severity weight values; (4) resource allocation among various crossing types; and (5) evaluation of an alternative countermeasure (i.e., light-emitting diode [LED] signs). Throughout all of these analyses, the **MORAP** mathematical model was solved with the MPSDR heuristic.

7.1. Sensitivity Analysis for the Total Available Budget

The impact of the total available budget on multi-objective resource allocation among the highway-rail grade crossings in Florida is investigated in this section. In particular, a total of 12 budget availability scenarios was developed, where the total available budget was increased from \$4.5M in scenario 1 to \$10.0M in scenario 12, with an increment of \$0.5M. This analysis investigated all the 6,109 public highway-rail grade crossings in Florida, which were found in the Federal Railroad Administration (FRA) crossing inventory database (FRA, 2016). Furthermore, a total of 11 countermeasures, which was adopted earlier in this project based on the GradeDec.NET Reference Manual (U.S. DOT, 2014a), were considered for implementation at the highway-rail grade crossings. Specifically, two cases of countermeasure availabilities were used for the budget availability scenarios, including the considerations of the first 6 countermeasures, which are comparatively more expensive, and all 11 countermeasures for further insights.

7.1.1. The Impact of the Total Available Budget on the MORAP Objective Functions

This project is associated with multi-objective optimization (i.e., multi-objective resource allocation). As such, a set of non-dominated solutions (i.e., a Pareto Front – PF) was generated instead of a single solution for each resource allocation decision. The number of PF points was set to 5. The PFs were plotted on a 2-D plane, where the horizontal axis and the vertical axis represent the overall hazard severity (denoted by F_1) and the overall traffic delay (denoted by F_2), respectively, at the considered highway-rail grade crossings. Figure 122 presents the PFs generated for the considered budget availability scenarios, when the first 6 countermeasures could be used for upgrading. Note that all the PFs in Figure 122 have the same limits for the horizontal and vertical axes, so that their movements can be observed with ease. It can be observed that the PFs moved from the lower-right corner in the plots to the upper-left corner, when the total available budget was increased. The PF in scenario 1 is at the lower-most-right corner, which denotes the highest overall hazard severity and the lowest overall traffic delay among the considered scenarios. On the other hand, the PF in scenario 12 is at the upper-most-left corner, which denotes the lowest overall hazard severity and the highest overall traffic delay among the considered scenarios. All these findings can be supported by the fact that when the total available budget was increased, more highway-rail grade crossings were upgraded with countermeasures. So, the overall hazard severity decreased. However, the overall traffic delay increased at the same time due to the installation of countermeasures.

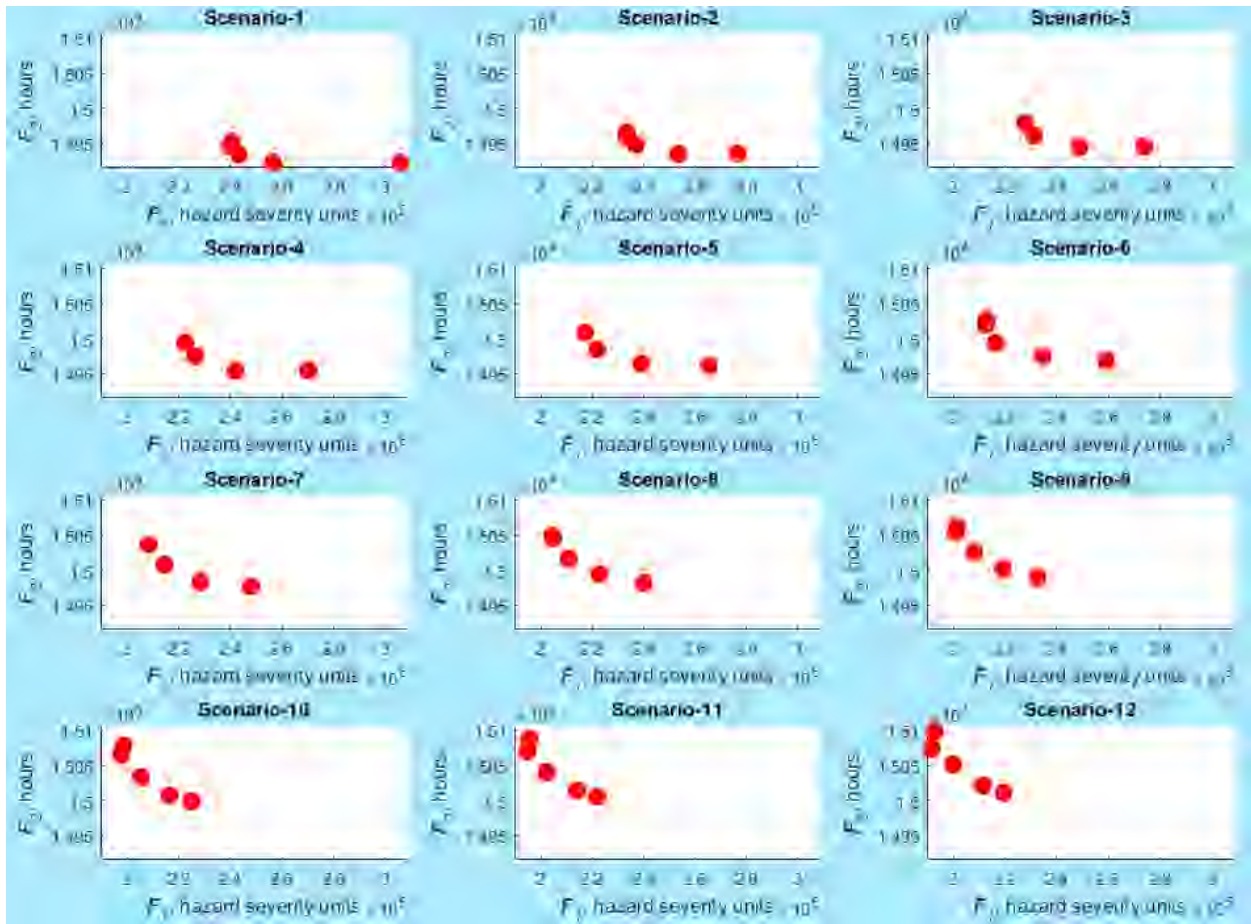


Figure 122 The PFs generated for each budget availability scenario (the first 6 countermeasures are available for upgrading).

Figure 123 presents the PFs generated for the considered budget availability scenarios, when all 11 countermeasures could be used for upgrading. Note that all the PFs in Figure 123 have the same limits for the horizontal and vertical axes, so that their movements can be observed with ease. It can be observed that the PFs moved from the lower-right corner in the plots to the upper-left corner, when the total available budget was increased. The PF in scenario 1 is at the lower-most-right corner, which denotes the highest overall hazard severity and the lowest overall traffic delay among the considered scenarios. On the other hand, the PF in scenario 12 is at the upper-most-left corner, which denotes the lowest overall hazard severity and the highest overall traffic delay among the considered scenarios. All these findings can be supported by the fact that when the total available budget was increased, more highway-rail grade crossings were upgraded with countermeasures. So, the overall hazard severity decreased. However, the overall traffic delay increased at the same time due to the installation of countermeasures. Moreover, the shapes of the PFs in Figure 123 are different from the ones presented in Figure 122. Such a pattern can be explained by the fact that the MPSDR heuristic started selecting countermeasures that are effective in terms of reducing both the overall hazard severity and the overall traffic delay after the introduction of low-cost countermeasures (i.e., countermeasures “7”, “8”, “9”, and “10”). Therefore, the PFs produced by the MPSDR heuristic for the scenarios with low-cost

countermeasures generally do not show a conflicting nature of the overall hazard severity minimization objective and the overall traffic delay minimization objective.

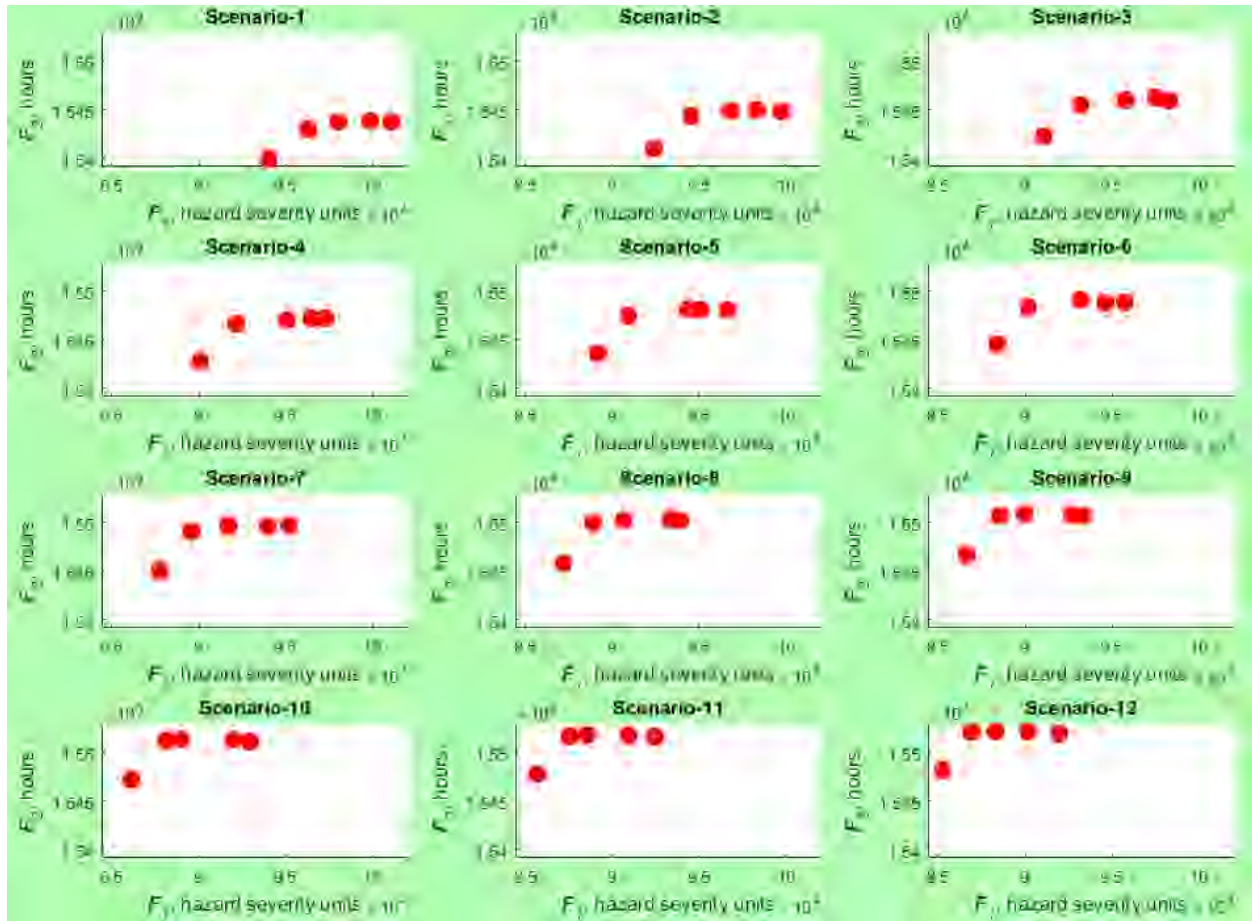


Figure 123 The PFs generated for each budget availability scenario (all 11 countermeasures are available for upgrading).

Figure 124 shows the average overall hazard severity over all the PF points for all the public highway-rail grade crossings for each one of the considered budget availability scenarios, when the first 6 countermeasures could be used for upgrading. On the other hand, Figure 125 shows the average overall hazard severity over all the PF points for all the public highway-rail grade crossings for each one of the considered budget availability scenarios, when all 11 countermeasures could be used for upgrading. Similar to the overall hazard severity for each of the PF points, the average overall hazard severity over all the PF points decreased with the availability of higher budgets. The latter pattern can be explained by the fact that the total number of highway-rail grade crossings, which were selected for upgrading by the **MORAP** mathematical model, increased with the total available budget and led to a reduction in the average overall hazard severity. The change in the average overall hazard severity in Figure 124 and Figure 125 is not perfectly linear, which can be supported by the complexity of multi-objective resource allocation based on the **MORAP** mathematical model, since many different factors are considered throughout the highway-rail grade crossing upgrading decisions (e.g., eligibility of a highway-rail grade crossing for the considered countermeasures, different

installation costs for the considered countermeasures, different effectiveness factors for the considered countermeasures, hazard severity and traffic delay at a highway-rail grade crossing).

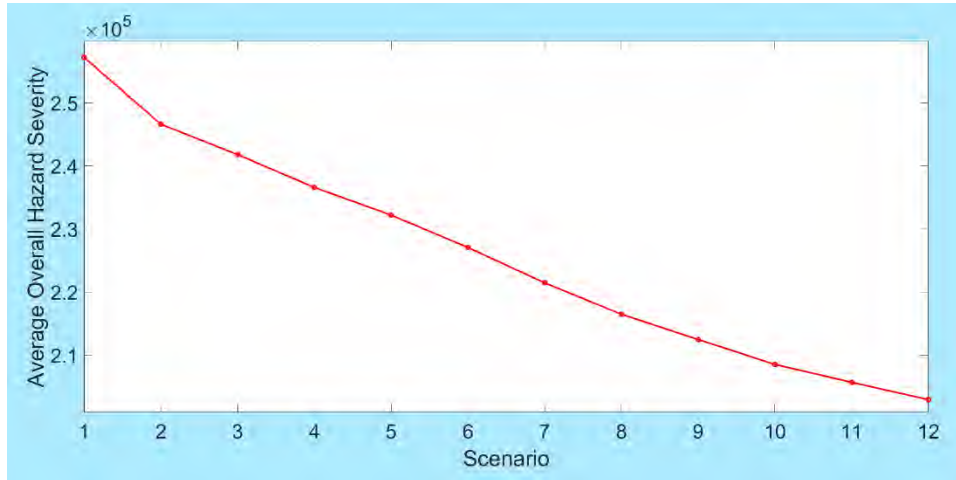


Figure 124 The average overall hazard severity over all the PF points for each budget availability scenario (the first 6 countermeasures are available for upgrading).

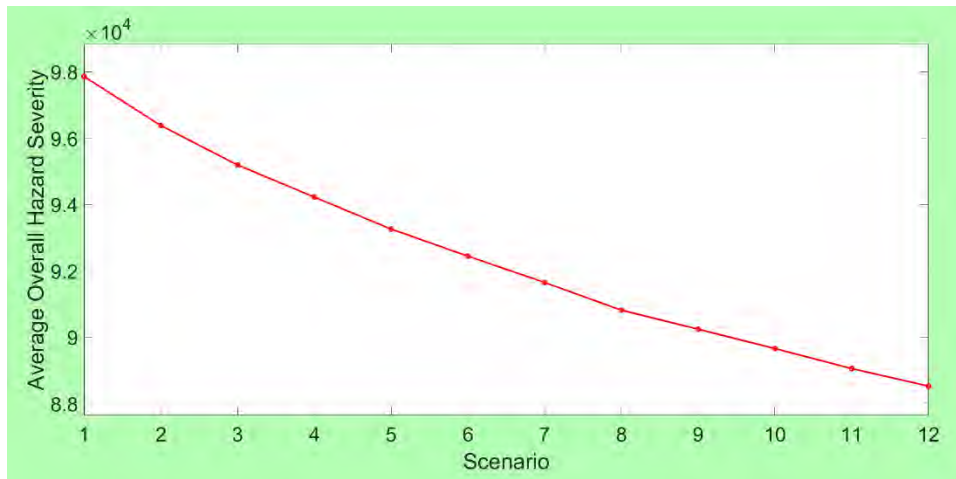


Figure 125 The average overall hazard severity over all the PF points for each budget availability scenario (all 11 countermeasures are available for upgrading).

Figure 126 illustrates the average overall traffic delay over all the PF points for all the public highway-rail grade crossings for each one of the considered budget availability scenarios, when the first 6 countermeasures could be used for upgrading. On the other hand, Figure 127 illustrates the average overall traffic delay over all the PF points for all the public highway-rail grade crossings for each one of the considered budget availability scenarios, when all 11 countermeasures could be used for upgrading. Similar to the overall traffic delay for each of the PF points, the average overall traffic delay over all the PF points increased with the availability of higher budgets. The latter pattern can be explained by the fact that the total number of highway-rail grade crossings, which were selected for upgrading by the **MORAP** mathematical model, increased with the total available budget and led to an increase in the average overall traffic delay.

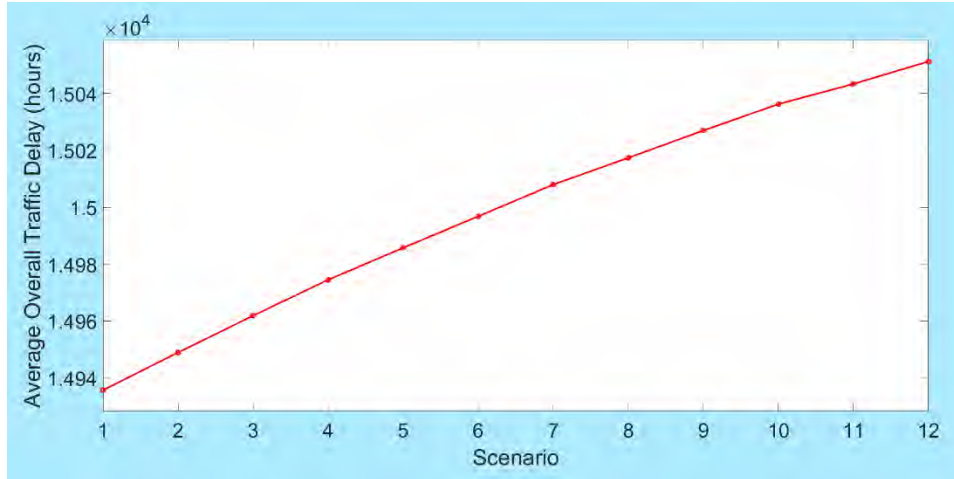


Figure 126 The average overall traffic delay over all the PF points for each budget availability scenario (the first 6 countermeasures are available for upgrading).

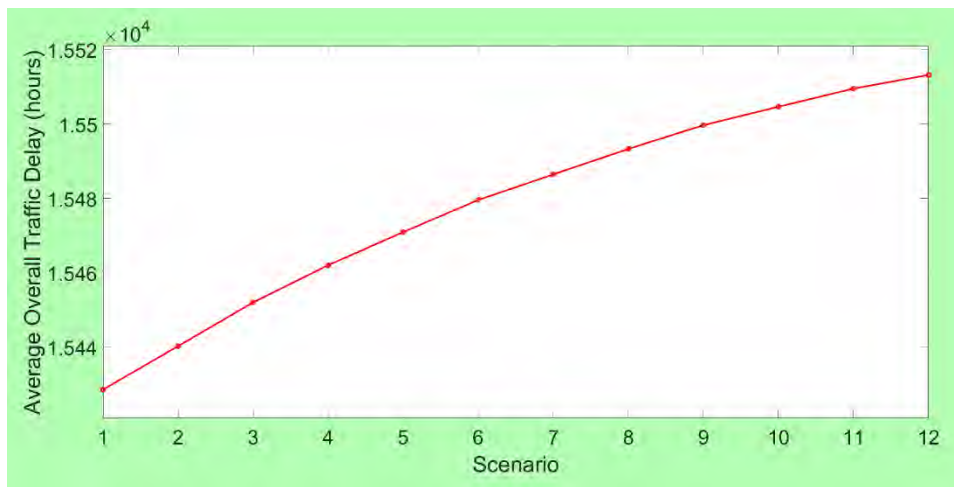


Figure 127 The average overall traffic delay over all the PF points for each budget availability scenario (all 11 countermeasures are available for upgrading).

7.1.2. The Impact of the Total Available Budget on the Number of Highway-Rail Grade Crossings Upgraded by MORAP

Figure 128 demonstrates the average total number of highway-rail grade crossings selected for upgrading over all the PF points for all the public highway-rail grade crossings for each one of the considered budget availability scenarios, when the first 6 countermeasures could be used for upgrading. As discussed earlier, the total number of upgraded highway-rail grade crossings increased with the total available budget for each one of the PF points. Similarly, the average total number of highway-rail grade crossings selected for upgrading over all the PF points increased as well. For example, the average total number of highway-rail grade crossings selected for upgrading out of the 6,109 public highway-rail grade crossings in Florida increased from 18.6 in scenario 1 to 41.8 in scenario 12. The small number of upgraded highway-rail grade crossings in case of Figure 128 is because of the high installation cost of countermeasures “1” to “6”, which were made available in this case. Moreover, the State of Florida has a number of gated highway-rail grade crossings, which are not eligible for countermeasures “1”, “2”, and “3”.

Hence, the selected gated highway-rail grade crossings were upgraded with countermeasures “4”, “5”, or “6” that are even more expensive than countermeasures “1”, “2”, and “3”. The change in the average total number of upgraded highway-rail grade crossings is not perfectly linear, which demonstrates the complexity of multi-objective resource allocation based on the **MORAP** mathematical model, since many different factors are considered throughout the highway-rail grade crossing upgrading decisions (e.g., eligibility of a highway-rail grade crossing for the considered countermeasures, different installation costs for the considered countermeasures, different effectiveness factors for the considered countermeasures, hazard severity and traffic delay at a highway-rail grade crossing).

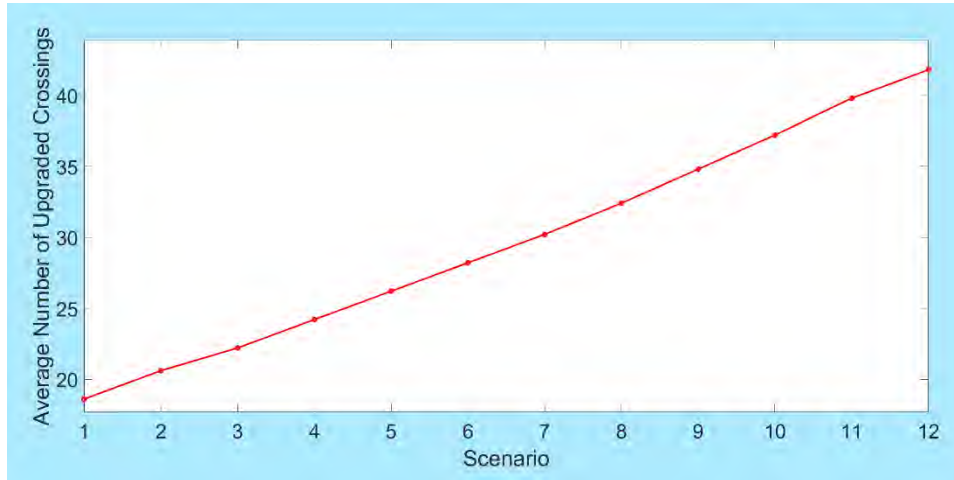


Figure 128 The average total number of highway-rail grade crossings selected for upgrading over all the PF points for each budget availability scenario (the first 6 countermeasures are available for upgrading).

Figure 129 demonstrates the average total number of highway-rail grade crossings selected for upgrading over all the PF points for all the public highway-rail grade crossings for each one of the considered budget availability scenarios, when all 11 countermeasures could be used for upgrading. As discussed earlier, the total number of upgraded highway-rail grade crossings increased with the total available budget for each one of the PF points. Similarly, the average total number of highway-rail grade crossings selected for upgrading over all the PF points increased as well. For example, the average total number of highway-rail grade crossings selected for upgrading out of the 6,109 public highway-rail grade crossings in Florida increased from 866.8 in scenario 1 to 1,780.4 in scenario 12. The number of upgraded highway-rail grade crossings in case of Figure 129 is substantially higher than that of Figure 128 due to the availability of more and cheaper countermeasures. The change in the average total number of upgraded highway-rail grade crossings is not perfectly linear, which demonstrates the complexity of multi-objective resource allocation based on the **MORAP** mathematical model, since many different factors are considered throughout the highway-rail grade crossing upgrading decisions (e.g., eligibility of a highway-rail grade crossing for the considered countermeasures, different installation costs for the considered countermeasures, different effectiveness factors for the considered countermeasures, hazard severity and traffic delay at a highway-rail grade crossing).

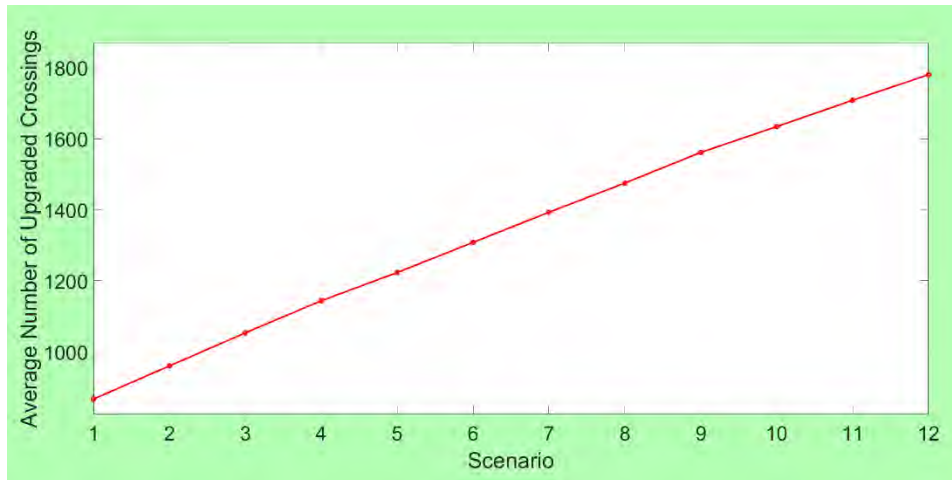


Figure 129 The average total number of highway-rail grade crossings selected for upgrading over all the PF points for each budget availability scenario (all 11 countermeasures are available for upgrading).

7.1.3. The Impact of the Total Available Budget on the Average Installation Cost and the Average Effectiveness of Countermeasures Selected by MORAP

Figure 130 shows the average installation cost of countermeasures implemented at highway-rail grade crossings selected for upgrading over all the PF points for all the public highway-rail grade crossings for each one of the considered budget availability scenarios, when the first 6 countermeasures could be used for upgrading. It can be observed that the average installation cost of countermeasures was fairly high (between \$237,881 and \$247,526), when only the first 6 countermeasures were considered for installation. The reason for such a high average cost is that the installation costs of countermeasures “1” to “6”, which were made available in this case, are between \$74,800 and \$260,000. Moreover, the State of Florida has a number of gated highway-rail grade crossings, which are not eligible for countermeasures “1”, “2”, and “3”. Hence, the selected gated highway-rail grade crossings were upgraded with countermeasures “4”, “5”, or “6” that are even more expensive than countermeasures “1”, “2”, and “3”. It can be seen that an increase in the total available budget allowed the **MORAP** mathematical model to select the countermeasures with higher installation costs for budget availability scenarios 1 to 7 as well as 12. However, there was a reduction in the average installation cost of countermeasures for budget availability scenarios 8 to 11. The latter pattern can be explained by the fact that the MPSDR heuristic, which was used to solve the **MORAP** mathematical model, creates a priority list of highway-rail grade crossing-countermeasure pairs based on the weighted sum of normalized hazard severity reduction and normalized traffic delay reduction to cost ratios. For budget availability scenarios 1 to 7, most of the selected highway-rail grade crossings, which were at the higher ranks of the aforementioned priority list, were not eligible for countermeasures “1”, “2”, and “3” that are comparatively less expensive than countermeasures “4”, “5”, and “6”. However, with an increase in the total available budget, especially for budget availability scenarios 8 to 11, more highway-rail grade crossings could be upgraded, and some of the selected highway-rail grade crossings, which were at the higher ranks of the aforementioned priority list, were eligible for countermeasures “1”, “2”, and “3”. Hence, a reduction in the average installation cost of countermeasures was noted.

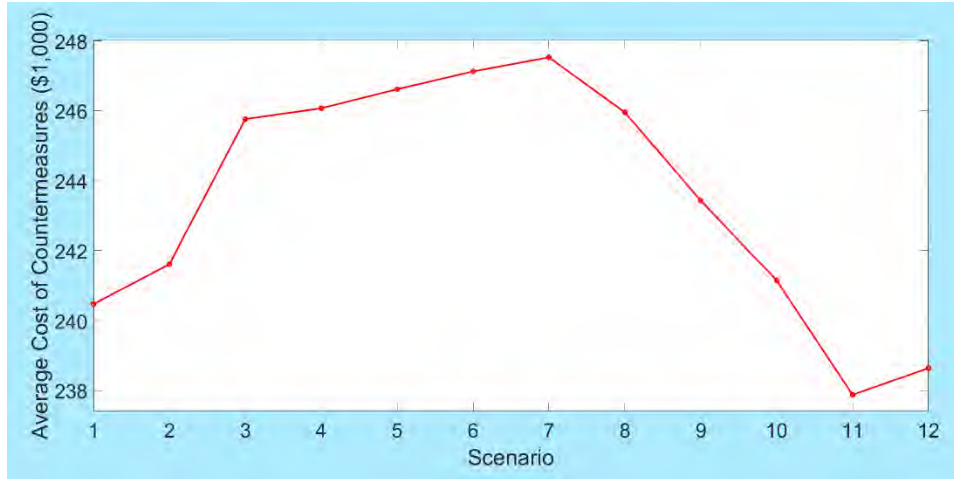


Figure 130 The average installation cost of countermeasures implemented at highway-rail grade crossings selected for upgrading over all the PF points for each budget availability scenario (the first 6 countermeasures are available for upgrading).

Figure 131 presents the average effectiveness of countermeasures implemented at highway-rail grade crossings selected for upgrading over all the PF points for all the public highway-rail grade crossings for each one of the considered budget availability scenarios, when the first 6 countermeasures could be used for upgrading. As evidenced by Figure 131, after increasing the total available budget from one scenario to another, the MPSDR heuristic still selected the countermeasures with fairly high effectiveness. The average effectiveness of the selected countermeasures varied between ≈ 0.840 and ≈ 0.860 for the considered budget availability scenarios, when the first 6 countermeasures could be selected throughout resource allocation.



Figure 131 The average effectiveness of countermeasures implemented at highway-rail grade crossings selected for upgrading over all the PF points for each budget availability scenario (the first 6 countermeasures are available for upgrading).

Figure 132 shows the average installation cost of countermeasures implemented at highway-rail grade crossings selected for upgrading over all the PF points for all the public highway-rail grade crossings for each one of the considered budget availability scenarios, when all 11

countermeasures could be used for upgrading. An increase in the total available budget allowed the **MORAP** mathematical model to select the countermeasures with higher installation costs. Still, when all of the 11 countermeasures were available for selection, the maximum average installation cost of the selected countermeasures did not exceed \$5,700 over all the developed budget availability scenarios, which can be supported by the fact that the MPSDR heuristic that was used to solve the **MORAP** mathematical model selects highway-rail grade crossings for upgrades and determines the appropriate countermeasure based on the weighted sum of normalized hazard severity reduction and normalized traffic delay reduction to cost ratios. Therefore, the low-cost countermeasures, such as countermeasure “7” (i.e., “mountable curbs [with channelized devices]”, which have an installation cost of \$15,000) or countermeasure “8” (i.e., “barrier curbs [with or without channelized devices]”, which have an installation cost of \$15,000) had better chances of being selected over the high-cost countermeasures, such as countermeasure “2” (i.e., “passive to flashing lights and gates”, which have an installation cost of \$180,900) or countermeasure “3” (i.e., “flashing lights to gates”, which have an installation cost of \$106,100). Lin et al. (2017) also indicated that considering monetary limitations, low-cost countermeasures could be efficient alternatives for safety improvements at the highway-rail grade crossings in Florida.

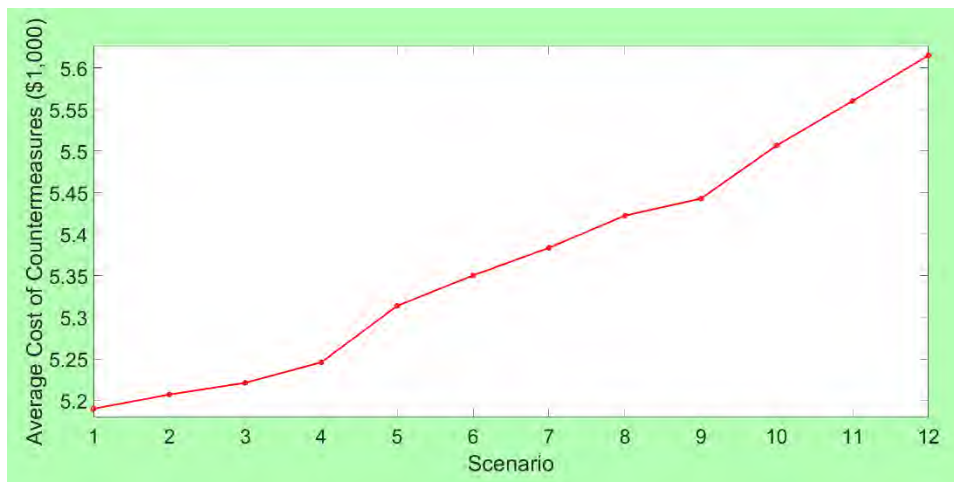


Figure 132 The average installation cost of countermeasures implemented at highway-rail grade crossings selected for upgrading over all the PF points for each budget availability scenario (all 11 countermeasures are available for upgrading).

Figure 133 presents the average effectiveness of countermeasures implemented at highway-rail grade crossings selected for upgrading over all the PF points for all the public highway-rail grade crossings for each one of the considered budget availability scenarios, when all 11 countermeasures could be used for upgrading. As evidenced by Figure 133, after increasing the total available budget from one scenario to another, the MPSDR heuristic still selected the countermeasures with fairly high effectiveness. The average effectiveness of the selected countermeasures varied between ≈ 0.818 and ≈ 0.819 for the considered budget availability scenarios, when all of the 11 countermeasures could be selected throughout resource allocation.

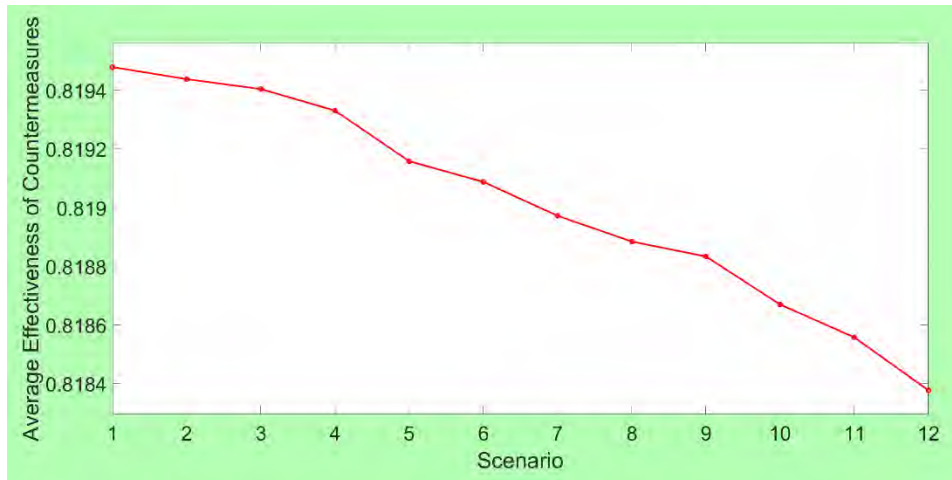


Figure 133 The average effectiveness of countermeasures implemented at highway-rail grade crossings selected for upgrading over all the PF points for each budget availability scenario (all 11 countermeasures are available for upgrading).

7.2. Sensitivity Analysis for the Number of Available Countermeasures

The impact of the number of available countermeasures on multi-objective resource allocation among the highway-rail grade crossings in Florida is investigated in this section. In particular, a total of 11 countermeasure availability scenarios was developed, where the number of countermeasures considered for multi-objective resource allocation was increased from 1 in scenario 1 to 11 in scenario 11, with an increment of 1 countermeasure per countermeasure availability scenario. This analysis investigated all the 6,109 public highway-rail grade crossings in Florida, which were found in the FRA crossing inventory database (FRA, 2016), and the total available budget was set to \$7.5M.

7.2.1. The Impact of the Countermeasure Availability on the MORAP Objective Functions

Figure 134 presents the PFs generated for the considered countermeasure availability scenarios. Note that all the PFs in Figure 134 have the same limits for the horizontal and vertical axes, so that their movements can be observed with ease. It can be observed that the PFs moved from the lower-right corner in the plots to the upper-left corner, when the number of available countermeasures was increased. Such a finding can be supported by the fact that when the number of available countermeasures was increased, more highway-rail grade crossings were upgraded (especially, after introducing low-cost countermeasures “7”, “8”, “9”, and “10”). So, the overall hazard severity decreased. However, the overall traffic delay increased at the same time due to the installation of countermeasures.

Figure 135 shows the average overall hazard severity over all the PF points for all the public highway-rail grade crossings for each one of the considered countermeasure availability scenarios. Similar to the overall hazard severity for each of the PF points, the average overall hazard severity over all the PF points decreased with the availability of more countermeasures. The latter pattern can be explained by the fact that the total number of highway-rail grade crossings, which were selected for upgrading by the **MORAP** mathematical model, increased with the number of available countermeasures and led to a reduction in the average overall hazard severity. The change in the average overall hazard severity in Figure 135 is not linear,

which can be supported by the complexity of multi-objective resource allocation based on the **MORAP** mathematical model, since many different factors are considered throughout the highway-rail grade crossing upgrading decisions (e.g., eligibility of a highway-rail grade crossing for the considered countermeasures, different installation costs for the considered countermeasures, different effectiveness factors for the considered countermeasures, hazard severity and traffic delay at a highway-rail grade crossing).

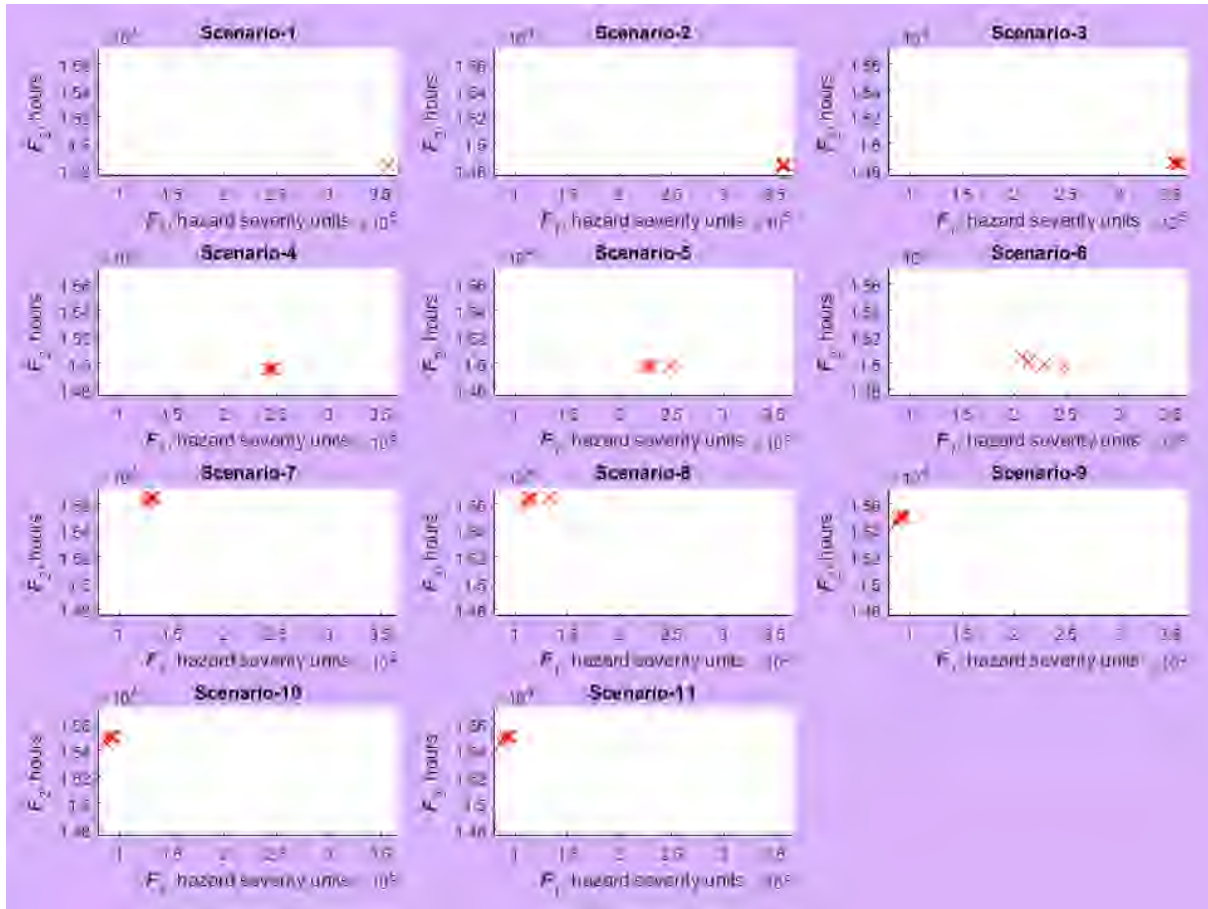


Figure 134 The PFs generated for each countermeasure availability scenario.

Figure 136 illustrates the average overall traffic delay over all the PF points for all the public highway-rail grade crossings for each one of the considered countermeasure availability scenarios. Similar to the overall traffic delay for each of the PF points, the average overall traffic delay over all the PF points increased with the availability of more countermeasures. The latter pattern can be explained by the fact that the total number of highway-rail grade crossings, which were selected for upgrading by the **MORAP** mathematical model, increased with the number of available countermeasures and led to an increase in the average overall traffic delay. The change in the average overall traffic delay in Figure 136 is not linear, which can be supported by the complexity of multi-objective resource allocation based on the **MORAP** mathematical model, since many different factors are considered throughout the highway-rail grade crossing upgrading decisions (e.g., eligibility of a highway-rail grade crossing for the considered countermeasures, different installation costs for the considered countermeasures, different

effectiveness factors for the considered countermeasures, hazard severity and traffic delay at a highway-rail grade crossing).



Figure 135 The average overall hazard severity over all the PF points for each countermeasure availability scenario.

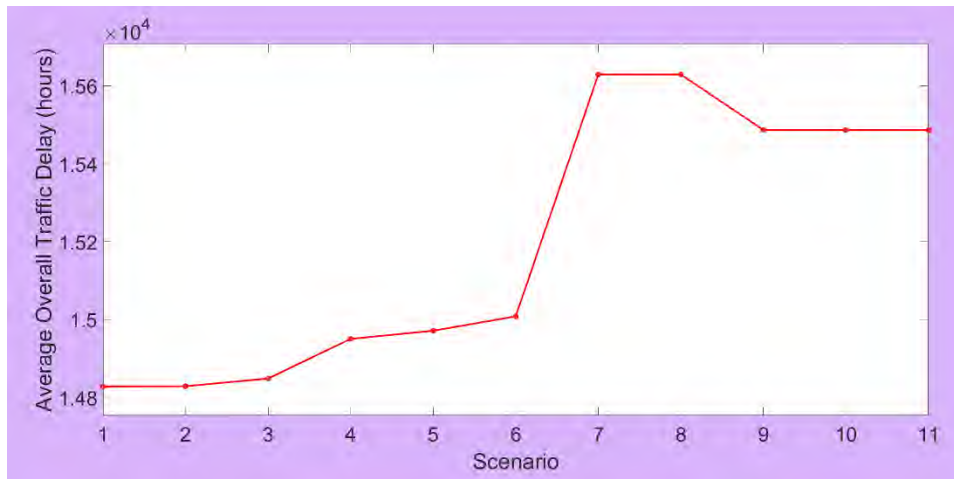


Figure 136 The average overall traffic delay over all the PF points for each countermeasure availability scenario.

7.2.2. The Impact of the Countermeasure Availability on the Number of Highway-Rail Grade Crossings Upgraded by MORAP

Figure 137 demonstrates the average total number of highway-rail grade crossings selected for upgrading over all the PF points for all the public highway-rail grade crossings for each one of the considered countermeasure availability scenarios. As discussed earlier, the total number of upgraded highway-rail grade crossings increased with the number of available countermeasures for each one of the PF points. Similarly, the average total number of highway-rail grade crossings selected for upgrading over all the PF points increased as well. For example, the average total number of highway-rail grade crossings selected for upgrading out of the 6,109 public highway-rail grade crossings in Florida was 100.0 in scenario 1 and 1,392.8 in scenario 11. The reason for such pattern is that the installation cost of the available countermeasures and

eligibility of the highway-rail grade crossings to implement them can significantly influence the number of highway-rail grade crossings to be upgraded. Specifically, the State of Florida has a number of gated highway-rail grade crossings which are not eligible for countermeasures “1”, “2”, and “3”. Hence, in the first 6 countermeasure availability scenarios, the selected gated highway-rail grade crossings were upgraded with countermeasures “4”, “5”, or “6” that are even more expensive than countermeasures “1”, “2”, and “3”. In addition, the number of upgraded highway-rail grade crossings in scenarios 1 to 6 is substantially less than that of scenarios 7 to 11 because of the high installation costs for the first 6 countermeasures, which vary from \$74,800 to \$260,000.

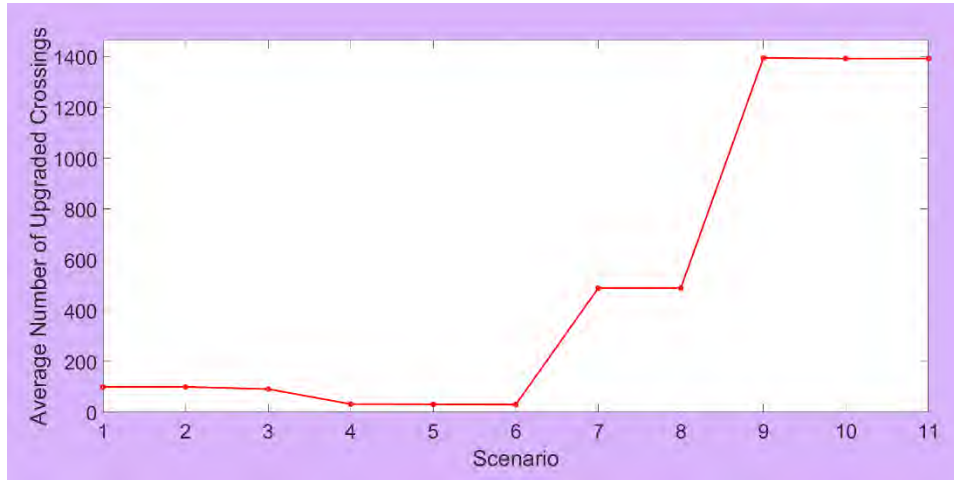


Figure 137 The average total number of highway-rail grade crossings selected for upgrading over all the PF points for each countermeasure availability scenario.

7.2.3. The Impact of the Countermeasure Availability on the Average Installation Cost and the Average Effectiveness of Countermeasures Selected by MORAP

Figure 138 shows the average installation cost of countermeasures implemented at highway-rail grade crossings selected for upgrading over all the PF points for all the public highway-rail grade crossings for each one of the considered countermeasure availability scenarios. The average installation cost of countermeasures was fairly high for scenarios 1 to 6 because of the high installation cost of the countermeasures available for selection in these scenarios (varying from \$74,800 to \$260,000). On the other hand, the average installation cost of countermeasures was significantly lower for scenarios 7 to 11 because of the low installation cost of the additional countermeasures available for selection in these scenarios (e.g., countermeasures “7”, “8”, and “9” with installations costs between \$5,000 and \$15,000). The importance of low-cost countermeasures for effective multi-objective resource allocation among the highway-rail grade crossings in Florida is accentuated by the latter finding.

Figure 139 presents the average effectiveness of countermeasures implemented at highway-rail grade crossings selected for upgrading over all the PF points for all the public highway-rail grade crossings for each one of the considered countermeasure availability scenarios. After increasing the number of the available countermeasures from one scenario to another, an overall increase was noted in the average effectiveness of the countermeasures, which were selected for the highway-rail grade crossings upgraded by the **MORAP** mathematical model. Such a pattern can

by justified by the comparatively high effectiveness factors of the low-cost countermeasures. For instance, “one-way street with gate”, whose installation cost is only \$5,000, has the effectiveness factor of 0.82. High installation costs also do not guarantee high effectiveness factors. For example, the effectiveness factor of “flashing lights to gates”, whose installation cost is \$106,100, is 0.63. Furthermore, the nature of the MPSDR heuristic, developed to solve the **MORAP** mathematical model, enables it to select the countermeasures with low installation costs and high effectiveness factors.

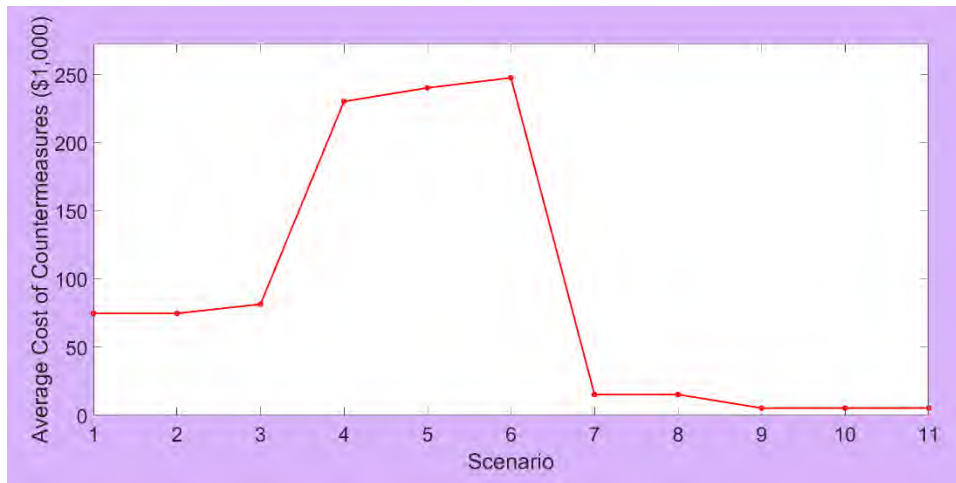


Figure 138 The average installation cost of countermeasures implemented at highway-rail grade crossings selected for upgrading over all the PF points for each countermeasure availability scenario.

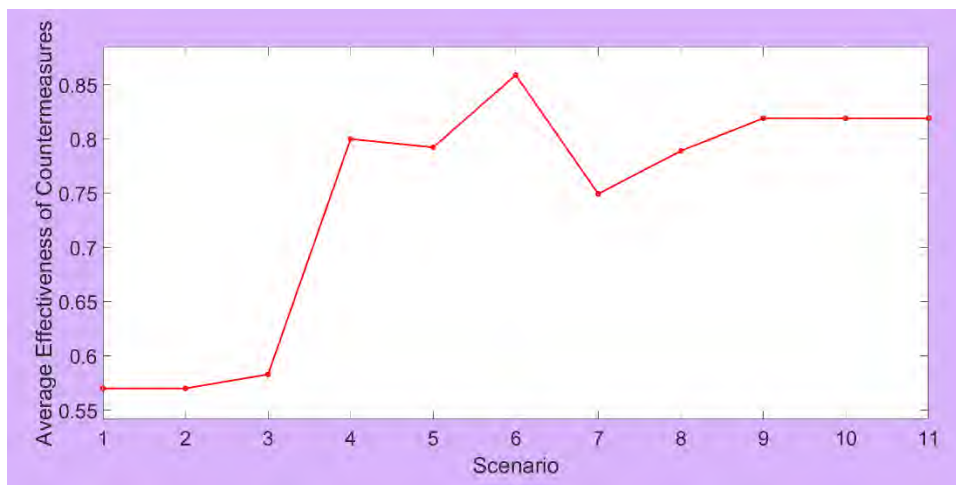


Figure 139 The average effectiveness of countermeasures implemented at highway-rail grade crossings selected for upgrading over all the PF points for each countermeasure availability scenario.

7.3. Sensitivity Analysis for the Hazard Severity Weight Values

The impact of the hazard severity weight values on multi-objective resource allocation among the highway-rail grade crossings in Florida is investigated in this section. In particular, a total of 20 hazard severity weight scenarios was developed, where the hazard severity weight values

were changed. Table 33 presents the hazard severity weight values that were used for the developed scenarios, where W_{FH} , W_{IH} , and W_{PH} denote the fatality hazard weight, the injury hazard weight, and the property damage hazard weight, respectively. This analysis investigated all the 6,109 public highway-rail grade crossings in Florida, which were found in the FRA crossing inventory database (FRA, 2016), and the total available budget was set to \$7.5M. Furthermore, a total of 11 countermeasures, which was adopted earlier in this project based on the GradeDec.NET Reference Manual (U.S. DOT, 2014a), were considered for implementation at the highway-rail grade crossings. Specifically, two cases of countermeasure availabilities were used for the hazard severity weight scenarios, including the considerations of the first 6 countermeasures, which are comparatively more expensive, and all 11 countermeasures for further insights.

Table 33 Developed scenarios for hazard severity weight values.

Scenario	W_{FH}	W_{IH}	W_{PH}
1	0.600	0.300	0.100
2	0.620	0.285	0.095
3	0.640	0.270	0.090
4	0.660	0.255	0.085
5	0.680	0.240	0.080
6	0.700	0.225	0.075
7	0.720	0.210	0.070
8	0.740	0.195	0.065
9	0.760	0.180	0.060
10	0.780	0.165	0.055
11	0.800	0.150	0.050
12	0.820	0.135	0.045
13	0.840	0.120	0.040
14	0.860	0.105	0.035
15	0.880	0.090	0.030
16	0.900	0.075	0.025
17	0.920	0.060	0.020
18	0.940	0.045	0.015
19	0.960	0.030	0.010
20	0.980	0.015	0.005

7.3.1. The Impact of the Hazard Severity Weight Values on the MORAP Objective Functions

Figure 140 presents the PFs generated for the considered hazard severity weight scenarios, when the first 6 countermeasures could be used for upgrading. Note that all the PFs in Figure 140 have the same limits for the horizontal and vertical axes, so that their movements can be observed with ease. It can be observed that the PFs moved from the right side in the plots to the left side, when the severity weight for the fatality hazard was increased, and the severity weights for the injury hazard and the property damage hazard were decreased. The PF in scenario 1 is at the right-most side, which denotes the highest overall hazard severity among the considered

scenarios. On the other hand, the PF in scenario 20 is at the left-most side, which denotes the lowest overall hazard severity among the considered scenarios. It can also be noted that there was no significant vertical shift in the PFs, which denotes no significant change in the overall traffic delay. All these findings can be supported by the fact that less highway-rail grade crossings were upgraded by the **MORAP** mathematical model, when the severity weight for the fatality hazard was increased, and the severity weights for the injury hazard and the property damage hazard were reduced. The highway-rail grade crossings with a higher fatality hazard received priority for upgrading.

Figure 141 presents the PFs generated for the considered hazard severity weight scenarios, when all 11 countermeasures could be used for upgrading. Note that all the PFs in Figure 141 have the same limits for the horizontal and vertical axes, so that their movements can be observed with ease. It can be observed that the PFs moved from the upper-right corner in the plots to the lower-left corner, when the severity weight for the fatality hazard was increased, and the severity weights for the injury hazard and the property damage hazard were decreased. The PF in scenario 1 is at the upper-most-right corner, which denotes the highest overall hazard severity and the highest overall traffic delay among the considered scenarios. On the other hand, the PF in scenario 20 is at the lower-most-left corner, which denotes the lowest overall hazard severity and the lowest overall traffic delay among the considered scenarios. All these findings can be supported by the fact that less highway-rail grade crossings were upgraded by the **MORAP** mathematical model, when the severity weight for the fatality hazard was increased, and the severity weights for the injury hazard and the property damage hazard were reduced. The highway-rail grade crossings with a higher fatality hazard received priority for upgrading.

Moreover, the shapes of the PFs in Figure 141 are different from the ones presented in Figure 140. Such a pattern can be explained by the fact that the MPSDR heuristic started selecting countermeasures that are effective in terms of reducing both the overall hazard severity and the overall traffic delay after the introduction of low-cost countermeasures (i.e. countermeasures “7”, “8”, “9”, and “10”). Therefore, the PFs produced by the MPSDR heuristic for the scenarios with low-cost countermeasures generally do not show a conflicting nature of the overall hazard severity minimization objective and the overall traffic delay minimization objective.

Figure 142 shows the average overall hazard severity over all the PF points for all the public highway-rail grade crossings for each one of the considered hazard severity weight scenarios, when the first 6 countermeasures could be used for upgrading. On the other hand, Figure 143 shows the average overall hazard severity over all the PF points for all the public highway-rail grade crossings for each one of the considered hazard severity weight scenarios, when all 11 countermeasures could be used for upgrading. Similar to the overall hazard severity for each of the PF points, the average overall hazard severity over all the PF points decreased with an increase in the severity weight for the fatality hazard and a reduction in the severity weights for the injury hazard and the property damage hazard. The latter pattern can be explained by the fact that the total number of highway-rail grade crossings, which were selected for upgrading by the **MORAP** mathematical model, decreased when the severity weight for the fatality hazard was increased, and the severity weights for the injury hazard and the property damage hazard were reduced. Furthermore, the highway-rail grade crossings with a higher fatality hazard received priority for upgrading.

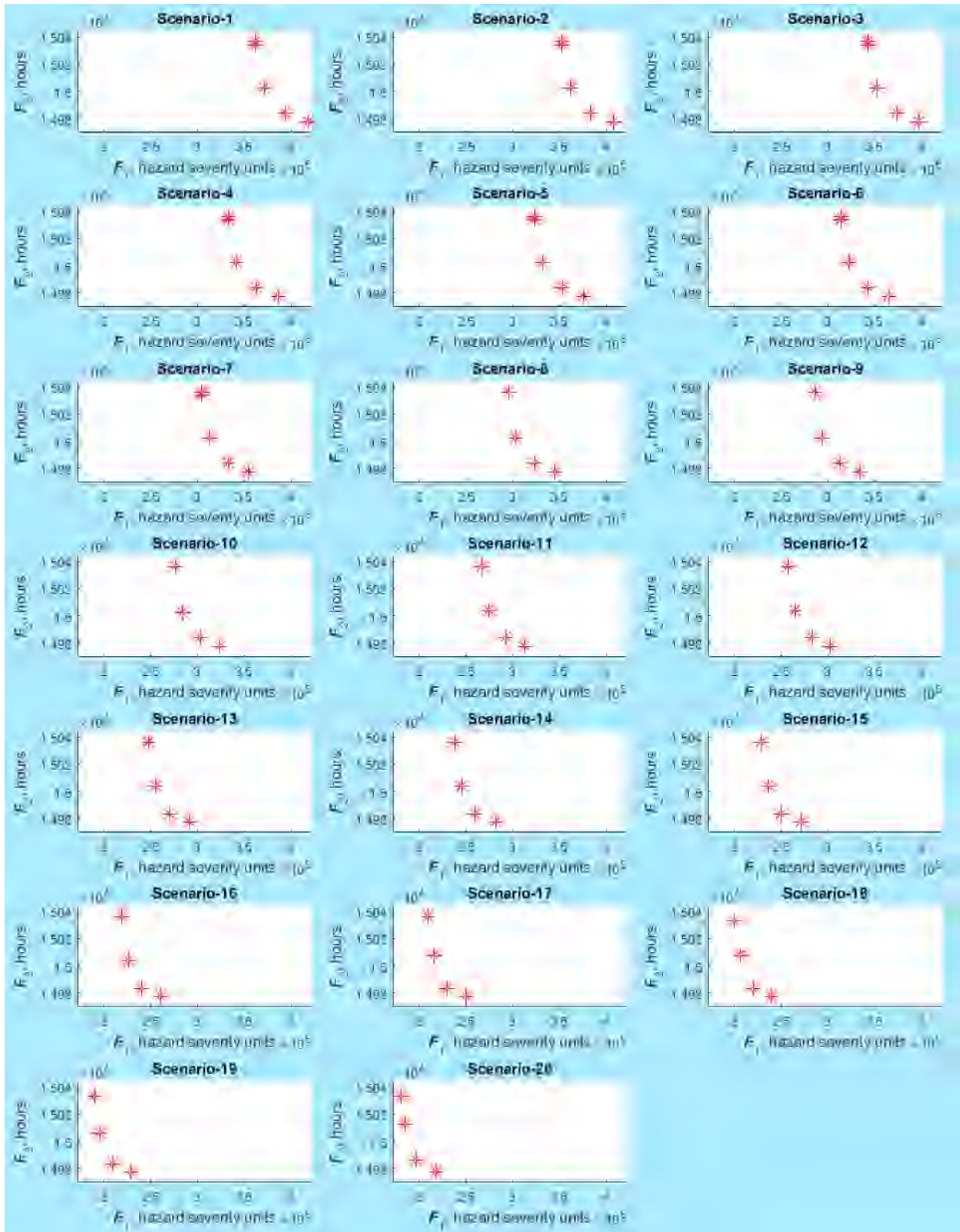


Figure 140 The PFs generated for each hazard severity weight scenario (the first 6 countermeasures are available for upgrading).

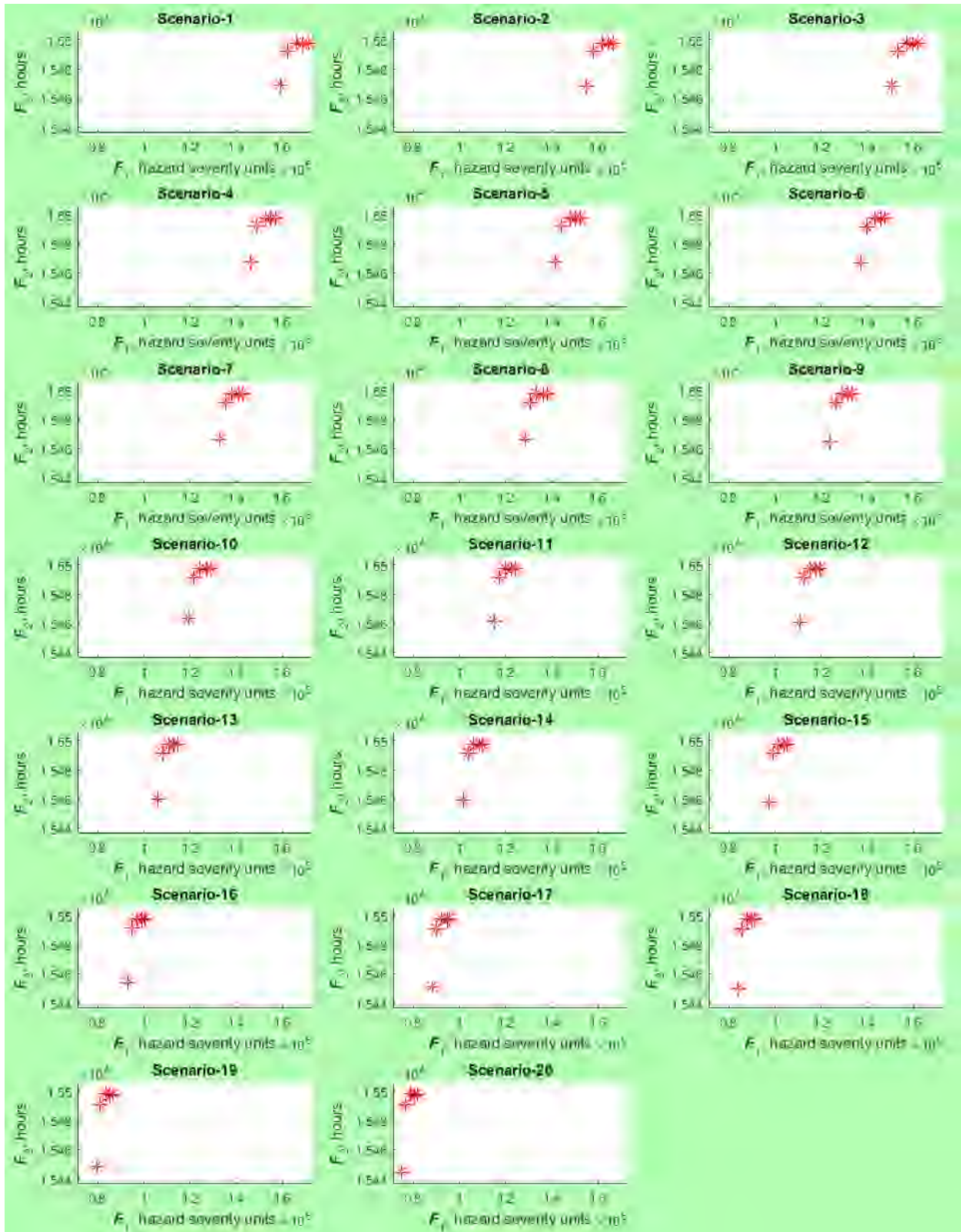


Figure 141 The PFs generated for each hazard severity weight scenario (all 11 countermeasures are available for upgrading).

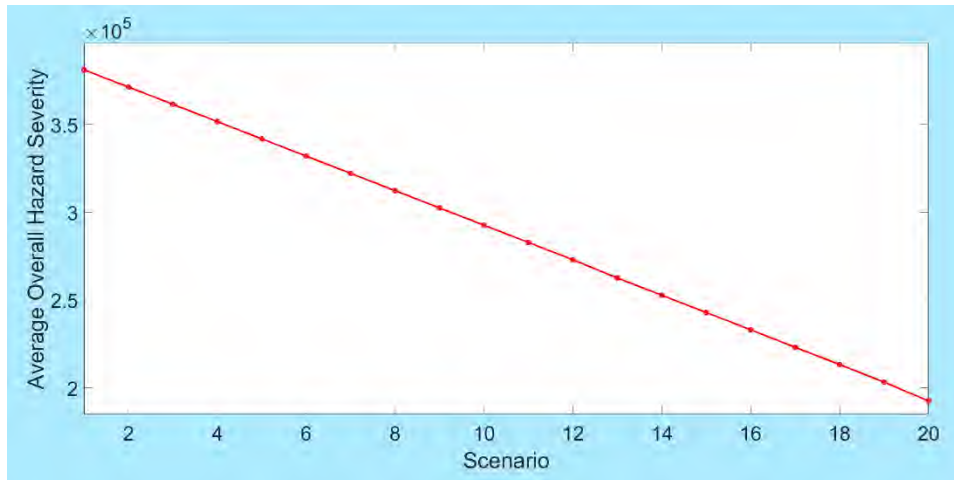


Figure 142 The average overall hazard severity over all the PF points for each hazard severity weight scenario (the first 6 countermeasures are available for upgrading).

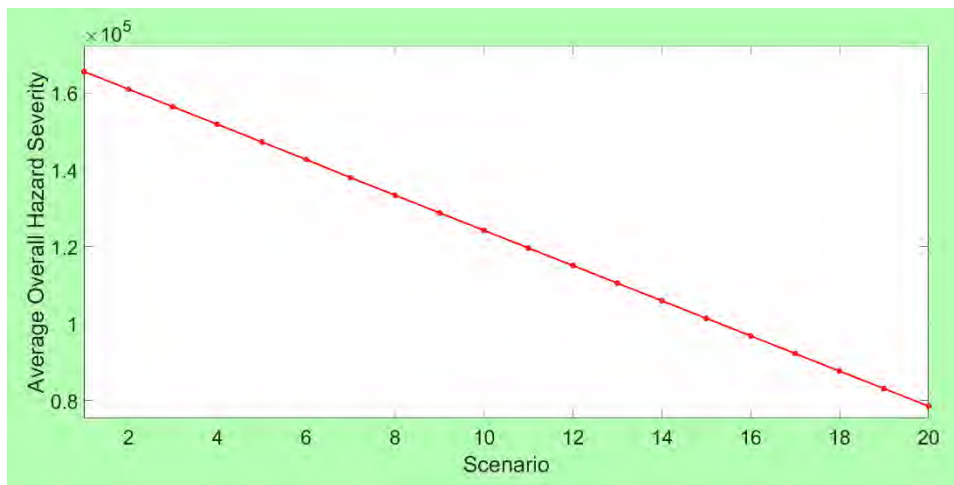


Figure 143 The average overall hazard severity over all the PF points for each hazard severity weight scenario (all 11 countermeasures are available for upgrading).

Figure 144 illustrates the average overall traffic delay over all the PF points for all the public highway-rail grade crossings for each one of the considered hazard severity weight scenarios, when the first 6 countermeasures could be used for upgrading. On the other hand, Figure 145 illustrates the average overall traffic delay over all the PF points for all the public highway-rail grade crossings for each one of the considered hazard severity weight scenarios, when all 11 countermeasures could be used for upgrading. Similar to the overall traffic delay for each of the PF points, no significant change in the average overall traffic delay over all the PF points was noted in case of Figure 144, when the first 6 countermeasures could be used for upgrading. On the other hand, the average overall traffic delay over all the PF points decreased in case of Figure 145, when all 11 countermeasures could be used for upgrading. Such a pattern can be explained by the fact that the MPSDR heuristic started selecting countermeasures that are effective in terms of reducing both the overall hazard severity and the overall traffic delay after the introduction of low-cost countermeasures (i.e. countermeasures “7”, “8”, “9”, and “10”).

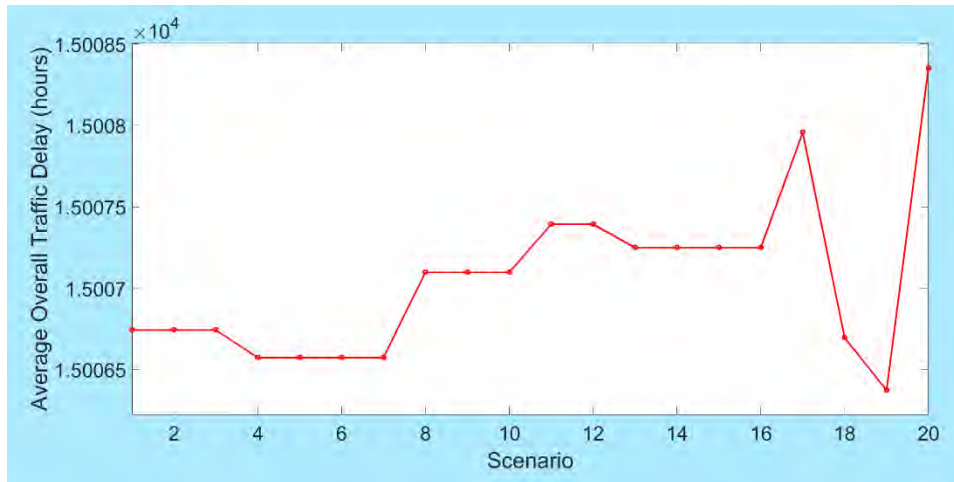


Figure 144 The average overall traffic delay over all the PF points for each hazard severity weight scenario (the first 6 countermeasures are available for upgrading).

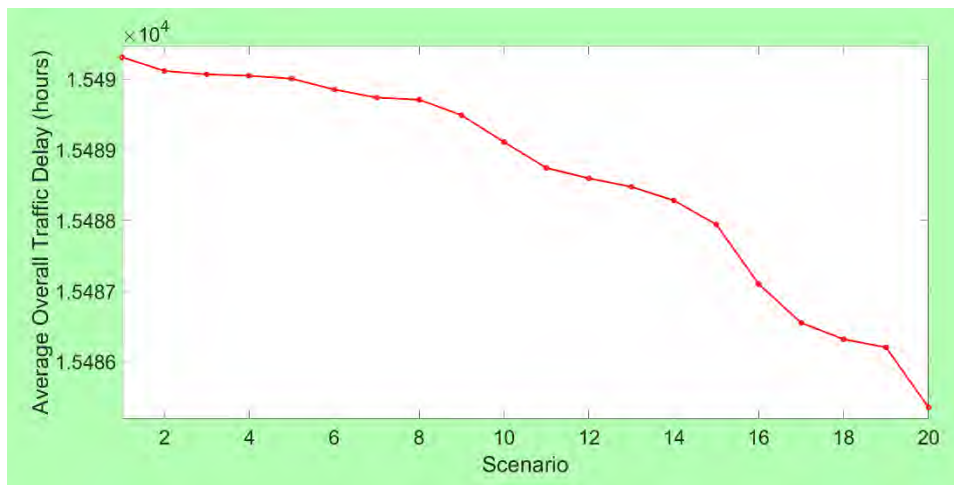


Figure 145 The average overall traffic delay over all the PF points for each hazard severity weight scenario (all 11 countermeasures are available for upgrading).

7.3.2. The Impact of the Hazard Severity Weight Values on the Number of Highway-Rail Grade Crossings Upgraded by MORAP

Figure 146 demonstrates the average total number of highway-rail grade crossings selected for upgrading over all the PF points for all the public highway-rail grade crossings for each one of the considered hazard severity weight scenarios, when the first 6 countermeasures could be used for upgrading. As discussed earlier, the total number of upgraded highway-rail grade crossings decreased with an increase in the severity weight for the fatality hazard and a reduction in the severity weights for the injury hazard and the property damage hazard for each one of the PF points. Similarly, the average total number of highway-rail grade crossings selected for upgrading over all the PF points decreased as well. For example, the average total number of highway-rail grade crossings selected for upgrading out of the 6,109 public highway-rail grade crossings in Florida decreased from 30.4 in scenario 1 to 30.2 in scenario 20. Such a finding can be justified by the fact that the MPSDR algorithm applied more expensive countermeasures with higher effectiveness factors as an attempt to achieve a greater reduction in the overall hazard

severity at the most hazardous public highway-rail grade crossings (i.e., the ones with the highest fatality hazard) in Florida. The small number of upgraded highway-rail grade crossings in case of Figure 146 is because of the high installation cost of countermeasures “1” to “6”, which were made available in this case. Moreover, the State of Florida has a number of gated highway-rail grade crossings, which are not eligible for countermeasures “1”, “2”, and “3”. Hence, the selected gated highway-rail grade crossings were upgraded with countermeasures “4”, “5”, or “6” that are even more expensive than countermeasures “1”, “2”, and “3”.

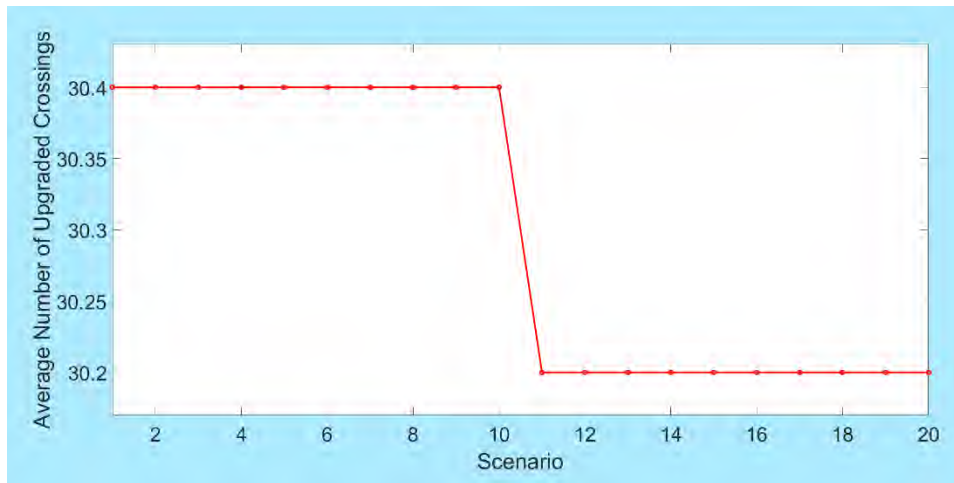


Figure 146 The average total number of highway-rail grade crossings selected for upgrading over all the PF points for each hazard severity weight scenario (the first 6 countermeasures are available for upgrading).

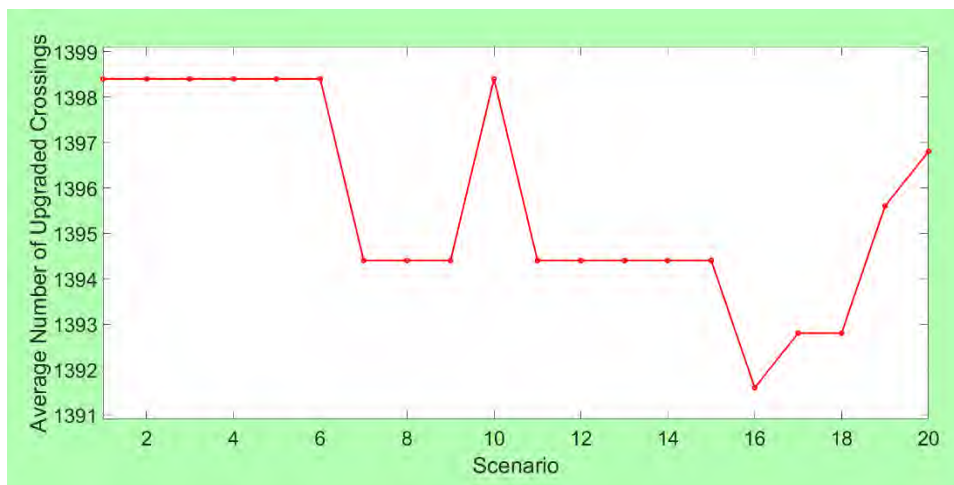


Figure 147 The average total number of highway-rail grade crossings selected for upgrading over all the PF points for each hazard severity weight scenario (all 11 countermeasures are available for upgrading).

Figure 147 demonstrates the average total number of highway-rail grade crossings selected for upgrading over all the PF points for all the public highway-rail grade crossings for each one of the considered hazard severity weight scenarios, when all 11 countermeasures could be used for upgrading. As discussed earlier, the total number of upgraded highway-rail grade crossings

deceased with an increase in the severity weight for the fatality hazard and a reduction in the severity weights for the injury hazard and the property damage hazard for each one of the PF points. Similarly, the average total number of highway-rail grade crossings selected for upgrading over all the PF points decreased as well. For example, the average total number of highway-rail grade crossings selected for upgrading out of the 6,109 public highway-rail grade crossings in Florida was 1,398.4 in scenario 1 and 1,391.6 in scenario 16. Such a finding can be justified by the fact that the MPSDR algorithm applied more expensive countermeasures with higher effectiveness factors as an attempt to achieve a greater reduction in the overall hazard severity at the most hazardous public highway-rail grade crossings (i.e., the ones with the highest fatality hazard) in Florida. The number of upgraded highway-rail grade crossings in case of Figure 147 is substantially higher than that of Figure 146 due to the availability of more and cheaper countermeasures. The change in the average total number of upgraded highway-rail grade crossings is nonlinear, which demonstrates the complexity of multi-objective resource allocation based on the **MORAP** mathematical model, since many different factors are considered throughout the highway-rail grade crossing upgrading decisions (e.g., eligibility of a highway-rail grade crossing for the considered countermeasures, different installation costs for the considered countermeasures, different effectiveness factors for the considered countermeasures, hazard severity and traffic delay at a highway-rail grade crossing).

7.3.3. The Impact of the Hazard Severity Weight Values on the Average Installation Cost and the Average Effectiveness of Countermeasures Selected by MORAP

Figure 148 shows the average installation cost of countermeasures implemented at highway-rail grade crossings selected for upgrading over all the PF points for all the public highway-rail grade crossings for each one of the considered hazard severity weight scenarios, when the first 6 countermeasures could be used for upgrading. An increase in the severity weight for the fatality hazard and a reduction in the severity weights for the injury hazard and the property damage hazard allowed the **MORAP** mathematical model to select the countermeasures with higher installation costs. It can be observed that the average installation cost of countermeasures was fairly high (between \$246,112 and \$247,526), when only the first 6 countermeasures were considered for installation. The reason for such a high average cost is that the installation costs of countermeasures “1” to “6”, which were made available in this case, are between \$74,800 and \$260,000. Moreover, the State of Florida has a number of gated highway-rail grade crossings, which are not eligible for countermeasures “1”, “2”, and “3”. Hence, the selected gated highway-rail grade crossings were upgraded with countermeasures “4”, “5”, or “6” that are even more expensive than countermeasures “1”, “2”, and “3”.

Figure 149 presents the average effectiveness of countermeasures implemented at highway-rail grade crossings selected for upgrading over all the PF points for all the public highway-rail grade crossings for each one of the considered hazard severity weight scenarios, when the first 6 countermeasures could be used for upgrading. As evidenced by Figure 149, after changing the hazard severity weight values from one scenario to another, the MPSDR heuristic still selected the countermeasures with fairly high effectiveness. The average effectiveness of the selected countermeasures varied between ≈ 0.856 and ≈ 0.861 for the considered hazard severity weight scenarios, when the first 6 countermeasures could be selected throughout resource allocation.

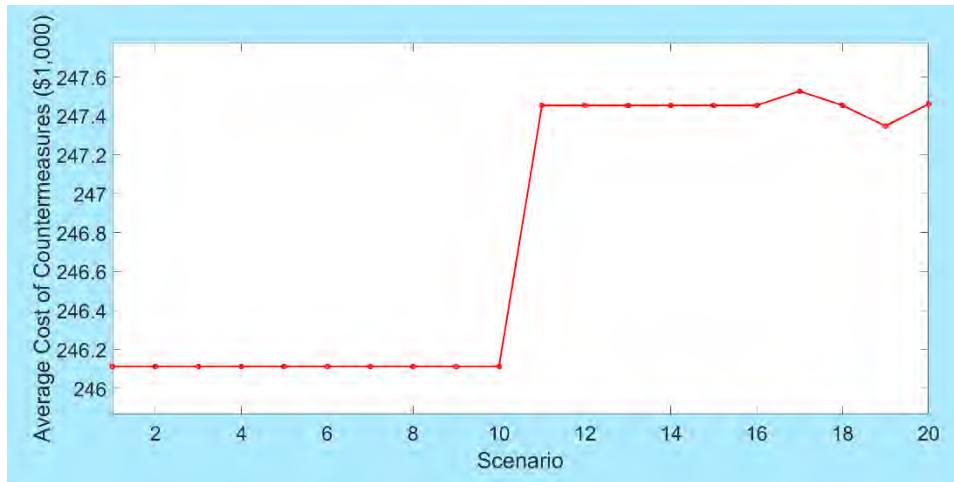


Figure 148 The average installation cost of countermeasures implemented at highway-rail grade crossings selected for upgrading over all the PF points for each hazard severity weight scenario (the first 6 countermeasures are available for upgrading).

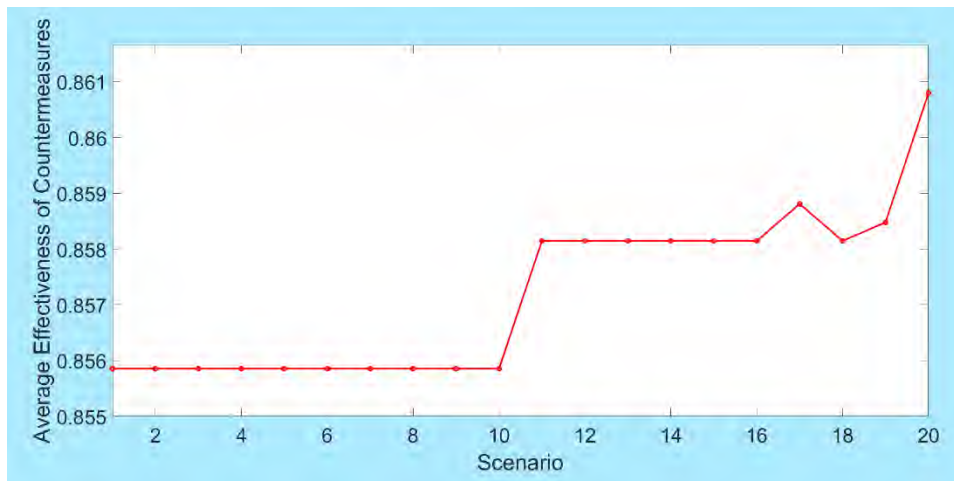


Figure 149 The average effectiveness of countermeasures implemented at highway-rail grade crossings selected for upgrading over all the PF points for each hazard severity weight scenario (the first 6 countermeasures are available for upgrading).

Figure 150 shows the average installation cost of countermeasures implemented at highway-rail grade crossings selected for upgrading over all the PF points for all the public highway-rail grade crossings for each one of the considered hazard severity weight scenarios, when all 11 countermeasures could be used for upgrading. An increase in the severity weight for the fatality hazard and a reduction in the severity weights for the injury hazard and the property damage hazard allowed the **MORAP** mathematical model to select the countermeasures with higher installation costs. Still, when all of the 11 countermeasures were available for selection, the maximum average installation cost of the selected countermeasures did not exceed \$5,400 over all the developed hazard severity weight scenarios, which can be supported by the fact that the MPSDR heuristic that was used to solve the **MORAP** mathematical model selects highway-rail grade crossings for upgrades and determines the appropriate countermeasure based on the weighted sum of normalized hazard severity reduction and normalized traffic delay reduction to

cost ratios. Therefore, the low-cost countermeasures, such as countermeasure “7” (i.e., “mountable curbs [with channelized devices]”, which have an installation cost of \$15,000) or countermeasure “8” (i.e., “barrier curbs [with or without channelized devices]”, which have an installation cost of \$15,000) had better chances of being selected over the high-cost countermeasures, such as countermeasure “2” (i.e., “passive to flashing lights and gates”, which have an installation cost of \$180,900) or countermeasure “3” (i.e., “flashing lights to gates”, which have an installation cost of \$106,100).

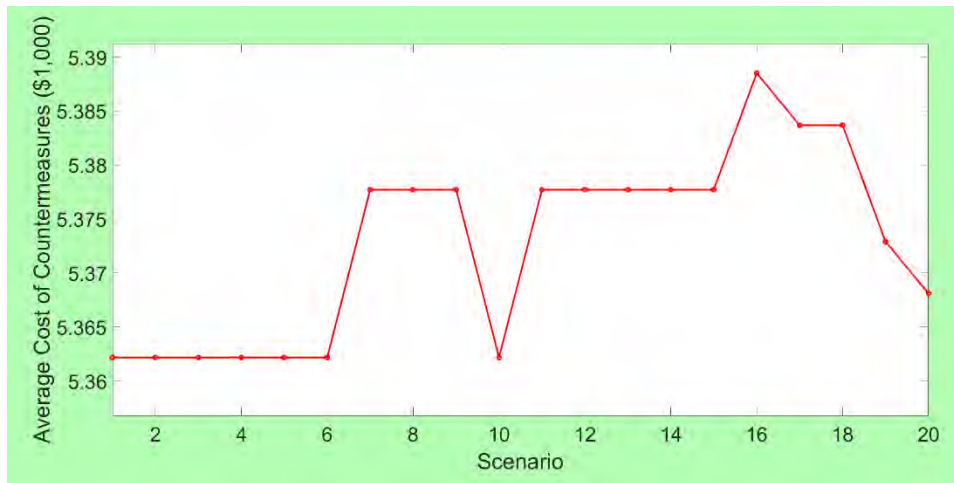


Figure 150 The average installation cost of countermeasures implemented at highway-rail grade crossings selected for upgrading over all the PF points for each hazard severity weight scenario (all 11 countermeasures are available for upgrading).

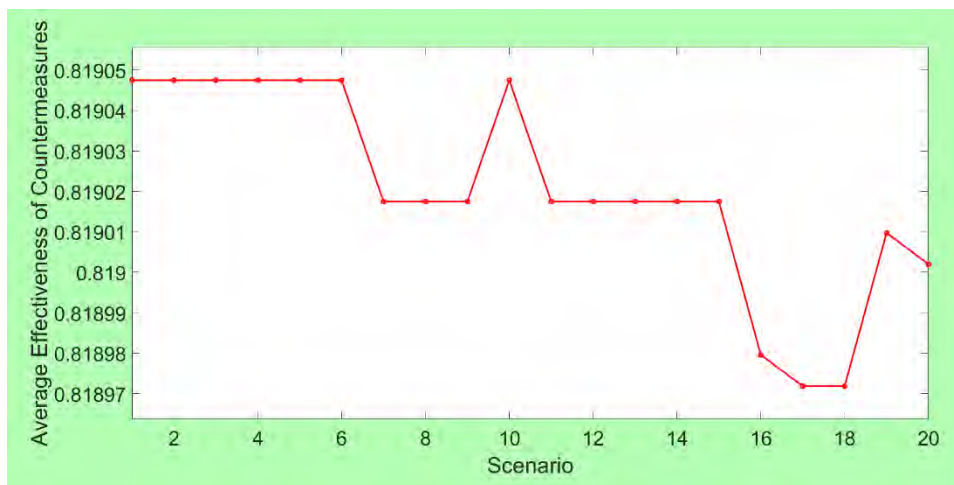


Figure 151 The average effectiveness of countermeasures implemented at highway-rail grade crossings selected for upgrading over all the PF points for each hazard severity weight scenario (all 11 countermeasures are available for upgrading).

Figure 151 presents the average effectiveness of countermeasures implemented at highway-rail grade crossings selected for upgrading over all the PF points for all the public highway-rail grade crossings for each one of the considered hazard severity weight scenarios, when all 11 countermeasures could be used for upgrading. As evidenced by Figure 151, after changing the

hazard severity weight values from one scenario to another, the MPSDR heuristic still selected the countermeasures with fairly high effectiveness. The average effectiveness of the selected countermeasures was about 0.819 for the considered hazard severity weight scenarios, when all of the 11 countermeasures could be selected throughout resource allocation.

7.4. Resource Allocation among Various Crossing Types

Multi-objective resource allocation among various types of highway-rail grade crossings in Florida is investigated in this section. In particular, a total of 3 crossing type scenarios was developed for this analysis. In scenario 1, all the 6,109 public highway-rail grade crossings in Florida were investigated. In scenario 2, all the 2,896 private highway-rail grade crossings in Florida were considered. Finally, in scenario 3, multi-objective resource allocation was conducted among all the 9,005 public and private highway rail-grade crossings in Florida. The relevant information regarding the public and private highway-rail grade crossings in Florida was obtained from the FRA crossing inventory database (FRA, 2016), while the total available budget was set to \$7.5M. Furthermore, a total of 11 countermeasures, which was adopted earlier in this project based on the GradeDec.NET Reference Manual (U.S. DOT, 2014a), were considered for implementation at the highway-rail grade crossings. Specifically, two cases of countermeasure availabilities were used for the crossing type scenarios, including the considerations of the first 6 countermeasures, which are comparatively more expensive, and all 11 countermeasures for further insights.

7.4.1. The Impact of the Crossing Type on the MORAP Objective Functions

Figure 152 presents the PFs generated for the considered crossing type scenarios, when the first 6 countermeasures could be used for upgrading. It can be observed that the PFs corresponding to scenario 1 (i.e., public highway-rail grade crossings) and scenario 3 (i.e., both types of highway-rail grade crossings) are at the upper-right corner of the plot, indicating higher overall hazard severity and higher overall traffic delay. This finding can be supported by the fact that the overall hazard severity and the overall traffic delay before upgrades at the public highway-rail grade crossings in Florida were substantially higher than the ones of the private highway-rail grade crossings. Furthermore, in scenario 3, almost all the highway-rail grade crossings selected for upgrading were public. On the other hand, the PF corresponding to scenario 2 is at the lower-left corner of the plot, which indicates the lowest overall hazard severity and the lowest overall traffic delay. The latter finding can be justified by the fact that the overall hazard severity and the overall traffic delay before upgrades at the private highway-rail grade crossings in Florida were comparatively lower.

Figure 153 presents the PFs generated for the considered crossing type scenarios, when all 11 countermeasures could be used for upgrading. It can be observed that the PFs corresponding to scenario 1 (i.e., public highway-rail grade crossings) and scenario 3 (i.e., both types of highway-rail grade crossings) are at the upper-right corner of the plot, indicating higher overall hazard severity and higher overall traffic delay. This finding can be supported by the fact that the overall hazard severity and the overall traffic delay before upgrades at the public highway-rail grade crossings in Florida were substantially higher than the ones of the private highway-rail grade crossings. Furthermore, in scenario 3, almost all the highway-rail grade crossings selected for upgrading were public.

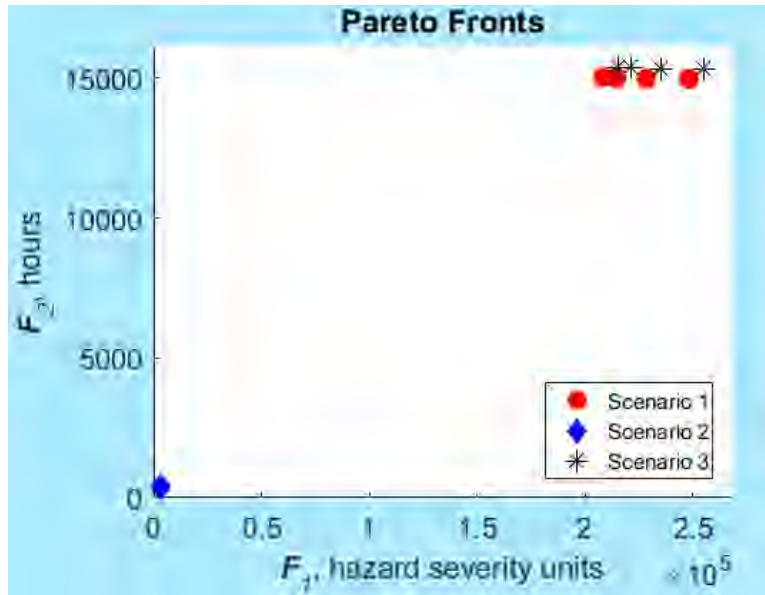


Figure 152 The PFs generated for each crossing type scenario (the first 6 countermeasures are available for upgrading).

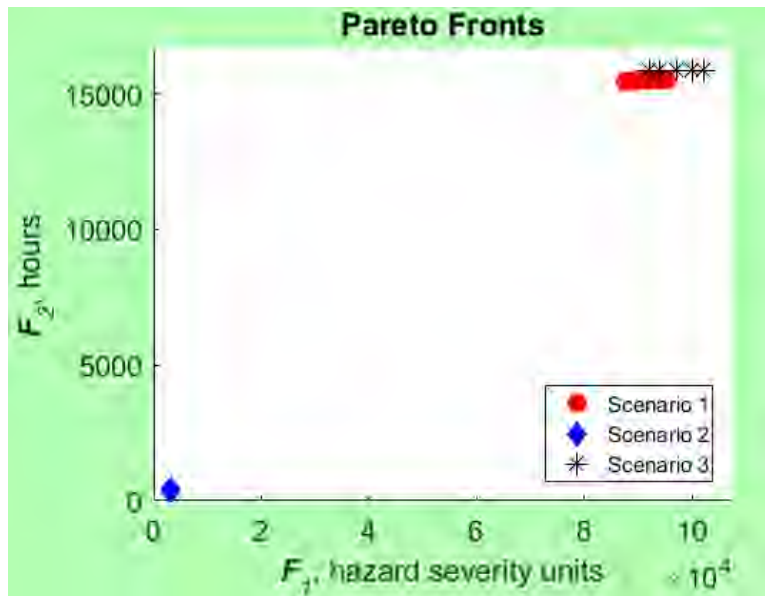


Figure 153 The PFs generated for each crossing type scenario (all 11 countermeasures are available for upgrading).

On the other hand, the PF corresponding to scenario 2 is at the lower-left corner of the plot, which indicates the lowest overall hazard severity and the lowest overall traffic delay. The latter finding can be justified by the fact that the overall hazard severity and the overall traffic delay before upgrades at the private highway-rail grade crossings in Florida were comparatively lower. Note that the shapes of the PFs in Figure 153 are different from the ones presented in Figure 152. Such a pattern can be explained by the fact that the MPSDR heuristic started selecting countermeasures that are effective in terms of reducing both the overall hazard severity and the overall traffic delay after the introduction of low-cost countermeasures (i.e., countermeasures

“7”, “8”, “9”, and “10”). Therefore, the PFs produced by the MPSDR heuristic for the scenarios with low-cost countermeasures generally do not show a conflicting nature of the overall hazard severity minimization objective and the overall traffic delay minimization objective.

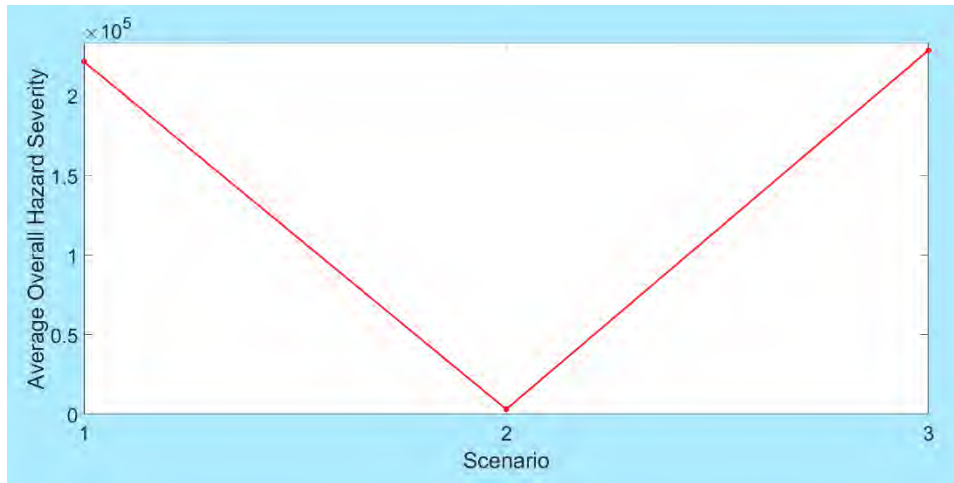


Figure 154 The average overall hazard severity over all the PF points for each crossing type scenario (the first 6 countermeasures are available for upgrading).

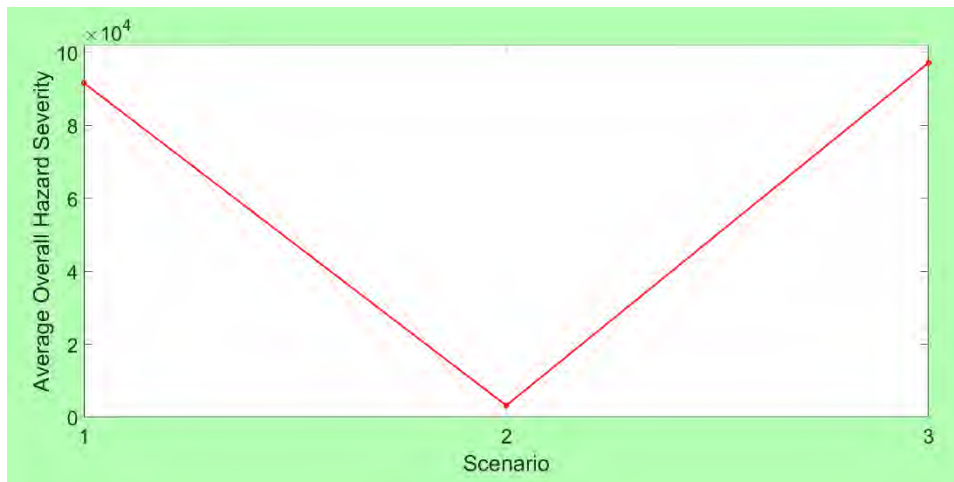


Figure 155 The average overall hazard severity over all the PF points for each crossing type scenario (all 11 countermeasures are available for upgrading).

Figure 154 shows the average overall hazard severity over all the PF points for each one of the considered crossing type scenarios, when the first 6 countermeasures could be used for upgrading. On the other hand, Figure 155 shows the average overall hazard severity over all the PF points for each one of the considered crossing type scenarios, when all 11 countermeasures could be used for upgrading. Similar to the overall hazard severity for each of the PF points, the average overall hazard severity over all the PF points for scenario 1 is significantly higher than that of scenario 2, due to the fact that the public highway-rail grade crossings in Florida were more hazardous before upgrades as compared to the private highway-rail grade crossings. Almost all the highway-rail grade crossings selected for upgrading in scenario 3 were public, and

so, the average overall hazard severity over all the PF points for scenario 3 is very close to that of scenario 1.

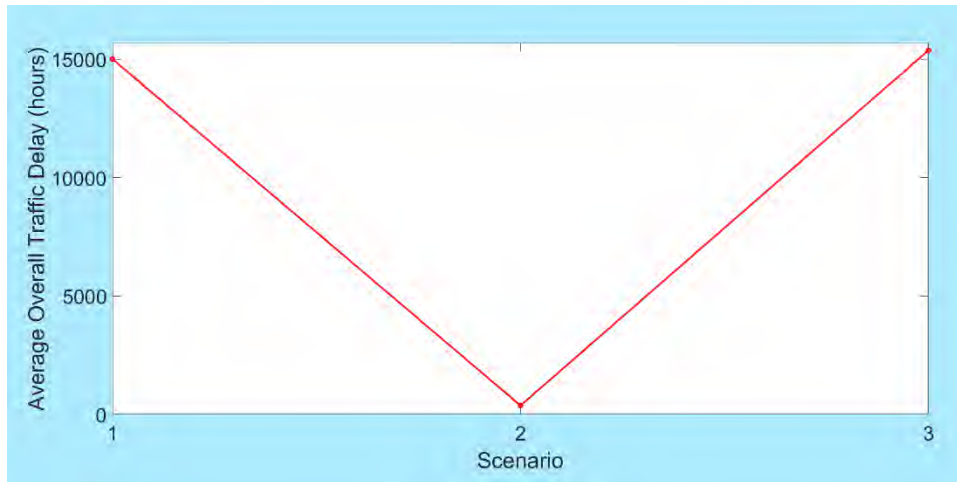


Figure 156 The average overall traffic delay over all the PF points for each crossing type scenario (the first 6 countermeasures are available for upgrading).

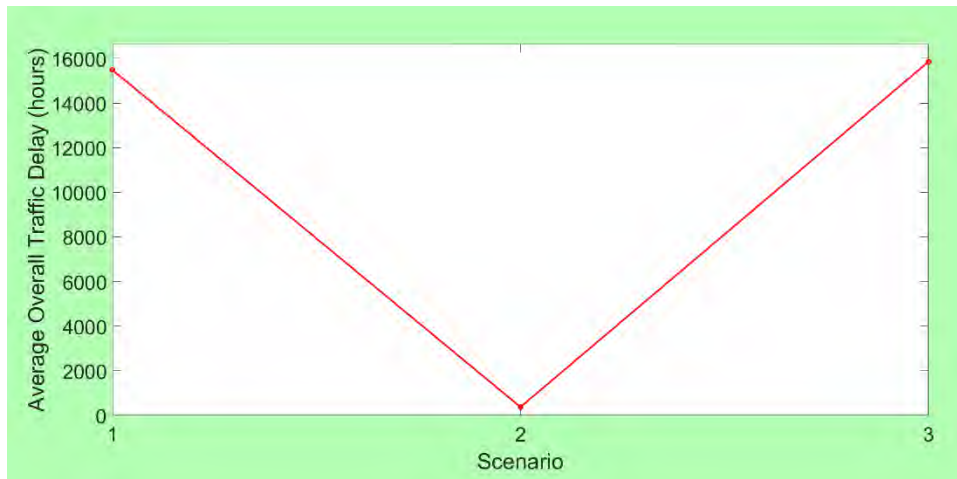


Figure 157 The average overall traffic delay over all the PF points for each crossing type scenario (all 11 countermeasures are available for upgrading).

Figure 156 shows the average overall traffic delay over all the PF points for each one of the considered crossing type scenarios, when the first 6 countermeasures could be used for upgrading. On the other hand, Figure 157 shows the average overall traffic delay over all the PF points for each one of the considered crossing type scenarios, when all 11 countermeasures could be used for upgrading. Similar to the overall traffic delay for each of the PF points, the average overall traffic delay over all the PF points for scenario 1 is significantly higher than that of scenario 2, due to the fact that the public highway-rail grade crossings in Florida were associated with more traffic delays before upgrades as compared to the private highway-rail grade crossings. Almost all the highway-rail grade crossings selected for upgrading in scenario 3 were public, and so, the average overall traffic delay over all the PF points for scenario 3 is very close to that of scenario 1.

7.4.2. The Impact of the Crossing Type on the Number of Highway-Rail Grade Crossings Upgraded by MORAP

Figure 158 demonstrates the average total number of highway-rail grade crossings selected for upgrading over all the PF points for each one of the considered crossing type scenarios, when the first 6 countermeasures could be used for upgrading. A total of 30.2 highway-rail grade crossings out of the 6,109 public highway-rail grade crossings in Florida was upgraded on average in scenario 1. In scenario 2, a total of 99.0 highway-rail grade crossings out of the 2,896 private highway-rail grade crossings was selected on average for upgrades. Furthermore, in scenario 3, a total of 31.2 highway-rail grade crossings out of the 9,005 public and private highway-rail grade crossings in Florida was upgraded on average. The small number of upgraded highway-rail grade crossings in case of Figure 158 is because of the high installation cost of countermeasures “1” to “6”, which were made available in this case. Furthermore, the State of Florida has a number of gated public highway-rail grade crossings, which are not eligible for countermeasures “1”, “2”, and “3”. So, the selected gated public highway-rail grade crossings were upgraded with countermeasures “4”, “5”, or “6” that are even more expensive than countermeasures “1”, “2”, and “3”. Hence, the average number of upgraded highway-rail grade crossings for scenario 1 is less than that of scenario 2. As discussed earlier, most of the highway-rail grade crossings selected for upgrades in scenario 3 were public, since only a small number of the private highway-rail grade crossings from the priority list, generated by the MPSDR heuristic, were ranked high enough for selection considering the total available budget. For this reason, the average number of upgraded highway-rail grade crossings for scenario 3 is very close to that of scenario 1.

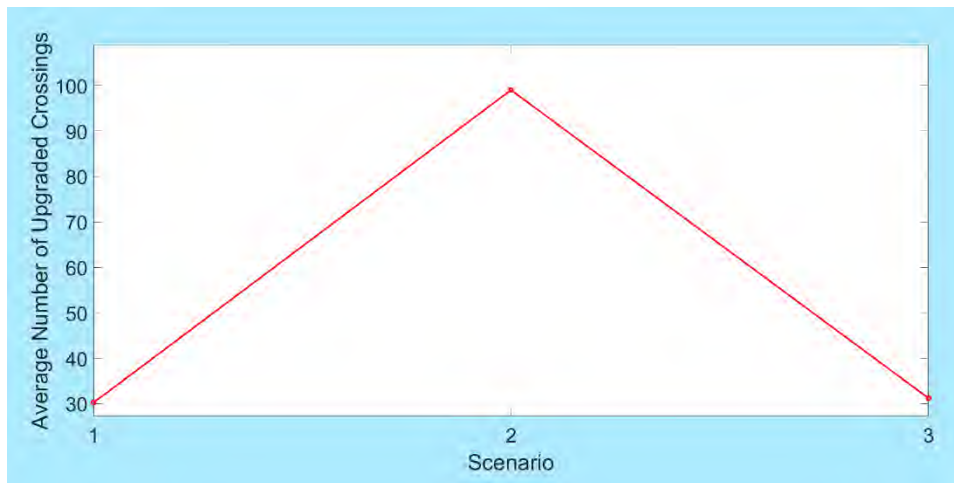


Figure 158 The average total number of highway-rail grade crossings selected for upgrading over all the PF points for each crossing type scenario (the first 6 countermeasures are available for upgrading).

Figure 159 demonstrates the average total number of highway-rail grade crossings selected for upgrading over all the PF points for each one of the considered crossing type scenarios, when all 11 countermeasures could be used for upgrading. A total of 1,392.8 highway-rail grade crossings out of the 6,109 public highway-rail grade crossings in Florida was upgraded on average in scenario 1. In scenario 2, a total of 110.4 highway-rail grade crossings out of the 2,896 private highway-rail grade crossings was selected on average for upgrades. Furthermore, in scenario 3, a

total of 1,346.4 highway-rail grade crossings out of the 9,005 public and private highway-rail grade crossings in Florida was upgraded on average. The number of upgraded highway-rail grade crossings in case of Figure 159 is substantially higher than that of Figure 158 due to the availability of more and cheaper countermeasures. Furthermore, when all 11 countermeasures were made available for selection, the average cost of implementing countermeasures at the public highway-rail grade crossings in Florida was significantly lower than that of the private highway-rail grade crossings. Hence, the average number of upgraded highway-rail grade crossings for scenario 1 is significantly higher than that of scenario 2. As discussed earlier, most of the highway-rail grade crossings selected for upgrades in scenario 3 were public, since only a small number of the private highway-rail grade crossings from the priority list, generated by the MPSDR heuristic, were ranked high enough for selection considering the total available budget. For this reason, the average number of upgraded highway-rail grade crossings for scenario 3 is very close to that of scenario 1.

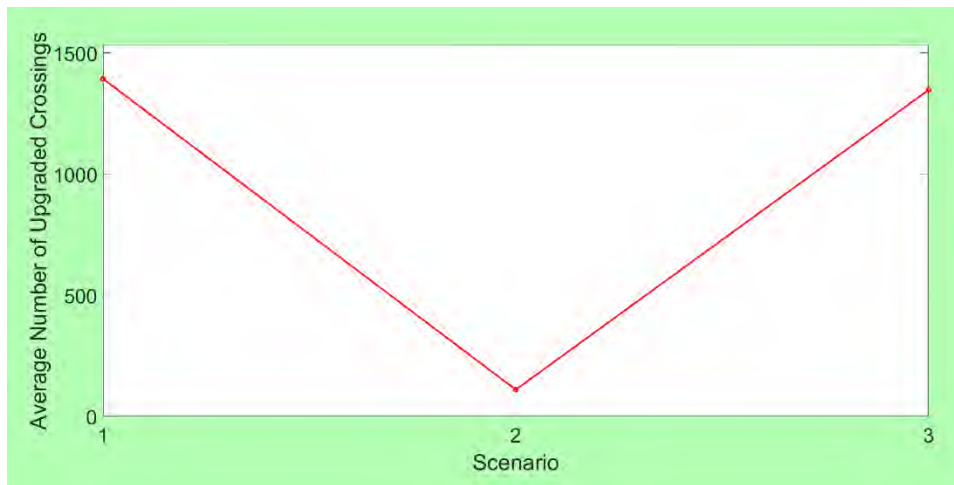


Figure 159 The average total number of highway-rail grade crossings selected for upgrading over all the PF points for each crossing type scenario (all 11 countermeasures are available for upgrading).

7.4.3. The Impact of the Crossing Type on the Average Installation Cost and the Average Effectiveness of Countermeasures Selected by MORAP

Figure 160 shows the average installation cost of countermeasures implemented at highway-rail grade crossings selected for upgrading over all the PF points for each one of the considered crossing type scenarios, when the first 6 countermeasures could be used for upgrading. When only the first 6 countermeasures were available for selection, the average installation cost of the selected countermeasures exceeded \$247,500, \$75,500, and \$239,600 in scenarios 1, 2, and 3 respectively. The high average installation cost of countermeasures in case of Figure 160 is because of the high installation cost of countermeasures “1” to “6”, which were made available in this case. Moreover, the State of Florida has a number of gated public highway-rail grade crossings, which are not eligible for countermeasures “1”, “2”, and “3”. So, the selected gated public highway-rail grade crossings were upgraded with countermeasures “4”, “5”, or “6” that are even more expensive than countermeasures “1”, “2”, and “3”. Therefore, the average installation cost of the selected countermeasures in scenario 1 is higher than that of scenario 2. The majority of the highway-rail grade crossings selected for upgrades in scenario 3 were public,

and so, the average installation cost of countermeasures in scenario 3 was close to that of scenario 1.

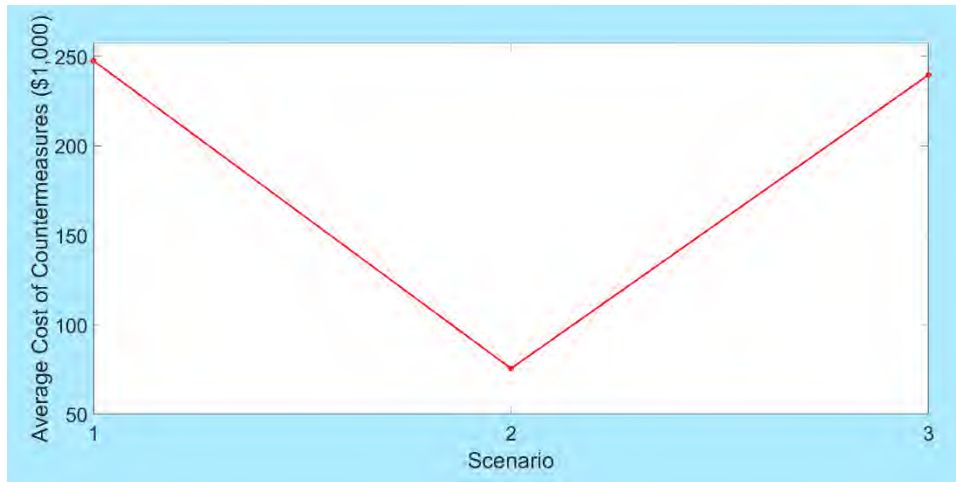


Figure 160 The average installation cost of countermeasures implemented at highway-rail grade crossings selected for upgrading over all the PF points for each crossing type scenario (the first 6 countermeasures are available for upgrading).

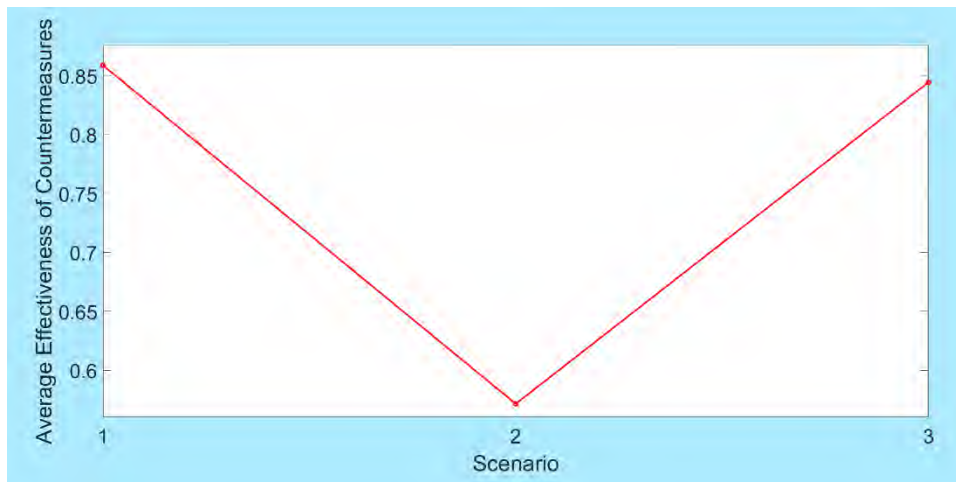


Figure 161 The average effectiveness of countermeasures implemented at highway-rail grade crossings selected for upgrading over all the PF points for each crossing type scenario (the first 6 countermeasures are available for upgrading).

Figure 161 presents the average effectiveness of countermeasures implemented at highway-rail grade crossings selected for upgrading over all the PF points for each one of the considered crossing type scenarios, when the first 6 countermeasures could be used for upgrading. The MPSDR heuristic, developed to solve the **MORAP** mathematical model, selected the countermeasures with higher effectiveness factors for scenarios 1 and 3, as the effectiveness factors for these scenarios exceeded 0.844. On the other hand, most of the private highway-rail grade crossings were not eligible for the countermeasures with fairly high effectiveness factors; hence, the countermeasures with comparatively lower effectiveness factors were recorded for scenario 2.

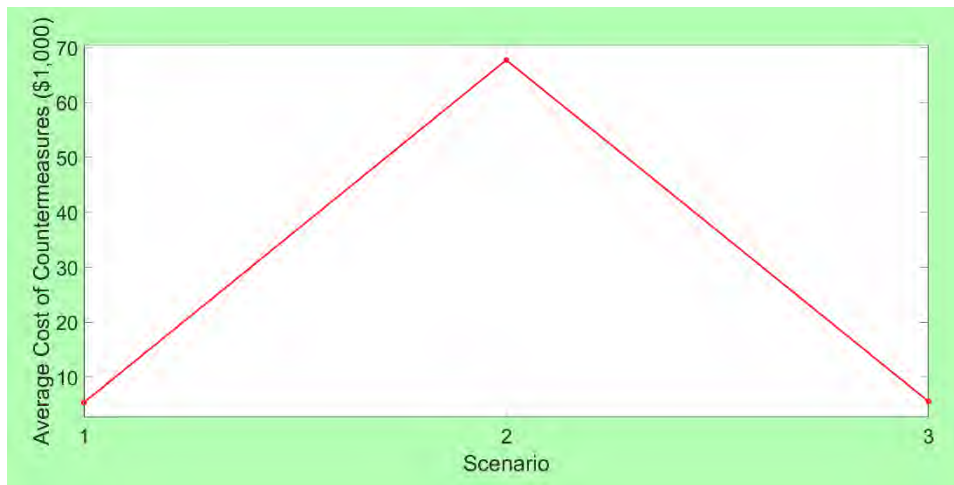


Figure 162 The average installation cost of countermeasures implemented at highway-rail grade crossings selected for upgrading over all the PF points for each crossing type scenario (all 11 countermeasures are available for upgrading).

Figure 162 shows the average installation cost of countermeasures implemented at highway-rail grade crossings selected for upgrading over all the PF points for each one of the considered crossing type scenarios, when all 11 countermeasures could be used for upgrading. When all of the 11 countermeasures were available for selection, the average installation cost of the selected countermeasures did not exceed \$5,400 in scenario 1, which can be supported by the fact that the MPSDR heuristic that was used to solve the **MORAP** mathematical model selects highway-rail grade crossings for upgrades and determines the appropriate countermeasure based on the weighted sum of normalized hazard severity reduction and normalized traffic delay reduction to cost ratios. Therefore, the low-cost countermeasures, such as countermeasure “7” (i.e., “mountable curbs [with channelized devices]”, which have an installation cost of \$15,000) or countermeasure “8” (i.e., “barrier curbs [with or without channelized devices]”, which have an installation cost of \$15,000) had better chances of being selected over the high-cost countermeasures, such as countermeasure “2” (i.e., “passive to flashing lights and gates”, which have an installation cost of \$180,900) or countermeasure “3” (i.e., “flashing lights to gates”, which have an installation cost of \$106,100). Moreover, only gated highway-rail grade crossings are eligible for the aforementioned low-cost countermeasures, and a significant portion of the public highway-rail grade crossings in Florida were gated (3,035 out of 6,109 public highway-rail grade crossings), according to the FRA crossing inventory database (i.e., WdCode = 8 or 9). On the other hand, the average installation cost of the selected countermeasures exceeded \$67,700 in scenario 2, which can be explained by the fact that only a small portion of the private highway-rail grade crossings in Florida were gated (13 out of 2,896 private highway-rail grade crossings), according to the FRA crossing inventory database (i.e., WdCode = 8 or 9). Thus, most of the private highway-rail grade crossings were not eligible for the low-cost countermeasures. Finally, the average installation cost of the selected countermeasures did not exceed \$5,600 in scenario 3. Thus, the average installation cost of countermeasures in scenario 3 was close to that of scenario 1. The latter finding can be justified by the fact that most of the highway-rail grade crossings selected for upgrades in scenario 3 were public and, therefore, were eligible for the low-cost countermeasures.

Figure 163 presents the average effectiveness of countermeasures implemented at highway-rail grade crossings selected for upgrading over all the PF points for each one of the considered crossing type scenarios, when all 11 countermeasures could be used for upgrading. The MPSDR heuristic, developed to solve the **MORAP** mathematical model, selected the countermeasures with higher effectiveness factors for scenarios 1 and 3, as the effectiveness factors for these scenarios exceeded 0.818. On the other hand, most of the private highway-rail grade crossings were not eligible for the low-cost countermeasures with fairly high effectiveness factors; hence, the countermeasures with comparatively lower effectiveness factors were recorded for scenario 2.

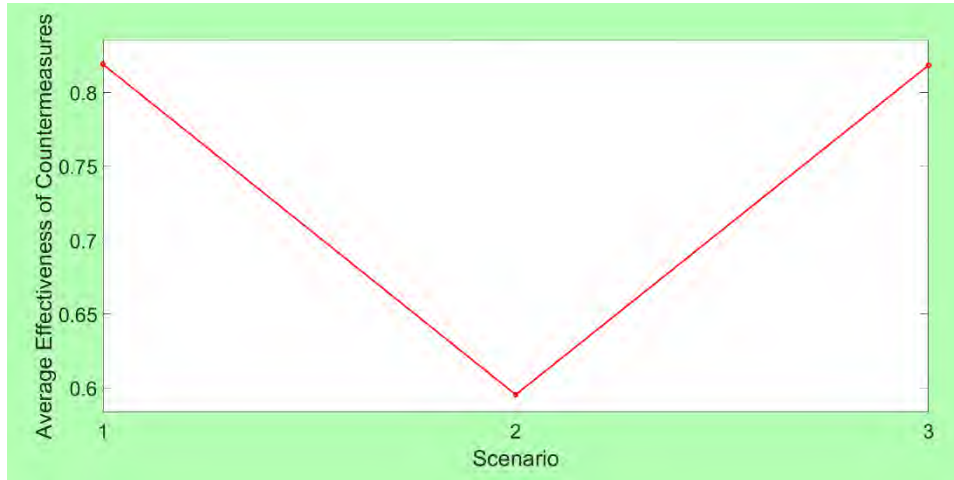


Figure 163 The average effectiveness of countermeasures implemented at highway-rail grade crossings selected for upgrading over all the PF points for each crossing type scenario (all 11 countermeasures are available for upgrading).

7.5. Evaluation of an Alternative Countermeasure

This section of the report evaluates the impact of a low-cost alternative countermeasure on multi-objective resource allocation among the highway-rail grade crossings in Florida. This alternative countermeasure is LED signs (see Figure 164). The approximate cost of an LED preemptive train warning sign is about \$1,800 to \$5,500 (TCRP-175, 2015). For the purpose of this analysis, the installation cost of LED signs was set to \$3,000, which is lower than that of the 11 default countermeasures (adopted earlier in this project based on the GradeDec.NET Reference Manual – U.S. DOT, 2014a). It is expected that many vehicles will not enter highway-rail grade crossings if they see activated LED signs. So, the effectiveness factor of LED signs was set as 0.90, which is comparable with the effectiveness factors of other low-cost countermeasures suggested by the GradeDec.NET Reference Manual. In addition, only gated highway-rail grade crossings in Florida were assumed to be eligible for installation of LED signs. Moreover, the additional delay due to application of LED signs at the highway-rail grade crossings in Florida was assumed to be the same as that of countermeasure “10” – “photo enforcement” (e.g., the drivers can be slowed down by staring at LED signs).



Figure 164 Examples of LED signs near highway-rail grade crossings.

Source: Signal-Tech. (2020). LED Light Rail Train Crossing Signals and Pedestrian Warning Signs

In order to evaluate the impact of the alternative countermeasure on multi-objective resource allocation among highway-rail grade crossings, a total of 12 budget availability scenarios was developed, where the total available budget was increased from \$4.5M in scenario 1 to \$10.0M in scenario 12, with an increment of \$0.5M. This analysis investigated all the 6,109 public highway-rail grade crossings in Florida, which were found in the FRA crossing inventory database (FRA, 2016). In order to analyze the benefits that could be achieved by the low-cost alternative countermeasure (i.e., LED signs) as compared to the 11 default countermeasures, two cases of countermeasure availabilities were used for the budget availability scenarios, including the considerations of the 11 default countermeasures as well as the 11 default countermeasures and LED signs.

7.5.1. The Impact of the Alternative Countermeasure on the MORAP Objective Functions

Figure 165 presents the PFs generated for the considered budget availability scenarios, when the 11 default countermeasures could be used for upgrading. Note that all the PFs in Figure 165 have the same limits for the horizontal and vertical axes, so that their movements can be observed with ease. It can be observed that the PFs moved from the lower-right corner in the plots to the upper-left corner, when the total available budget was increased. The PF in scenario 1 is at the lower-most-right corner, which denotes the highest overall hazard severity and the lowest overall traffic delay among the considered scenarios. On the other hand, the PF in scenario 12 is at the upper-most-left corner, which denotes the lowest overall hazard severity and the highest overall traffic delay among the considered scenarios. All these findings can be supported by the fact that

when the total available budget was increased, more highway-rail grade crossings were upgraded with countermeasures. So, the overall hazard severity decreased. However, the overall traffic delay increased at the same time due to the installation of countermeasures.

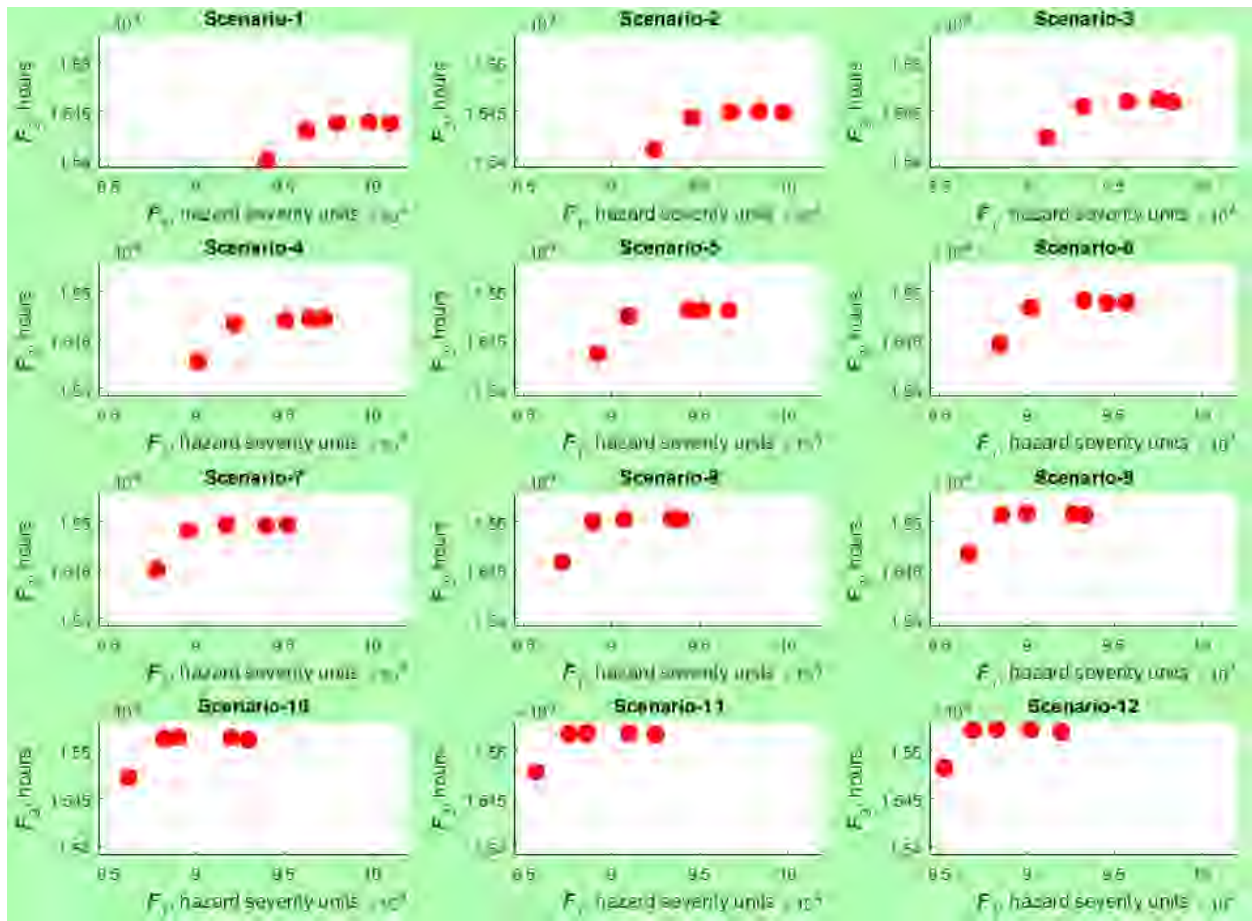


Figure 165 The PFs generated for each budget availability scenario (all 11 countermeasures are available for upgrading).

Figure 166 presents the PFs generated for the considered budget availability scenarios, when the 11 default countermeasures and LED signs could be used for upgrading. Note that all the PFs in Figure 166 have the same limits for the horizontal and vertical axes, so that their movements can be observed with ease. It can be observed that the PFs moved from the lower-right corner in the plots to the upper-left corner, when the total available budget was increased. The PF in scenario 1 is at the lower-most-right corner, which denotes the highest overall hazard severity and the lowest overall traffic delay among the considered scenarios. On the other hand, the PF in scenario 12 is at the upper-most-left corner, which denotes the lowest overall hazard severity and the highest overall traffic delay among the considered scenarios. All these findings can be supported by the fact that when the total available budget was increased, more highway-rail grade crossings were upgraded with countermeasures. So, the overall hazard severity decreased. However, the overall traffic delay increased at the same time due to the installation of countermeasures. Moreover, the shapes of the PFs in Figure 166 are different from the ones presented in Figure 165. In particular, the introduction of the low-cost alternative countermeasure (i.e., LED signs) caused a significant reduction in the overall hazard severity,

while no substantial increase was observed in terms of the overall traffic delay. Such a finding confirms the effectiveness of LED signs when comparing to the 11 default countermeasures.

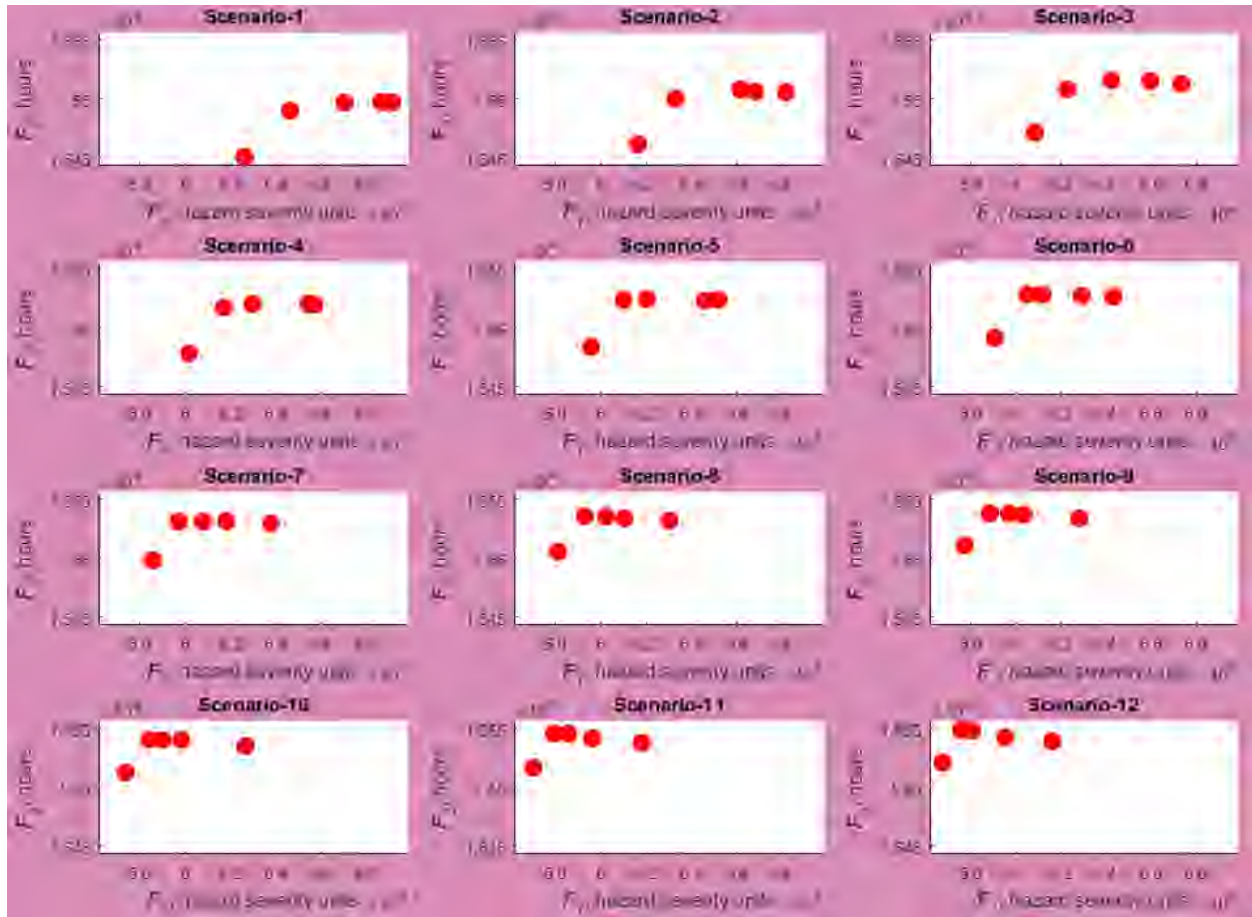


Figure 166 The PFs generated for each budget availability scenario (all 11 countermeasures and LED signs are available for upgrading).

Figure 167 shows the average overall hazard severity over all the PF points for all the public highway-rail grade crossings for each one of the considered budget availability scenarios, when the 11 default countermeasures could be used for upgrading. On the other hand, Figure 168 shows the average overall hazard severity over all the PF points for all the public highway-rail grade crossings for each one of the considered budget availability scenarios, when the 11 default countermeasures and LED signs could be used for upgrading. Similar to the overall hazard severity for each of the PF points, the average overall hazard severity over all the PF points decreased with the availability of higher budgets. The latter pattern can be explained by the fact that the total number of highway-rail grade crossings, which were selected for upgrading by the **MORAP** mathematical model, increased with the total available budget and led to a reduction in the average overall hazard severity. The change in the average overall hazard severity in Figure 167 and Figure 168 is not perfectly linear, which can be supported by the complexity of multi-objective resource allocation based on the **MORAP** mathematical model, since many different factors are considered throughout the highway-rail grade crossing upgrading decisions (e.g., eligibility of a highway-rail grade crossing for the considered countermeasures, different installation costs for the considered countermeasures, different effectiveness factors for the

considered countermeasures, hazard severity and traffic delay at a highway-rail grade crossing). The average overall hazard severity in case of Figure 168 is significantly lower than that of Figure 167 for each one of the considered budget availability scenarios. The latter finding showcases the safety benefits of LED signs.

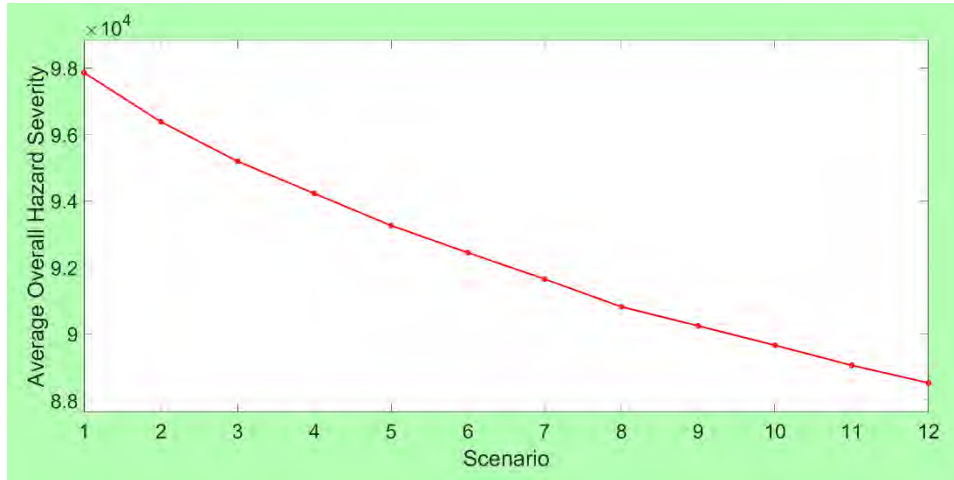


Figure 167 The average overall hazard severity over all the PF points for each budget availability scenario (all 11 countermeasures are available for upgrading).

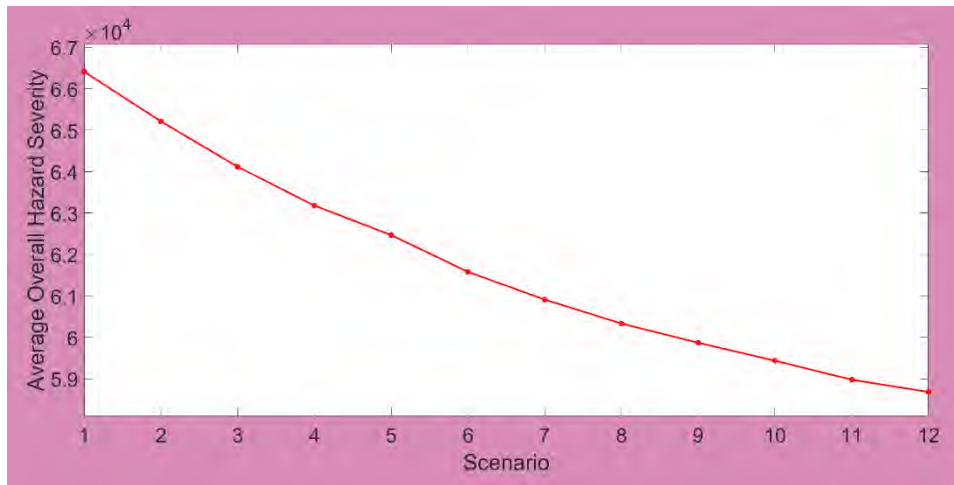


Figure 168 The average overall hazard severity over all the PF points for each budget availability scenario (all 11 countermeasures and LED signs are available for upgrading).

Figure 169 illustrates the average overall traffic delay over all the PF points for all the public highway-rail grade crossings for each one of the considered budget availability scenarios, when the 11 default countermeasures could be used for upgrading. On the other hand, Figure 170 illustrates the average overall traffic delay over all the PF points for all the public highway-rail grade crossings for each one of the considered budget availability scenarios, when the 11 default countermeasures and LED signs could be used for upgrading. Similar to the overall traffic delay for each of the PF points, the average overall traffic delay over all the PF points increased with the availability of higher budgets. The latter pattern can be explained by the fact that the total number of highway-rail grade crossings, which were selected for upgrading by the **MORAP**

mathematical model, increased with the total available budget and led to an increase in the average overall traffic delay. The change in the average overall traffic delay in Figure 169 and Figure 170 is not perfectly linear, which can be supported by the complexity of multi-objective resource allocation based on the **MORAP** mathematical model, since many different factors are considered throughout the highway-rail grade crossing upgrading decisions (e.g., eligibility of a highway-rail grade crossing for the considered countermeasures, different installation costs for the considered countermeasures, different effectiveness factors for the considered countermeasures, hazard severity and traffic delay at a highway-rail grade crossing).

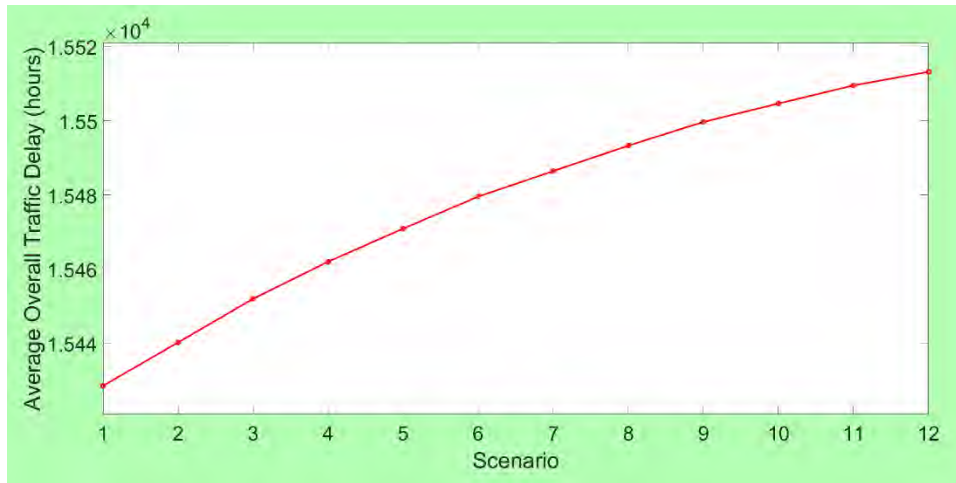


Figure 169 The average overall traffic delay over all the PF points for each budget availability scenario (all 11 countermeasures are available for upgrading).

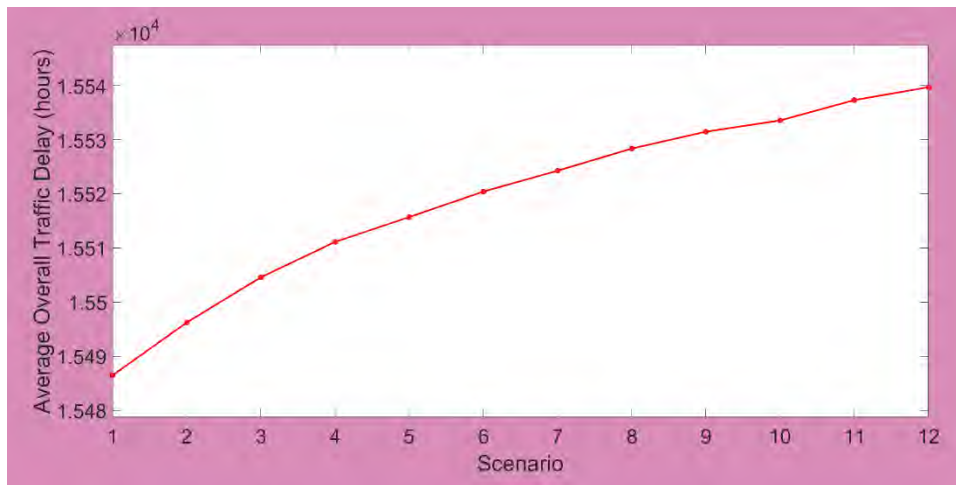


Figure 170 The average overall traffic delay over all the PF points for each budget availability scenario (all 11 countermeasures and LED signs are available for upgrading).

7.5.2. The Impact of the Alternative Countermeasure on the Number of Highway-Rail Grade Crossings Upgraded by MORAP

Figure 171 demonstrates the average total number of highway-rail grade crossings selected for upgrading over all the PF points for all the public highway-rail grade crossings for each one of the considered budget availability scenarios, when the 11 default countermeasures could be used

for upgrading. As discussed earlier, the total number of upgraded highway-rail grade crossings increased with the total available budget for each one of the PF points. Similarly, the average total number of highway-rail grade crossings selected for upgrading over all the PF points increased as well. For example, the average total number of highway-rail grade crossings selected for upgrading out of the 6,109 public highway-rail grade crossings in Florida increased from 866.8 in scenario 1 to 1,780.4 in scenario 12. The change in the average total number of upgraded highway-rail grade crossings is not perfectly linear, which demonstrates the complexity of multi-objective resource allocation based on the **MORAP** mathematical model, since many different factors are considered throughout the highway-rail grade crossing upgrading decisions (e.g., eligibility of a highway-rail grade crossing for the considered countermeasures, different installation costs for the considered countermeasures, different effectiveness factors for the considered countermeasures, hazard severity and traffic delay at a highway-rail grade crossing).

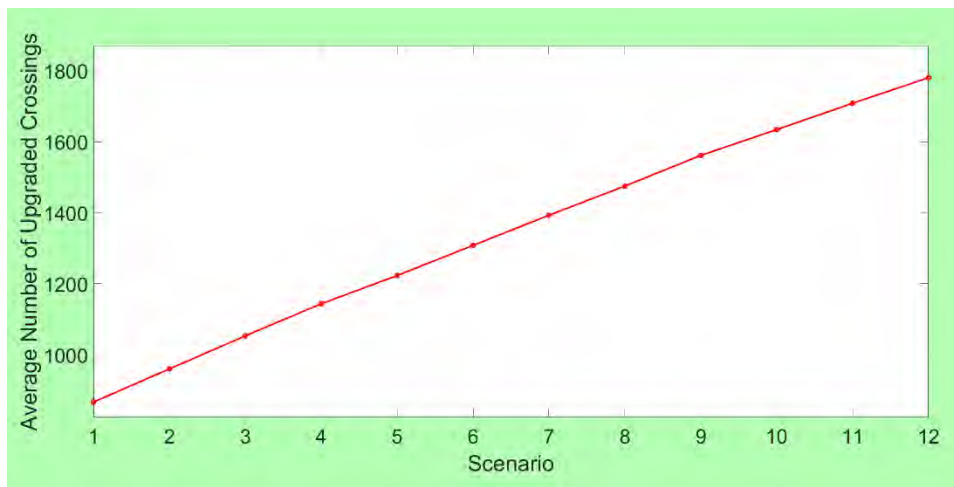


Figure 171 The average total number of highway-rail grade crossings selected for upgrading over all the PF points for each budget availability scenario (all 11 countermeasures are available for upgrading).

Figure 172 demonstrates the average total number of highway-rail grade crossings selected for upgrading over all the PF points for all the public highway-rail grade crossings for each one of the considered budget availability scenarios, when the 11 default countermeasures and LED signs could be used for upgrading. As discussed earlier, the total number of upgraded highway-rail grade crossings increased with the total available budget for each one of the PF points. Similarly, the average total number of highway-rail grade crossings selected for upgrading over all the PF points increased as well. For example, the average total number of highway-rail grade crossings selected for upgrading out of the 6,109 public highway-rail grade crossings in Florida increased from 1,415.4 in scenario 1 to 2,417.2 in scenario 12. The number of upgraded highway-rail grade crossings in case of Figure 172 is significantly higher than that of Figure 171 due to the availability of the alternative countermeasure (i.e., LED signs), which has the lowest installation cost and a high effectiveness factor. The change in the average total number of upgraded highway-rail grade crossings is nonlinear, which demonstrates the complexity of multi-objective resource allocation based on the **MORAP** mathematical model, since many different factors are considered throughout the highway-rail grade crossing upgrading decisions (e.g., eligibility of a highway-rail grade crossing for the considered countermeasures, different

installation costs for the considered countermeasures, different effectiveness factors for the considered countermeasures, hazard severity and traffic delay at a highway-rail grade crossing).

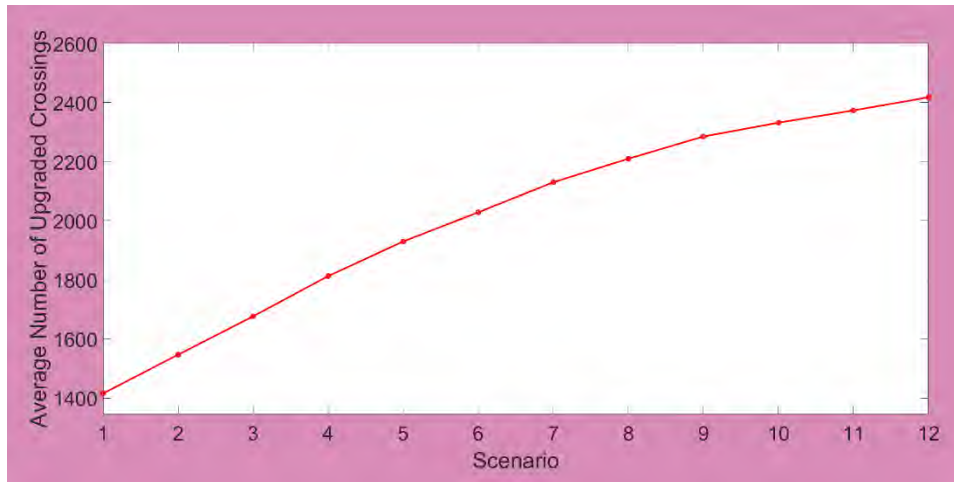


Figure 172 The average total number of highway-rail grade crossings selected for upgrading over all the PF points for each budget availability scenario (all 11 countermeasures and LED signs are available for upgrading).

7.5.3. The Impact of the Alternative Countermeasure on the Average Installation Cost and the Average Effectiveness of Countermeasures Selected by MORAP

Figure 173 shows the average installation cost of countermeasures implemented at highway-rail grade crossings selected for upgrading over all the PF points for all the public highway-rail grade crossings for each one of the considered budget availability scenarios, when the 11 default countermeasures could be used for upgrading. An increase in the total available budget allowed the **MORAP** mathematical model to select the countermeasures with higher installation costs. Still, when all of the 11 countermeasures were available for selection, the maximum average installation cost of the selected countermeasures did not exceed \$5,700 over all the developed budget availability scenarios, which can be supported by the fact that the MPSDR heuristic that was used to solve the **MORAP** mathematical model selects highway-rail grade crossings for upgrades and determines the appropriate countermeasure based on the weighted sum of normalized hazard severity reduction and normalized traffic delay reduction to cost ratios. Therefore, the low-cost countermeasures, such as countermeasure “7” (i.e., “mountable curbs [with channelized devices]”, which have an installation cost of \$15,000) or countermeasure “8” (i.e., “barrier curbs [with or without channelized devices]”, which have an installation cost of \$15,000) had better chances of being selected over the high-cost countermeasures, such as countermeasure “2” (i.e., “passive to flashing lights and gates”, which have an installation cost of \$180,900) or countermeasure “3” (i.e., “flashing lights to gates”, which have an installation cost of \$106,100). Lin et al. (2017) also indicated that considering monetary limitations, low-cost countermeasures could be efficient alternatives for safety improvements at the highway-rail grade crossings in Florida.

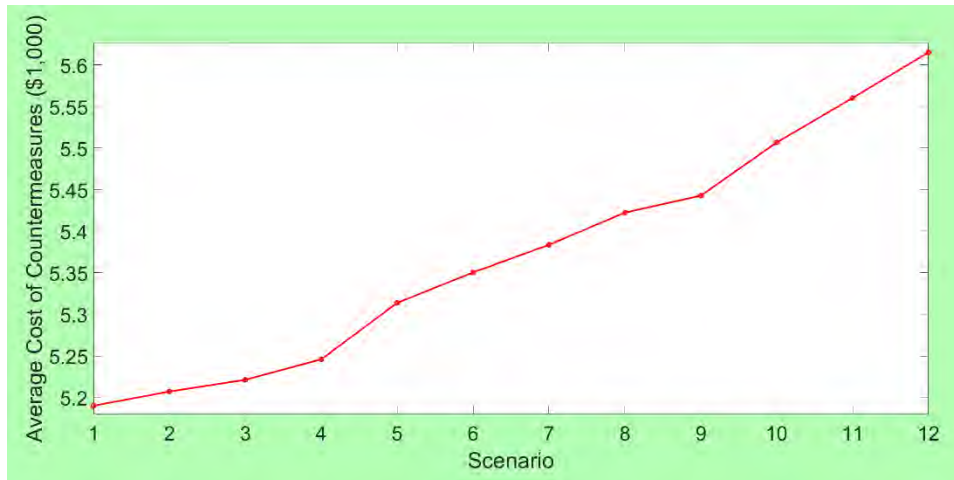


Figure 173 The average installation cost of countermeasures implemented at highway-rail grade crossings selected for upgrading over all the PF points for each budget availability scenario (all 11 countermeasures are available for upgrading).

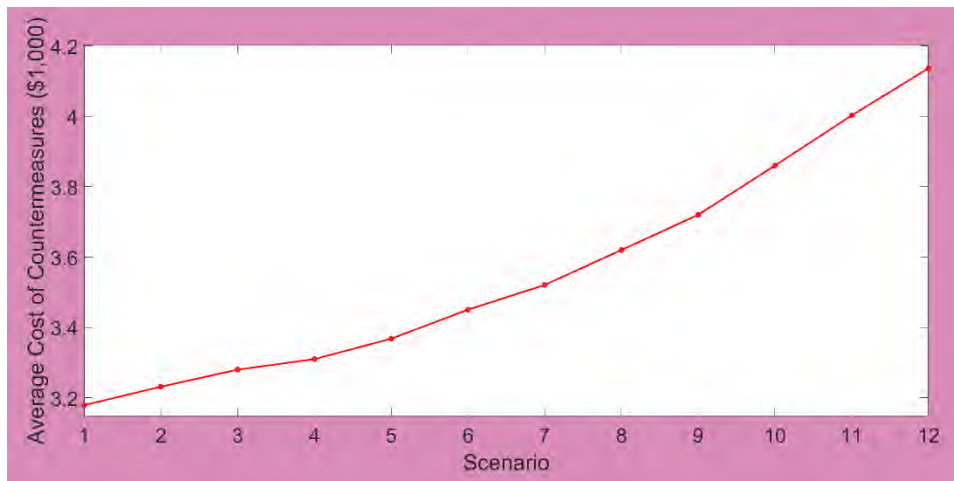


Figure 174 The average installation cost of countermeasures implemented at highway-rail grade crossings selected for upgrading over all the PF points for each budget availability scenario (all 11 countermeasures and LED signs are available for upgrading).

Figure 174 shows the average installation cost of countermeasures implemented at highway-rail grade crossings selected for upgrading over all the PF points for all the public highway-rail grade crossings for each one of the considered budget availability scenarios, when the 11 default countermeasures and LED signs could be used for upgrading. An increase in the total available budget allowed the **MORAP** mathematical model to select the countermeasures with higher installation costs. Still, when all of the 11 countermeasures were available for selection, the maximum average installation cost of the selected countermeasures did not exceed \$4,200 over all the developed budget availability scenarios, which can be supported by the fact that the **MPSDR** heuristic that was used to solve the **MORAP** mathematical model selects highway-rail grade crossings for upgrades and determines the appropriate countermeasure based on the weighted sum of normalized hazard severity reduction and normalized traffic delay reduction to cost ratios. The average installation cost of countermeasures in case of Figure 174 is significantly

lower than that of Figure 173. The latter finding can be justified by the fact that more highway-rail grade crossings were upgraded with the same total available budget because of the introduction of LED signs, whose installation cost is lower than that of the 11 default countermeasures.

Figure 175 presents the average effectiveness of countermeasures implemented at highway-rail grade crossings selected for upgrading over all the PF points for all the public highway-rail grade crossings for each one of the considered budget availability scenarios, when the 11 default countermeasures could be used for upgrading. As evidenced by Figure 175, after increasing the total available budget from one scenario to another, the MPSDR heuristic still selected the countermeasures with fairly high effectiveness. The average effectiveness of the selected countermeasures varied between ≈ 0.818 and ≈ 0.819 for the considered budget availability scenarios, when all of the 11 countermeasures could be selected throughout resource allocation.

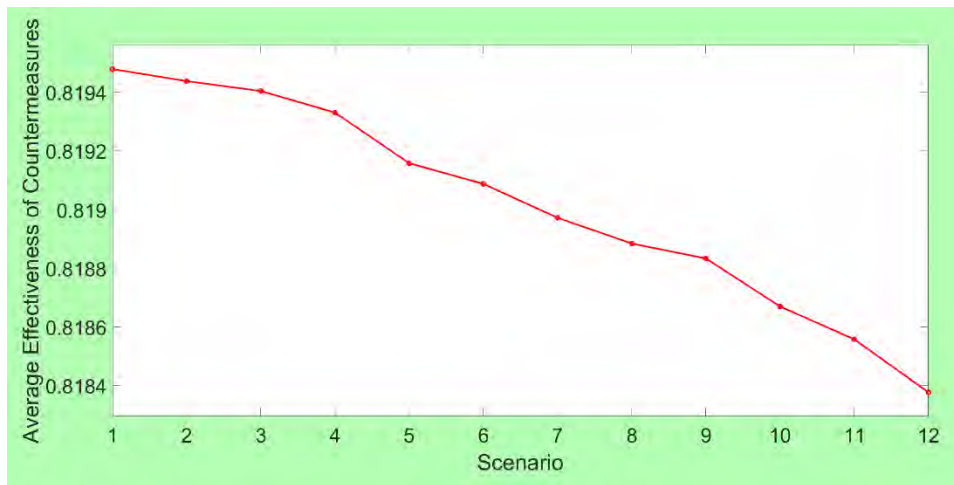


Figure 175 The average effectiveness of countermeasures implemented at highway-rail grade crossings selected for upgrading over all the PF points for each budget availability scenario (all 11 countermeasures are available for upgrading).

Figure 176 presents the average effectiveness of countermeasures implemented at highway-rail grade crossings selected for upgrading over all the PF points for all the public highway-rail grade crossings for each one of the considered budget availability scenarios, when the 11 default countermeasures and LED signs could be used for upgrading. As evidenced by Figure 176, after increasing the total available budget from one scenario to another, the MPSDR heuristic still selected the countermeasures with fairly high effectiveness. The average effectiveness of the selected countermeasures varied between ≈ 0.896 and ≈ 0.899 for the considered budget availability scenarios, when the 11 default countermeasures and LED signs could be selected throughout resource allocation. The average effectiveness of countermeasures in case of Figure 176 is significantly higher than that of Figure 175 for each one of the considered budget availability scenarios. The latter finding demonstrates the safety benefits offered by LED signs.

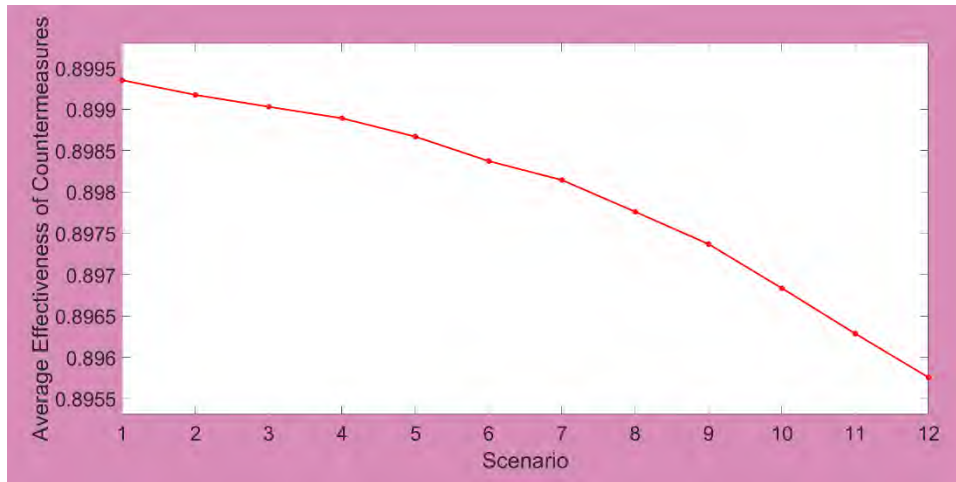


Figure 176 The average effectiveness of countermeasures implemented at highway-rail grade crossings selected for upgrading over all the PF points for each budget availability scenario (all 11 countermeasures and LED signs are available for upgrading).

8. CONCLUSIONS AND FUTURE RESEARCH

The State of Florida is currently the third most populous state in the U.S. More and more residents from other states are now migrating to Florida, thus increasing the population of this state faster than that of the nation. Because of this increasing population, a substantial amount of freight is transported in Florida. Moreover, Florida is now the 17th largest economy in the world, which boosts the Gross Domestic Product (GDP) that is more than \$1 trillion. Freight-associated industries, which are also growing, play a major role in the economic growth of the State of Florida. As such, a large volume of freight is handled in the state by various modes (e.g., road, rail, sea). Rail is an important mode of freight transportation in Florida, as 15.8% of freight tonnage is exported by rail in Florida. Railroad transportation-based activities have increased in Florida, leading to greater economic impacts as well as more highway-rail crossing accidents. For instance, a total of 135 highway-rail crossing accidents was recorded in Florida in the year 2019, as compared to 51 highway-rail crossing accidents in the year 2009.

Since the number of highway-rail grade crossing accidents in Florida has been increasing, safety issues at the state highway-rail grade crossings should be mitigated. The latter objective can be achieved with various countermeasures, such as installation of various warning devices, traffic signal preemption, grade separation, and others. However, installation of countermeasures along with halting of the associated highway traffic, because of passing trains, may add delays at a highway-rail grade crossing. Various ways to quantify such delays have been discussed in this study, which include the methodologies suggested by the Institute of Transportation Engineers (ITE), the U.S. DOT Highway Rail Crossing Handbook, NCHRP Report 288, Okitsu et al. (2010), the Southern California International Gateway Draft EIR, the Center for Urban Transportation Research (the University of South Florida), and the Surface Transportation Board (STB). Moreover, upgrading all the highway-rail grade crossings in Florida is not feasible with the limited budget that is set aside for safety improvement projects. Therefore, the Florida Department of Transportation (FDOT) needs to assign countermeasures to the highway-rail grade crossings in Florida in an effective manner, so that safety issues at these highway-rail grade crossings are addressed, while passenger and freight flows are not significantly impaired.

In order to address the aforementioned issues, this project has developed a mathematical model, named the Multi-Objective Resource Allocation Problem (**MORAP**), which aims to minimize the overall hazard severity and to minimize the overall traffic delay at the considered highway-rail grade crossings with the application of selected countermeasures. The highway-rail grade crossing hazard was assessed based on the Florida Priority Index Formula that incorporates several factors, such as the average daily traffic volume, average daily train volume, train speed, protection factor, and accident history parameter (the total number of accidents in the last five years or since the year of last improvement in case there was an upgrade). A novel approach was developed for estimation of the overall traffic delay due to application of a countermeasure at a highway-rail grade crossing based on the number of blockage occurrences (i.e., number of trains) and the overall delay experienced by queued vehicles during each blockage. In particular, the overall delay experienced by queued vehicles during each blockage was computed based on the delay time for a given highway-rail grade crossing caused by the implemented countermeasure, average train length, average train speed, average number of vehicles arriving per day, and number of highway lanes.

A total of three solution algorithms was developed for the **MORAP** mathematical model, including the following: (1) Epsilon-Constraint (ECON) method; (2) Multi-Objective Profitable Severity and Delay Reduction (MPSDR) heuristic; and (3) Multi-Objective Effective Severity and Delay Reduction (MESDR) heuristic. All the developed candidate algorithms were evaluated in terms of both solution quality and computational time criteria. Based on the analysis results, the MPSDR heuristic was recommended as a solution approach for the **MORAP** mathematical model, as it demonstrated a competitive performance in terms of both solution quality and computational time criteria. In particular, the PFs produced by the MPSDR heuristic did not differ by more than 1.05% and 1.80% on average as compared to the optimal PFs produced by the ECON method in terms of the best overall hazard severity and traffic delay values, respectively. Moreover, the MPSDR maximum computational time did not exceed 192.1 seconds over the generated scenarios and developed problem instances.

Furthermore, a standalone application “HRX Safety Improvement” was developed as a part of this project to assist the FDOT personnel with the following functions: (1) estimation of the overall hazard severity for the considered highway-rail grade crossings; (2) estimation of the overall traffic delay for the considered highway-rail grade crossings before and after application of the candidate countermeasures; and (3) resource allocation for the considered highway-rail grade crossings (i.e., assign countermeasures to the considered highway-rail grade crossings in order to minimize the overall hazard severity and to minimize the overall traffic delay based on the total available budget). The purpose of the application, installation guidelines, and basic user guidelines were outlined in this report.

A set of computational experiments was performed to illustrate applicability of the proposed methodology for conducting multi-objective resource allocation in order to minimize the overall hazard severity and to minimize the overall traffic delay at the existing highway-rail grade crossings in Florida. A comprehensive description of the computational experiments was presented in this report. Specifically, the following analyses were performed as a part of the experiments: (1) sensitivity analysis for the total available budget; (2) sensitivity analysis for the number of available countermeasures; (3) sensitivity analysis for the hazard severity weight values; (4) resource allocation among various crossing types; and (5) evaluation of an alternative countermeasure (i.e., light-emitting diode [LED] signs). Throughout all of these analyses, the **MORAP** mathematical model was solved with the MPSDR heuristic.

The computational experiments explicitly demonstrated that the developed methodology, including the **MORAP** mathematical model, the MPSDR heuristic, and the “HRX Safety Improvement” standalone application, can serve as an effective decision support system for the FDOT personnel and assist with reducing the overall hazard severity and the overall traffic delay at the highway-rail grade crossings in Florida under different budget availability, countermeasure availability, hazard severity weight, and crossing type scenarios. Moreover, the introduction of alternative countermeasures, such as LED signs, could facilitate multi-objective resource allocation among highway-rail grade crossings and make it more efficient.

The future research opportunities for this study include, but are not limited to, the following:

- First, the methodology proposed in this study does capture the overall hazard severity and overall traffic delay at highway-rail grade crossings. Additional features can be captured throughout multi-objective resource allocation among highway-rail grade crossings as well to account for certain important practical considerations. In particular, the emissions produced by the vehicles queued at highway-rail grade crossings can be accounted for, as these emissions cause the environmental problems and negatively impact the quality of life in the areas surrounding a given highway-rail grade crossing. Furthermore, extensive traffic delays at highway-rail grade crossings may create long vehicle queues and increase the risk of queue spillbacks at the adjacent highway intersections. Minimizing the risk of queue spillbacks at the highway intersections adjacent to highway-rail grade crossings can be another important objective function.
- Second, this study used an approach for assessing the hazard severity at highway-rail grade crossings (i.e., the expected fatality hazard, injury hazard, and property damage hazard), which was recommended by the U.S. DOT. The future research can focus on the development of more advanced and accurate approaches for assessing hazard severity at highway-rail grade crossings.
- Third, as a part of the future research, a set of simulation models can be developed to accurately emulate collisions between highway vehicles and passing trains at highway-rail grade crossings. Such models could be further used to accurately assess the impacts of collisions on the passengers inside highway vehicles and trains.
- Fourth, COVID-19 substantially affected passenger and traffic flows across the U.S. The future research could investigate the COVID-19 effects on rail transportation in Florida with a particular focus on accidents at highway-rail grade crossings (i.e., determine whether the COVID-19 pandemic caused any changes in the accident patterns at highway-rail grade crossings in Florida). Some managerial insights can be obtained regarding the features and causes of highway-rail grade crossing accidents during the COVID-19 pandemic.

REFERENCES

1. Abioye, O.F., Dulebenets, M.A., Kavooosi, M., Pasha, J. and Theophilus, O., 2020. Vessel Schedule Recovery in Liner Shipping: Modeling Alternative Recovery Options. *IEEE Transactions on Intelligent Transportation Systems*, pp.1-15.
2. Abioye, O.F., Dulebenets, M.A., Pasha, J. and Kavooosi, M., 2019. A vessel schedule recovery problem at the liner shipping route with emission control areas. *Energies*, 12(12), p.2380.
3. Abraham, J., Datta, T.K., and Datta, S., 1998. Driver Behavior at Rail–Highway Crossings. *Transportation Research Record*, 1648, pp. 28-34.
4. ALFAZETA, 2020. Advantages of Flip Dot Boards. [online]. Available at: <https://flipdots.com/en/advantages-of-electromagnetic-flip-disc-technology/>. [Accessed 20 August 2020].
5. AREMA, 2004. Highway-Rail Grade Crossing Warning Systems. Communications and Signal Manual, Section 3. Landover, MD.
6. Association of American Railroads, 2020. Freight Rail & Highly Automated Vehicles. [online]. Available at: <https://www.aar.org/article/freight-rail-highly-automated-vehicles/>. [Accessed 20 August 2020].
7. Bazgan, C., Hugot, H. and Vanderpooten, D., 2009. Solving efficiently the 0–1 multi-objective knapsack problem. *Computers & Operations Research*, 36(1), pp. 260-279.
8. BEA, 2020. Gross Domestic Product by State: 4th Quarter and Annual 2019. [online]. Available at: <https://www.bea.gov/system/files/2020-04/qgdpstate0420.pdf>. [Accessed 27 May 2020].
9. BNSF Railway, 2017. Positive Train Control and BNSF in the Pacific Northwest. [online]. Available at: <https://bnsfnorthwest.com/news/2017/12/22/positive-train-control-bnsf-pacific-northwest/>. [Accessed 20 August 2020].
10. Briginshaw, D., 2019. Rail is on the Way to Autonomous Trains. *International Railway Journal*. [online]. Available at: <https://www.railjournal.com/opinion/rail-autonomous-trains>. [Accessed 20 August 2020].
11. California Short Line Railroad Association, 2019. Railroad Day in Sacramento. [online]. Available at: <https://www.csra.org/?m=201903>. [Accessed 20 August 2020].
12. Carlson, P.J. and Fitzpatrick, K., 1999. Violations at Gated Highway–Railroad Grade Crossings. *Transportation Research Record*, 1692, pp. 66-73.
13. Chang, C.S., Wang, W., Liew, A.C., Wen, F.S. and Srinivasan, D., 1995. Genetic algorithm based bicriterion optimization for traction substations in DC railway system. In: *Proceedings of the IEEE Conference on Evolutionary Computation*. [online]. Perth, Australia: IEEE, pp. 11-16. Available at: <https://ieeexplore.ieee.org/document/489111>. [Accessed 01 Oct 2018].
14. Chang, T.J., Meade, N., Beasley, J.E. and Sharaiha, Y.M., 2000. Heuristics for cardinality constrained portfolio optimisation. *Computers & Operations Research*, 27(13), pp.1271-1302.
15. Chekuri, C. and Khanna, S., 2005. A polynomial time approximation scheme for the multiple knapsack problem. *SIAM Journal on Computing*, 35(3), pp. 713-728.
16. Chicago Metropolitan Agency for Planning, 2015. Highway Capacity Measurements: Grade Crossing Saturation Flows Chicago Region, 2013. Draft Technical Update. [online]. Available at: https://www.cmap.illinois.gov/documents/10180/481346/GradeCrossingCapacityReport_20151020.pdf/c3520921-b26c-449b-a020-ffcc236fa7ba. [Accessed 27 May 2020].

17. Coleman, F., and Venkataraman, K., 2001. Driver Behavior at Vehicle Arresting Barriers: Compliance and Violations during the First Year at the McLean Site. *Transportation Research Record*, 1754, pp. 68-76.
18. Cook, J., 2018. The Right Tool for the Job: Active and Passive Infrared Sensors. [online]. Available at: <https://www.arrow.com/>. [Accessed 20 August 2020].
19. Cook, S., 2006. *The P versus NP Problem*. [online] Oxford, U.K.: Clay Mathematics Institute. [online]. Available at: <http://www.claymath.org/sites/default/files/pvsnp.pdf>. [Accessed 21 Dec 2018].
20. CUTR, 2014. Coordinated Pre-Preemption of Traffic Signals to Enhance Railroad Grade Crossing Safety in Urban Areas and Estimation of Train Impacts to Arterial Travel Time Delay. Prepared for the Florida Department of Transportation. [online]. Available at: https://rosap.ntl.bts.gov/view/dot/26860/dot_26860_DS1.pdf. [Accessed 27 May 2020].
21. Dammeyer, F. and Voss, S., 1991. *Application of Tabu Search Strategies for Solving Multiconstraint Zero-One Knapsack Problems*. Working Paper. Technische Hochschule Darmstadt.
22. Donahey, M., 2019. Council Evaluating Railroad ‘Quiet Zones’. Available at: <https://www.timesrepublican.com/news/todays-news/2019/07/council-evaluating-railroad-quiet-zones/>. [Accessed 20 August 2020].
23. Drexl, A., 1988. A Simulated Annealing approach to the multiconstraint zero-one knapsack problem. *Computing*, 40(1), pp. 1-8.
24. Dulebenets, M.A., 2015. Bunker consumption optimization in liner shipping: A metaheuristic approach. *International Journal on Recent and Innovation Trends in Computing and Communication*, 3(6), pp.3766-3776.
25. Dulebenets, M.A., 2016. Advantages and disadvantages from enforcing emission restrictions within emission control areas. *Maritime Business Review*, 1(2), pp.107-132.
26. Dulebenets, M.A., 2018a. A comprehensive multi-objective optimization model for the vessel scheduling problem in liner shipping. *International Journal of Production Economics*, 196, pp.293-318.
27. Dulebenets, M.A., 2018b. Application of evolutionary computation for berth scheduling at marine container terminals: Parameter tuning versus parameter control. *IEEE Transactions on Intelligent Transportation Systems*, 19(1), pp.25-37.
28. Dulebenets, M.A., 2018c. A comprehensive evaluation of weak and strong mutation mechanisms in evolutionary algorithms for truck scheduling at cross-docking terminals. *IEEE Access*, 6, pp.65635-65650.
29. Dulebenets, M.A., 2018d. A diploid evolutionary algorithm for sustainable truck scheduling at a cross-docking facility. *Sustainability*, 10(5), p.1333.
30. Dulebenets, M.A., 2018e. A novel memetic algorithm with a deterministic parameter control for efficient berth scheduling at marine container terminals. *Maritime Business Review*, 2(4), pp.302-330.
31. Dulebenets, M.A., 2018f. Evaluation of non-parametric selection mechanisms in evolutionary computation: A case study for the machine scheduling problem. In: J. Del Ser Lorente, E. Osaba, eds., *Nature-inspired Methods for Stochastic, Robust and Dynamic Optimization*, 1st ed. IntechOpen: United Kingdom, pp. 23-45.
32. Dulebenets, M.A., 2018g. Green vessel scheduling in liner shipping: Modeling carbon dioxide emission costs in sea and at ports of call. *International Journal of Transportation Science and Technology*, 7(1), pp.26-44.

33. Dulebenets, M.A., 2018h. The green vessel scheduling problem with transit time requirements in a liner shipping route with Emission Control Areas. *Alexandria Engineering Journal*, 57(1), pp.331-342.
34. Dulebenets, M.A., 2018i. The vessel scheduling problem in a liner shipping route with heterogeneous fleet. *International Journal of Civil Engineering*, 16(1), pp.19-32.
35. Dulebenets, M.A., 2019a. A Delayed Start Parallel Evolutionary Algorithm for just-in-time truck scheduling at a cross-docking facility. *International Journal of Production Economics*, 212, pp.236-258.
36. Dulebenets, M.A., 2019b. Minimizing the total liner shipping route service costs via application of an efficient collaborative agreement. *IEEE Transactions on Intelligent Transportation Systems*, 20(1), pp.123-136.
37. Dulebenets, M.A., 2020. An Adaptive Island Evolutionary Algorithm for the berth scheduling problem. *Memetic Computing*, 12(1), pp.51-72.
38. Dulebenets, M.A., Kavooosi, M., Abioye, O. and Pasha, J., 2018. A self-adaptive evolutionary algorithm for the berth scheduling problem: towards efficient parameter control. *Algorithms*, 11(7), p.100.
39. Dulebenets, M.A., Moses, R., Sobanjo, J., Ozguven, E.E., Abioye, O.F., Kavooosi, M. and Pasha, J., 2020a. Development of the Optimization Model for Improving Safety at Rail Crossings in Florida. A Technical Report Prepared for the Florida Department of Transportation. Florida Department of Transportation. Tallahassee, FL.
40. Dulebenets, M.A., Pasha, J., Abioye, O.F., Kavooosi, M., Ozguven, E.E., Moses, R., Boot, W.R. and Sando, T., 2019. Exact and heuristic solution algorithms for efficient emergency evacuation in areas with vulnerable populations. *International Journal of Disaster Risk Reduction*, 39, p.101114.
41. Dulebenets, M.A., Pasha, J., Kavooosi, M., Abioye, O.F., Ozguven, E.E., Moses, R., Boot, W.R. and Sando, T., 2020b. Multiobjective optimization model for emergency evacuation planning in geographical locations with vulnerable population groups. *Journal of Management in Engineering*, 36(2), p.04019043.
42. Elliott, D., Keen, W., and Miao, L., 2019. Recent Advances in Connected and Automated Vehicles. *Journal of Traffic and Transportation Engineering (English Edition)*, 6(2), pp. 109-131.
43. Elmore Group, 2020. Microwave Vehicle Detection. [online]. Available at: <http://www.elmore.ie/its/microwave-vehicle-detection/>. [Accessed 25 August 2020].
44. FDOT, 2010. The Florida Rail System Plan: Investment Element. [online]. Available at: <https://fdotwww.blob.core.windows.net/sitefinity/docs/default-source/content/rail/plandevl/documents/finalinvestmentelement/a-2010flrailplan-investmentelement.pdf>. [Accessed 27 May 2020].
45. FDOT, 2011. Florida's Highway-Rail Grade Crossing Safety Action Plan. Florida. [online]. Available at: https://fdotwww.blob.core.windows.net/sitefinity/docs/default-source/rail/plans/safety-action-plan/fcsap0811.pdf?sfvrsn=85d8a4e9_4. [Accessed 27 November 2020].
46. FDOT, 2013. Improved Traffic Control Measures to Prevent Incorrect Turns at Highway-Rail Grade Crossings. [online]. Available at: <https://www.nctr.usf.edu/wp-content/uploads/2013/12/77950.pdf>. [Accessed 20 August 2020].
47. FDOT, 2018. Florida Rail System Plan – 2018 Update. [online]. Available at: <https://fdotwww.blob.core.windows.net/sitefinity/docs/default->

- source/rail/publications/plans/rail/2018/rail-plan_dec-2018.pdf?sfvrsn=40a652e2_2. [Accessed 27 May 2020].
48. FDOT, 2020. Freight Mobility and Trade Plan. [online]. Available at: https://fdotwww.blob.core.windows.net/sitefinity/docs/default-source/rail/fmtp/april-2020/fmtp-tm-vp-april-2020.pdf?sfvrsn=5ec40f68_8. [Accessed 27 May 2020].
49. FHWA, 2002. Status of the Nation's Highways, Bridges, and Transit: 2002 Conditions and Performance Report. Chapter 26: Highway-Rail Grade Crossings. [online]. Available at: <https://www.fhwa.dot.gov/policy/2002cpr/ch26.cfm>. [Accessed 27 May 2020].
50. FHWA, 2007. A Summary of Vehicle Detection and Surveillance Technologies Used in Intelligent Transportation Systems. [online]. Available at: <https://www.fhwa.dot.gov/policyinformation/pubs/vdstits2007/vdstits2007.pdf>. [Accessed 20 August 2020].
51. FHWA, 2016. Freight Analysis Framework Inter-Regional Commodity Flow Forecast Study: Final Forecast Results Report. U.S. Department of Transportation. Federal Highway Administration. [online]. Available at: <https://ops.fhwa.dot.gov/publications/fhwahop16043/fhwahop16043.pdf>. [Accessed 27 May 2020].
52. FHWA, 2019. Status of the Nation's Highways, Bridges, and Transit: Conditions and Performance Report – 23rd edition. [online]. Available at: <https://www.fhwa.dot.gov/policy/23cpr/pdfs/23cpr.pdf>. [Accessed 27 May 2020].
53. FIERCE Telecom, 2020. Nokia Turns up AI for Railroad Crossing Safety Trials in Japan. [online]. Available at: <https://www.fiercetelecom.com/ai/nokia-turns-up-ai-for-railroad-crossing-safety-trials-japan>. [Accessed 20 August 2020].
54. FRA, 2004. Benefits and Costs of Positive Train Control. Report in Response to Request of Appropriations Committees. [online]. Available at: <https://rsac.fra.dot.gov/radcms.rsac/File/DownloadFile?id=39>. [Accessed 20 August 2020].
55. FRA, 2016. FRA Data Dictionary for External Use Grade Crossing Inventory System (GCIS) v2.5.0.0. U.S. Department of Transportation. Federal Railroad Administration. Office of Railroad Safety.
56. FRA, 2020a. Highway-Rail Crossing Inventory Data. [online]. Available at: <https://safetydata.fra.dot.gov/officeofsafety/publicsite/downloaddbf.aspx>. [Accessed 27 May 2020].
57. FRA, 2020b. Accident/Incident Data. [online]. Available at: https://safetydata.fra.dot.gov/OfficeofSafety/publicsite/on_the_fly_download.aspx. [Accessed 27 May 2020].
58. Fréville, A., 2004. The multidimensional 0–1 knapsack problem: An overview. *European Journal of Operational Research*, 155(1), pp. 1-21.
59. GAMS, 2020. Cutting Edge Modeling. [online]. Available at: <https://www.gams.com/>. [Accessed 27 November 2020].
60. GAO, 2019. RAIL SAFETY: Freight Trains are Getting Longer, and Additional Information is Needed to Assess Their Impact. [online]. Available at: <https://www.gao.gov/assets/700/699396.pdf> [Accessed 10 December 2020].
61. Gebauer, O., Pree, W., Hanis, G., and Stadlmann, B., 2012. Towards Autonomously Driving Trains on Tracks with Open Access. *19th ITS World Congress*. Vienna, Austria. October 22-26, 2012. [online]. Available at:

- <https://www.softwareresearch.net/fileadmin/src/docs/publications/ITS.pdf>. [Accessed 20 August 2020].
62. Gilmore, P.C. and Gomory, R.E., 1966. The theory and computation of knapsack functions. *Operations Research*, 14(6), pp. 1045-1074.
63. Green, C.J., 1967. *Two Algorithms for Solving Independent Multidimensional Knapsack Problems*. Management Sciences Report, no. 110, Carnegie institute of Technology, Graduate School of Industrial Administration, Pittsburgh, PA.
64. Güntzer, M.M. and Jungnickel, D., 2000. Approximate minimization algorithms for the 0/1 knapsack and subset-sum problem. *Operations Research Letters*, 26(2), pp. 55-66.
65. Hanafi, S., Fréville, A. and El Abdellaoui, A., 1996. Comparison of heuristics for the 0–1 multidimensional knapsack problem. In: I.H. Osman, J.P. Kelly, eds., *Meta-Heuristics*, 1st ed. Springer: Boston, MA, pp. 449-465.
66. Harb, J., 2019. Challenges of the Autonomous Train. [online]. Available at: <https://blog.irt-systemx.fr/challenges-of-the-autonomous-train>. [Accessed 20 August 2020].
67. Hartong, M., Goel, R., and Wijesekera, D., 2011. Positive Train Control (PTC) Failure Modes. *Journal of King Saud University – Science*, 23(3), pp. 311-321.
68. Hilleary, T.N. and John, R.S., 2011. Development and Testing of a Radar-Based Non-Embedded Vehicle Detection System for Four Quadrant Gate Warning Systems and Blocked Crossing Detection. [online]. Available at: https://www.arena.org/files/library/2011_Conference_Proceedings/Development-Testing-Radar-Based_Non-Embedded_Vehicle_Detection_System-4_Quadrant_Gate_Warning_Systems-Blocked_Crossing_Detection.pdf. [Accessed 20 August 2020].
69. Ibaraki, T., 1987. Enumerative Approaches to Combinatorial Optimization - Part II. *Annals of Operations Research*, 11.
70. Iowa DOT, 2020. Use of a Benefit-Cost Ratio to Prioritize Projects for Funding. [online]. Available at: https://www.iowadot.gov/iowarail/assistance/130/130SelectionProcess_final.pdf. [Accessed 10 October 2020].
71. Isaka S., 1983. *Double Relaxation Dynamic Programming Methods for the Multi-Dimensional Knapsack Problem*. Master Thesis. Kyoto University.
72. ITE, 2006. Preemption of Traffic Signals Near Railroad Crossings: An ITE Recommended Practice. Institute of Transportation Engineers. [online]. Available at: <https://www.ite.org/pub/?id=e1dca8bc%2D2354%2Dd714%2D51cd%2Dbd0091e7d820>. [Accessed 27 May 2020].
73. Jusayan, J., 2015. Delay Due to Level Crossing. [online]. Available at: https://levelcrossings.vic.gov.au/__data/assets/pdf_file. [Accessed 27 September 2020].
74. Karp, R.M., 1972. Reducibility among combinatorial problems. In: R.E. Miller, J.W. Thatcher, J.D. Bohlinger, eds., *Complexity of Computer Computations*, 1st ed. Springer: Boston, MA, pp. 85-103.
75. Kavooosi, M., Dulebenets, M.A., Abioye, O.F., Pasha, J., Wang, H. and Chi, H., 2019. An augmented self-adaptive parameter control in evolutionary computation: A case study for the berth scheduling problem. *Advanced Engineering Informatics*, 42, p.100972.
76. Kavooosi, M., Dulebenets, M.A., Pasha, J., Abioye, O.F., Moses, R., Sobanjo, J. and Ozguven, E.E., 2020a. Development of Algorithms for Effective Resource Allocation among Highway–Rail Grade Crossings: A Case Study for the State of Florida. *Energies*, 13(6), p.1419.

77. Kavvoosi, M., Dulebenets, M.A., Abioye, O., Pasha, J., Theophilus, O., Wang, H., Kampmann, R. and Mikijeljević, M., 2020b. Berth scheduling at marine container terminals. *Maritime Business Review*, 5(1), pp.30-36.
78. Khattak, A., 2014. Investigation of Train Warning Times and Gate Violations. *Transportation Research Record*, 2458, pp. 104-109.
79. Khuri, S., Bäck, T. and Heitkötter, J., 1994. The zero/one multiple knapsack problem and Genetic Algorithms. In: *Proceedings of the 1994 ACM Symposium on Applied Computing*. [online]. Phoenix, AZ: ACM, pp. 188-193. Available at: <http://citeseerx.ist.psu.edu/viewdoc/download?doi=10.1.1.51.2713&rep=rep1&type=pdf>. [Accessed 01 Oct 2018].
80. Klassy, T., 2017. Railroad Crossing Lights. Available at: <https://fineartamerica.com/featured/railroad-crossing-lights-todd-klassy.html>. [Accessed 20 August 2020].
81. Lin, P., Wang, Z., Vasili, A., and Schultz, D., 2017. A Pilot Study for Preventing Incorrect Turns at Highway-Rail Grade Crossings. A Technical Report Prepared for Florida Department of Transportation.
82. Magnetic Signal Co., 2020. Magnetic Wigwag Crossing Flagman. Signal Accessories and Supplies. [online]. Available at: http://www.rrsignalpix.com/pdf/Magnetic1_ocr_sec.pdf. [Accessed 20 August 2020].
83. Marsten, R.E. and Morin, T.L., 1976. *MMPD, a Computer Code for Solving Multiconstraint Knapsack Problems in Integer Variables*. User's Guide. Operations Research Center, MIT, Cambridge, MA.
84. Mathews, G.B., 1896. On the partition of numbers. *Proceedings of the London Mathematical Society*, 1(1), pp. 486-490.
85. MathWorks, 2020. MATLAB. [online]. Available at: <https://www.mathworks.com/>. [Accessed 27 November 2020].
86. Minnesota DOT, 2000. Cost of Pavement Marking Materials. [online]. Available at: <https://www.lrrb.org/media/reports/200011.pdf>. [Accessed 20 August 2020].
87. Minnesota DOT, 2005. Low-Cost Highway-Rail Intersection Active Warning System Field Operational Test. Evaluation Report. [online]. Available at: https://www.dot.state.mn.us/guidestar/2001_2005/hri/HRI_Evaluation_Report_Final.pdf. [Accessed 20 August 2020].
88. Moeur, R., 2019. Manual of Traffic Signals. [online]. Available at: <http://www.trafficsign.us/signcost.html>. [Accessed 20 August 2020].
89. MUTCD, 2009. Manual on Uniform Traffic Control Devices. Federal Highway Administration. U.S. Department of Transportation.
90. NCHRP, 1987. National Cooperative Highway Research Program Report 288. Evaluating Grade-Separated Rail and Highway Crossing Alternatives. [online]. Available at: http://onlinepubs.trb.org/Onlinepubs/nchrp/nchrp_rpt_288.pdf. [Accessed 27 May 2020].
91. Okitsu, W., Louie, J., and Lo, K., 2010. Simulation-Free Railroad Grade Crossing Delay Calculations. *Western District, Institute of Transportation Engineers 2010 Annual Meeting*.
92. Pasha, J., Dulebenets, M.A., Abioye, O.F., Kavvoosi, M., Moses, R., Sobanjo, J. and Ozguven, E.E., 2020a. A Comprehensive Assessment of the Existing Accident and Hazard Prediction Models for the Highway-Rail Grade Crossings in the State of Florida. *Sustainability*, 12(10), p.4291.

93. Pasha, J., Dulebenets, M.A., Kavooosi, M., Abioye, O.F., Theophilus, O., Wang, H., Kampmann, R. and Guo, W., 2020b. Holistic tactical-level planning in liner shipping: an exact optimization approach. *Journal of Shipping and Trade*, 5, pp.1-35.
94. Pasha, J., Dulebenets, M.A., Kavooosi, M., Abioye, O.F., Wang, H. and Guo, W., 2020c. An optimization model and solution algorithms for the vehicle routing problem with a “factory-in-a-box”. *IEEE Access*, 8, pp.134743-134763.
95. Pasha, J., Dulebenets, M.A., Singh, P., Moses, R., Sobanjo, J., and Ozguven, E.E., 2021. Safety and delays at level crossings in the United States: Addressing the need for multi-objective resource allocation. In: M. Marinov, J.K. Piip, eds., *Sustainable Rail Transport 4*, 4th ed. Springer Nature: Switzerland – accepted.
96. Photon Play, 2020. VMS Signs & VMS Boards. [online]. Available at: <http://www.photonplayinc.com/traffic-signs/vms-signs-vms-boards/>. [Accessed 20 August 2020].
97. Pisinger, D., 2007. The quadratic knapsack problem – a survey. *Discrete Applied Mathematics*, 155(5), pp. 623-648.
98. Progressive Railroading, 2009. C&S Technology - Remote Monitoring Systems. [online]. Available at: https://www.progressiverailroading.com/c_s/article/CampS-Technology-Remote-monitoring-systems--20603. [Accessed 20 August 2020].
99. Resor, R., Smith, M., and Patel, P., 2005. Positive Train Control (PTC): Calculating Benefits and Costs of a New Railroad Control Technology. *Journal of the Transportation Research Forum*, 44(2), pp. 77-98.
100. Richards, S.H. and Heathington, K.W., 1990. Assessment of Warning Time Needs at Railroad–Highway Grade Crossings with Active Traffic Control. *Transportation Research Record*, 1254, pp. 72-84.
101. Rilett, L. and Appiah, J., 2008. Microsimulation Analysis of Highway-Rail Grade Crossings: A Case Study in Lincoln, Nebraska. *IEEE/ASME/ASCE Joint Rail Conference*. Wilmington, DE. [online]. Available at: <https://asmedigitalcollection.asme.org/JRC/proceedings-abstract/JRC2008/48124/279/323315>. [Accessed 20 August 2020].
102. SAE International, 2019. SAE Standards News: J3016 Automated-Driving Graphic Update. [online]. Available at: <https://www.sae.org/news/2019/01/sae-updates-j3016-automated-driving-graphic>. [Accessed 20 August 2020].
103. Safety Pilot, 2012. Technology. [online]. Available at: http://safetypilot.umtri.umich.edu/index.php?content=technology_overview. [Accessed 20 August 2020].
104. Siemens, 2020a. Crossings – Train Detection. [online]. Available at: <https://www.mobility.siemens.com/global/en/portfolio/rail/automation/signaling-on-board-and-crossing-products/crossings-overview/crossings-train-detection.html>. [Accessed 20 August 2020].
105. Siemens, 2020b. 2020 Siemens Rail Infrastructure Price Guide. [online]. Available at: <https://assets.new.siemens.com/siemens/assets/api/uuid:1d87f2eb-cd2c-4a15-bc35- ea7a51808301/sie-pg-estimatorpriceguide.pdf>. [Accessed 20 August 2020].
106. Signal-Tech, 2020. LED Light Rail Train Crossing Signals and Pedestrian Warning Signs. [online]. Available at: https://www.signal-tech.com/products/rail/light_rail_and_pedestrian_warning. [Accessed 20 August 2020].
107. Singh, J., Desai, A., and Spicer, T., 2010. Intelligent Transportation System to Improve Safety at Level Crossing. *Conference on Railway Engineering*. Wellington, New Zealand.

- September 12-15, 2010. [online]. Available at:
<http://railknowledgebank.com/Presto/content/GetDoc.axd?ctID=MTk4MTRjNDUtNWQ0My00OTBmLTllYWUtzWFjM2U2OTE0ZDY3&rID=ODk=&pID=NzIx&attchmnt=True&uSesDM=False&rIdx=MjU0MA==&rCFU>. [Accessed 20 August 2020].
108. Southern California International Gateway Draft EIR, 2011. Appendix H2: Grade Crossing Delay Calculation Methodology Including Mathematical Derivation of Delay Equation. [online]. Available at: <https://kentico.portoflosangeles.org/getmedia/f4bf4445-de75-4c43-b780-6ff4244894a9/Appendix-H2-At-Grade-Crossing-Memo>. [Accessed 27 May 2020].
109. STB, 2020. Appendix K – Transportation Safety and Delay. Northern Rail Extension Draft Environmental Impact Statement. [online]. Available at:
https://www.stb.gov/FD34658Files/Appendix_K_Trans_Safety_and_Delay.pdf. [Accessed 27 May 2020].
110. TAPCO, 2020. Safe Travels. [online]. Available at: <https://www.tapconet.com/>. [Accessed 20 August 2020].
111. TCRP-175, 2015. Guidebook on Pedestrian Crossings of Public Transit Rail Services. [online]. Available at: https://www.ssti.us/wp/wp-content/uploads/2015/04/tcrp_rpt_175_.pdf. [Accessed 20 August 2020].
112. Texas DOT, 1995. Enhanced Traffic Control Devices and Railroad Operations for Highway-Railroad Grade Crossings: First Year Activities. [online]. Available at:
<https://static.tti.tamu.edu/tti.tamu.edu/documents/1469-1.pdf>. [Accessed 20 August 2020].
113. Toyoda, Y., 1975. A simplified algorithm for obtaining approximate solutions to zero-one programming problems. *Management Science*, 21(12), pp. 1417-1427.
114. Trains, 2019. Computer Runs Train at Test Track, NYAB Announces. [online]. Available at: <https://trn.trains.com/news/news-wire/2019/09/13-computer-runs-train-at-test-track-nyab-announces>. [Accessed 20 August 2020].
115. trainweb.org, 2020. Exeter Branch Wigwags. [online]. Available at:
http://www.trainweb.org/dansrailpix/WIG_WAG_PAGE12a.htm. [Accessed 20 August 2020].
116. U.S. Access Board, 2020. Advancing Full Access and Inclusion for All. [online]. Available at: <https://www.access-board.gov/>. [Accessed 20 August 2020].
117. U.S. DOT, 2007. Railroad-Highway Grade Crossing Handbook. Second Edition 2007. [online]. Available at: <https://www.fra.dot.gov/Elib/Document/1464>. [Accessed 20 August 2020].
118. U.S. DOT, 2014a. GradeDec.NET Reference Manual. [online]. Available at:
<https://www.fra.dot.gov/Elib/Document/14852>. [Accessed 24 September 2018].
119. U.S. DOT, 2014b. Connected Commercial Vehicles-Retrofit Safety Device Kit Project. Model Deployment Operational Analysis Report. [online]. Available at:
https://rosap.ntl.bts.gov/view/dot/3494/dot_3494_DS1.pdf. [Accessed 20 August 2020].
120. U.S. DOT, 2014c. Vehicle-to-Vehicle Communications: Readiness of V2V Technology for Application. [online]. Available at:
<https://www.nhtsa.gov/staticfiles/rulemaking/pdf/V2V/Readiness-of-V2V-Technology-for-Application-812014.pdf>. [Accessed 20 August 2020].
121. U.S. DOT, 2014d. Effect of Dynamic Envelope Pavement Markings on Vehicle Driver Behavior at a Highway-Rail Grade Crossing. [online]. Available at:
https://railroads.dot.gov/sites/fra.dot.gov/files/fra_net/3627/Dynamic%20Envelope%20Pavement%20Markings_FINAL.pdf. [Accessed 20 August 2020].

122. U.S. DOT, 2015. Status of the Dedicated Short-Range Communications Technology and Applications. [online]. Available at: https://www.its.dot.gov/research_archives/connected_vehicle/pdf/DSRCReportCongress_FINAL_23NOV2015.pdf. [Accessed 20 August 2020].
123. U.S. DOT, 2017. Vehicle to Infrastructure Prototype Rail Crossing Violation Warning Application. [online]. Available at: https://rosap.ntl.bts.gov/view/dot/34852/dot_34852_DS1.pdf. [Accessed 20 August 2020].
124. U.S. DOT, 2018. Automated Vehicles at Highway-Rail Grade Crossings: Final Report. [online]. Available at: https://railroads.dot.gov/sites/fra.dot.gov/files/fra_net/18267/AVs%20at%20Highway-Rail%20Grade%20Crossings.pdf. [Accessed 20 August 2020].
125. U.S. DOT, 2019. Highway-Rail Crossing Handbook. Third Edition. [online]. Available at: https://safety.fhwa.dot.gov/hsip/xings/com_roaduser/fhwasa18040/fhwasa18040v2.pdf. [Accessed 27 May 2020].
126. U.S. DOT, 2020. Costs Database. Intelligent Transportation Systems. Joint Program Office. [online]. Available at: <https://www.itscosts.its.dot.gov/its/benecost.nsf/CostHome>. [Accessed 20 August 2020].
127. University of Hawaii, 2020. ICS 311 #24: NP-Completeness. [online]. Available at: <https://www2.hawaii.edu/~nodari/teaching/s17/Notes/Topic-24.html>. [Accessed 10 October 2020].
128. Van Leeuwen, J., 1990. *Algorithms and Complexity. Handbook of Theoretical Computer Science*. 1st ed. Netherlands: Elsevier.
129. Village of Glendale, 2007. Quiet Zone. [online]. Available at: [armorypark.files.wordpress.com > quietzonepowerpoint](http://armorypark.files.wordpress.com/quietzonepowerpoint). [Accessed 20 August 2020].
130. Whippany Railway Museum, 2020. Railroad Crossing Gates & Signals. [online]. Available at: <http://www.whippanyrailwaymuseum.net/exhibits/structures/railroad-crossing-gates-a-signals>. [Accessed 20 August 2020].
131. Wikimedia Commons, 2020. File:Flip-dots.jpg. [online]. Available at: <https://commons.wikimedia.org/wiki/File:Flip-dots.jpg>. [Accessed 20 August 2020].
132. Witzgall, C., 1975. *Mathematical Methods of Site Selection for Electronic Message Systems (EMS)*. [online]. Washington, D.C. Available at: <https://nvlpubs.nist.gov/nistpubs/Legacy/IR/nbsir75-737.pdf>. [Accessed 24 Sept 2018].
133. Young, R., 2017. *2017 Grade Crossing Research Needs Conference*. BNSF Railway. August 2017. [online]. Available at: <https://www.fra.dot.gov/conference/2017/rnw/pdf/Presentations/Engineering%20and%20Technologies/Wireless%20Crossing%20Technology.pdf>. [Accessed 20 August 2020].
134. Zaouk, B. and Ozdemir, K., 2017. Implementing Connected Vehicle and Autonomous Vehicle Technologies at Highway-Rail Grade Crossings. *2017 Grade Crossing Research Needs Workshop*. August 15, 2017. [online]. Available at: <https://www.fra.dot.gov/conference/2017/rnw/pdf/Presentations/Engineering%20and%20Technologies/Implementing%20Connected%20Vehicle%20and%20Autonomous%20Vehicle%20Technologies%20at%20Highway-Rail%20Grade%20Crossings.pdf>. [Accessed 20 August 2020].